Thiosemicarbazones Target Multiple Resistance Pathways in Cancer

Alexandra Stacy B.Sc. (Hons. I)

Department of Pathology, Faculty of Medicine

The University of Sydney

A thesis submitted in fulfilment of the requirements for the degree of Doctor of Philosophy 13.10.2016

Acknowledgements

I would like to thank my supervisor, Prof Des Richardson, for his contributions to my PhD project. His support, both intellectual and financial, allowed me to achieve results that would otherwise have not been possible.

My co-supervisor, Dr Patric Jansson, has been my greatest resource for ideas, trouble-shooting and encouragement. This thesis would not be where it is today without Patś optimism and input.

To Dr Durai Palanimuthu, Prof Paul Bernhardt and Dr Danuta Kalinowski, I am grateful for their help in completing scientific experiments and in preparing the manuscripts of my chapters for publication. Their contributions were critical in getting the manuscripts accepted.

To Dr Michael Carnell, Dr Alexander MacMillan and Dr Renee Whan of The Biomedical Imaging Facility, I am thankful for their microscopy expertise and input regarding experimental design. The knowledge and experience I gained from working in their facility was truly invaluable.

To my family, I owe my deepest gratitude for their constant support over the duration of my studies. I never would have been able to complete this thesis without them.

Declaration

I certify that the intellectual content of this thesis is the product of my own work and that all the assistance received in preparing this thesis and sources have been acknowledged. This thesis has not been submitted for any degree or any other purposes.

Alexandra Stacy

Authorship Attributions

Chapter 3 of this thesis is published as ñStacy AE, Palanimuthu D, Bernhardt PV, Kalinowski DS, Jansson PJ, Richardson DR. (2016). Structure-Activity Relationships of Di-2-Pyridylketone, 2-Benzoylpyridine and 2-Acetylpyridine Thiosemicarbazones for Overcoming Pgp-Mediated Drug Resistance *J. Med. Chem.* **59**(18): 8601-20.ò

I designed the studies with P.J.J. and D.R.R., interpreted the data, performed experiments and wrote the manuscript. D.P. and P.V.B performed experiments and contributed to the manuscript preparation. P.J.J, D.S.K. and D.R.R contributed to the manuscript preparation.

Chapter 4 of this thesis is published as ñStacy AE, Palanimuthu D, Bernhardt PV, Kalinowski DS, Jansson PJ, Richardson DR. (2016). Zinc(II)-thiosemicarbazone complexes are localised to the lysosomal compartment where they transmetallate with copper ions to induce cytotoxicity. *J. Med. Chem.* **59**(10): 4965-84.ò

I designed the studies with P.J.J. and D.R.R., interpreted the data, performed experiments and wrote the manuscript. D.P. and P.V.B performed experiments and contributed to the manuscript preparation. P.J.J, D.S.K. and D.R.R contributed to the manuscript preparation.

In addition to the statement above, where I am not the corresponding author of the published item, permission to include the published material has been granted by the corresponding author

Alexandra Stacy		22.08.2016
Student Name	Signature	Date

As supervisor for the candidature upon which this thesis is based, I can confirm that the authorship attribution statement above is correct.

Professor Des Richardson	Des Richardson 22/8/2016.	
Supervisor Name	Signature	Date

Abstract

Multidrug resistance (MDR) is a significant obstacle in the successful treatment of cancer. To date, no therapies that target MDR have reached the clinic. Our thiosemicarbazone compound, di-2-pyridylketone 4,4-dimethyl-3-thiosemicarbazone (Dp44mT), induces greater cytotoxicity in drug resistant cancer cells that express the drug efflux transporter, P-glycoprotein (Pgp), than in their non-drug resistant counterparts.

Herein, the structure-activity relationships of selected thiosemicarbazones were explored and the novel mechanism underlying their ability to overcome MDR was examined. Only thiosemicarbazones with electron-withdrawing substituents at the imine carbon mediated Pgp-dependent potentiated cytotoxicity and caused Pgp-dependent lysosomal membrane permeabilisation (LMP). This LMP relied on copper(II) chelation, reactive oxygen species generation and increased relative lipophilicity.

We also synthesised fluorescent zinc(II) complexes of our potently anti-cancer thiosemicarbazones to assess their intracellular distribution. The Zn(II) complexes generally showed significantly greater cytotoxicity than the thiosemicarbazones alone. Confocal fluorescence imaging showed that the Zn(II) complex of our lead compound, di-2-pyridylketone 4-cyclohexyl-4-methyl-3-thiosemicarbazone (DpC), was localised to lysosomes. Under lysosomal conditions, the Zn(II) complexes were shown to transmetallate with copper ions, leading to redox-active Cu(II) complexes that induced LMP and cytotoxicity.

Furthermore, we investigated the anti-cancer efficacy of Dp44mT and DpC in Bcl-2 over-expressing, melanoma cells. Herein, we demonstrated that DpC decreased Bcl-2 expression, while Dp44mT did not. Furthermore, we showed that the mechanism by which DpC and Dp44mT exerted their cytotoxicity in melanoma cells did not involve copper ion binding or ROS generation. DpC, but not Dp44mT, induced autophagosome formation and increased the accumulation of acidic vesicles (***e.g.***, autolysosomes), regardless of Bcl-2 expression.

This thesis significantly expands current knowledge regarding novel strategies of overcoming MDR, which can be implemented in the design of innovative therapeutics.

Abbreviations

311 ï 2-hydroxy-1-naphthylaldehyde isonicotinoyl hydrazone

3-AP - 3-aminopyridine-2-carboxaldehyde thiosemicarbazone

A1A - Bcl-2-like protein A1A

ABC transporters ï ATP Binding Cassette Transporters

ABCG2 ï ATP binding cassette subfamily G isoform 2

AKT ï protein kinase B

AO - acridine orange

ApT - 2-acetylpyridine thiosemicarbazone

Ap44mT - 2-acetylpyridine 4,4-dimethyl-3-thiosemicarbazone

ATP ï adenosine triphosphate

Bad- Bcl-2 antagonist of cell death

Bak - Bcl-2 antagonist/killer

Bax - Bcl-2-associated X protein

Bcl-2 ï B cell lymphoma 2

Bcl-B - Bcl-2 like protein 10

Bcl-W ï Bcl-2 like protein 2

Bcl-X_L ï Bcl-2 like protein 1

BH3 - Bcl-2 homology 3

Bid - BH3-interacting domain death agonist

Bik- Bcl-2-interacting killer

Bim - Bcl-2-interacting mediator of cell death

Bmf - Bcl-2 modifying factor

Bok - Bcl-2-related ovarian killer protein

BBB ï blood-brain barrier

BCRP ï breast cancer resistance protein

BpT - 2-benzoylpyridine thiosemicarbazone

Bp2mT - 2-benzoylpyridine 2-methyl-3-thiosemicarbazone

Bp44mT - 2-benzoylpyridine 4,4-dimethyl-3-thiosemicarbazone

c-Src - cellular-sarcoma kinase

DCF - 2N7Ndichlorofluorescein

DMSO ï dimethyl sulfoxide

DpT - di-2-pyridylketone thiosemicarbazone

Dp44mT - di-2-pyridylketone 4,4-dimethyl-3-thiosemicarbazone

DpC - di-2-pyridylketone 4-cyclohexyl-4-methyl-3-thiosemicarbazone

Ela ï Elacridar

ERKs - extracellular regulated kinases

GSH - glutathione

H_2DCF-DA - 2',7'-dichlorodihydrofluorescein

HIF-1Ŭ - hypoxia-inducible factor 1Ŭ

HO^{Å} - hydroxyl radical

Hrk - Harakiri

JNK - c-Jun *N*-terminal kinase

LC3- microtubule-associated protein 1 light chain 3

LAMP1 ï lysosomal-associated membrane protein 1

LAMP2 - lysosomal-associated membrane protein 2

LMP - lysosomal membrane permeabilisation

MAPK - p38 mitogen-activated protein kinase

MDR - multidrug resistance;

MRP1 - multidrug resistance associated protein 1

MTT - 3-(4,5-dimethylthiazol-2-yl)-2,5-diphenyltetrazolium bromide

NAC - *N*-acetylcysteine

NBD - nucleotide binding domain

NDRG1 - N-myc downstream-regulated gene 1

$O_2^{Å ô}$ - superoxide radical

Pgp ï P-glycoprotein

PI3K - phosphatidylinositol-3-kinase

PKIH - di-2-pyridylketone isonicotinyl hydrazone

Puma - p53 up-regulated modulator of apoptosis

ROCK1/pMLC2 pathways ï Rho-associated Coiled-coil-containing protein Kinase 1/phosphorylated Myosin Light Chain 2

ROS - reactive oxygen species

RR - ribonucleotide reductase

STAT3 - signal transduce and activator of transcription 3

TGF-ƃ - transforming growth factor-ƃ

TM - ammonium tetrathiomolybdate

TMD - transmembrane domain

Publications In Support of This Thesis

Stacy AE, Palanimuthu D, Bernhardt P, Kalinowski DS, Jansson PJ, Richardson DR (2016). Zinc(II)ī thiosemicarbazone complexes are localised to the lysosomal compartment where they transmetallate with copper ions to induce cytotoxicity. *J Med Chem*. **59**(10):4965-84

Stacy AE, Jansson PJ, Richardson DR (2013). Molecular pharmacology of ABCG2 and its role in chemoresistance. *Mol. Pharmacol*. **84**(5):655-69

Stacy, AE, Palanimuthu D, Bernhardt P, Kalinowski DS, Jansson PJ, Richardson DR (2016). Structure-activity relationships of di-2-pyridylketone, 2-benzoylpyridine and 2-acetylpyridine thiosemicarbazones for overcoming Pgp-mediated drug resistance. *J. Med Chem.* **59**(18): 8601-20.

Stacy, AE, Richardson DR, Jansson, PJ. DpC, but not Dp44mT, overcomes Bcl-2 mediated multidrug resistance in melanoma. Manuscript in preparation.

Additional publications during this candidature:

Jansson PJ, Yamagishi T, Arvind A, Seebacher N, Gutierrez E, Stacy A, Maleki S, Sharp D, Sahni S, Richardson DR (2015). Di-2-pyridylketone 4,4-dimethyl-3-thiosemicarbazone (Dp44mT) overcomes multidrug resistance by a novel mechanism involving the hijacking of lysosomal P-glycoprotein (Pgp). *J Biol Chem*. **290**(15):9588-603

Competitive Awards

Australian Postgraduate Award, $25,000 *per annum*

1st Runner Up, Three Minute Thesis Competition, Bosch Annual Meeting (2014), $500

Conference Presentations

- ñOvercoming Multidrug Resistance with Dp44mTò- Pathology Department Seminar Series - 2015

- ñStructure-Activity Relationships of Di-2-Pyridylketone, 2-Benzoylpyridine and 2-Acetylpyridine Thiosemicarbazones for Overcoming Pgp-Mediated Drug Resistanceò- EORTC-AACR-NCI Symposium on Molecular Therapeutics, 2014

- ñA Novel Mechanism of Targeting Multidrug Resistance in CanceròThree Minute Thesis Competition, Bosch Institute Annual Scientific Meeting, 2014

- ñThe Structure-Activity Relationships of Novel Thiosemicarbazones: Overcoming Multidrug ResistanceòBosch Young Investigators Meeting, 2014

- ñStructure-Activity Relationships of Di-2-Pyridylketone, 2-Benzoylpyridine and 2-Acetylpyridine Thiosemicarbazones for Overcoming Pgp-Mediated Drug Resistanceò- Bosch Young Investigators Seminar Series, 2014

- ñOvercoming Multidrug Resistance Using Novel Thiosemicarbazonesò- Pathology Department Seminar Series - 2013

List of Figures

List of Tables

Table of Contents

Chapter 1 - Introduction

1.1Aroylhyrdrazone and Thiosemicarbazones for Cancer Treatment

For more than 25 years, our laboratory has developed ligands as anti-cancer agents (Baker et al., 1992; Becker et al., 2003; Darnell and Richardson, 1999; Richardson et al., 1995; Richardson and Milnes, 1997). Aroylhydrazones such as hydroxy-1-naphthylaldehyde isonicotinoyl hydrazone (311) were investigated first, and are biologically effective iron ion chelators, forming tridentate ligands *via* their O-N-O system (Fig. 1.1) (Ponka et al., 1979).

These agents possess favourable properties such as oral availability, high membrane permeability, and simple synthesis (Kalinowski and Richardson, 2005; Kalinowski et al., 2007; Richardson et al., 1995; Richardson, 1997). Investigations of the biological activity of 311 found that it inhibits ribonucleotide reductase (RR), resulting in growth inhibition and apoptosis of cancer cells(Green et al., 2001; Richardson, 1997). Additional molecular targets include cell cycle regulators cyclins D1, D2, and D3, cyclin-dependent kinase 2 and the cyclins A and B1; the expression of which is reduced by 311 and results in cell cycle arrest (Gao and Richardson, 2001).

In an attempt to increase the cytotoxicity of aroylhydrazones such as 311, analogues with additional lipophilic groups were synthesised (Richardson et al., 1995). These

ligands have similar yet more potent properties to 311, with di-2-pyridylketone isonicotinyl hydrazone (PKIH) (Fig. 1.1) emerging as the lead compound from the series. Aside from their selective anti-proliferative activity towards cancer cells, they also affect the cell cycle by increasing the expression of proteins involved in G_1/S arrest (Becker et al., 2003). Furthermore, the redox activity of the complexes of PKIH and its analogues plays an important role in their cytotoxicity (Becker et al., 2003).

Thiosemicarbazones were originally developed for the treatment of tuberculosis (Domagk et al., 1946; Donovick et al., 1950), however they have been found to have a broad range of therapeutic uses ranging from anti-viral to anti-cancer (Brockman et al., 1956; Brownlee and Hamre, 1951; Hamre et al., 1950; Klayman et al., 1979; Liberta and West, 1992; Shipman et al., 1986). Indeed, 2-formylpyridine thiosemicarbazone was the first agent of this class to demonstrate potent anti-cancer activity (Brockman et al., 1956). This property has since made thiosemicarbazones the focus of extensive research and development (Kalinowski and Richardson, 2005). Similarly to aroylhydrazones, one of the mechanisms that mediates the anti-cancer activity of thiosemicarbazones is the inhibition of RR through iron ion chelation (Cory et al., 1994; Finch et al., 2000; Green et al., 2001; Sartorelli et al., 1971; Yu et al., 2011). Subsequent studies demonstrated that this was only one of a multitude of anti-cancer mechanisms mediated by thiosemicarbazones including the inhibition of oncogenic signalling pathways and the formation of redox-active transition metal complexes which are coordinated *via* the N-N-S system (Fig. 1.1, 1.3) (Jansson et al., 2010a; Jansson et al., 2010b; Kovacevic et al., 2011; Kovacevic et al., 2013; Lovejoy et al., 2011; Lovejoy et al., 2012; Richardson et al., 2006; Yu et al., 2009b; Yuan et al., 2004).

One of the first thiosemicarbazones to enter clinical trials was 3-amino-2-pyridinecarboxaldehyde thiosemicarbazone (3-AP), which has been in greater than 20 multi-centre clinical trials (Fig. 1.1) (Knox et al., 2007; Merlot et al., 2013; Odenike et al., 2008; Traynor et al., 2010). However, 3-AP has suffered multiple problems, including low efficacy in some tumour types and serious side effects such as methaemoglobinaemia (Knox et al., 2007; Merlot et al., 2013; Traynor et al., 2010).

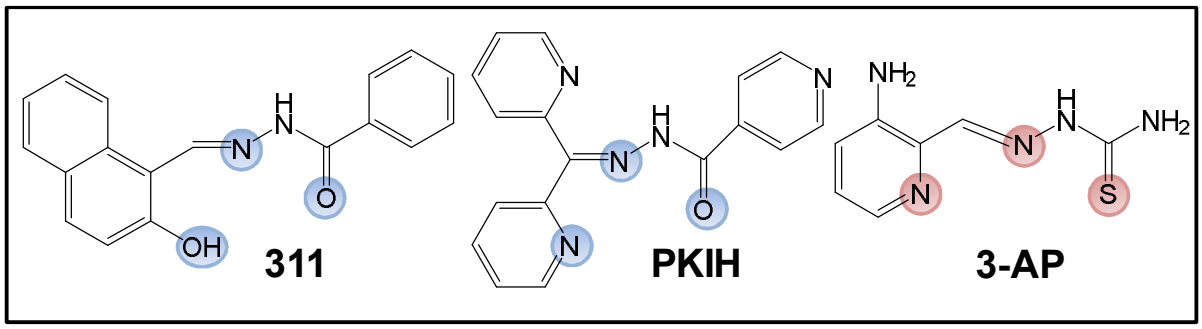

Figure 1.1 Structures of 311, PKIH and 3-AP

Whereas 311 has an O-N-O system, PKIH, an aroylhydrazone, chelates transition metals through its N-N-O system (blue highlights). 3-AP, a thiosemicarbazone, chelates transition metals through its N-N-S system (red highlights).

1.2 Development of New Generation Thiosemicarbazones for Cancer Treatment

The anti-cancer efficacy of aroylhydrazones, such as 311 and PKIH, and thiosemicarbazones, such as 3-AP, prompted the development of aroylhydrazone/thiosemicarbazone hybrids (Kalinowski and Richardson, 2005). Concerted structure-activity studies identified several series of ligands with marked and selective anti-tumour activity *in vitro* and/or *in vivo* (Kalinowski et al., 2007;

Richardson et al., 2009; Yu et al., 2012). These series included the di-2-pyridylketone thiosemicarbazone (DpT) series (Chen et al., 2012; Liu et al., 2012; Lovejoy et al., 2012; Richardson et al., 2006; Whitnall et al., 2006; Yuan et al., 2004), the 2-benzoylpyridine thiosemicarbazone (BpT) (Kalinowski et al., 2007) and 2-acetylpyridine thiosemicarbazone (ApT) series of ligands (Richardson et al., 2009) that also showed marked and selective anti-tumour activity *in vitro* and/or *in vivo* (Fig. 1.2) (Kalinowski et al., 2007; Richardson et al., 2009; Yu et al., 2012).

The DpT series was developed first, based on the high activity of PKIH and 3-AP (Becker et al., 2003; Knox et al., 2007; Merlot et al., 2013; Odenike et al., 2008; Traynor et al., 2010). The success of the DpT series led to the synthesis of the BpT series, which was developed in order to explore the role of aromatic substituents on the anti-proliferative effects of the DpT series (Fig. 1.2) (Kalinowski et al., 2007). The ApT series explored the effects of replacing the parent ketone of DpT series, di-2-pyridylketone, with 2-acetylpyridine in order to create an agent similar to the clinically trialled 3-AP (Fig. 1.2) (Richardson et al., 2009).

1.2.1 Efficacy of the DpT Series

Of the DpT analogues, di-2-pyridylketone 4,4-dimethyl-3-thiosemicarbazone (Dp44mT) is the best characterised. Dp44mT acts in a polypharmacological manner, targeting primary tumour growth, metastasis and drug resistance (Jansson et al., 2015a).

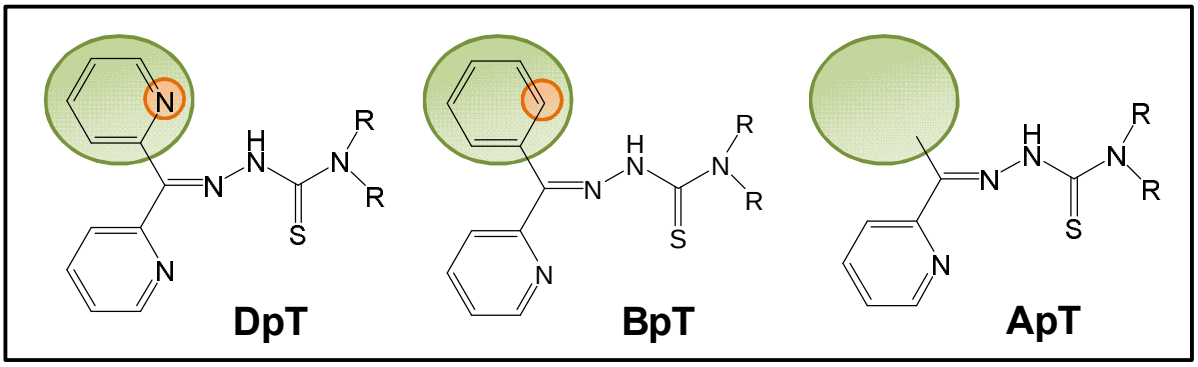

Figure 1.2 Hybrid aroylhydrazones-thiosemicarbazones of the DpT, BpT and ApT series

Hybrid aroylhydrazone-thiosemicarbazones chelate transition metals through their N-N-S systems. The DpT and BpT series differ to the ApT series in that the ApT series possesses only 1 aromatic ring on its imine carbon, as opposed to 2 like the DpT and BpT series (green highlights). The BpT and DpT series differ in the type of aromatic substituents on the imine carbon (orange highlights): DpT has a dipyridyl substituent; BpT possesses a phenyl ring and a pyridyl ring.

Specifically, Dp44mT can target tumour growth by inducing G1/S cell cycle arrest (Dixon et al., 2013; Noulsri et al., 2009) and inhibiting oncogenic signalling pathways including transforming growth factor-ƃ (TGF-ƃ) (Kovacevic et al., 2013), c-Jun N-terminal kinase (JNK) and p38 mitogen-activated protein kinase (MAPK) (Yu and Richardson, 2011), Ras/extracellular regulated kinase (ERK) (Kovacevic et al., 2013), protein kinase B (AKT)/phosphatidylinositol-3-kinase (PI3K) (Dixon et al., 2013; Kovacevic et al., 2013), STAT3 (Lui et al., 2015), cellular-sarcoma kinase (c-Src) (Liu et al., 2015) and Rho-associated Coiled-coil-containing protein Kinase 1 (ROCK1)/phosphorylated Myosin Light Chain 2 (pMLC2) pathways (Sun et al., 2013).

Dp44mT can suppress metastasis through up-regulation of N-myc downstream-regulated gene 1 (NDRG1), which inhibits primary tumour growth, angiogenesis and metastasis of cancer *in vivo* (Bae et al., 2013; Kovacevic and Richardson, 2006; Maruyama et al., 2006). The metastasis suppressor NDRG1 is up-regulated by Dp44mT *via* hypoxia-inducible factor-1Ŭ (HIF-1Ŭ)-dependent (Le and Richardson, 2004) and -independent mechanisms (Lane et al., 2013), both related to iron depletion. The anti-tumour activity of Dp44mT is also mediated by the formation of complexes with iron and copper ions that exhibit pronounced redox activity (Jansson et al., 2010a; Jansson et al., 2010b; Lovejoy et al., 2011). Furthermore, Dp44mT is able to overcome multidrug resistance (MDR) in cancer, which will be discussed further in Section 1.6 (Jansson et al., 2015a; Seebacher et al., 2016a; Whitnall et al., 2006).

Significantly, Dp44mT demonstrated markedly more pronounced anti-proliferative activity *in vitro* than the clinically trialled 3-AP (Whitnall et al., 2006; Yuan et al., 2004). Additionally, Dp44mT demonstrated greater tolerability with less side effects (Richardson et al., 2006; Whitnall et al., 2006), which has been independently validated by a number of research groups (Gaal et al., 2014; Ishiguro et al., 2014; Liu et al., 2012; Rao et al., 2009). Unfortunately, Dp44mT induced cardiac fibrosis at high non-optimal doses (Whitnall et al., 2006) and this led to the design and synthesis of a second generation of DpT analogues (Kovacevic et al., 2011; Lovejoy et al., 2012). These novel agents were derived from previous studies which showed that increasing lipophilicity *via* the replacement of the terminal H at N4 with an alkyl group, also increased anti-proliferative activity (Kalinowski and Richardson, 2005; Lovejoy and Richardson, 2002; Richardson et al., 2006; Yuan et al., 2004). Of these

ligands, di-2-pyridylketone 4-cyclohexyl-4-methyl-3-thiosemicarbazone (DpC) was identified as the lead agent (Kovacevic et al., 2011; Lovejoy et al., 2012). DpC possessed many advantages over Dp44mT, such as: potent anti-tumour activity *in vitro* and *in vivo* against multiple tumour-types; greater tolerability when administered orally, as well as intravenously (Lovejoy et al., 2012; Yu et al., 2012); and an improved side-effect profile inducing less cardiotoxicity and methaemoglobin generation (Kovacevic et al., 2011; Lovejoy et al., 2012; Quach et al., 2012). Notably, due to its optimal properties, DpC has entered clinical trials towards the end of 2016 (ClinicalTrials.gov Identifier NCT02688101) for the treatment of advanced cancers (Jansson et al., 2015a).

1.2.2 Efficacy of the BpT Series

Another strategy that was taken in an attempt to overcome the cardiotoxicity induced by high, non-optimal doses of Dp44mT, led to the generation of the BpT series. In order to increase lipophilicity and redox cycling, the non-coordinating 2-pyridyl ring was removed and replaced with a less electron-withdrawing phenyl group (Fig. 1.2) (Kalinowski et al., 2007). Indeed, the anti-proliferative activity of the BpT series was found to be greater than that of the DpT series *in vitro* (Kalinowski et al., 2007; Yu et al., 2012).

The redox activity of the BpT- complexes was demonstrated to be greater than the DpT- complexes, likely due to the lowered redox potentials due to the phenyl moiety found in the BpT but not DpT series (Fig. 1.2) (Kalinowski et al., 2007). The greater redox activity potentially accounts for the increased anti-proliferative activity of the

BpT series (Kalinowski et al., 2007). Furthermore, the lead analogue of the series, 2-benzoylpyridine-4,4-dimethyl-3-thiosemicarbazone (Bp44mT), was shown to be orally active against the growth of a human lung xenograft model (Yu et al., 2012). In this model Bp44mT also caused a marked decrease in cyclin D1 and p21CIP1/WAF1 expression in the tumours, which should prevent cell cycle progression and induce apoptosis (Yu et al., 2012). Compared to Dp44mT, Bp44mT had a better side-effect profile, as it did not induce weight loss or cardiac fibrosis (Yu et al., 2012). However, Bp44mT treatment was associated with mild reversible anaemia and hepatotoxicity (Yu et al., 2012).

1.2.3 Efficacy of the ApT Series

In order to examine the effects of substituents at the imine carbon and to create a thiosemicarbazone similar to the clinically trialled 3-AP (Knox et al., 2007; Odenike et al., 2008; Traynor et al., 2010), the ApT series of analogues was developed (Fig. 1.2) (Richardson et al., 2009). The electron-withdrawing aromatic rings that are found in the DpT and BpT series were, in the ApT series, replaced with an inductively-donating methyl group (Fig.1.2) (Richardson et al., 2009). Four of the six ApT chelators showed potent anti-proliferative effects, comparable to the DpT and BpT series (Richardson et al., 2009).

The chelation efficiency of the ApT series was also similar to the DpT and BpT series (Richardson et al., 2009). However, the ApT-Fe(III) complexes demonstrated lower Fe(II/III) redox potentials than the DpT or BpT series (Richardson et al., 2009), and the Cu(II) complex of 2-acetylpyridine-4,4-dimethyl-3-thiosemicarbazone (Ap44mT)

exhibited lower Cu(ll/l) redox potentials than the Cu(II) complex of Dp44mT (Jansson et al., 2010a). This was attributed to the inductively donating imine methyl group in close proximity to the metal centre (Jansson et al., 2010a; Richardson et al., 2009). Despite this, the [Fe(III)-ApT] complexes were still able to oxidise ascorbate at levels similar to the DpT series (Richardson et al., 2009); and although the Cu(II) complex of Ap44mT was less redox-active than the Cu(II) complex of Dp44mT *in vitro*, both complexes displayed similar redox activity *in vivo* (Jansson et al., 2010a). However, the anti-proliferative activity of the Cu(II) complex of Ap44mT was less than the Cu(II) complex of Dp44mT (Jansson et al., 2010a)

1.3 Thiosemicarbazones, Transition Metals and Redox Cycling

Thiosemicarbazones chelate transition metals, such as iron, copper and zinc, in a tridentate fashion *via* their N-N-S system (French and Blanz, 1966). They can form both 1:1 transition metal/ligand complexes, and 1:2 complexes (Jansson et al., 2010b). In particular, Ŭ-*N*-heterocyclic can bind a vast range of transition metals (Fig. 1.3). The formation of redox-active complexes with transition metals has been demonstrated to increase thiosemicarbazone cytotoxicity both *in vitro* (Antholine et al., 1976; Blanz et al., 1970; Crim and Petering, 1967; Jansson et al., 2010b; Kalinowski et al., 2007; Lovejoy et al., 2011; Richardson et al., 2006; Richardson et al., 2009; Saryan et al., 1979; Van Giessen et al., 1973) and *in vivo* (Petering et al., 1967; Yu et al., 2012).

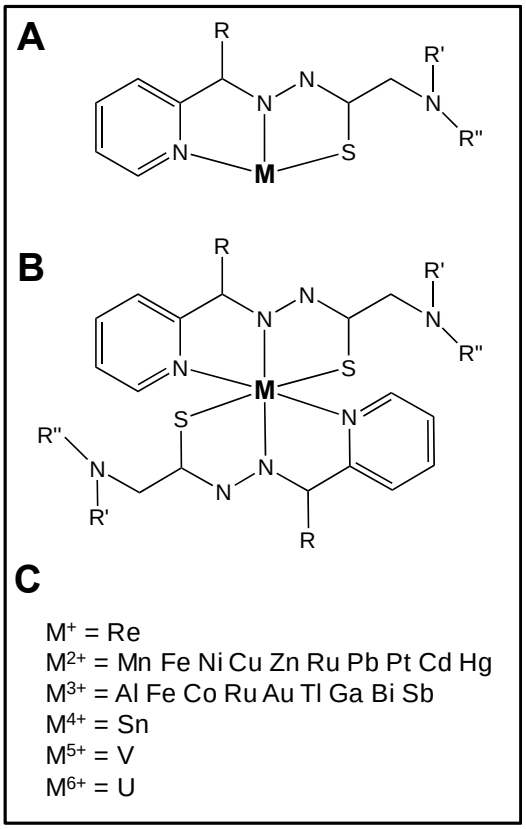

Figure 1.3 Structure of α-pyridyl thiosemicarbazones and their transition metal (M) complexes

A Ŭ-pyridyl thiosemicarbazones can form 1:1 complexes with a range of transition metals (M) **B** Ŭ-pyridyl thiosemicarbazones can form 1:2 complexes with M. **C** M that Ŭ-pyridyl thiosemicarbazones can form complexes with.

1.3.1 Transition Metals and Redox Cycling

The transition metals are located in the d block of the periodic table and form stable ions that have incompletely filled d sub-shells (Petrucci et al., 2002). The presence of unpaired electrons in their d orbitals makes transition metals highly reactive and also means that they have multiple oxidation states (Petrucci et al., 2002). This unique electronic structure generally allows transition metals to participate in redox reactions, involving the loss (oxidation) or gain (reduction) of one or more electrons (Young and Woodside, 2001). This makes transition metals ideal co-factors in

enzymes that carry out fundamental biological functions. However, transition metals can cause damage to biomolecules, either through direct interaction or by mediating the formation of reactive oxygen species (ROS) through redox cycling (Gutteridge et al., 1979). Thus, transition metals are tightly regulated within the cell to prevent metal-induced toxicity (Stohs and Bagchi, 1995).

Of the transition metals, there is ample evidence for the roles of both iron and copper in oxidative stress-induced disease (Stohs and Bagchi, 1995; Young and Woodside, 2001). These elements play a key role in the formation of the hydroxyl radical ($HO^{\cdot}$) *in vivo*, *via* the Haber-Weiss reaction (Fig. 1.4) (Haber and Weiss, 1932). The reaction occurs in two parts, first involving the reduction of a transition metal by $O_2^{\cdot-}$; followed by the oxidation of the transition metal with H_2O_2 to form the $HO^{\cdot}$ radical and HO^{-}, which is known as the Fenton Reaction (Fig. 1.4) (Haber and Weiss, 1932).

$$Fe^{3+} + O_2^{\cdot-} \longrightarrow Fe^{2+} + O_2$$

Fenton reaction:

$$Fe^{2+} + H_2O_2 \longrightarrow Fe^{3+} + HO^{-} + HO^{\cdot}$$

Net reaction:

$$O_2^{\cdot-} + H_2O_2 \longrightarrow O_2 + HO^{-} + HO^{\cdot}$$

Figure 1.4 The Haber-Weiss Reaction.

1.3.2 Important Transition Metals Chelated by Thiosemicarbazones

1.3.2.1. Iron

Iron is a vital element for living organisms, as it is essential for the functioning of many proteins and enzymes that are involved in cell growth and division (Kovacevic et al., 2011; Lovejoy et al., 2012). Indeed, iron depletion results in cell cycle arrest (Kovacevic et al., 2011; Lovejoy et al., 2012). Intracellular iron may be present as part of the labile iron pool, bound to the iron storage protein, ferritin, or bound to enzymes where it acts as a cofactor (Jansson et al., 2015a; Lovejoy et al., 2012; Quach et al., 2012; Yu et al., 2012). However, it is the very feature which makes iron a powerful catalyst that also makes it potentially toxic to cells: the redox cycling of iron ions leads to the generation of the $HO^{\bullet}$ *via* the Haber-Weiss reaction (Fig. 1.4, Section 1.3.1) (Gutteridge et al., 1979; Halliwell, 1978). Hence, iron is carefully regulated within cells in order to prevent the formation of harmful free radicals and the resultant oxidative stress (Richardson et al., 2009).

In the context of human disease, iron-induced oxidative stress is evident in iron overload diseases such as β-thalassaemia and Friedreich's ataxia (Blanz et al., 1970; Crim and Petering, 1967). Furthermore, the ROS produced by iron redox cycling have been implicated in many disease states due to the damage they cause to DNA, lipids and proteins (Section 1.3.3) (Gutteridge, 1995; Imlay et al., 1988; Stadtman, 1990).

1.3.2.2 Copper

Similarly to iron, copper is also essential to the function of most organisms, acting as a co-factor for a variety of enzymes that have roles as diverse as anti-oxidant defence *e.g.* superoxide dismutase; mitochondrial respiration *e.g.* cytochrome c oxidase; and nervous system function *e.g.* dopamine ß-monooxygenase (Antholine et al., 1976; Gaggelli et al., 2006; Petering et al., 1967; Van Giessen et al., 1973). Once taken up by the cell, copper can be found bound to metallothionein proteins and bound to enzymes; or it is incorporated into ceruloplasmin which contains up to 95% of the copper found in serum (Cowley et al., 2005; Kalinowski et al., 2007; Kowol et al., 2010; Richardson et al., 2006; Richardson et al., 2009; Saryan et al., 1979; Yuan et al., 2004). Lysosomes also contain a large proportion of intracellular copper due to degradation of copper-containing metalloproteins by lysosomal cathepsins (Gupte and Mumper, 2009; Kurz et al., 2010; Terman and Kurz, 2013). Under standard physiological conditions, an upper limit of 1×10^{-18} M of free Cu(II) has been calculated (Jansson et al., 2010b; Lippard, 1999; Rae et al., 1999). Unbound copper ions virtually non-existent within the cell as it is too redox-active and acts as a catalyst in the generation of damaging ROS and free radicals (Gaggelli et al., 2006). Furthermore, copper out-competes other divalent metals to bind cellular ligands, thereby affecting the functioning of biomolecules directly (Gaal et al., 2014; Irving and Williams, 1953; Kalinowski et al., 2007).

Even when bound to proteins or enzymes, copper is still able to directly catalyse the formation of ROS or exert pro-oxidant effects on biomolecules (Jansson et al., 2010b; Lovejoy et al., 2011). Indeed, copper causes DNA and protein oxidation and lipid peroxidation (Antholine et al., 1976; Blanz et al., 1970; Crim and Petering, 1967;

Gutierrez et al., 2014; Gutteridge, 1984; Jansson et al., 2010a; Petering et al., 1967; Van Giessen et al., 1973). Unsurprisingly, copper has been linked to disease progression or severity where oxidative stress is involved in the pathogenesis, such as cancer, arteriosclerosis and Alzheimerôs disease (Cowley et al., 2005; Jansson et al., 2010a; Jansson et al., 2010b; Kalinowski et al., 2007; Kowol et al., 2010; Richardson et al., 2009; Saryan et al., 1979). Moreover, serum and tumour copper levels are significantly elevated in cancer patients (Goodman et al., 2004; Gupte and Mumper, 2009). The importance of copper homeostasis is also highlighted by the genetic disorders, Menkes disease and Wilsonôs disease, that result in fatal copper deficiency or damaging copper build-up in the liver and brain, respectively (Jansson et al., 2015a; Sartorelli et al., 1970).

1.3.2.3 Zinc

Zinc is an essential trace element and is the second most abundant transition metal found in the human body after iron (Kovacevic et al., 2011; Outten and O'Halloran, 2001; Vallee, 1988). Zinc can act as a co-factor in the formation of a structural motif in proteins, which is commonly referred to as a zinc finger (Lovejoy et al., 2011; Vallee, 1988). However, zinc is generally directly involved in catalysis and is found in the active site of enzymes such as human carbonic anhydrase II (Outten and O'Halloran, 2001; Richardson et al., 2009). In biological systems zinc always occurs as a divalent cation, Zn^{2+}/Zn(II), with a fully occupied *d* shell (Cowley et al., 2005). Zn(II) is therefore not redox-active as neither the potential oxidised form, Zn^{3+}, nor the reduced form, Zn^{+}, can be formed under physiological conditions (Kowol et al., 2010). As a structural element in nucleic acid-binding and gene regulatory proteins, Zn^{2+} therefore possess an advantage over redox-active transition metals such as

iron and copper ions, which promote free radical generation and DNA damage (Cowley et al., 2005).

1.3.3 Redox Damage to Biomolecules Mediated by Iron and Copper Ions

Iron and copper ions can mediate damage to biomolecules either by interacting with them directly or by mediating the formation of the free radical, $HO^{Å}$, *via* the Fenton Reaction (Fig. 1.4,1.5). The production of ROS is inevitable in aerobic life and their damaging interactions with DNA, lipids and proteins (Fig. 1.5) (Antholine et al., 1976; Blanz et al., 1970; Crim and Petering, 1967; Gutierrez et al., 2014; Gutteridge, 1995; Imlay et al., 1988; Jansson et al., 2010a; Petering et al., 1967; Stadtman, 1990; Van Giessen et al., 1973) have acknowledged roles in the aetiology and pathogenesis of many diseases (Blanz et al., 1970; Cowley et al., 2005; Crim and Petering, 1967; Gutteridge, 1984; Jansson et al., 2010a; Jansson et al., 2010b; Kalinowski et al., 2007; Kowol et al., 2010; Richardson et al., 2009; Saryan et al., 1979).

ROS act as oxidising agents, accepting electrons from biomolecules that result in the reduction of the ROS and oxidation of the biomolecules (Gaetke and Chow, 2003; Welch et al., 2002). Transition metal ions such as Fe(II/III) and Cu(I/II) bind with high affinity to DNA, meaning that the $HO^{Å}$ radical can be produced in close proximity to DNA *via* the Fenton Reaction (Gutteridge, 1984; Kohen et al., 1986). Importantly, the $HO^{Å}$ radical is known to react with all components of DNA (purines, pyrimidines and the deoxyribose backbone) and is responsible for the majority of ROS-mediated DNA damage that occurs (Domagk et al., 1946; Donovick et al., 1950; Liberta and

West, 1992). Oxidative damage to DNA can result from the formation of DNA-protein cross-links (Hamre et al., 1950), apurinic sites (Hamre et al., 1950) and DNA strand breaks (Shipman et al., 1986) all of which lead to mutations (Fig. 1.5) (Brownlee and Hamre, 1951). Additionally, the presence of iron and copper ions can greatly enhance the oxidative degradation of lipids (Blanz et al., 1970; Gutteridge et al., 1979; Petering et al., 1967). Cell membranes are vulnerable to oxidation, known as lipid peroxidation, as the double bonds found in polyunsaturated fatty acids are a ready target for attack by $HO^{Å}$ produced by the redox cycling of iron or copper ions (Gutteridge, 1995; Reichard and Ehrenberg, 1983; Sartorelli et al., 1970). It has been estimated that around 60 molecules of linoleic acid (the most common poly-unsaturated fatty acid found in cell membranes) are consumed per oxidant that reacts with the lipid bilayer (Crim and Petering, 1967). The consequences of lipid peroxidation affect the functioning of the cell membrane by disrupting ion channels, membrane transport proteins or by causing the membrane to become permeable, leading to cell death (Fig. 1.5) (Van Giessen et al., 1973).

Almost all amino acids are vulnerable to oxidation by $HO^{Å}$ radicals, produced when H_2O_2 encounters iron or copper ions found in the binding sites of proteins (Saryan et al., 1979; Stadtman, 1990). Radicals can target and cause damage to both the backbone and the amino acid side chains of proteins (Knox et al., 2007; Stadtman, 1990). This damage may result in inter- and intra-protein cross-links, protein fragmentation and conformational changes in structure (Fig. 1.5.) (Baker et al., 1992; Darnell and Richardson, 1999; Merlot et al., 2013; Richardson et al., 1995; Richardson and Milnes, 1997; Stadtman, 1990). Oxidative damage to proteins can therefore affect cell functioning due to the loss of enzymatic, transport and regulatory

protein function (Becker et al., 2003; Stadtman, 1990; Whitnall et al., 2006; Yuan et al., 2004).

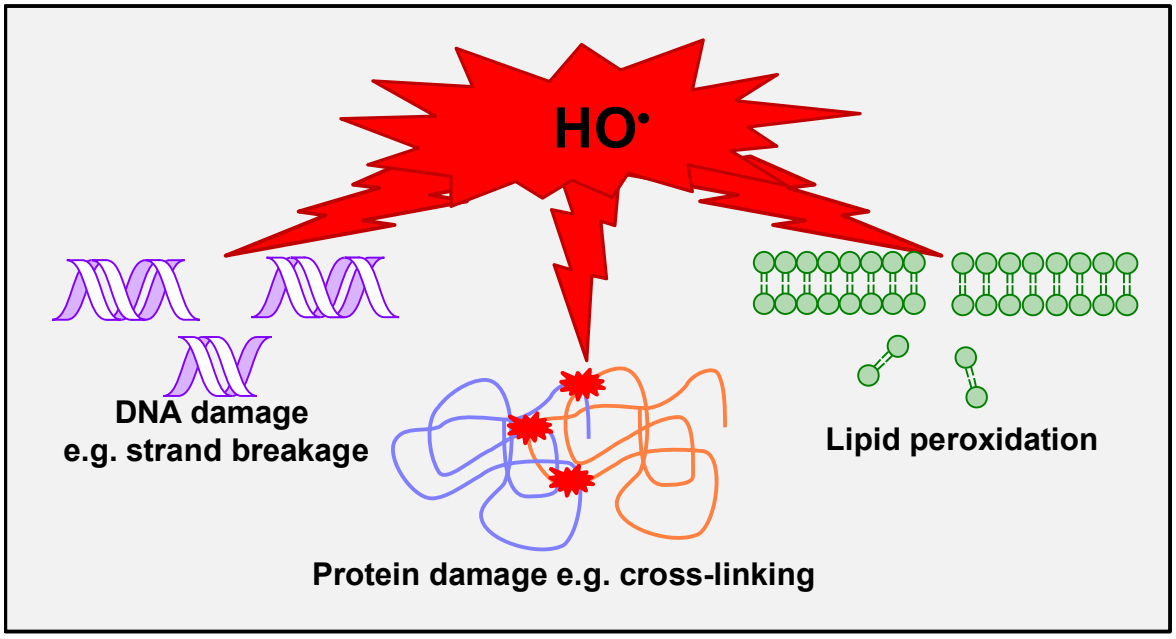

Figure 1.5 Examples of damage to biomolecules caused by the HO• radical.
The redox cycling of copper and iron ions produces the highly reactive HO• radical *via* the Fenton reaction. The HO• radical induces oxidative damage to biomolecules including: DNA damage such as strand breaks and apurinic sites; protein damage such as cross-linking and fragmentation; and lipid peroxidation in membranes.

1.4 Multidrug Resistance and Cancer

When cancer patients fail to respond to surgical excision and/or radiotherapy or their cancer is too advanced, the next line of treatment is chemotherapy (Gillet and Gottesman, 2010; Gottesman, 2002). While some patients go into complete remission following treatment, others show only a transient response or fail to respond at all (Gillet and Gottesman, 2010; Gottesman, 2002). This resistance to chemotherapy is commonly conferred against a variety of both structurally and

mechanistically unrelated drugs and is known as cancer multidrug resistance (MDR), which may be inherent or acquired (Gillet and Gottesman, 2010; Gottesman, 2002).

The mechanisms behind this failure to respond can be divided into three categories: **(1)** pharmacokinetic resistance *e.g.* increased metabolism (Ekhart et al., 2009) or poor tumour penetration (Minchinton and Tannock, 2006); **(2)** intrinsic tumour cell resistance *e.g.* altered drug transport (Gottesman, 2002) or inhibition of apoptosis (Dunn et al., 1997; Kroemer, 1997); and **(3)** tumour microenvironment-related factors (Minchinton and Tannock, 2006; Tomida and Tsuruo, 1999) *e.g.* hypoxia or acidosis (Fig. 1.6) (Gerweck et al., 2006; Seebacher et al., 2016a). Although there are multiple mechanisms that tumour cells use to evade apoptosis, two of the best-characterised mechanisms involve increased drug efflux by members of the adenosine triphosphate (ATP)-binding cassette (ABC) family (Fig. 1.6) (Gillet and Gottesman, 2010; Gottesman, 2002), and evasion of apoptosis by increased expression of B cell lymphoma 2 (Bcl-2) (Fig. 1.6) (Thomas et al., 2013; Youle and Strasser, 2008). An additional mechanism of MDR involves sequestration of cytotoxic chemotherapeutics inside lysosomes, which prevents them from reaching their intended intracellular targets and thus decreases their cytotoxicity (Fig. 1.6) (Appelqvist et al., 2013; Zhitomirsky and Assaraf, 2016).

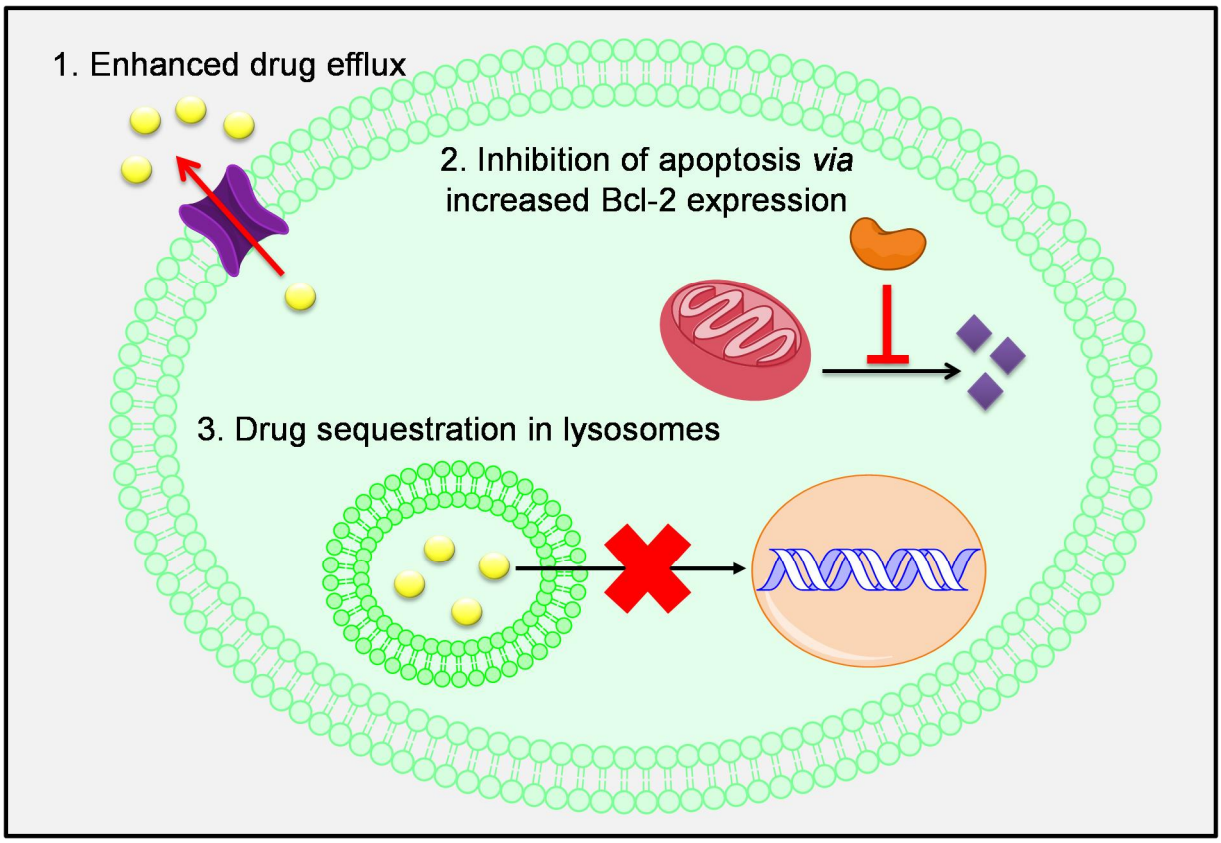

Figure 1.6 Mechanisms of MDR

The three mechanisms of MDR that will be the focus of this thesis are **(1)** Enhanced drug (yellow circle) efflux by ABC transporters; **(2)** Inhibition of intrinsic apoptosis by increased expression of Bcl-2 family members (orange oval); **(3)** Drug sequestration in lysosomes, preventing the drug from reaching its target e.g. DNA in the nucleus.

1.4.1 Pgp, a Member of the ABC Family of Drug Efflux Transporters

Members of the ABC family are transmembrane proteins that bind and hydrolyse ATP, the energy from which is then utilised to efflux substrates across cell membranes (Fletcher et al., 2010; Gillet and Gottesman, 2010; Gottesman and Pastan, 1993; Gottesman et al., 2002). The substrate specificity of the family members varies widely; they are responsible for the transport of biological substrates such as hormones, lipids, metabolic products, and also xenobiotics, including

chemotherapeutics (Fletcher et al., 2010; Gillet and Gottesman, 2010; Gottesman and Pastan, 1993; Gottesman et al., 2002). There are 48 known members of the ABC superfamily which are divided into seven subfamilies, designated A to G, on the basis of sequence and structural homology (Fletcher et al., 2010; Gillet and Gottesman, 2010; Gottesman and Pastan, 1993; Gottesman et al., 2002).

The ABC transporters are highly conserved in evolution, generally consisting of two nucleotide (ATP) binding domains (NBDs) and two transmembrane domains (TMDs), although some exist as half transporters which must at least homo- or hetero-dimerise to become functional transporters (Fletcher et al., 2010; Gillet and Gottesman, 2010; Gottesman and Pastan, 1993; Gottesman et al., 2002). The TMDs are usually found at the N-terminal and contain 6-12 Ŭ-helices that span the membrane and confer substrate specificity. The NBDs are located at the C-terminal in the cytoplasm and contain both the ATP-binding sequences, Walker A and B motifs, found in other ATPases; and the ABC signature or C motif, which is unique to the family (Fletcher et al., 2010; Gillet and Gottesman, 2010; Gottesman and Pastan, 1993; Gottesman et al., 2002).

When a substrate binds to the transporter, one of the NBDs is activated to hydrolyse ATP, which results in a major conformational change in the transporter, releasing the substrate on the other side of the membrane (Fletcher et al., 2010; Gillet and Gottesman, 2010; Gottesman and Pastan, 1993; Gottesman et al., 2002). The hydrolysis of a second molecule of ATP then returns the transporter to its native

conformation, ready to repeat the cycle (Fletcher et al., 2010; Gillet and Gottesman, 2010; Gottesman and Pastan, 1993; Gottesman et al., 2002).

The three ABC transporters that are most extensively studied in the context of MDR are P-glycoprotein (Pgp, also known as MDR1 or ABCB1), multidrug resistance associated protein 1 (MRP1, also known as ABCC1) and ATP-binding cassette, sub-family G, isoform 2 protein (ABCG2, also known as breast cancer resistance protein, BCRP) (Cole et al., 1992; Doyle et al., 1998; Fletcher et al., 2010; Gillet and Gottesman, 2010; Gottesman and Pastan, 1993; Gottesman, 2002; Gottesman et al., 2002; Stacy et al., 2013). Of these three, Pgp has been the focus of concentrated research as its clinical relevance in the MDR phenotype is well established (Gottesman et al., 2002; Juliano and Ling, 1976). Thus, Pgp will be discussed in depth as a major focus of this thesis.

Juliano and Ling (1976) first discovered Pgp almost 40 years ago in Chinese hamster ovary cells selected for colchicine resistance. However, Pgp was found to also confer resistance to a variety of mechanistically and structurally unrelated drugs (Juliano and Ling, 1976). The 170 kDa protein is encoded by the *MDR1* gene located on chromosome 7q21 (Ganapathi et al., 1996), and is the most thoroughly characterised of the ABC transporters (Fletcher et al., 2010; Gillet and Gottesman, 2010; Gottesman and Pastan, 1993; Gottesman et al., 2002). Pgp is expressed in a wide variety of cancers where it effluxes chemotherapeutics from the cell, thus decreasing their cytotoxicity and contributing to treatment failure (Fletcher et al.,

2010; Gillet and Gottesman, 2010; Gottesman and Pastan, 1993; Gottesman et al., 2002). Pgp has therefore been the focus of research aimed at overcoming MDR.

1.4.1.1 Structure and Transport Models of Pgp

Pgp is synthesised as a 140 kDa polypeptide precursor that is later N-glycosylated in the first extracellular linker region to become a 170 kDa transmembrane protein containing 1280 amino acids (Fig. 1.7) (Chen et al., 1986; Greer and Ivey, 2007; Gros et al., 1986; Juliano and Ling, 1976). To date, no high-resolution crystal structures of human Pgp have been generated, thus it is difficult to make concrete assertions regarding the structure of human Pgp. Current homology models are based on mouse and *Caenorhabditis elegans* Pgp proteins, which have 87% and 46% sequence homology with human Pgp, respectively (Aller et al., 2009; Jin et al., 2012; Li et al., 2014). The transporter consists of 2 halves with 6 N-terminal TMDs and 1 C-terminal NBD each, joined by a linker region (Fig. 1.7) (Li et al., 2014; Rosenberg et al., 2005). The N- and C-terminals as well as the NBDs are both intracellular (Fig. 1.7) (Kartner et al., 1985). The TMDs are predicted to form the substrate-binding sites and the central pore through which substrates are transported across the membrane (Li et al., 2014; Rosenberg et al., 2005). The presence of aromatic residues in the mammalian Pgp translocation pathway likely facilitates the recognition and transport of neutral/cationic molecules (Ferreira et al., 2013; Li et al., 2014). It has been suggested that there are up to three binding sites within the central pore: two that are substrate-binding sites, and one that is a modulator-binding site (Ferreira et al., 2013; Shapiro and Ling, 1997; Sharom et al., 2005).

Substrates of Pgp, being relatively hydrophobic (Section 1.4.1.4), partition into the lipid bilayer where they interact with the transporterôs substrate binding sites (Fig. 1.7) (Aller et al., 2009; Higgins and Gottesman, 1992; Kessel, 1989; Pearce et al., 1989; Sharom, 1997; Sharom, 2014). Although the exact mechanism of Pgp substrate binding and transport remains elusive, Pgp and other ABC transporters are thought to act by an alternating access model, whereby substrate binding to the inward-facing conformation of the transporter stimulates ATPase activity (Fig. 1.7) (Callaghan et al., 2006; Senior et al., 1995; Urbatsch et al., 1995). The hydrolysis of one molecule of ATP then generates the energy needed to cause a switch to an outward-facing conformation of the transporter, resulting in the release of the substrate into the extracellular space (Aller et al., 2009; Higgins and Gottesman, 1992; Kessel, 1989; Pearce et al., 1989; Sharom, 1997; Sharom, 2014). Hydrolysis of another ATP molecule is then needed to ór e-setô the transporter so that it can bind substrates again (Aller et al., 2009; Higgins and Gottesman, 1992; Kessel, 1989; Pearce et al., 1989; Sharom, 1997; Sharom, 2014).

1.4.1.2 Pgp in Normal Physiology

Despite Pgp being thought of mainly as a drug resistance protein, like all ABC transporters, it also plays a role in normal physiology. The transporter is widely distributed throughout the body and its localisation suggests that its main physiological role is to protect the body from exposure to toxins (Gottesman et al., 2002; Sharom, 2011).

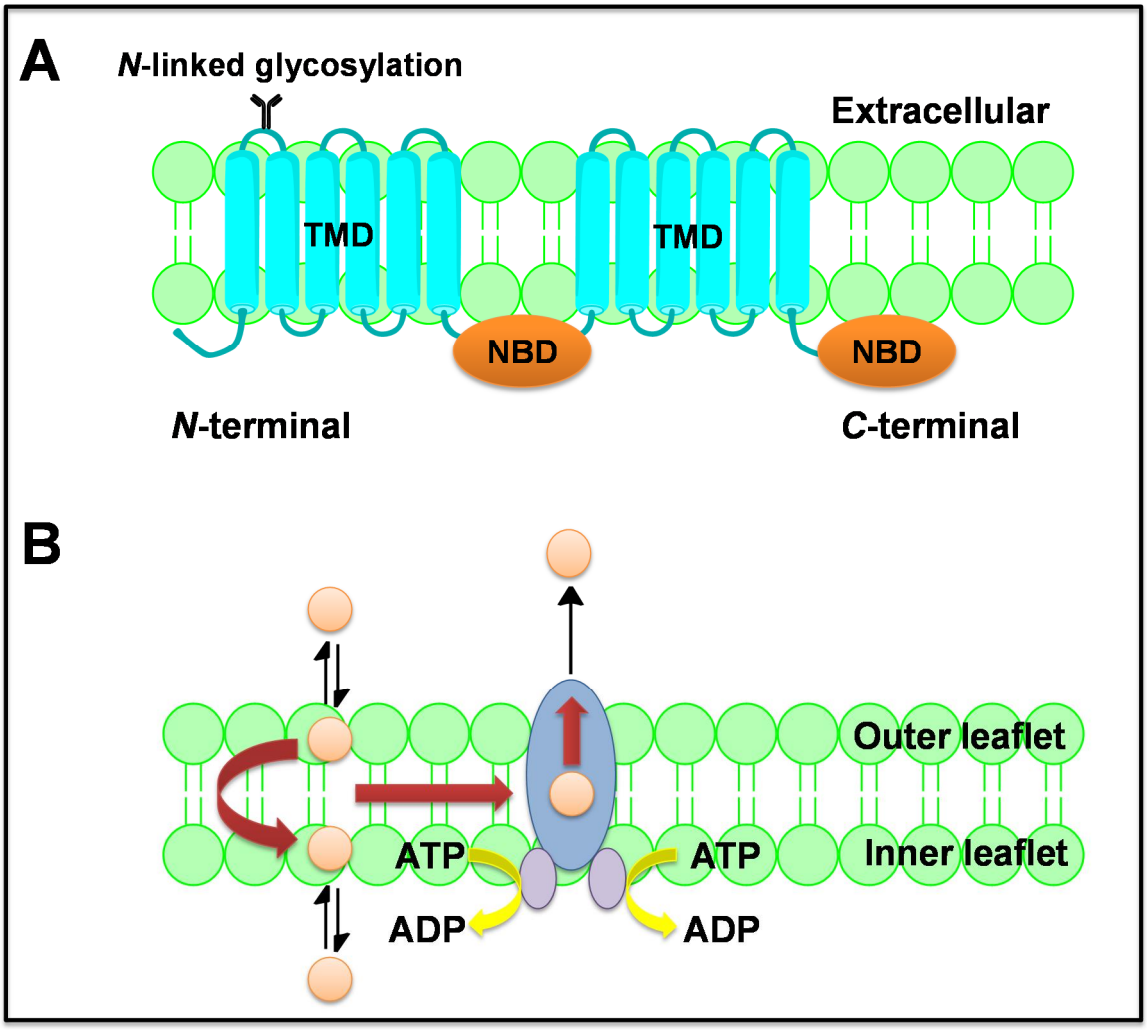

Figure 1.7 Membrane topology and transport model of Pgp

A Pgp consists of 2 halves with 6 N-terminal TMDs and 1 C-terminal NBD each, joined by a linker region. The N- and C-terminals as well as the NBDs are both intracellular. The 140 kDa polypeptide precursor that is N-glycosylated in the first extracellular linker region to become a 170 kDa transmembrane protein. **B** Substrates partition into the lipid bilayer where they interact with the transporterôs substrate binding sites. The hydrolysis of one molecule of ATP then generates the energy needed to cause a switch to an outward-facing conformation of the transporter, resulting in the release of the substrate into the extracellular space. Hydrolysis of another ATP molecule is then needed to ôre-setô the transporter so that it can bind substrates again.

Pgp has been found in the apical membrane of the large and small intestine, liver bile ductules and kidney proximal tubules, which all have excretory roles; as well as in the adrenal glands, the placenta and the apical membrane of endothelial cells lining the capillaries of the brain (Cordon-Cardo et al., 1990; Fojo et al., 1987; Thiebaut et al., 1987; Thiebaut et al., 1989; van der Valk et al., 1990).

Pgp protects against xenobiotic exposure in three main ways: **(1)** Pgp is expressed in the apical membrane of enterocytes in the gastrointestinal mucosa, where it pumps substrates in the basal to apical membrane direction into the lumen of the gastrointestinal tract, thus limiting drug absorption and oral bioavailability (Thiebaut et al., 1987); **(2)** if a xenobiotic reaches the blood circulation, Pgp is constitutively expressed in the canalicular membrane of hepatocytes and the luminal membrane of proximal tubule cells in the kidney, promoting xenobiotics excretion into bile and urine, respectively (Cordon-Cardo et al., 1990; Sugawara et al., 1988; Thiebaut et al., 1987); **(3)** finally, Pgp expression in the brain, testis and foetal circulation, limits the penetration of xenobiotics to sensitive tissues (Cordon-Cardo et al., 1990; Sugawara et al., 1988). In this way, Pgp limits absorption, actively eliminates and limits the tissue distribution of xenobiotics.

1.4.1.3 Pgp in Cancer and MDR

Generally, intrinsic Pgp expression is found in solid tumours originating from areas where Pgp is endogenously expressed, specifically, the kidney, liver, colon, pancreas and adrenal glands (Fojo et al., 1987; Goldstein et al., 1989; Kakehi et al., 1988; Kanamaru et al., 1989). Additionally, Pgp is found in leukaemia, non-Hodgkin's

lymphoma, neuroblastoma, sarcoma, and astrocytoma and non-small cell lung cancer (Bourhis et al., 1989a; Chan et al., 1997; Goldstein et al., 1989; Herweijer et al., 1990; Lai et al., 1989; Oka et al., 1997; Pirker et al., 1989; Pirker et al., 1991; Rothenberg et al., 1989; Sato et al., 1990a; Sato et al., 1990b). Pgp expression can also be selected for by exposure to chemotherapy, and has been found following treatment and relapse in breast cancer, ovarian cancer, lymphoma, leukaemia, neuroblastoma, pheochromocytoma, rhabdomyosarcoma and multiple myeloma (Bourhis et al., 1989b; Dalton et al., 1989; Gerlach et al., 1987; Izquierdo et al., 1995; Ro et al., 1990; Schneider et al., 1989).

While several of the ABC transporters have been associated with MDR in cancer, Pgp especially has been demonstrated to play a significant role in clinical drug resistance (Gillet and Gottesman, 2010; Gottesman, 2002; Gottesman et al., 2002; Sharom, 2011). Many lines of evidence highlight the importance of Pgp in MDR, including: **(1)** high levels of Pgp expression has been found in a wide variety of tumour types and cancer cell lines, and its expression is associated with MDR (Alvarez et al., 1995; Cordon-Cardo et al., 1990; Fojo et al., 1987; Szakacs et al., 2004); **(2)** increased Pgp expression is associated with acquired drug resistance following chemotherapy in patients or exposure of cells to Pgp substrates (Abolhoda et al., 1999; Bell et al., 1985; Bourhis et al., 1989b; Dalton et al., 1989; Gerlach et al., 1987; Goldstein et al., 1989; Ro et al., 1990; Schneider et al., 1989); **(3)** modulation of Pgp with inhibitors (Section 1.5.1) sensitises cells (de Bruin et al., 1999; Hyafil et al., 1993; Solary et al., 1991) and in some cases, patients (Advani et al., 1999; Greenberg et al., 2004; Sonneveld et al., 1996; Tidefelt et al., 2000), to anti-cancer agents that are Pgp substrates; **(4)** expression of Pgp in tumours is associated with

poor clinical outcomes such as treatment failure, decreased overall survival and an aggressive phenotype (Chan et al., 1991; Colone et al., 2008; Katoh et al., 2008; Miletti-Gonzalez et al., 2005; Oda et al., 2005; Ohtsuki et al., 2007; Weinstein et al., 1991).

Despite ample evidence for Pgp playing a significant role in MDR, attempts to target Pgp using inhibitors have been largely unsuccessful (Section 1.5.1). It has been suggested that this may be due to the high degree of functional redundancy within the ABC family (Holohan et al., 2013). Indeed, there is considerable substrate overlap between Pgp and MRP1 (Cole, 2014), which is also thought to play a role in MDR (Nooter et al., 1995; Triller et al., 2006; Zalcberg et al., 2000). It has also been estimated that as many as half of the 48 identified ABC transporters may be involved in drug resistance (Szakacs et al., 2004).

1.4.1.4 Pgp Substrates

Pgp can detect a wide variety of substrates, likely due to the presence of multiple binding sites that give it more flexibility than many other transport pumps (Table 1.1) (Aller et al., 2009). Pgp substrates range in size from small molecules like organic cations and amino acids, to large macromolecules such as polysaccharides and proteins (Gottesman and Pastan, 1993).

In general Pgp substrates are hydrophobic, and a ñrule of fourò has been developed to predict whether a compound will be a Pgp substrate (Didziapetris et al., 2003;

Ford and Hait, 1990). Briefly, if a compound has at least 8 nitrogen and oxygen atoms, a molecular weight of over 400 and is an acid with a pK_a of greater than 4, it is likely to be a Pgp substrate (Didziapetris et al., 2003). In addition to biological substrates such as steroid hormones, Pgp also transports a multitude of xenobiotics ranging from chemotherapeutics, HIV protease inhibitors, steroids, immunosuppressants, antibiotics, antihistamines, antiarrhythmics, *etc* (Table 1.1) (Fletcher et al., 2010; Gottesman et al., 2002; Kim, 2002).

Class	Compound
Chemotherapeutics	Colchicine, Doxorubicin, Daunorubicin, Etoposide, Paclitaxel, Vinblastine, Vincristine, Imatinib, Topotecan, Methotrexate
HIV Protease Inhibitors	Amprenavir, Indinavir, Nelfinavir, Saquinavir
Steroid hormones	Aldosterone, Estradiol-17B-d-glucuronide, Cortisol, Dexamethasone, Methylprednisolone
Immunosuppressants and their analogues	Cyclosporine, Valspodar, Sirolimus, Tacrolimus
Antibiotics	Tetracycline, Rifampicin, Doxycycline, Erythromycin
Anti-arrhythmics	Digoxin, Diltiazem, Nifedipine
Antihistamines	Cimetidine, Fexofenadine, Terfenadine
Natural substrates	Flavonoids, Curcuminoids, Colchicine, Actinomycin D
Fluorescent substrates	Rhodamine 123, Hoechst 33342, LysoTracker, Calcein AM

Table 1.1 Substrates of Pgp

1.4.2 The Bcl-2 Family and Regulation of Apoptosis

A hallmark of B cell follicular lymphoma was discovered to be chromosomal translocations in a previously unknown gene, *BCL2* (Tsujimoto et al., 1985). This gene encodes the Bcl-2 protein, which due to the chromosomal translocations was greatly over-expressed (Bakhshi et al., 1985); and led to the discovery of the Bcl-2 family. Bcl-2 is the founding member of the Bcl-2 family of proteins, which have shared sequence homology within conserved Bcl-2 homology (BH) domains (Cory and Adams, 2002; Danial, 2007). The Bcl-2 family proteins act as master regulators of the intrinsic pathway of apoptosis (Cory and Adams, 2002; Czabotar et al., 2014; Youle and Strasser, 2008).

The family members are grouped into three classes: **(1)** multi-domain anti-apoptotic which includes Bcl-2 (Tsujimoto et al., 1985); B cell lymphoma extra-large (Bcl-X_L) (Boise et al., 1993); Bcl-2-like protein 2 (Bcl-w) (Gibson et al., 1996); Bcl-2-like protein A1A (A1A) (Savitsky et al., 1995); myeloid cell leukaemia sequence 1 (Mcl1) (Kozopas et al., 1993); Bcl-2 like protein 10 (Bcl-B) (Kozopas et al., 1993) (Table 1.2) **(2)** multi-domain pro-apoptotic which includes BCL-2-associated X protein (Bax) (Oltvai et al., 1993); Bcl-2 antagonist/killer (Bak) (Chittenden et al., 1995; Kiefer et al., 1995); Bcl-2-related ovarian killer protein (Bok) (Hsu et al., 1997) (Table 1.2); and **(3)** Bcl-2 homology 3 (BH3)-only proteins that exert pro-apoptotic effects, including Bcl-2 antagonist of cell death (Bad) (Yang et al., 1995); Bcl-2-interacting killer (Bik) (Boyd et al., 1995); Bcl-2-interacting mediator of cell death (Bim) (O'Connor et al., 1998); BH3-interacting domain death agonist (Bid) (Wang et al., 1996); harakiri (Hrk) (Inohara et al., 1997); Bcl-2 modifying factor (BmF) (Puthalakath et al., 2001); Noxa

(Oda et al., 2000); p53 up-regulated modulator of apoptosis (Puma) (Nakano and Vousden, 2001) (Table 1.2).

The BH3-only proteins can be further divided into activators (Bim and Bid), which interact directly with Bax and Bak to activate them (Certo et al., 2006; Kuwana et al., 2005; Letai et al., 2002; Oh et al., 2006; Walensky et al., 2006); and sensitisers, which bind to anti-apoptotic family members and inhibit their function (Table 1.2) (Chen et al., 2005; Willis et al., 2005; Willis et al., 2007).

The balance between BH3-only and pro-apoptotic family members, and anti-apoptotic family members, regulates mitochondrial outer membrane permeabilisation, the critical õpoint of no returnò in apoptosis (Cheng et al., 2001; Chipuk et al., 2006; Huang and Strasser, 2000). When BH3-only proteins are induced by cytotoxic stresses, they promote apoptosis by neutralising anti-apoptotic Bcl-2 family members and releasing activated Bax and Bak (Fig. 1.8) (Czabotar et al., 2014; Merino et al., 2009; Youle and Strasser, 2008).

In the direct activation model, the binding of sensitisers to anti-apoptotic Bcl-2 family members results in the release of activator BH3-only proteins which can then directly activate Bax and Bak (Fig. 1.8) (Cory and Adams, 2002; Danial, 2007; Youle and Strasser, 2008). Sensitiser BH3-only proteins do not activate Bax and Bak directly, but lower the threshold for apoptosis by occupying anti-apoptotic members and releasing activators to trigger Bax and Bak oligomerisation (Fig. 1.8) (Cory and

Adams, 2002; Danial, 2007; Youle and Strasser, 2008). Alternatively, in the indirect activation model, binding of BH3 only proteins to anti-apoptotic family members triggers the release of activated Bax and Bak (Fig. 1.8) (Cory and Adams, 2002; Danial, 2007; Youle and Strasser, 2008).

Activated Bax and Bak can homo-oligomerise and permeabilise the mitochondrial outer membrane (Fig. 1.8) (Czabotar et al., 2014; Wei et al., 2001; Youle and Strasser, 2008). Proteins from within the mitochondrial intermembrane space then diffuse into the cytosol (Fig. 1.8). The best studied of these proteins is cytochrome *c* (Kluck et al., 1997), which binds to apoptotic protease-activating factor-1 (APAF1) and assembles into the apoptosome (Riedl and Salvesen, 2007; Zou et al., 1997). The apoptosome then induces the activation of caspase 9 (Li et al., 1997; Riedl and Salvesen, 2007), which in turn activates the effector caspases that orchestrate the death of the cell.

Multi-domain anti-apoptotic	**Multi-domain pro-apoptotic**	**BH3-only**	
		Activators	**Sensitisers**
Bcl-2	Bax	Bik	Bad
Bcl-X_L	Bak	Bim	Puma
Bcl-w	Bok		Bid
A1A			BmF
Mcl-1			Hrk
Bcl-B			Noxa

Table 1.2 The Bcl-2 family members

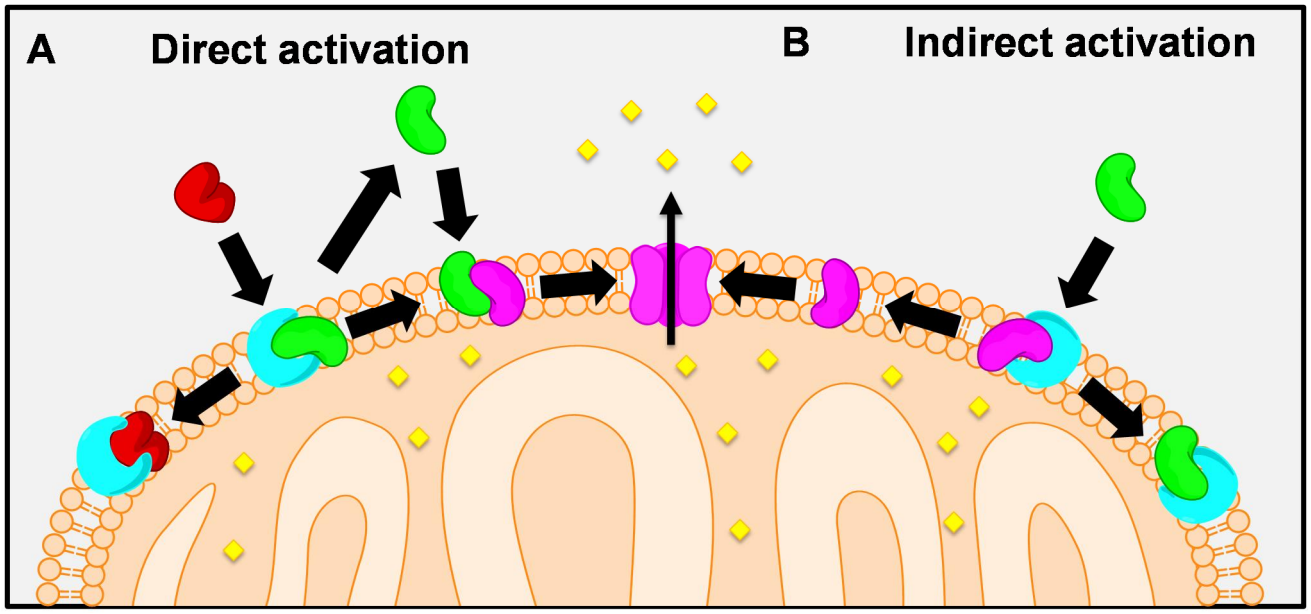

Figure 1.8 The Bcl-2 family members and the regulation of apoptosis

(A) In the direct activation model, the binding of sensitisers (red) to anti-apoptotic Bcl-2 family members (blue) results in the release of activator BH3-only proteins (green), which can then directly activate Bax and Bak (purple). **(B)** Alternatively, in the indirect activation model, binding of BH3 only proteins (green) to anti-apoptotic family members (blue) triggers the release of activated Bax and Bak (purple). In both cases, Bax and Bak can then homoligomerise and form a pore in the mitochondrial outer membrane, resulting in mitochondrial outer membrane permeabilisation. Proteins from inside the mitochondria, such as cytochrome *c* (yellow), can diffuse into the cytosol, triggering the intrinsic cascade of cell death effectors.

1.4.2.1 Bcl-2 Structure and Interactions with Bcl-2 Family Members

Bcl-2 has four BH domains that each consist of a helical bundle of hydrophobic helix-turn-helices, surrounding a hydrophobic core helix (Petros et al., 2001). This hydrophobic fold is formed by the BH1, BH2 and BH3 domains and is the interface for interactions with the amphipathic alpha helix of BH3 domains belonging to pro-apoptotic family members and BH3-only proteins (Lee et al., 2008; Liu et al., 2003; Petros et al., 2001; Sattler et al., 1997). These interactions mainly occur at the mitochondrial outer membrane, where Bcl-2 is anchored by a C-terminal hydrophobic transmembrane domain (Nguyen et al., 1993). However, Bcl-2 is also

found anchored to the endoplasmic reticulum and the nuclear envelope (Lithgow et al., 1994). Bcl-2 family can be post-translationally modified, predominantly *via* phosphorylation of Ser and Thr residues within the α1-α2 loop (Dai et al., 2013). For example, the phosphorylation of the Ser70 residue of Bcl-2 alters the conformation of the α1-α2 loop and increases its binding to Bak and Bim, making the cell resistant to chemotherapeutic agents (Dai et al., 2013).

Bcl-2 exerts its anti-apoptotic function by binding to the pro-apoptotic family members Bax and Bak, which prevents them from causing mitochondrial outer membrane permeabilisation (Certo et al., 2006). Bcl-2 can also be bound by the amphipathic BH3 helix (Lee et al., 2008; Liu et al., 2003; Petros et al., 2001; Sattler et al., 1997) of the BH3-only proteins Bid, Bim, Bad, Puma, Bmf and to a lesser extent, Bik (Chen et al., 2005). In this case, the binding of the BH3-only domain proteins neutralise the anti-apoptotic activity of Bcl-2. Bcl-2 will also bind to the autophagy inducer, Beclin 1, which contains a region that resembles a BH3 domain (Chang et al., 2010; Liang et al., 1998). This happens only at the endoplasmic reticulum and appears to inhibit autophagy (Chang et al., 2010; Pattingre et al., 2005). Phosphorylation of the α1-α2 loop prevents Bcl-2 from binding Beclin 1 and inhibiting autophagy (Wei et al., 2008).

1.4.2.2 Bcl-2 in Cancer and MDR

Dysregulated expression of the Bcl-2 family members has been demonstrated to be an underlying cause or contributor in many different types of cancer, as impaired apoptosis is a key aspect of tumour development (Thomas et al., 2013). Indeed, in

90% of B cell lymphoma the expression of Bcl-2 is greatly increased (Weiss et al., 1987) due to the chromosomal translocation t(14, 18) that places Bcl-2 next to the enhancer of the immunoglobulin heavy chain promoter (Cleary et al., 1986). Aside from haematopoietic cancers (Bincoletto et al., 1999; Hermine et al., 1996; Tothova et al., 2002), other, diverse types of cancer where Bcl-2 over-expression has been found include glioma (Weller et al., 1995) melanoma (Grover and Wilson, 1996), breast (Joensuu et al., 1994), prostate (McDonnell et al., 1992), small cell lung cancer (Jiang et al., 1995), colorectal cancer (Sinicrope et al., 1995) and bladder cancer (Gazzaniga et al., 1996). In many of these cancers, Bcl-2 has been linked to severity of malignancy, poor clinical response and poor prognosis (Bincoletto et al., 1999; Grover and Wilson, 1996; Hermine et al., 1996; Joensuu et al., 1994; McDonnell et al., 1992; Tothova et al., 2002).

BH3-only proteins are essential transducers of stress signals generated in response to many chemotherapeutics. Over-expression of anti-apoptotic family members such as Bcl-2, which bind to BH3 only proteins and prevent them from activating Bak/Bax, allows cancer cells to ignore apoptotic signals generated in response to chemotherapeutics which contributes to MDR (Amundson et al., 2000; Dole et al., 1994; Miyashita and Reed, 1993; Schmitt et al., 2000; Shibata et al., 1999; Strasser et al., 1993; Thomas et al., 1996; Vaux et al., 1988; Wang et al., 2013). In this manner, over-expression of Bcl-2 mediates resistance to a variety of structurally and mechanistically unrelated chemotherapeutics including dexamethasone (Skommer et al., 2006), doxorubicin (Skommer et al., 2006) 5-fluorouracil (Wu et al., 2015), etoposide (Wang et al., 2013), and cisplatin (Wang et al., 2013).

1.4.3 Lysosomes as More than 'Suicide Bags'

Lysosomes are degradative organelles which digest macromolecules and organelles so that their components may be recycled (Appelqvist et al., 2013). These components are delivered to lysosomes as a result of either endocytosis or autophagy (Appelqvist et al., 2013). Lysosomes consist of a lipid/protein bilayer (Saftig et al., 2010) and an acidic lumen that contains the digestive enzymes, acid hydrolases (Lübke et al., 2009). Since their discovery in the 1950ôs, our knowledge of the physiological roles of lysosomes has expanded beyond that of simple ósuicide bagsô a term coined by Christian de Duve, who won the Nobel Prize in Physiology in Medicine for their discovery (Appelmans et al., 1955; De Duve et al., 1955; De Duve, 1965). We now know that beyond their basic digestive role, lysosomes also play a role in processes such as plasma membrane repair (McNeil, 2002), exocytosis (Rodriguez et al., 1997), apoptosis (Turk et al., 2002) and regulation of metabolites such as cholesterol (Carstea et al., 1997).

1.4.3.1 Formation and Properties of Lysosomes

Lysosomes are formed through a dynamic process involving fusions of vesicles from the trans-Golgi network with endosomes (Huotari and Helenius, 2011; Saftig and Klumperman, 2009). The vesicles of the endolysosomal pathway are characterised as early endosomes that form *via* endocytosis (pH 6), which mature into late endosomes (pH 5) and finally lysosomes (pH < 5) (Dunn and Maxfield, 1992; Geuze et al., 1988; Stoorvogel et al., 1991).

The maturation process takes approximately 40 mins and involves exchange of membrane components, movement to the perinuclear area, formation of intraluminal vesicles, a decrease in luminal pH, acquisition of lysosomal components, and changes in morphology (Huotari and Helenius, 2011; Saftig and Klumperman, 2009). The maturation requires a series of exchanges with vesicles which contain acid hydrolases and membrane proteins like lysosomal membrane associated protein 1 (LAMP1) and LAMP2, trafficked from the trans-Golgi network (Huotari and Helenius, 2011; Saftig and Klumperman, 2009). Although it is difficult to distinguish between intermediates in the endolysosomal pathway, markers of early endosomes include early endosomal antigen 1 (EEA1) (Mu et al., 1995) and Rab5 (Rink et al., 2005), whereas endosomes have mannose-6-phosphate receptors; both of which are not found in lysosomes (Brown et al., 1986). Once lysosomes are formed, they are able to fuse with autophagosomes. In the autophagic pathway, a new double membrane called a phagophore is formed, which engulfs cytoplasmic contents and forms an autophagosome. The formation of the double membrane vesicle, the autophagosome, involves a complex interplay of proteins such as the class III phosphoinositide 3-kinaseÂBeclin 1 complex, ATG5·ATG12, and microtubule-associated protein 1 light chain 3 (LC3)-phosphatidylethanolamine conjugation system (Kondo et al., 2005). The fusion of autophagosomes with lysosomes results in the degradation of the cytoplasmic contents of the autophagosome (Kondo et al., 2005).

The purpose of this process is to recycle cellular components (Kondo et al., 2005). However, autophagy plays a more complex role in maintaining cellular homeostasis, as it can either protect the cell against stressors such as nutrient deprivation, or it

can promote apoptosis, depending on the stimulus received (Mukhopadhyay et al., 2014). Furthermore, autophagy has also been linked to tumour progression, drug resistance (Tsuchihara et al., 2009) and metastasis (Kenific et al., 2010).

Lysosomes have a pH of below 5, maintained by a membrane vacuolar H^+-ATPase (V-ATPase), which pumps protons into the lysosome against the concentration gradient (Mellman et al., 1986; Ohkuma et al., 1982; Schneider, 1981). The low pH is optimal for the functioning of the acid hydrolases, as it loosens the structures of macromolecules, making them easier to digest (Coffey and De Duve, 1968; Schneider, 1981). More than 60 acid hydrolases have been found in lysosomes, including proteases (Bohley and Seglen, 1992), phosphatases (Pohlmann et al., 1988), nucleases (Slor and Lev, 1971), sulphatases (Bond et al., 1997), lipases (Goldstein et al., 1975), and glycosidases (Appelmans et al., 1955). The cathepsin family of proteases has been widely studied (Bohley and Seglen, 1992). Within this family, the three subtypes are serine, cysteine and aspartic proteases, named according to which amino acid is found in their active site (Bohley and Seglen, 1992; Rossi et al., 2004; Turk et al., 2002). The hydrolases that are found in the highest concentrations are the cysteine proteases cathepsins B and L and the aspartic protease cathepsin D (Bohley and Seglen, 1992). The highly-glycosylated lysosomal membrane is thought to protect the lipid bilayer from degradation by acid hydrolases (Granger et al., 1990). More than 25 membrane proteins have been identified, of which 50% are LAMP 1 and LAMP2 (Saftig et al., 2010). LAMP1 and LAMP2 are important in maintaining lysosomal membrane integrity, and regulating lysosomal trafficking and fusion with autophagosomes (Saftig et al., 2010).

Lysosomes have relatively high concentrations of transition metals such as iron and copper ions, due to the degradation of proteins that contain transition metals in their active site (Gupte and Mumper, 2009; Kurz et al., 2006; Yu et al., 2003). Oxidative stressors can activate Fenton-type reactions, generating the HOĘ radical; the presence of high levels of iron and copper ions therefore make lysosomes sensitive to oxidative stress (Gupte and Mumper, 2009; Kurz et al., 2006; Terman and Kurz, 2013; Yu et al., 2003). Additionally, the redox capacity of Cu(II) is promoted by the acidic pH and milieu of lysosomes (Gupte and Mumper, 2009; Kurz et al., 2010; Terman and Kurz, 2013) The HOĘradical attacks the lipid bilayer of the lysosome causing lipid peroxidation that can ultimately result in permeabilisation of the lysosomal membrane (Gupte and Mumper, 2009; Kurz et al., 2006; Yu et al., 2003).

1.4.3.2 Lysosomes in Cancer and MDR

Lysosomes in cancer cells differ dramatically from those in normal cells in terms of their volume, cellular distribution and enzyme activity (Kallunki et al., 2013). These changes have been linked to increased tumourigenic potential, progression and metastasis (Kallunki et al., 2013; Yu et al., 2016). Lysosomes are not only linked to cancer as drivers of malignant transformation and progression; they are also involved in MDR due to drug sequestration (Appelqvist et al., 2013; Piao and Amaravadi, 2015; Zhitomirsky and Assaraf, 2016).

Several cathepsins, namely cathepsins B, S, E and L, are negative prognostic indicators in cancer (Gocheva et al., 2006; Keliher et al., 2013; Kos and Lah, 1998; Small et al., 2013). Cathepsin B, for example, is associated with increased

progression, invasion and metastasis in *in vitro*, *in vivo* and clinical studies (Bengsch et al., 2014; Chen et al., 2011; Gocheva et al., 2006; Premzl et al., 2003; Withana et al., 2012). It is thought that the increased expression of lysosomal cathepsins in cancer may result in their increased excretion into the extracellular space, which in turn promotes invasion and metastasis due to their digestion of basement membranes (Gocheva et al., 2006; Recklies et al., 1982; Sloane et al., 1981). Other lysosomal changes that have been associated with cancer include increased LAMP-1 expression on the surface of highly metastatic cells (Furuta et al., 2001); and alterations to the tumour microenvironment by V-ATPase, which promotes invasion (Fais et al., 2007)

Lysosomes act as mediators of MDR primarily by sequestering chemotherapeutics (Fig. 1.9). Hydrophobic weak bases, such as sunitinib (Gotink et al., 2011), doxorubicin (Herlevsen et al., 2007), daunorubicin (Gong et al., 2006) and vincristine (Groth-Pedersen et al., 2007), are able to easily diffuse through both the plasma membrane of the cell and the lysosomal membrane (Zhitomirsky and Assaraf, 2015a). Once inside lysosomes, these drugs become protonated due to the low pH and their ionised forms are ótrappedô inside lysosomes, unable to diffuse out (Fig. 1.9) (Mahoney et al., 2003). The sequestered chemotherapeutics are unable to access their targets, so are rendered ineffective (Fig. 1.9) (Zhitomirsky and Assaraf, 2015a). Indeed, increased lysosomal trapping of chemotherapeutics has been observed in MDR cell lines (Gong et al., 2003; Hurwitz et al., 1997; Schindler et al., 1996). Interestingly, the pH of lysosomes in MDR cells has been shown to be more acidic than in lysosomes of drug-sensitive cells, which facilitates enhanced drug sequestration in MDR cell lines (Altan et al., 1998; Gong et al., 2003; Kramer et al.,

1998). In addition to diffusion, there is also evidence of active transport of chemotherapeutics into the lysosome by ABC transporters such as Pgp, MRP1 and ABCA3 (Chapuy et al., 2008; Jansson et al., 2015b; Rajagopal and Simon, 2003b; Seebacher et al., 2016a; Yamagishi et al., 2013).

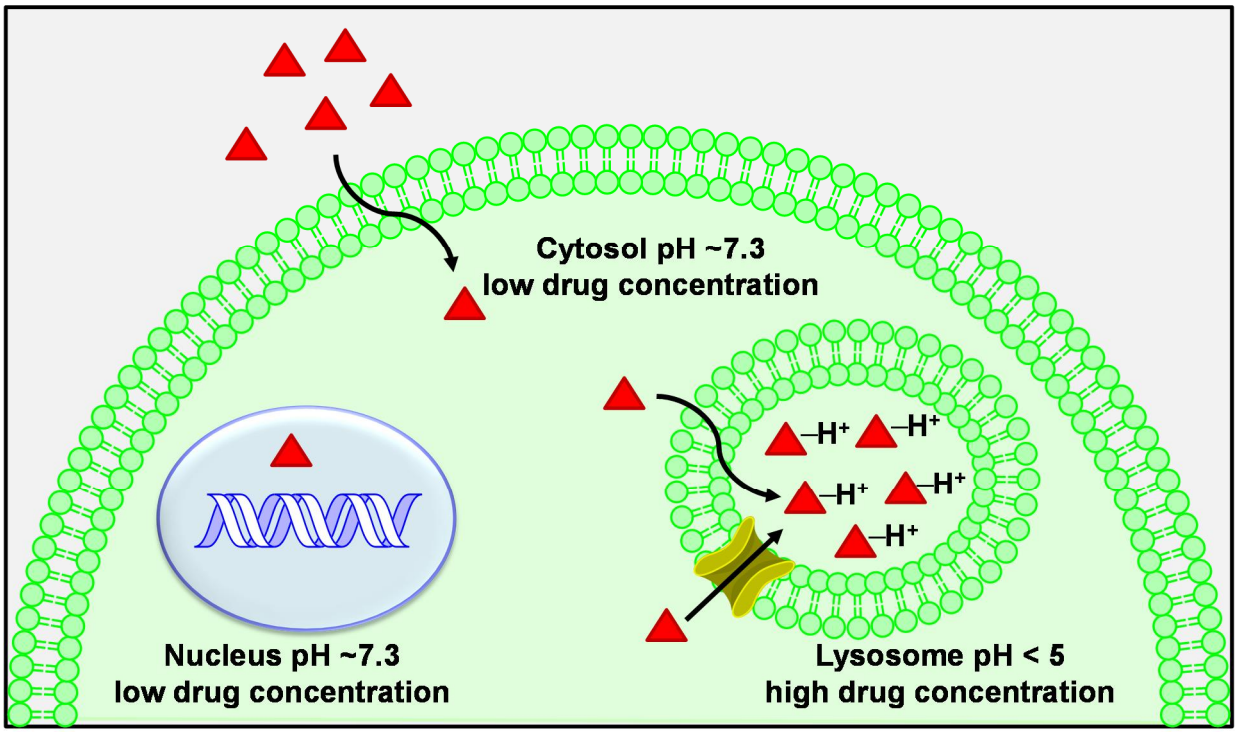

Figure 1.9 Lysosomal drug sequestration

Hydrophobic weak bases (red triangle) diffuse through the plasma membrane and the lysosomal membrane. ABC transporters in the lysosomal membrane can also actively transport drugs into lysosomes. Once inside lysosomes, the hydrophobic weak bases are protonated by the low pH of the lysosomal lumen. The hydrophobic weak bases are unable to diffuse back out of lysosomes and access their targets, such as DNA in the nucleus.

1.5 Targeting MDR

Targeting MDR is clinically important as it is a major factor that contributes to treatment failure (Gillet and Gottesman, 2010). Resistance can develop by numerous mechanisms including increased drug efflux (Pgp), evasion of drug-induced apoptosis (Bcl-2), and activation of detoxifying systems (lysosomal drug sequestration) (Gillet and Gottesman, 2010). Specific targeting of each of these mechanisms in order to overcome MDR has been thoroughly investigated, with varying degrees of success.

1.5.1 Targeting Pgp-Mediated MDR

As Pgp mediates the resistance to many common anti-cancer drugs, the majority of efforts to target Pgp have focused on Pgp inhibitors (Gottesman et al., 2002). Initial trials using 1st generation inhibitors failed as the inhibitors used, such as verapamil and cyclosporine A, were only weak inhibitors of Pgp and toxic at high doses (Benson et al., 1985; Damiani et al., 1998; Lum et al., 1992; Miller et al., 1991). Novel 2nd generation inhibitors with greater Pgp specificity were then developed aiming to overcome these obstacles (Table 1.3). For example, valspodar (PSC-833) has 10- to 20-fold greater specificity for Pgp than cyclosporine A, although it also inhibits ABCG2 and MRP1 (Jachez et al., 1993; Keller et al., 1992). However, valspodar and other 2nd generation inhibitors also failed to demonstrate clinical efficacy in several clinical trials involving cancers such as acute myeloid leukaemia and ovarian cancer (Table 1.3) (Baer et al., 2002; Fracasso et al., 2001; van der Holt et al., 2005).

These issues led researchers to design 3rd generation inhibitors with increased specificity and potency towards Pgp (Table 1.3). Elacridar (Ela, GF120918) was the first of the 3rd generation inhibitors to be developed (Hyafil et al., 1993) and has shown minimal toxicity in phase I clinical trials (Elgie et al., 1999; Kuppens et al., 2007). Although Ela inhibits Pgp potently, it also inhibits ABCG2 (de Bruin et al., 1999; Maliepaard et al., 2001). Tariquidar (XR9051), another 3rd generation inhibitor, exhibited many favourable characteristics in pre-clinical studies (Dale et al., 1998; Martin et al., 1999). Being 10- to 30-fold more potent than valspodar, tariquidar was able to increase sensitivity of Pgp-expressing cells to Pgp substrates such as doxorubicin and paclitaxel at concentrations as low as 25 to 80 nM (Table 1.3) (Dale et al., 1998; Martin et al., 1999; Mistry et al., 2001). While tariquidar demonstrated the ability to increase the efficacy of doxorubicin or taxane chemotherapy, toxicity was a serious issue and resulted in the abandonment of phase III clinical trials (Fox and Bates, 2007; Pusztai et al., 2005). However, the National Cancer Institute is still conducting further phase I/II trials of tariquidar, with results pending (Fox and Bates, 2007). Although pre-clinical data was promising, other 3rd generation inhibitors such as zosuquidar (LY335979) and ONT-093 failed to produce significant results in clinical trials (Cripe et al., 2006; Kuppens et al., 2005; Rubin et al., 2002; Sandler et al., 2004). Despite the apparent lack of clinical efficacy to date, research into the area of Pgp inhibitors remains ongoing and it is hoped that by selecting for specific clinical scenarios, these agents may yet demonstrate clinical efficacy.

Name	Alias	Specificity	Generation
Valspodar	PSC-833	Pgp	2nd
Biricodar	VX-710	Pgp, ABCG2, MRP1	2nd
Tariquidar	XR-9576	Pgp and ABCG2	3rd
Zosuquidar	LY335979	Pgp, ABCG2, MRP1	3rd
Laniquidar	R101933	Pgp	3rd
Elacridar	GF120918	Pgp and ABCG2	3rd
ONT-93		Pgp	3rd

Table 1.3 Inhibitors of Pgp

1.5.2 Targeting Bcl-2-Mediated MDR

Impaired apoptosis is a key aspect of tumour development and also contributes to MDR (Thomas et al., 2013). Indeed, Bcl-2 mediates resistance to structurally and mechanistically unrelated chemotherapeutics (Skommer et al., 2006; Wang et al., 2013; Wu et al., 2015). Targeting Bcl-2 is an important approach in overcoming MDR, and has taken three main directions: **(1)** antisense oligonucleotides and antibody targeting; **(2)** BH3-only peptidomimetics; and **(3)** small molecule inhibitors (Lessene et al., 2008; Thomas et al., 2013). The two approaches that have been explored and are pertinent to Bcl-2 are antisense antisense oligonucleotides and antibodies, and small molecule inhibitors (Table 1.4).

Antisense oligonucleotides function by binding to target mRNA and forming a DNA heteroduplex which is susceptible to degradation by RNAse H (Olie and

Zangemeister-Wittke, 2001). This reduces the levels of the target mRNA and thus the expression of the target protein (Olie and Zangemeister-Wittke, 2001). Oblimersen (G-3139), an 18-mer oligonucleotide complimentary to the *BCL2* gene, was one of the first antisense oligonucleotides trialled (Olie and Zangemeister-Wittke, 2001). Oblimersen did not obtain Food and Drug Administration approval as it failed to show survival advantage in melanoma, multiple myeloma and chronic myelocitic leukaemia (O'Brien et al., 2009). However, in a Phase II combination study with dacarbazine, oblimersen demonstrated improved survival and progression-free survival in melanoma patients (Bedikian et al., 2006).

Unfortunately, the clinical use of antisense oligonucleotides will always be limited due to their susceptibility to DNAse-mediated degradation and non-specific targeting (Dai et al., 2005). Similarly, although antibodies have been produced that inhibit Bcl-2 expression and one has been show to increase cytotoxicity in response to chemotherapies in cancer; their instability *in vivo* limits its practical use as a therapy (Piche et al., 1998).

A more promising approach has been the development of small molecule Bcl-2 inhibitors, which are defined as organic molecules with molecular weights less than 750 Da (Thomas et al., 2013). The principle mechanism of small molecule inhibitors is to mimic the action of BH3-only proteins by binding to the hydrophobic fold in Bcl-2 and other anti-apoptotic Bcl-2 family members (Lessene et al., 2008; Thomas et al., 2013). In doing so, the small molecule inhibitors antagonise the anti-apoptotic activity of Bcl-2 by preventing its heterodimerisation with the pro-apoptotic family members,

Bax and Bak (Thomas et al., 2013). Gossypol (BL-193) is a natural polyphenol (Wu, 1989) that binds to the hydrophobic fold of Bcl-2 and Bcl-X_L and was the first small molecule inhibitor investigated (Table 1.4) (Kitada et al., 2003). The demonstrated anti-proliferative effects of Gossypol in cancer cells (Gilbert et al., 1995; Le Blanc et al., 2002; Wu et al., 1989) has led to it entering clinical trials (Stein et al., 1992; Van Poznak et al., 2001), however toxicity issues (Stein et al., 1992) spurned the further development of second and third generation derivatives such as TW37 (Table 1.4) (Mohammad et al., 2007; Verhaegen et al., 2006; Wang et al., 2006) and Apogossypolone (ApoG2) (Becattini et al., 2004; Hu et al., 2009; Sun et al., 2009), respectively. Both TW37 and ApoG2 have the advantage of inhibiting not only Bcl-2 and Bcl-X_L, but also Mcl-1 (Mohammad et al., 2007; Verhaegen et al., 2006; Wang et al., 2006). To date, TW37 and ApoG2 have been shown to induce apoptosis in cancer (Hu et al., 2009; Mohammad et al., 2007; Sun et al., 2009; Verhaegen et al., 2006; Wang et al., 2006).

Abbott Laboratories has also developed a series of small molecule inhibitors (MW less than 750 Da), starting with ABT-737 (Table 1.4) (Oltersdorf et al., 2005). ABT-737 binds to Bcl-2, Bcl-X_L and Bcl-W by mimicking the BH3 domain of Bad. The primary target of ABT-737 is Bcl-2-Bim dimers, which it disrupts more effectively than Bcl-X_L-Bim and Bcl-W-Bim dimers (Merino et al., 2012; van Delft et al., 2006). Bim released by the binding of ABT-737 to Bcl-2 can directly activate Bax and Bak, leading to apoptosis (Merino et al., 2012; van Delft et al., 2006). The orally-available derivative of ABT-737, ABT-263 (Navitoclax), has demonstrated efficacy as both a single agent an in combination studies in clinical trials (Table 1.4) (Tse et al., 2008). However, the ability of ABT-263 to bind Bcl-X_L, has resulted in dose-limiting toxicity

issues, as Bcl-X_L controls platelet lifespan (Mason et al., 2007; Zhang et al., 2007). A more recently developed analogue, ABT-199 that is selective for Bcl-2, seems to have overcome this issue (Souers et al., 2013). More recently, Bcl-2 inhibitors have been developed that also bind to Mcl-1, such as Obatoclax (Konopleva et al., 2008), HA14-1 (Manero et al., 2006), Sabutoclax (Dash et al., 2011) and BI-97D6 (Table 1.4) (Wei et al., 2011).

Name	Alias	Specificity	Class/Generation
Oblimersen	G-3139		Antisense oligonucleotide
Gossypol	BL-193	Bcl-2, Bcl-X_L	Small molecule inhibitor
TW37		Bcl-2, Bcl-X_L, Mcl-1	Small molecule inhibitor/ 2nd generation Gossypol derivative
ApoG2		Bcl-2, Bcl-X_L, Mcl-1	Small molecule inhibitor/ 3rd generation Gossypol derivative
ABT-737	Navitoclax	Bcl-2, Bcl-X_L, Bcl-W	Small molecule inhibitor
ABT-263		Bcl-2, Bcl-X_L, Bcl-W	Small molecule inhibitor, 2nd generation
ABT-199		Bcl-2>>>>	
AT-101		Bcl-2, Bcl-X_L, Mcl-1	Small molecule inhibitor
Obatoclax	GX015-070	Bcl-2, Bcl-X_L, Bcl-W, Mcl-1	Small molecule inhibitor
HA14-1		Bcl-2, Bcl-X_L	
Sabutoclax	BI-97C1	Bcl-2, Bcl-X_L, Mcl-1 Bfl-1	Small molecule inhibitor/ 3rd generation Gossypol derivative
BI-97D6		Bcl-2, Bcl-X_L, Mcl-1 Bfl-1	

Table 1.4 Bcl-2 inhibitors

1.5.3 Targeting Lysosomes in MDR

Overcoming lysosomal drug sequestration has been an important objective for successful treatment of MDR cancer. Several approaches have been taken to overcome lysosomal drug sequestration including altering the structure of drugs to decrease their pKa (Duvvuri et al., 2005), increasing lysosomal pH using V-ATPase inhibitors and inducing apoptosis using lysosomotropic agents (Zhitomirsky and Assaraf, 2016).

Modifying the structures of existing drugs to improve efficacy against specific targets has long been a validated method of drug discovery. Doxorubicin and daunorubicin are examples of weakly basic chemotherapeutics, which are sequestered in lysosomes as the low pH inside the lysosome favours their protonation (Duvvuri et al., 2005; Egorin et al., 1980). Once protonated they become trapped, unable to diffuse back through the lipid bilayer to reach their nuclear target (Duvvuri et al., 2005; Rutherford and Willingham, 1993). It has been shown that altering the structure of daunorubicin to decrease its pKa and thus decrease its lysosomal sequestration, significantly increases the efficacy of daunorubicin against MDR cancer cells (Duvvuri et al., 2005). Interestingly, it has also been demonstrated that the presence of Pgp in the lysosomal membrane can also enhance lysosomal sequestration of doxorubicin and other anti-cancer agents (Seebacher et al., 2016a; Seebacher et al., 2015; Yamagishi et al., 2013).

Increasing lysosomal pH can decrease sequestration of hydrophobic weak bases. There are several well-known inhibitors of V-ATPase which are generally of microbial

origin, such as baflomycin A1, and concanamycin A (Fais et al., 2007). Such inhibitors have been shown to increase sensitivity to doxorubicin, daunorubicin and epirubicin as the alkalisation of the lysosome results in their release from the lysosome and redistribution to the cytosol and nucleus (Altan et al., 1998; Ouar et al., 2003; Schindler et al., 1996; Zhitomirsky and Assaraf, 2015b). However, these agents generally have multiple other targets and effects within the cell, which makes them somewhat unsuitable for this purpose (Zhitomirsky and Assaraf, 2015a)

Lysosomotropic agents such as chloroquine have been shown to reduce lysosomal drug sequestration and increase MDR cancer cell sensitivity to chemotherapeutics (Yamagishi et al., 2013). Disrupting the lysosomal membrane can cause apoptosis or necrosis, as the acidic and degradative contents of the lysosomal lumen spill out into the cytosol of the cell (Erdal et al., 2005; Repnik et al., 2014). Unfortunately, lysosomotropic agents can also trigger lysosomal biogenesis, which ultimately only serves to increase drug sequestration (Zhitomirsky and Assaraf, 2015a). However, it has been shown that Dp44mT can selectively and potently target the lysosomes in MDR cells and induce cell death by rupturing the lysosomal membrane (Section 1.6) (Jansson et al., 2015b). Additional methods of inducing cell death using lysosomotropic mechanisms include loading lysosomes with photosensitisers which when activated cause cell death by disrupting the stability of the lysosomal membrane (Adar et al., 2012; Nowak-Sliwinska et al., 2015).

1.6 Selective activity of Dp44mT against MDR

Dp44mT possesses a number of characteristics that enable it to target lysosomes. For many weakly basic drugs, including chemotherapeutics, lysosomal sequestration decreases their efficacy by preventing them from reaching their intended targets (Gong et al., 2003; Hurwitz et al., 1997; Schindler et al., 1996). Similarly, Dp44mT sequestered in lysosomes as it is polyprotic and is protonated at the lower pH of lysosomal lumens (Lovejoy et al., 2011). However, as part of the mechanism of action of Dp44mT, it forms redox-active Fe(III) and Cu(II) complexes (Jansson et al., 2010a; Jansson et al., 2010b; Kalinowski et al., 2007; Lovejoy et al., 2011; Richardson et al., 2006; Richardson et al., 2009; Yuan et al., 2004).

The redox activity of these complexes of Dp44mT produces $HO^{\bullet}$ radicals that damage lysosomal membranes through lipid peroxidation (Gutierrez et al., 2014; Jansson et al., 2010b; Lovejoy et al., 2011). The permeabilisation of lysosomal membranes by the redox-active Dp44mT complexes results in apoptosis due to the release of degradative lysosomal cathepsins into the cytosol (Gutierrez et al., 2014; Jansson et al., 2015a; Lovejoy et al., 2011; Repnik et al., 2014; Roberg et al., 1999; Turk et al., 2002; Turk and Turk, 2009).

Interestingly, Dp44mT and its Cu(II) complex are potently more cytotoxic in drug resistant cells expressing Pgp, relative to their non-Pgp expressing counterparts (Jansson et al., 2015b; Whitnall et al., 2006). Pgp, expressed in lysosomal membranes, actively transports Dp44mT into lysosomes, where it is protonated by

the acidic environment and trapped (Jansson et al., 2015b; Lovejoy et al., 2011). In this manner, Dp44mT is able to ñhijackò mechanisms that the cell normally uses to evade cell death, namely: ABC transporter drug efflux and lysosomal drug sequestration. Furthermore, Dp44mT targets the pro-survival autophagy pathway (Gutierrez et al., 2014), which also regulates tumour progression, drug resistance (Tsuchihara et al., 2009) and metastasis (Kenific et al., 2010). Although Dp44mT induces the autophagic-initiation pathway, Dp44mT also induced permeabilisation of the lysosomal membrane (Gutierrez et al., 2014). This led to cell death by a combination of preventing the cancer cells from completing the autophagic process and leaking of degradative lysosomal enzymes into the cytosol (Gutierrez et al., 2014).

The ability of Dp44mT to selectively target MDR cells and overcome MDR is an exciting therapeutic prospect. While key components of the mechanism by which Dp44mT selectively targets MDR are established (Jansson et al., 2015b), it has also been demonstrated that Dp44mT is an inappropriate drug candidate due to undesirable side effects *in vivo* such as methaemoglobinaemia (Quach et al., 2012) and cardiotoxicity (Whitnall et al., 2006). It would therefore be of interest to establish whether other thiosemicarbazones are capable of similarly targeting MDR cells, as Dp44mT does (Jansson et al., 2015b; Whitnall et al., 2006). Furthermore, many other mechanisms of drug resistance exist in addition to ABC transporter drug efflux and lysosomal drug sequestration, such as evasion of apoptosis mediated by Bcl-2 family members.

1.7 Aims of the Thesis

1. Assess the structure-activity relationships and mechanisms that enable thiosemicarbazones and their Cu(II) complexes to overcome Pgp mediate MDR

2. Examine the effects of zinc binding on thiosemicarbazone cytotoxicity and intracellular localisation. Elucidate mechanisms of action where relevant.

3. Explore the efficacy of thiosemicarbazones (Dp44mT and DpC) against Bcl-2-mediated MDR in melanoma. Examine mechanisms of action where applicable.

Chapter 2 - Materials and Methods

2.1 Reagents

General Reagents	Source
2',7'-dichlorodihydrofluorescein (H_2DCF-DA)	Sigma-Aldrich (St. Louis, MO, USA)
3-(4,5-Dimethylthiazol-2-yl)-2,5-diphenyltetrazolium bromide (MTT)	Sigma-Aldrich (St. Louis, MO, USA)
Ammonium tetrathiomolybdate (TM)	Sigma-Aldrich (St. Louis, MO, USA)
Dimethyl sulphoxide (DMSO)	Sigma-Aldrich (St. Louis, MO, USA)
Elacridar (Ela)	Sigma-Aldrich (St. Louis, MO, USA)
N-acetylcysteine (NAC)	Sigma-Aldrich (St. Louis, MO, USA)
Phosphate buffered saline (PBS)	Sigma-Aldrich (St. Louis, MO, USA)

Cell Culture Reagents	Source
DMEM	Gibco® (Life Technologies Australia Pty Ltd, Mulgrave, VIC, Australia)
Foetal bovine serum	Sigma-Aldrich (St. Louis, MO, USA)
Fungizone	Gibco® (Life Technologies Australia Pty Ltd, Mulgrave, VIC, Australia)
Non-essential amino acids	Gibco® (Life Technologies Australia Pty Ltd, Mulgrave, VIC, Australia)
Penicillin, streptomycin, L-glutamine	Gibco® (Life Technologies Australia Pty Ltd, Mulgrave, VIC, Australia)
Vinblastine	Sigma-Aldrich (St. Louis, MO, USA)

Synthetic Reagents	Source
2-benzoylpyridine	Sigma-Aldrich (St. Louis, MO, USA)
2-methyl-3-thiosemicarbazide	Sigma-Aldrich (St. Louis, MO, USA)
3-AP	Synthesised as previously reported (Liu et al., 1992)
4,4-dimethyl-3-thiosemicarbazide	Alfa Aesar (Ward Hill, MA, USA)
Ap44mT	Synthesised as previously reported (Richardson et al., 2009)
Dp44mT	Synthesised as previously reported (Richardson et al., 2006)}
DpC	Synthesised as previously reported (Lovejoy et al., 2012)
Bp44mT	Synthesised as previously reported (Kalinowski et al., 2007)
$CuCl_2.2H_2O$	Sigma-Aldrich (St. Louis, MO, USA)
$Cu(ClO_4)_2.6H_2O$	Sigma-Aldrich (St. Louis, MO, USA)
Di-2-pyridyl ketone	Sigma-Aldrich (St. Louis, MO, USA)
Diethyl ether	Sigma-Aldrich (St. Louis, MO, USA)
Ethanol	Sigma-Aldrich (St. Louis, MO, USA)
Triethylamine	Sigma-Aldrich (St. Louis, MO, USA)
$ZnCl_2$	Sigma-Aldrich (St. Louis, MO, USA)
$ZnClO_4$	Sigma-Aldrich (St. Louis, MO, USA)

Fluorescent Reagents	Source
Acridine Orange (AO)	Sigma-Aldrich (St. Louis, MO, USA)
Deep Red, DRAQ5Ê	ThermoFisher Scientific Australia Pty Ltd (Scoresby, VIC, Australia)
FITC conjugated secondary antibody	Life Technologies Australia Pty Ltd (Mulgrave, VIC, Australia)
LysoTracker® Deep Red	ThermoFisher Scientific Australia Pty Ltd (Scoresby, VIC, Australia)
MitoTracker® Deep Red	ThermoFisher Scientific Australia Pty Ltd (Scoresby, VIC, Australia)
ProLong® Gold Antifade Mountant with DAPI	ThermoFisher Scientific Australia Pty Ltd (Scoresby, VIC, Australia)
TexasRed conjugated secondary antibody	Cell Signaling (Danvers, MA, USA)

Antibodies	Source
ɓ actin	Sigma-Aldrich (St. Louis, MO, USA)
Bcl-2	Cell Signaling Technology
LC3	Sigma-Aldrich (St. Louis, MO, USA)

2.2 Synthesis of Novel Thiosemicarbazones and Complexes

2.2.1 Bp2mT

To a solution of 2-methyl-3-thiosemicarbazide (1.05 g, 10 mmol) in ethanol (25 mL), 2-benzoylpyridine (1.83 g, 10 mmol) and glacial acetic acid (10 drops) were added and refluxed for 1 h. The precipitated thiosemicarbazide was filtered and discarded. The ligand, Bp2mT, was isolated as light brown crystals from the slow evaporation of mother liquor. Yield: 60%. ^{1}H NMR (DMSO-d_6) ŭ ppm 8.53, 8.77 (1H, d, C*H, E*/*Z* isomers), 8.18 (1H, d, C*H*), 7.91, 8.00 (1H, t, C*H*), 7.71 (2H, bs, NH_2), 7.41-7.53 (5H, m, Ph), 7.27 (1H, m, C*H*), 2.99, 3.02 (3H, s, CH_3). ^{13}C NMR (DMSO-d_6) ŭ ppm 181.5, 181.4, 162.6, 161.9, 155.4, 154.4, 150.3, 149.1, 137.7, 137.1, 136.7, 135.4, 131.2, 129.8, 129.3, 129.0, 128.8, 128.7, 125.3, 124.9, 124.8, 123.8, 41.6, 41.3. ESI-MS in MeOH: found mass: 293.00, Calcd. mass for $C_{14}H_{14}N_4SNa$: 293.08 $[M+Na^+]^+$. Anal. Calcd. for $C_{14}H_{14}N_4S$ (%): C, 62.20; H, 5.22; N, 20.72; S, 11.80. Found (%): C, 62.02; H, 5.22; N, 20.74; S, 11.78.

2.2.2 Cu(II) Complexes Synthesis

The 1:2 Cu(II) complexes with Bp44mT, DpC and 3-AP were prepared using a reported procedure with slight modifications, as described below (Jansson et al., 2010a). To a hot solution of Bp44mT, 3-AP or DpC·HCl (0.5 mmol) in ethanol (5 mL), triethylamine (56 mg, 0.55 mmol for 3-AP or Bp44mT; 112 mg, 1.1 mmol for DpC·HCl) followed by $Cu(ClO_4)_2.6H_2O$ (93 mg, 0.25 mmol) were added and refluxed for 60 min. After cooling to room temperature, the solution was poured into diethyl ether (20 mL). The precipitate formed was collected by vacuum filtration, washed with copious amounts of diethyl ether and dried *in vacuo*.

2.2.2.1 [Cu(Bp44mT)(Bp44mT-H)](ClO4)

Dark brown solid. 90 mg, yield: 57%. The single crystals suitable for X-ray diffraction were obtained from the slow diffusion of diethyl ether into a methanol solution. Mass data (ESI+, CH_3CN): m/z: Calcd. for $CuC_{30}H_{31}N_8S_2$: 630.15 $[M\bar{\imath}\ ClO_4]^+$; found: 630.13. Anal. Calcd. (%) for $CuC_{30}H_{31}N_8S_2ClO_4\cdot(H_2O)_4(C_2H_5OH)$: C 45.28, H 5.34, N 13.20, S 7.55. Found: C 45.47, H 5.22, N 12.94, S 7.44. IR, cm-1: 3510 (br, O-H), 1550 (m, C=N), 1393 (s), 1320 (s), 1253 (s), 1091 (vs, ClO4), 913 (m), 789 (s, C$\bar{\imath}$ S), 700 (s), 624 (s) (br, broad; vs, very strong; s, strong; m, medium; w, weak). UV$\bar{\imath}$ visible in DMSO [ə max, nm (Ů Mī 1 cmī 1)]: 425 (18 500), 351 (19 500), 310 (27 700).

2.2.2.2 [Cu(3-AP)(3-AP-H)](ClO4)

Brown solid. Yield: 75%. Mass data (ESI+, CH_3CN): m/z: Calcd. for $CuC_{14}H_{16}N_{10}S_2$, 452.05 $[M\bar{\imath}\ ClO_4]^+$; found: 551.97 (100%). Anal. Calcd. (%) for

$CuC_{14}H_{17}N_{10}S_2ClO_4\cdot(H_2O)_1(C_2H_5OH)_{0.5}$: C 30.35, H 3.74, N 23.60, S 10.81. Found: C 30.11, H 3.56, N 23.24, S 11.27. IR, cm^{-1}: 3428 (m, N-H), 3358 (m, NH), 3176, 2151 (w), 1632 (m), 1597 (m, C=N), 1469 (s), 1442 (s), 1323 (m), 1250 (m), 1097 (vs, ClO_4), 900 (m), 848 (m), 801 (m, Cī S), 704 (w), 626 (vs). UVī visible in DMSO [ə$_{max}$, nm (Ů M$^{ī\ 1}$ cm$^{ī\ 1}$)]: 444 (25 200), 458(sh) (24 200), 385 (20 800), 295 (45 500).

2.2.2.3 [Cu(DpC)(DpC-H)]ClO_4

Dark brown solid. Yield: 41%. Mass data (ESI+, CH_3CN): m/z: Calcd. for $CuC_{38}H_{45}N_{10}S_2$, 768.27 $[M+H^+]^+$; found: 768.22 (100%). Anal. Calcd. (%) for $CuC_{38}H_{45}N_{10}S_2ClO_4\cdot(H_2O)_2(C_2H_5OH)_1$: C 50.52, H 5.83, N 14.73, S 6.74. Found: C 50.45, H 5.67, N 14.63, S 6.19. IR, cm^{-1}: 3428 (br, O-H), 2929 (m), 2855 (m), 1486 (s, C=N), 1305 (s), 1247 (m), 1088 (vs, ClO_4), 929 (w), 792 (m, Cī S), 742 (m), 623 (s). UVī visible in DMSO [ə$_{max}$, nm (Ů M$^{ī\ 1}$ cm$^{ī\ 1}$)]: 430 (25 700), 384 (18 000) (sh), 314 (26 400).

Caution: *Perchlorate salts are potentially explosive and should only be handled in small quantities, never be heated in the solid state or scraped from sintered glass frits.*

2.2.2.4 [Cu(Bp44mT-H)Cl]

The 1:1 Cu(II) complex, [Cu(Bp44mT-H)Cl] was synthesised following a literature procedure, as described (West et al., 1995). Bp44mT (142 mg, 0.5 mmol) and $CuCl_2.2H_2O$ (86 mg, 0.5 mmol) was added to ethanol (7 mL) and refluxed for 30 min to provide a dark brown solid. This was filtered off, washed with ethanol followed by

diethyl ether and dried *in vacuo* to afford 160 mg of the desired product. The single crystals were obtained by slow diffusion of diethyl ether into a methanol solution. Yield: 95%. Mass data (ESI+, CH_3CN): m/z: Calcd. for: $CuC_{15}H_{15}N_4SClNa$, 403.99 $[M+Na^+]^+$; Found: 403.83 (80%); Calcd. for $Cu_2C_{30}H_{32}N_8S_2Cl$, 729.07 $[2M\bar{\imath}\ Cl+2H^+]^+$; Found: 728.96 (100%). Anal. Calcd. (%) for: $CuC_{15}H_{15}N_4SCl$: C 47.12, H 3.95, N 14.65, S 8.38. Found: C 47.31, H 3.95, N 14.60, S 8.23. IR, cm^{-1}: 2919 (w), 1592 (m), 1548 (m), 1515 (s, C=N), 1393 (vs), 1299 (vs), 1245 (vs), 1128 (s), 970 (m), 791 (s, C$\bar{\imath}$ S), 726 (m), 655 (s). UV$\bar{\imath}$ visible in DMSO [λ_{max}, nm ($Å\ M^{\bar{\imath}\,1}\ cm^{\bar{\imath}\,1}$)]: 430 (18 400), 310 (16 300).

2.2.3 Zinc Complexes Synthesis

2.2.3.1 General procedure

Complexes $[Zn(Dp44mT)Cl_2]$, $[Zn(Ap44mT)Cl_2]$ and $[Zn(DpC)Cl_2]$ were synthesised as described below. One mole equivalent of $ZnCl_2$ was added to hot ethanolic (30 mL) solution of either Dp44mT or Ap44mT or DpC·HCl and refluxed for 30 min. Precipitate formed was collected by filtration under hot condition and washed with ethanol, diethylether and dried *in vacuo.* Complexes $[Zn(Dp44mT)_2]$, $[Zn(Ap44mT)_2]$ and $[Zn(DpC)_2](ClO_4)_2$ were prepared by a general procedure where either Dp44mT or Ap44mT or DpC·HCl (1 mmol) in ethanol (25 mL) was reacted with $ZnClO_4$ (0.186 g, 0.5 mmol) in the presence of triethyl amine (0.51 g, 5 mmol) under reflux for 30 min. After cooling to room temperature, precipitate was filtered off, washed with ethanol followed by copious amounts of diethylether and dried *in vacuo.*

2.2.3.2 [Zn(Dp44mT)Cl_2]

Dp44mT (0.4 g, 1.40 mmol) and $ZnCl_2$ (0.195 g, 1.43 mmol) were used as substrates for the preparation of [Zn(Dp44mT)Cl_2]. Product was isolated as a bright yellow solid (0.52 g). Yield: 88%. ^{1}H NMR (500 MHz, $CDCl_3$): ŭ 3.32 (6H, bs, N(C*H*$_3$)$_2$), ŭ 7.53-7.57 (2H, m, C*H*$_{py}$), ŭ 7.74 (2H, bs, C*H*$_{py}$), ŭ 7.97-8.03 (2H, m, C*H*$_{py}$), ŭ 8.64 (1H, d, C*H*$_{py}$), ŭ 8.83 (1H, d, C*H*$_{py}$), ŭ 14.83 (1H, bs, N*H*). ^{13}C NMR (125 MHz, d^6-DMSO): ŭ 49.07 (N(*C*H$_3$)$_2$), ŭ 124.71 (py), ŭ 125.22 (py), ŭ 125.60 (py), ŭ 127.43 (py), ŭ 139.30 (py), ŭ 139.98 (py), ŭ 141.27 (py), ŭ 148.35 (py), ŭ 148.60 (py), ŭ 150.00 (*C*=N), ŭ 180.46 (*C*=S). ESI-MS (+ve mode in MeOH) found mass: 347.92 (67%), 632.86 (100%). Calc. mass for $C_{14}H_{14}N_5SZn$ ([Mī 2Cl$^-$ī H$^+$]$^+$: 348.02, $C_{28}H_{29}N_{10}S_2Zn$ ([Mī 2Cl$^-$ +L+H$^+$]$^+$: 633.13. Anal. Calc. for $C_{14}H_{15}N_5SCl_2Zn\cdot H_2O$ (%): C 38.25, H 3.90, N 15.93, S 7.29. Found (%): C 38.22, H 3.81, N 15.75, S 7.26. IR Data/ cm^{-1}: 3495 (w, NH), 2981 (w, CH), 2883 (w, CH), 2827 (w, CH), 1598 (m), 1547 (vs, C=N), 1439 (m), 1420 (m), 1388 (m), 1317 (s), 1235 (m, thioamide), 1138 (m), 1055 (m), 1006 (m), 904 (m), 802 (m, C=S), 751 (m), 650 (s), 630 (s). UV-Vis in DMSO: [ə$_{max}$ (nm) (Ů M^{-1} cm^{-1})]: 309 (10600), 420 (14600).

2.2.3.3 [Zn(Ap44mT)Cl_2]

Zn(Ap44mT)Cl_2 was prepared using general procedure except that Ap44mT (0.50 g, 2.25 mmol) and $ZnCl_2$ (0.31 g, 2.27 mmol) were used. Yellow solid (0.7 mg). Yield: 88%. ^{1}H NMR (500 MHz, d^6-DMSO): ŭ 2.53 (3H, s, C*H*$_3$), ŭ 3.32 (6H, s, N(C*H*$_3$)$_2$), ŭ 7.49-7.67 (1H, broad doulet, C*H*$_{py}$), ŭ 7.99 (1H, bs, C*H*$_{py}$), ŭ 8.14 (1H, bs, C*H*$_{py}$), ŭ 8.67 (1H, bs, C*H*$_{py}$). ESI-MS in MeOH: found mass: 284.99 (95%), 506.79 (100%). Calc. mass for $C_{10}H_{13}SN_4Zn$ ([Mī 2Cl$^-$ī H$^+$]$^+$): 285.02, $C_{20}H_{26}S_2N_8Zn$ ([Mī 2Cl$^-$ +L+H$^+$]$^+$): 507.11. Anal. Calc. for $C_{10}H_{14}N_4SCl_2Zn$ (%): C 33.50, H 3.94, N 15.62, S

8.94. Found (%): C 33.46, H 4.03, N 15.26, S 8.98. IR Data/ cm^{-1}: 3262 (w, NH), 2976 (w, CH), 1626 (m), 1563 (vs, C=N), 1473 (m), 1440 (m), 1388 (m), 1352 (m), 1307 (s), 1222 (s, thioamide), 1110 (m), 1017 (m), 898 (m), 814 (s, C=S), 777 (vs), 747 (m), 733 (m), 640 (m). UV-Vis in DMSO: [λ_{max} (nm) (ε M^{-1} cm^{-1})]: 307 (11300), 404 (18400).

2.2.3.4 [Zn(DpC)Cl_2]

Zn(DpC)Cl_2 was prepared using general procedure where DpC·HCl (0.350 g, 0.90 mmol) and $ZnCl_2$ (0.122 g, 0.90 mmol) were used. Yellow solid (0.36 g). Yield: 82%. ^{1}H NMR (500 MHz, d^6-DMSO): δ 1.17-1.81 (11H, m, cyclohexyl), δ 3.13 (3H, bs, NC*H*$_3$), δ 7.59 (1H, t, $^3J_{H,H}$ = 8.5 Hz, py), δ 7.65 (1H, t, $^3J_{H,H}$ = 7.0 Hz, py), δ 7.80 (2H, bs, py), δ 8.04 (1H, t, $^3J_{H,H}$ = 9.5 Hz, py), δ 8.11 (1H, t, $^3J_{H,H}$ = 9.0 Hz, py), δ 8.67 (1H, s, py), δ 8.86 (1H, dd, $^3J_{H,H}$ = 5.5 Hz, py). ^{13}C NMR (125 MHz, d^6-DMSO): δ 18.83 (*C*H$_2$, cyclohexyl), δ 25.35 (*C*H$_2$, cyclohexyl), δ 25.82 (*C*H$_2$, cyclohexyl), δ 29.73 (N*C*H, cyclohexyl), δ 56.31 (N*C*H$_3$), δ 124.41 (py), δ 124.47 (py), δ 125.28 (py), δ 127.42 (py), δ 138.81 (py), δ 139.39 (py), δ 148.33 (py), δ 148.69 (*C*=N). ESI-MS in MeOH: found mass: 416.05, 768.98. Calc. mass for $C_{19}H_{22}SN_5Zn$ [M − 2Cl^- − H^+]$^+$: 416.09, $C_{38}H_{45}S_2N_{10}Zn$ [M − 2Cl^-+L+H^+]$^+$: 769.26. Anal. Calc. for $C_{19}H_{23}N_5SCl_2Zn$ (%): C 46.59, H 4.73, N 14.30, S 6.55. Found (%): C 46.46, H 4.78, N 13.96, S 6.51. IR Data/ cm^{-1}: 3071 (w, CH), 2944 (w, CH), 2862 (CH), 1597 (m), 1514 (vs, C=N), 1473 (m), 1445 (m), 1403 (m), 1326 (m), 1296 (s), 1230 (s, thioamide), 1190 (m), 1151 (m), 1002 (s), (m), 808 (vs, C=S), 776 (m), 749 (s), 639 (s), 614 (m). UV-Vis in DMSO: [λ_{max} (nm) (ε M^{-1} cm^{-1})]: 310 (11500), 423 (11500).

2.2.3.5 [Zn(Dp44mT)$_2$]

Orange yellow solid (0.28 g). Yield: 88%. ^{1}H NMR (500 MHz, $CDCl_3$): ŭ 3.21 (6H, s, N(C*H*$_3$)$_2$), ŭ 7.05 (1H, ddd, C*H*$_{py}$), ŭ 7.33 (1H, ddd, C*H*$_{py}$), ŭ 7.31-7.35 (1H, m, C*H*$_{py}$), ŭ 7.49-7.54 (1H, td, C*H*$_{py}$), ŭ 7.82-7.87 (1H, td, C*H*$_{py}$), 7.94 (1H, d, C*H*$_{py}$), 8.14 (1H, dd, $^3J_{H,H}$ = 6.0 Hz, C*H*$_{py}$), 8.77 (1H, dd, $^3J_{H,H}$ = 4.0 Hz, C*H*$_{py}$). ^{13}C NMR (125 MHz, $CDCl_3$): ŭ 122.95 (py), ŭ 123.10 (py), 123.44 (py), 127.89 (py), ŭ 135.37 (py), ŭ 137.80 (py), ŭ 142.41 (py), ŭ 147.17 (*C*=N), ŭ 149.16 (py), 150.15 (py), 153.80 (py), ŭ 183.07 (*C*-S). ESI-MS in MeCN: found mass: 632.86 (100%). Calc. mass for $C_{28}H_{29}N_{10}S_2Zn$ ([M+H$^+$]$^+$: 633.13. Anal. Calc. for $C_{28}H_{28}N_{10}S_2Zn$ (%): C 53.04, H 4.45, N 22.09, S 10.11. Found (%): C 52.84, H 4.38, N 20.76, S 9.63. IR Data/ cm^{-1}: 3077 (w, NH), 2936 (w, CH), 1559 (m, C=N), 1473 (m), 1317 (m), 1238 (m, thioamide), 1006 (m), 975 (m), 906 (m), 803 (m, C=S), 622 (s). UV-Vis in DMSO: [ə$_{max}$ (nm) (Ů M^{-1} cm^{-1})]: 309 (21900), 418 (26800).

2.2.3.6 [Zn(Ap44mT)$_2$]

Yellow solid (0.21 g). Yield: 84%. Single crystals suitable for X-ray diffraction were grown in a NMR tube. ^{1}H NMR (500 MHz, $CDCl_3$): ŭ 2.59 (3H, s, C*H*$_3$C=N), ŭ 3.32 (6H, s, N(C*H*$_3$)$_2$), ŭ 7.01 (1H, dd, C*H*$_{py}$), ŭ 7.46 (1H, d, $^3J_{H,H}$ = 5 Hz, C*H*$_{py}$), ŭ 7.61-7.64 (1H, m, C*H*$_{py}$), ŭ 7.90 (1H, d, $^3J_{H,H}$ = 5.0 Hz, C*H*$_{py}$). ^{13}C NMR (125 MHz, $CDCl_3$): ŭ 13.65 (*C*H$_3$C=N), ŭ 39.70 (N(*C*H$_3$)$_2$), ŭ 120.41 (py), ŭ 123.18 (py), ŭ 138.14 (py), 143.33 (py), ŭ 146.80 (*C*=N), ŭ 151.06 (py), ŭ 178.9 (*C*-S). ESI-MS in MeCN: found mass: 285.00 (100%), 506.87 (85%), 792.93 (80%). Calc. mass for $C_{10}H_{13}SN_4Zn$ [Mī L]$^+$: 285.02, $C_{20}H_{27}N_8S_2Zn$ [M+H$^+$]$^+$: 507.11, $C_{30}H_{39}S_3N_{12}Zn_2$ [2M+L]$^+$: 793.11. Anal. Calc. for $C_{20}H_{26}N_8S_2Zn\cdot0.5H_2O$ (%): C 46.46, H 5.26, N 21.67, S 12.41. Found (%): C 46.59, H 5.04, N 21.64, S 12.47. IR Data/ cm^{-1}: 1561 (m, C=N), 1479 (w),

1310 (m), 1226 (m, thioamide), 1018 (m), 902 (m), 813 (m, C-S), 788 (m), 623 (s). UV-Vis in DMSO: [λ_{max} (nm) (ε M^{-1} cm^{-1})]: 309 (22300), 404 (30600).

2.2.3.7 $[Zn(DpC)_2]\cdot(ClO_4)_2$

$[Zn(DpC)_2](ClO_4)_2$ was prepared using general procedure without addition of triethyl amine. Yellow solid (0.29 g). Yield: 59%. ^{1}H NMR (500 MHz, d^6-DMSO): δ 1.13-1.76 (11H, m, cyclohexyl), δ 3.12 (3H, s, NCH_3), δ 7.60 (1H, t, $^3J_{H,H}$ = 6.5 Hz, CH_{py}), δ 7.67 (1H, t, $^3J_{H,H}$ = 6.0 Hz, CH_{py}), δ 7.82 (2H, bs, CH_{py}), δ 8.04 (1H, t, CH_{py}), δ 8.13 (1H, bs, CH_{py}), δ 8.66 (1H, bs, CH_{py}), δ 8.86 (1H, d, CH_{py}), δ 8.88 (1H, d, $^3J_{H,H}$ = 5.0 Hz, CH_{py}). ^{13}C NMR (125 MHz, d^6-DMSO): δ 19.01 (*C*H_2, cyclohexyl), δ 25.27 (*C*H_2, cyclohexyl), δ 25.77 (*C*H_2, cyclohexyl), δ 29.63 (N*C*H, cyclohexyl), δ 56.50 (N*C*H_3), δ 125.07 (*C*H_{py}), δ 125.60 (py), δ 125.82 (py), δ 126.09 (py), δ 127.65 (py), δ 128.08 (py), δ 139.50 (py), δ 140.76 (py), δ 147.60 (py), δ 148.42 (py), 149.33 (*C*=N), δ 180.16 (*C*=S). ESI-MS in MeCN: found mass: 768.98 (100%). Calc. mass for $C_{32}H_{42}S_3N_{12}Zn$ ($[M - 2ClO_4+CH_3CN - H^+]^+$): 769.22. Anal. Calc. for $C_{38}H_{46}N_{10}S_2O_8Cl_2Zn$ (%): C 46.99, H 4.77, N 14.42, S 6.60. Found (%): C 46.74, H 4.74, N 14.36, S 6.21. IR Data/ cm^{-1}: 2931 (w), 2856 (w), 1501 (m, C=N), 1477 (m), 1301 (m), 1238 (m, thioamide), 1090 (vs, ClO_4), 1006 (m), 927 (m), 807 (s, C=S), 704 (m), 623 (s). UV-Vis in DMSO: [λ_{max} (nm) (ε M^{-1} cm^{-1})]: 315 (22700), 423 (31500).

2.3 X-ray Crystallography

Data were collected at 190 K on an Oxford Diffraction Gemini CCD diffractometer (Abingdon, United Kingdom) with Cu-KŬ radiation (1.54184 Å). Data reduction and empirical absorption corrections (multiscan) were carried out using Oxford Diffraction CrysAlisPro software. The structure was solved by direct methods with SHELX-86 and refined by full matrix least-squares on F^2 with SHELXL-97 (Farrugia, 1999; Sheldrick, 2008). All non-hydrogen atoms were refined anisotropically except O-atoms attached to Cl5, Cl6, Cl7 and Cl8 (disordered perchlorates). Hydrogen atoms were included at their calculated positions using a riding model. The N-H protons were first identified from difference maps, but then constrained. Molecular structure diagrams were produced with ORTEP3 (Farrugia, 1997). Crystal data in CIF format have been deposited with the Cambridge Crystallographic Data Centre (CCDC 1062686 & 1062687).

2.4 Binding Studies

Zn-ligand binding studies were carried out in Mops buffer (pH=7.3, 50 mM, NaCl, 100 mM, DMSO, 10% (v/v)) and in DMSO alone. To the ligand (50 µM) solution, increasing concentration of $ZnCl_2$ was added gradually and incubated. After 3 min, absorption spectra were measured, subsequently their binding ratio was calculated by plotting λ_{max} that appeared between 380-450 nm against Zn/ligand molar ratio.

2.5 Cell Culture

The KB31 (-Pgp) and the vinblastine-resistant variant KBV1 (+Pgp) cell lines were grown in DMEM. SW480 cells were grown in RPMI. M14 Bcl-2 and PC cells were grown in RPMI with G418 (800 εM). All cells were grown under standard growth conditions. All media were supplemented with foetal bovine serum (10%), penicillin (100 U/mL), streptomycin (100 mg/mL), L-glutamine (2 mM), non-essential amino acids, sodium pyruvate (1 mM) and fungizone (0.25 εg/mL). KBV1 (+Pgp) cells were grown constantly in the presence of vinblastine (1 εg/mL) to ensure high Pgp expression (Jansson et al., 2015a; Yamagishi et al., 2013).

2.6 Determination of Pgp-ATPase Activity

Whether or not the thiosemicarbazones and their Fe(III) and Cu(II) complexes are Pgp substrates was assessed using the Pgp GloÊ Assay System (Promega Corporation, Madison, WI, USA). The assay was performed according to the manufacturerôs instructions as described previously, using thiosemicarbazones and their Fe(III) or Cu(II) complexes (50 εM). Briefly, Pgp-enriched membranes (0.5 mg/mL) and Mg(II)-ATP (5 mM) were incubated for 40 min/37 °C with the test agents, and ATP levels were detected as a luciferase-generated luminescent signal. As relevant negative controls, the well characterised Pgp inhibitor, vanadate, was utilised (Urbatsch et al., 1994). As a positive control, verapamil-stimulated Pgp-ATPase activity was measured in the presence of the Pgp control substrate, verapamil (200 µM) (Ogihara et al., 2006).

2.7 Cellular Proliferation Assay

Proliferation was examined using the MTT assay. Briefly, cells were seeded in 96 well plates and allowed to adhere overnight. The seeding densities used were of 5 x 10^3 cells/well for KBV1 cells, 2 x 10^3 cells/well for KB31 cells, 10 x 10^3 cells/well for SW480 cells and 1 x 10^4 for M14 Bcl-2 and PC cells. The thiosemicarbazones and Zn-thiosemicarbazone complexes were added to the plates and incubated for 24 h/37°C. In studies involving the use of the Pgp inhibitor, Ela, thiosemicarbazones were added to the plates in the presence of absence of Ela (0.1 εM) and incubated for 24 h/37°C. For assays conducted with TM, TM was added to cells 3 h before the addition of Zn complexes, followed by a 24 h incubation with the Zn complexes. As shown previously, MTT colour formation was directly proportional to the number of viable cells (Richardson et al., 1995), validating its use in these studies. Results were processed and analysed according to standard procedures (Kalinowski et al., 2007; Lovejoy et al., 2012; Richardson et al., 2006; Richardson et al., 2009; Whitnall et al., 2006; Yuan et al., 2004). For assays conducted with N-acetyl cysteine (NAC), NAC (10 mM) was added to the cells 3 h prior to the thiosemicarbazones.

2.8 Redox Activity Assessment

2.8.1 *In Vivo*

In order to assess ROS generation by the thiosemicarbazones and their Fe(III) and Cu(II) complexes, H_2DCF-DA oxidation was assessed *in vitro* using standard experimental procedures and conditions (Jansson et al., 2010a; Lovejoy et al., 2011). Briefly, KBV1 cells were seeded to give approximately 50% confluence the

next day. H_2DCF-DA (30 μM) and Ela (0.1 μM) were then added and the cells were incubated at 37°C/30 min. The H_2DCF-DA was then removed, before the thiosemicarbazones (10 μM) and Ela were added and the cells were again incubated at 37°C/30 min. The treatments were subsequently removed and the cells were harvested with PBS/EDTA and centrifuged (1000 rpm/5 min) prior to being re-suspended in cold PBS prior to conducting flow cytometry using a FACS Canto (Becton Dickinson, USA). In these studies, 10,000 events/sample were recorded and the data analysis conducted using FloJo software version 7.5.5. (Tree Star, Inc; Ashland, OR, USA).

2.8.2 *In Vitro*

Studies were conducted as described with H_2DCF (5 εmol/L)(Lovejoy et al., 2011; Myhre et al., 2003). As a positive control, Zn(II), Cu(II) at 5 εmol/L was reduced using cysteine (100 εmol/L) in either Hanks Buffered Saline Solution (HBSS, pH = 7.4) or 150 mmol/L acetate buffer (pH = 5.0). Hydrogen peroxide (100 εmol/L) was then added to initiate hydroxyl radical generation. Dp44mT, [Zn(Dp44mT)$_2$], Ap44mT, [Zn(Ap44mT)$_2$] DpC and [Zn(DpC)$_2$] (5 εmol/L) were added to examine hydroxyl radical production, in the presence or absence of Cu(II) (5 εmol/L) or TM (250 εmol/L).

2.9 Microscopy

2.9.1 Lysosomal Membrane Permeabilisation Assays

Lysosomal membrane permeabilisation (LMP) was assessed using a Zeiss Axio Observer:Z camera and AxioVision Rel. 4.7 Software (Zeiss, Oberkochen, Germany) 1 fluorescence microscope equipped with GFP and TexasRed filters. Images were captured using an AxioCam camera and AxioVision Rel. 4.7 Software (Zeiss). Data analysis was performed using ImageJ v 1.48 software. For acridine orange (AO) studies (Yu et al., 2009a), cells were seeded to give 50% confluence and left to adhere overnight. Cells were then incubated with AO (2.5 εg/mL) for 12 min/37°C, washed 3 times with PBS and then incubated for 30 min/37°C with the thiosemicarbazones (10 or 30 εM), either alone, or pre-coordinated with Fe(III) or Cu(II) (10 εM), +/- Ela (0.1 εM), +/- NAC (5 mM) or +/-TM (10 εM). Further studies were also conducted where cells were incubated for 1 h/37°C with the thiosemicarbazones (10 εM), or the Zn complexes (10 εM), +/-TM (250 εM). The cells were then washed 3 times and imaged. Alternatively, cells were incubated with thiosemicarbazones for 24 h prior to incubation with AO, as previously described.

LMP was also assessed *via* immunofluorescence using the lysosomal markers, lysosomal-associated membrane protein 2 (LAMP2) and Cathepsin D (Yu et al., 2009a). KBV1 cells were seeded onto coverslips at a density of 3 x 10^4 cells/ml and left to adhere overnight/37^{o}C. Cells were then treated with Dp44mT or Ap44mT (25 μM), +/- Ela (0.1 μM), +/-NAC (5 mM), +/- TM (25 μM) for 24 h/37^{o}C. Treatment was followed by methanol fixation for 15 min and digitonin permeabilisation (100 μM/10 min) at room temperature. After blocking with 1% bovine serum albumin for 30 min at

room temperature, immunocytochemistry was performed with LAMP2 (Cell Signaling, Danvers, MA, USA) and cathepsin D (Cell Signaling), using TexasRed and FITC conjugated secondary antibodies. Coverslips were mounted on slides using ProLong® Gold Antifade Mountant with DAPI (ThermoFisher Scientific).

2.9.2 Intracellular Localisation of (Zn[DpC])

Intracellular localisation of [Zn(DpC)] was examined using the fluorescent probes LysoTracker® Deep Red, MitoTracker® Deep Red and DRAQ5Ê . Images were acquired using a Zeiss LSM 780 confocal microscope with a 100 x oil-immersion objective. Data analysis was performed using ImageJ v 1.48 software and the associated JACoP plugin. To examine nuclear localisation, DRAQ5Ê was added to cells at concentrations recommended by the manufacturer. Cells were incubated with DRAQ5Ê for 10 min/37°C, followed by another 10 min/37°C incubation with [Zn(DpC)]. Cells were then washed 3 x with PBS prior to imaging in Live Cell Imaging Solution. Excitation wavelengths were set at 405 and 633 nm, and emission detected between 410-510 nm and 685-695 nm.

Mitochondrial localisation was assessed using MitoTracker® Deep Red. Cells were treated with 50 nM of Mitotracker® Deep Red for 10 min/37°C, before 100 mM of [Zn(DpC)] was added and cells were incubated for 10 min/ 37°C. Cells were then washed 3 x with PBS prior to imaging in Live Cell Imaging Solution. Excitation wavelengths were set at 405 and 633 nm, and emission detected between 410-510 nm and 685-695 nm. Lysosomal localisation was assessed using LysoTracker® Deep Red. Cells were treated with 50 nM of LysoTracker® Deep Red for 10 min/

37°C, before 100 mM of [Zn(DpC)] was added and cells were incubated for 10 min/ 37°C. Cells were then washed 3 x with PBS prior to imaging in Live Cell Imaging Solution. Excitation was set at 405 nm (LysoTracker® Deep Red exhibits a small excitation peak at ~400 nm) and emission detected between 410-510 nm and 685-695 nm.

2.10 Western Blotting

Protein extraction and Western blotting were performed using standard methods (Gao and Richardson, 2001). Immunodetection of proteins was carried out using antibodies against Bcl-2 (catalogue number 2872; Cell Signalling Technology), LC3 (catalogue number MBPM036; Abacus-ALS, Meadowbrook, QLD, Australia) and β-actin (catalogue number A1978; Sigma Aldrich). Secondary antibodies included horseradish peroxidase-conjugated anti-rabbit (catalogue number A6154; Sigma Aldrich) and anti-mouse (catalogue number A4416; Sigma Aldrich). The membrane was developed using enhanced chemiluminescence and imaged using a ChemiDoc (Bio-Rad) imager. Densitometric analysis was performed using Image Lab Software (Bio-Rad), normalised to β-actin.

2.11 Silencing using RNA Interference

Cells were seeded into plates and allowed to adhere overnight. Cells were transfected with ONTARGET plus siRNA oligos (Dharmacon, Lafayette, CO) for 8 h/37°C in serum-free OPTIMEM (Sigma Aldrich) media using Lipofectamine 2000 (Invitrogen), according to the manufacturerôs instructions. The cells were then

incubated in MEM media supplemented with FCS for 96 h/37°C, prior to further experiments. The siRNAs purchased from Dharmacon were: ONTARGET plus non-targeting pool (negative control siRNA, catalogue number D-001810-01) and SMART pool ONTARGET plus Bcl-2 siRNA (catalogue number L-003307-00-005).

2.12 Statistical Analysis

All statistical analysis using two-way ANOVA or Student's *t*-test were performed using GraphPad Prism (v6.0, GraphPad Software, Inc, La Jolla, CA, USA).

Chapter 3 - Structure-Activity Relationships of Di-2-Pyridylketone, 2-Benzoylpyridine and 2-Acetylpyridine Thiosemicarbazones for Overcoming Pgp-Mediated Drug Resistance

(Taken from Stacy *et al* (2016) *J. Med. Chem.*)

3.1 Introduction

Cancer remains a major cause of mortality and morbidity worldwide and new anti-cancer agents are essential to develop (Jansson et al., 2015a). One class of compounds that has been extensively investigated is the thiosemicarbazone group that exert their effects through their ability to effectively sequester transition metals (Yu et al., 2009b). Of these, 3-AP (Fig. 3.1A), has entered greater than 20 multi-centre clinical trials, but has suffered multiple problems, including low efficacy in some tumour-types and significant side effects, including methaemoglobinemia (Knox et al., 2007; Merlot et al., 2013; Traynor et al., 2010).

Over the last 20 years, our laboratory has focused on the development of ligands for clinical use, with a particular emphasis on agents for cancer treatment (Baker et al., 1992; Becker et al., 2003; Darnell and Richardson, 1999; Richardson et al., 1995; Richardson and Milnes, 1997). Through concerted structure-activity relationship studies, novel ligands of the DpT series that show potent and selective anti-tumour activity and anti-metastatic activity both *in vitro* and *in vivo* were developed (Chen et

al., 2012; Liu et al., 2012; Lovejoy et al., 2012; Richardson et al., 2006; Whitnall et al., 2006; Yuan et al., 2004). Of these DpT analogues, Dp44mT (Fig. 3.1B), is the most well characterised and has been shown to target the lysosome to induce lysosomal membrane permeabilisation (LMP) (Gutierrez et al., 2014; Jansson et al., 2015b; Lovejoy et al., 2011).

Significantly, Dp44mT demonstrated markedly more pronounced anti-proliferative activity than 3-AP and greater tolerability with less side effects (Whitnall et al., 2006; Yuan et al., 2004). However, Dp44mT induced cardiac fibrosis at high non-optimal doses (Whitnall et al., 2006) and this undesirable property led to the design and synthesis of a second generation of DpT analogues (Kovacevic et al., 2011; Lovejoy et al., 2012). These new agents were designed based upon a key structureī activity relationship derived from our previous studies in which the replacement of the terminal H at N4 with an alkyl group increased anti-proliferative activity (Lovejoy and Richardson, 2002; Richardson et al., 2006; Yuan et al., 2004). Of these ligands, DpC (Fig. 3.1C) was identified as the lead agent (Kovacevic et al., 2011; Lovejoy et al., 2012). Both Dp44mT and DpC demonstrate selectivity towards cancer cells over normal cells both *in vitro* and *in vivo* (Kalinowski et al., 2007; Lovejoy et al., 2012; Stefani et al., 2011; Stefani et al., 2013; Whitnall et al., 2006). However, the advantages of DpC over Dp44mT include: **(1)** that DpC demonstrates greater anti-tumour activity than Dp44mT *in vivo* against pancreatic tumour xenografts, showing substantially enhanced efficacy than the gold standard agent for this disease, gemcitabine (Kovacevic et al., 2011); **(2)** DpC demonstrates pronounced anti-tumour activity and tolerability when administered orally, as well as intravenously, while Dp44mT is toxic when given *via* the oral route (Lovejoy et al., 2012; Yu et al., 2012);

(3) DpC demonstrates potent anti-tumour activity *in vitro* and *in vivo* against multiple belligerent tumour-types without inducing cardiotoxicity (Kovacevic et al., 2011; Lovejoy et al., 2012); and **(4)** unlike Dp44mT, DpC is markedly and significantly less active at inducing methaemoglobin generation (Quach et al., 2012). Moreover, due to its optimal properties, DpC has entered clinical trials in early 2016 for the treatment of advanced and resistant cancers (NCT02688101) which highlights its selectivity and tolerability (Jansson et al., 2015a).

Concurrently with the DpT series of ligands, the synthesis and characterisation of several other series of thiosemicarbazones were also initiated in our laboratories (Jansson et al., 2015a). These included the BpT (*e.g.*, Bp44mT; Fig. 3.1D) and ApT (*e.g.* Ap44mT; Fig. 3.1E) series of ligands that also showed marked and selective anti-tumour activity *in vitro* and/or *in vivo* (Kalinowski et al., 2007; Richardson et al., 2009; Yu et al., 2012). As a relevant control, 2-benzoylpyridine 2-methylthiosemicarbazone (Bp2mT), a BpT analogue that cannot chelate metals, was also synthesised where a methyl group substituted at N2 prevents electron delocalisation and the binding of metal ions (Fig. 3.1F).

Integral to the mechanism of action of these ligands, it was demonstrated that they form redox-active Fe(III) and Cu(II) complexes (Jansson et al., 2010a; Jansson et al., 2010b; Kalinowski et al., 2007; Lovejoy et al., 2011; Richardson et al., 2006; Richardson et al., 2009; Yuan et al., 2004). Moreover, two of these agents, namely Dp44mT and DpC are substrates of the drug transporter, Pgp, and are effluxed out of cells, but also are transported into lysosomes by utilising Pgp on the lysosomal

membrane (Jansson et al., 2015b; Seebacher et al., 2016b; Seebacher et al., 2016c). Notably, as a part of endocytosis in Pgp expressing cells, the Pgp-containing plasma membrane buds inward to form an early endosome. Upon endocytosis there is inversion of the topology of Pgp in the endosomal membrane that leads to the transport of Pgp substrates, including Dp44mT and DpC, into the lysosomal interior (Jansson et al., 2015b; Seebacher et al., 2016b; Seebacher et al., 2016c; Yamagishi et al., 2013). During this process, the catalytic active site and ATP-binding domain of Pgp are still exposed to the cytosol and enable Pgp to õpumpò substrates from the cytosol into lysosomes (Yamagishi et al., 2013). Within the lysosomes, these agents become trapped due to protonation of the compounds at the acidic pH of the organelle, bind copper and redox cycle to generate reactive oxygen species that induce LMP, and apoptotic cell death (Gutierrez et al., 2016; Jansson et al., 2015b; Lovejoy et al., 2011). Clearly, the ability of Dp44mT to õhijackò Pgp and markedly overcome resistance to standard chemotherapies is an important advantage, as MDR is a major impediment to the successful treatment of cancer (Jansson et al., 2015a; Leonard et al., 2003).

The ATP-binding cassette transporters, such as Pgp, are one of the most commonly encountered MDR mechanisms, and are responsible for the cellular efflux of a broad variety of cytotoxic drugs and one of the most clinically significant drug transport mechanisms (Higgins, 2007; Leonard et al., 2003). In fact, Pgp has been linked to poorer clinical outcomes in solid tumours and haematological malignancies (Higgins, 2007; Leonard et al., 2003). Past efforts aimed at targeting Pgp have largely focused on direct inhibitors, although clinical trials have yet to provide convincing proof of their efficacy (Coley, 2010; Szakacs et al., 2006). Hence, alternative strategies at

overcoming resistance, such as that offered by Dp44mT (Jansson et al., 2015b; Whitnall et al., 2006), are critical to develop.

Considering the marked activity of Dp44mT in overcoming drug resistance, the current study investigated the structural requirements of thiosemicarbazones necessary to target drug resistant cancer cells using the aforementioned mechanism of hijacking lysosomal Pgp to potentiate lysosomal targeting (Jansson et al., 2015b). To assess this, four structurally-related thiosemicarbazones belonging to the DpT, BpT, and ApT series were examined, namely: Dp44mT (Fig. 3.1B), DpC (Fig. 3.1C), Bp44mT (Fig. 3.1D) and Ap44mT (Fig. 3.1E). This choice of agents was based on their marked and selective anti-cancer efficacy (Kalinowski et al., 2007; Lovejoy et al., 2012; Richardson et al., 2009; Yu et al., 2012; Yuan et al., 2004). The activity of these compounds was compared to the clinically trialled thiosemicarbazone, 3-AP (Knox et al., 2007; Traynor et al., 2010) (Fig. 3.1A) and the negative control BpT analogue, Bp2mT (Fig. 3.1F).

Herein, we identify crucial structural-activity relationships that enable thiosemicarbazones of these classes to overcome MDR which includes: **(1)** the presence an electron-withdrawing substituent at the imine carbon (that results in an appropriate redox potential of its Cu complex to oxidise biological substrates and induce ROS generation); **(2)** sufficient relative lipophilicity to enable facile membrane transport and to act as an effective Pgp substrate; and **(3)** the ability of the ligand to bind Cu(II) and generate ROS that is essential for inducing LMP that kills drug resistant tumour cells.

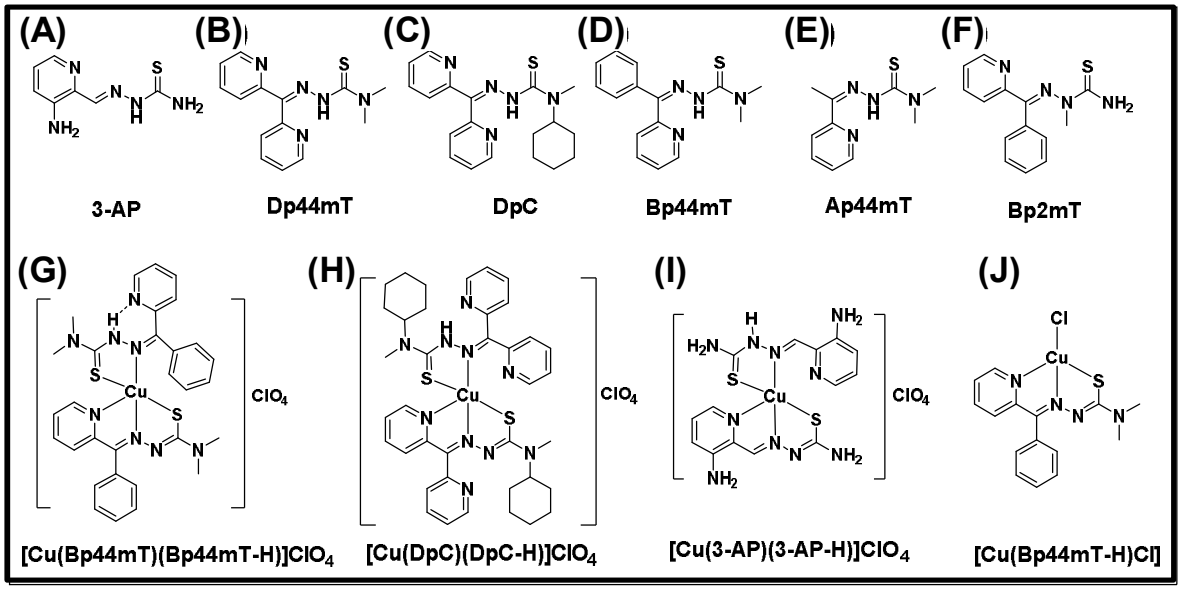

Figure 3.1. Line drawings of the ligands (A-F); mechanism of action of thiosemicarbazones in Pgp-mediated drug resistance (G); and line drawings of new copper complexes examined in this investigation (H-K).

Structure of **(A)** 3-AP, 3-aminopyridine-2-carboxaldehyde thiosemicarbazone; **(B)** Dp44mT, di-2-pyridylketone 4,4-dimethyl-3-thiosemicarbazone; **(C)** DpC, di-2-pyridylketone 4-cyclohexyl-4-methyl-3-thiosemicarbazone; **(D)** Bp44mT, 2-benzoylpyridine 4,4-dimethyl-3-thiosemicarbazone; **(E)** Ap44mT, 2-acetylpyridine 4,4-dimethyl-3-thiosemicarbazone; and **(F)** Bp2mT, 2-benzoylpyridine 2-methyl-3-thiosemicarbazone. **Structure of new thiosemicarbazones Cu complexes (G)** [Cu(Bp44mT)(Bp44mT-H)]ClO_4; **(H)** [Cu(DpC)(DpC-H)]ClO_4; **(I)** [Cu(3-AP)(3-AP-H)]ClO_4; and **(J)** [Cu(Bp44mT-H)Cl].

3.3 Results and Discussion

3.3.1 Synthesis and Characterisation of Novel Thiosemicarbazones

The tridentate thiosemicarbazone ligands, Dp44mT, DpC, Bp44mT and Ap44mT (Fig. 3.1B-E), were synthesised and characterised, as previously described (Kalinowski et al., 2007; Lovejoy et al., 2012; Richardson et al., 2006; Richardson et al., 2009). The compound, Bp2mT (Fig. 3.1F), was synthesised in an analogous manner by refluxing equimolar amounts of 2-benzoylpyridine and 2-methyl-3-

thiosemicarbazide in ethanol with glacial acetic acid as a catalyst. ^{1}H and ^{13}C NMR spectral analysis revealed the presence of both *E* and *Z* isomers of Bp2mT in 50:50 ratio in d_6-DMSO (Fig. 3.2, 3.3). Furthermore, our group has already demonstrated that the same class of 2-benzoylpyridine thiosemicarbazones exist as interconvertible *E/Z* isomers in solution (Stariat et al., 2010).

The 1:1 and 1:2 Cu(II)/ligand complexes with selected ligands were also synthesised (Figs. 3.1G-J). Significantly, the thiosemicarbazone Cu(II) complexes were important to characterise as it is well known that the Dp44mT-Cu(II) complex is markedly active and crucial in terms of inducing LMP and overcoming drug resistance (Jansson et al., 2015b; Lovejoy et al., 2011). The 1:2 Cu(II)/ligand complexes of Bp44mT (Fig. 3.1G), DpC (Fig. 3.1H) and 3-AP (Fig. 3.1I) were obtained by refluxing 2 equivalents of the respective thiosemicarbazone with one equivalent of $Cu(ClO_4)_2.6H_2O$ in ethanol in the presences of the base, triethylamine, for 1 h. On the other hand, the 1:1 Cu(II)/ligand complex, [Cu(Bp44mT-H)Cl] (Fig. 3.1J), was prepared by refluxing an ethanolic solution of equimolar amounts of Bp44mT and $CuCl_2$. All complexes were characterised by ESI-MS, UV–visible and IR spectroscopy and their purity was confirmed by elemental analysis.

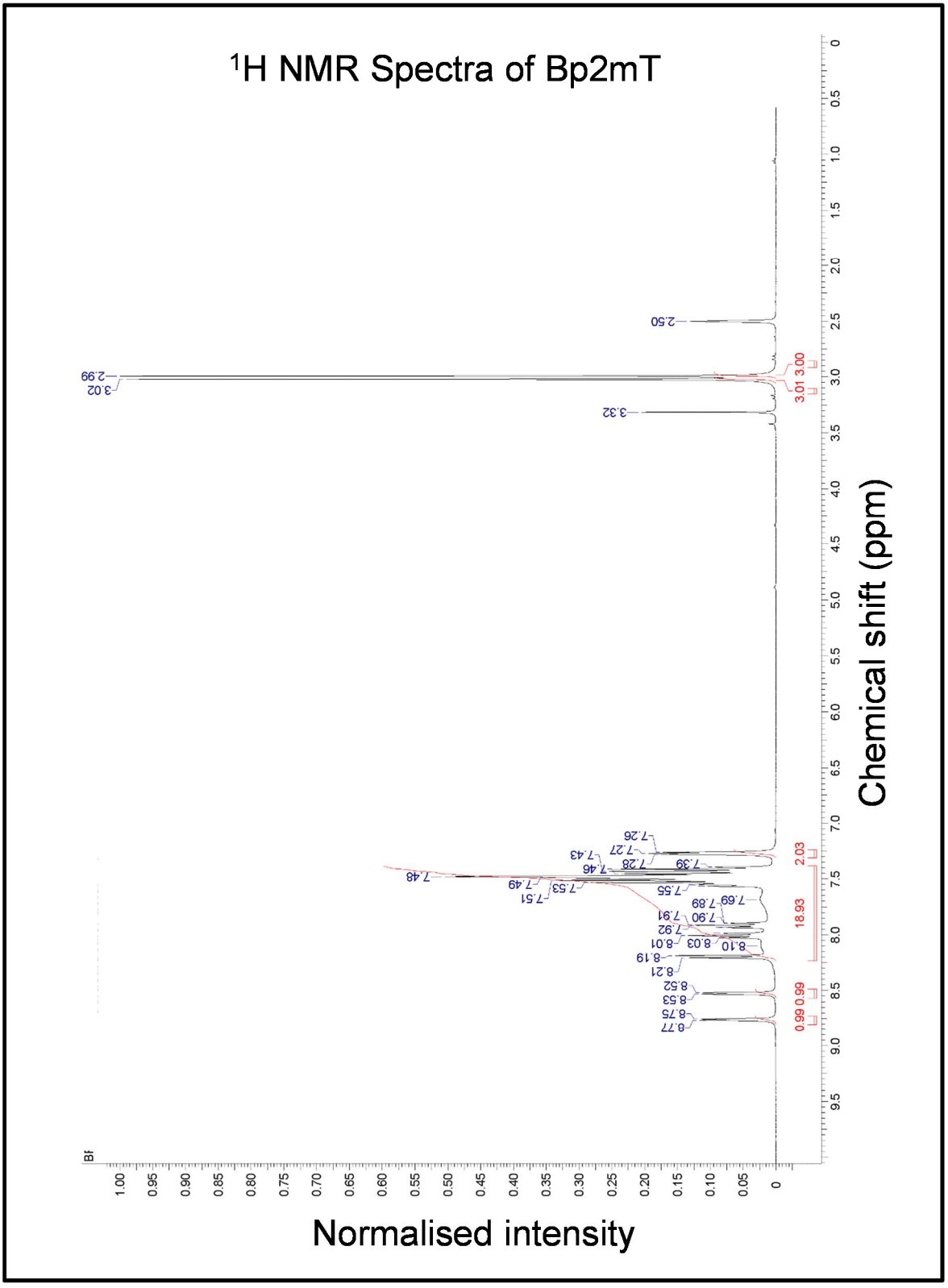

Fig. 3.2 ^{1}H NMR spectrum of Bp2mT.

^{1}H NMR spectral analysis revealed the presence of both *E* and *Z* isomers of Bp2mT in 50:50 ratio in d_6-DMSO.

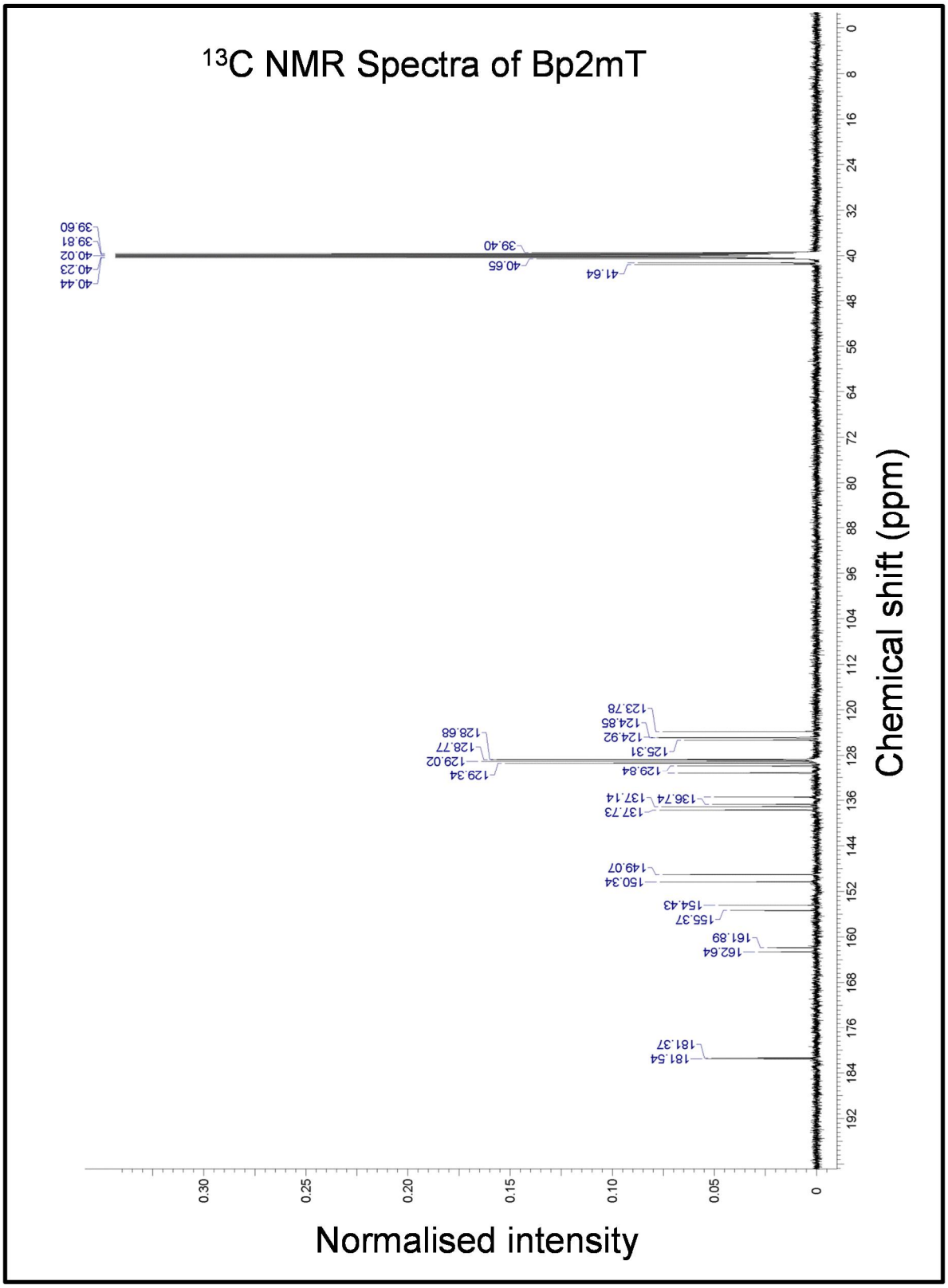

Fig. 3.3 ^{13}C NMR spectrum of Bp2mT.

^{13}C NMR spectral analysis revealed the presence of both *E* and *Z* isomers of Bp2mT in 50:50 ratio in d_6-DMSO.

3.3.2 Novel Crystal Structures

Single crystals of the Cu(II) complexes of Bp44mT (both 1:1 and 1:2 Cu/ligand) suitable for X-ray diffraction were obtained by slow vapour diffusion of diethyl ether into methanol solutions of each compound. The molecular structures of [Cu(Bp44mT)(Bp44mT-H)]ClO_4 and [Cu(Bp44mT-H)Cl] are shown in Figures 3.3A and B, respectively, and their crystal data are presented in Table 3.1. The structure of [Cu(Bp44mT)(Bp44mT-H)]ClO_4 comprised four complex cations in the asymmetric unit, each with essentially the same coordination geometry (Fig. 3.4A).

The Cu ion was coordinated to two ligands in an asymmetric manner to give a distorted square pyramidal geometry, where the deprotonated ligand acted as a tridentate chelator (N-N-S), while the neutral ligand acted as a bidentate (N-S) chelator (Fig. 3.4A). The bidentate coordinated ligand is found in its *Z*-isomeric form which is incapable of binding as a tridentate ligand. The positions of the phenyl and pyridyl rings are reversed by comparison with the tridentate deprotonated ligand, which is in its *E*-isomeric form. The fact that both isomers are observed here within the same complex illustrates that conversion between the two is facile in solution and that they equilibrate, as shown by NMR.

The presence of the proton on the thiosemicarbazone group most likely stabilises the ligand in the *Z*-isomeric form (through the intra-molecular H-bond to the pyridine ring; Fig. 3.4A). This prevents the ligand from isomerising to the *E*-form, where the three donor atoms are on the same side of the ligand. The intra-molecular hydrogen bonding between the NH and the N of the pyridine ring in the neutral *Z*-isomeric

Bp44mT ligand was preserved (Fig. 3.4A) In fact, the conformation of the neutral ligand in [Cu(Bp44mT)(Bp44mT-H)]ClO_4 is almost the same as found in the free ligand (Jayakumar et al., 2011), except that the phenyl ring is rotated out of the plane of the ligand by the presence of the Cu atom. Two of the four independent perchlorate anions were well defined, but the other two were disordered over several sites and refined with partial occupancies. The coordination geometry of the [Cu(Bp44mT)(Bp44mT-H)]ClO_4 complex was quite different from the geometries of other analogous 1:2 Cu(II)/ligand complexes, namely [Cu(Ap44mT-H)$_2$] and [Cu(Dp44mT-H)$_2$], that were reported earlier by our group as tridentate ligands both in their deprotonated form (Bernhardt et al., 2009; Jansson et al., 2010b). The structure of the 1:1 complex, [Cu(Bp44mT-H)Cl], was more conventional and crystallised in a centrosymmetric dimeric five-coordinate configuration, where the S atom of an adjacent complex coordinated weakly in the axial site (Cué $S1^{\delta}$> 2.9 Å). A view of the dimer seen in the solid state is shown in Figure 3.3B.

There are other Cu(II) complexes of Bp44mT that have been characterised, including a bis-acetato-bridged dimer [(Bp44mT-H)Cu(μ-OAc)$_2$Cu(Bp44mT-H)] and a bis-azido bridged dimer [(Bp44mT-H)Cu(μ-N_3)$_2$Cu(Bp44mT-H)] (Jayakumar et al., 2014; Kunnath et al., 2012). There are also examples of related 2-benzoylpyridine thiosemicarbazones coordinating to Cu(II) in either their deprotonated (monoanionic) or protonated (neutral) forms (Dobritzsch et al., 2005; Joseph et al., 2004; Lobana et al., 2012; Sreekanth and Kurup, 2003; West et al., 1995; Yang et al., 2013a). However, the structure of [Cu(Bp44mT)(Bp44mT-H)]$^+$ reported herein is a hybrid of both forms within the same complex. Significantly, no similar examples are known in the literature where the acid and base forms of a benzoylpyridine thiosemicarbazone

are coordinated to the same metal ion. The closest analogue is the Cu(II) complex of acetylpyridine thiosemicarbazone, where one of the two ligands is deprotonated, but in that case, both ligands bind in a tridentate manner to give a six-coordinate complex (Souza et al., 1996).

The C-S bond length of the thiosemicarbazone is a reliable indicator of the state of deprotonation. Deprotonation of the NH-C=S moiety leads to the N=C-S^- form being the dominant contributor to the structure and the C-S bond is invariably longer than 1.73 Å. By contrast, when the neutral ligand is bound, the C=S bond retained double bond character (C-S < 1.7 Å). This was also seen here in the structure of [Cu(Bp44mT)(Bp44mT-H)]ClO_4 (Fig. 3.4A) and [Cu(Bp44mT-H)Cl] (Fig. 3.4B).

As observed previously, Cu(II) complexes of the tridentate thiosemicarbazones preferred to form 1:1 complexes due to the Jahn-Teller effect operative on the d^9 electronic ground state, which weakens the two axial coordinate bonds perpendicular to the more strongly bound thiosemicarbazone (Jansson et al., 2010b). This is essentially the case with [Cu(Bp44mT)(Bp44mT-H)]ClO_4, where the bidentate coordinated ligand was the one that occupies the axial coordination site, and the axial Cu-N bonds of all four molecules in the asymmetric unit are long (Fig. 3.4A). The Cu-N and Cu-S bond lengths in [Cu(Bp44mT-H)Cl] and the tridentate (deprotonated) ligand in [Cu(Bp44mT)(Bp44mT-H)]ClO_4 were not significantly different. As expected, the central Cu-N imine bond was the shortest in the meridionally coordinated ligand.

Herein, the *in situ* generated 1:1 Cu(II)/ligand complexes were used in all biological studies. This was done as comprehensive EPR studies with the 1:2 Cu(II)/ligand complexes, namely [Cu(Dp44mT-H)$_2$] and [Cu(Ap44mT-H)$_2$], clearly demonstrated that these complexes partially dissociate to form the corresponding 1:1 Cu(II)/ligand complexes as the dominant species in solution (Jansson et al., 2010b). Moreover, the 1:1 complexes were found to be the active species that mediated tumour cell cytotoxicity (Jansson et al., 2010b; Lovejoy et al., 2012). The *in situ* 1:1 Cu(II)/ligand complexes were prepared by the addition of equimolar amounts of the ligand and $CuCl_2$ in DMSO to give a final 10 mM solution of the complex. A rapid change in colour of the solution was observed upon mixing the ligand and $CuCl_2$, indicating the formation of the resultant complex. Notably, all *in situ* complexes in this study were checked against our pre-synthesised metal-ligand complexes using UV-Vis spectrophotometry to ensure complexation (Jansson et al., 2010b).

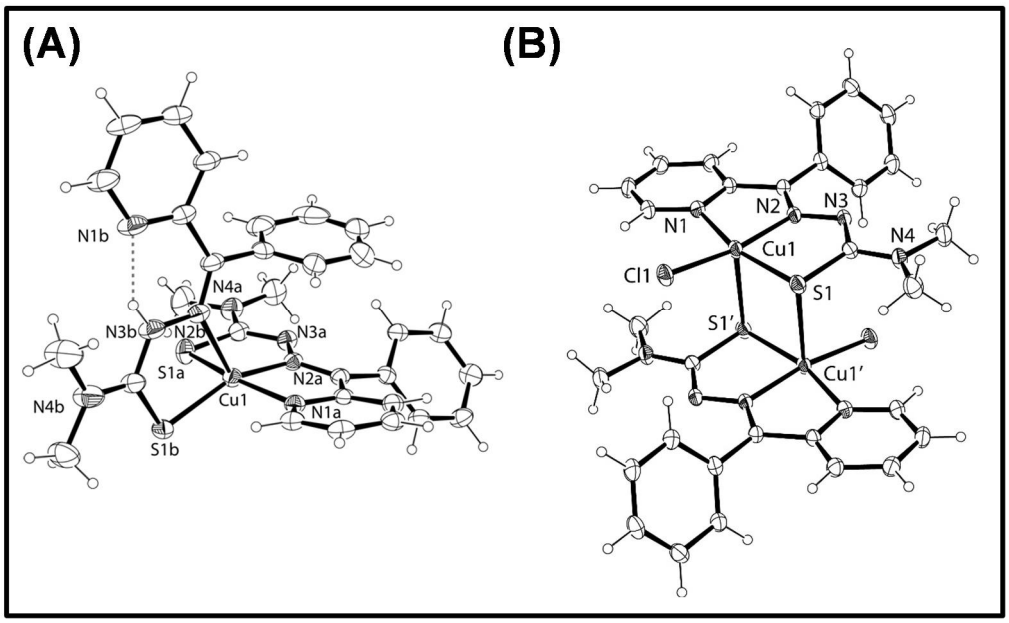

Figure 3.4. ORTEP views (30% probability ellipsoids) of the Cu(II) complexes (A) [Cu(Bp44mT)(Bp44mT-H)]$^+$; and **(B)** [Cu(Bp44mT-H)Cl].

	[Cu(Bp44mT)(Bp44mT-H)]ClO_4	[Cu(Bp44mT-H)Cl]
Formula	$C_{30}H_{31}ClCuN_8O_4S_2$	$C_{15}H_{15}ClCuN_4S$
Formula weight	730.74	382.36
Crystal system	Triclinic	Monoclinic
Space group	$P\bar{1}$	$P2_1/c$
Colour	Dark-brown	Dark-brown
a (Å)	9.2567(1)	9.6179(4)
b (Å)	14.1387(1)	8.2794(5)
c (Å)	51.6543(4)	20.0050(9)
α (deg)	90.287(1)	
β (deg)	94.629(1)	90.344(4)
γ (deg)	91.203(1)	
V (Å^3)	6736.71(1)	1592.98(14)
T (K)	190(2)	190(2)
Z	8	4
R_1 (obsd data)	0.0734	0.0406
wR_2	0.2188	0.1037
GOF	1.040	1.076
CCDC	1062686	1062687

Table 3.1 Crystal Data

3.3.3 Structural Analysis of Novel Thiosemicarbazones

The thiosemicarbazones assessed in this investigation were chosen based upon previous studies demonstrating their potent and selective *in vitro* and *in vivo* activities (Kalinowski et al., 2007; Kovacevic et al., 2011; Lovejoy et al., 2012; Richardson et al., 2009; Whitnall et al., 2006; Yu et al., 2012; Yuan et al., 2004). Particular attention was paid to choosing structurally diverse thiosemicarbazones in order to develop an understanding of which pharmacophores confer the novel ability to overcome MDR, demonstrated previously for Dp44mT (Jansson et al., 2015b). Hence, the ligands, Bp44mT, DpC, Ap44mT and 3-AP (Fig. 3.5), were selected and

possess the following common features, including that all ligands are Ŭ-*N*-heterocyclic thiosemicarbazones that bind transition metals through their pyridyl nitrogen, imine nitrogen and thiocarbonyl sulfur atoms (Bernhardt et al., 2009; Jansson et al., 2010b; Kalinowski et al., 2007; Lovejoy et al., 2012; Richardson et al., 2009). Moreover, each of these selected thiosemicarbazones possess the same ionisable sites (Gutierrez et al., 2014) as Dp44mT that allow the ligand to be neutral at physiological pH (pH 7.4), but become charged at lysosomal pH (pH ~ 5-5.5), resulting in lysosomal trapping of the ligand and Cu(II) complex formation that enables LMP (Lovejoy et al., 2011).

However, each analogue contains substitutional variations at the: **(1)** imine carbon and **(2)** terminal N4 atom that will lead to differences in lipophilicity, inductive effects *etc.*, that will alter biological activity. For example, Bp44mT differs from Dp44mT only in that it possesses a phenyl ring relative to the pyridyl ring at the imine position of Dp44mT (Fig. 3.5; see blue highlight). On the other hand, DpC also contains the di-2-pyridyl moiety present in Dp44mT (Fig. 3.5; see blue highlight), but possesses a methyl and a cyclohexyl ring at the N4 position instead of the dimethyl moiety found in Dp44mT (Fig. 3.5; see green highlight). The ligand, Ap44mT, contains a methyl group at the imine carbon instead of the pyridyl or phenyl moiety (Fig. 3.5; see blue highlight) and possesses a dimethyl substitution at the terminal N4 atom similar to that of Dp44mT and Bp44mT (Fig. 3.5; see green highlight).

The well-characterised thiosemicarbazone, 3-AP, that has entered clinical trials (Knox et al., 2007; Traynor et al., 2010), was used as a reference compound for

comparison to the other thiosemicarbazones. In contrast to Dp44mT, Bp44mT, DpC and Ap44mT, 3-AP is unsubstituted at the imine carbon (Fig. 3.5; see blue highlight) and at the terminal N4 atom (Fig. 3.5; see green highlight). Additionally, 3-AP contains an amine substituent at the 3-position of the coordinating pyridyl ring (Fig. 3.5; see orange highlight). As a negative control, we also included Bp2mT in our studies, as this compound has a methyl substituent at the N2 position of the thiosemicarbazone backbone (Fig. 3.5; see purple highlight). This prevents electron delocalisation and like its close structural analogue, Dp2mT, this prevents metal binding and leads to a compound devoid of activity (Chen et al., 2012; Yuan et al., 2004). Notably, Bp2mT, contains the 2-benzoylpyridine moiety of Bp44mT (Fig. 3.5; see blue highlight), but is unsubstituted at the terminal N4 atom (Fig. 3.5; see green highlight).

3.3.4 Differential Thiosemicarbazone Cytotoxicity in Pgp-Expressing Cells

The ability of Dp44mT to mediate potentiated cytotoxicity in drug resistant cancer cells is inherently related to the fact that it is a Pgp substrate (Jansson et al., 2015b). Others have also demonstrated that structurally different thiosemicarbazones are selectively cytotoxic towards Pgp-expressing MDR cells, although the precise molecular mechanism involved was not clearly established (Hall et al., 2009; Hall et al., 2011). Therefore, we first investigated whether any of the other thiosemicarbazones in this study also mediated Pgp-potentiated cytotoxicity similar to that observed with Dp44mT (Jansson et al., 2015b).

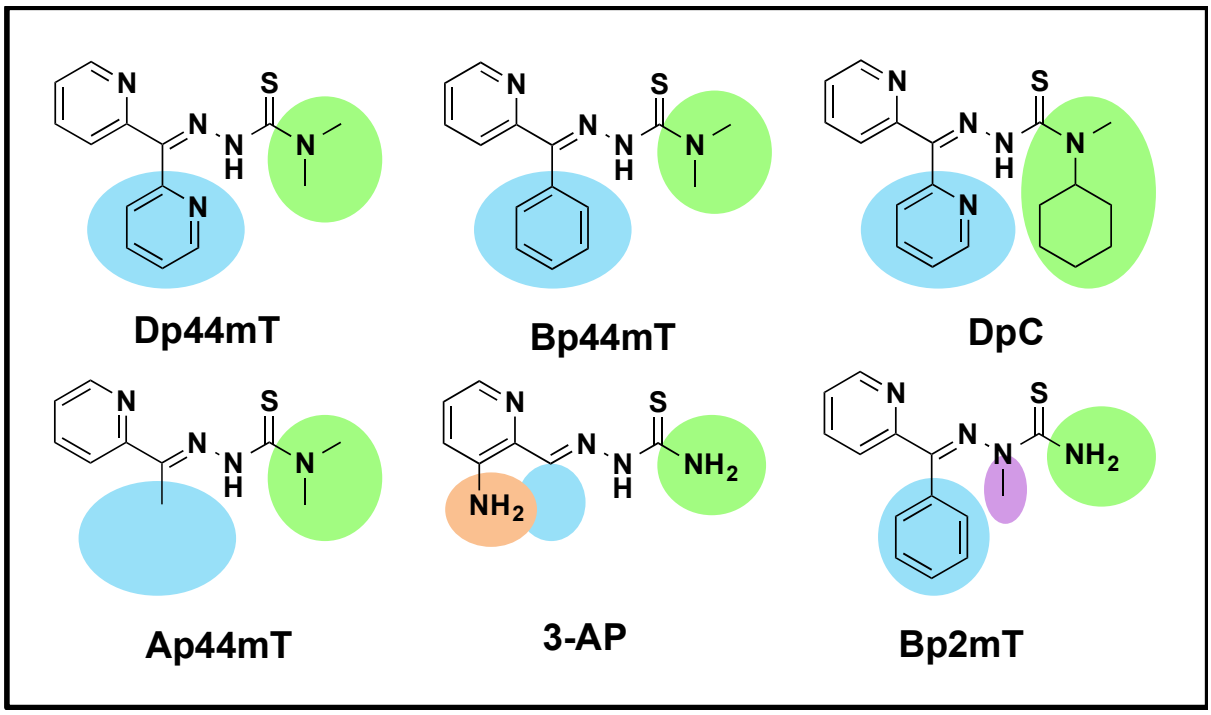

Figure 3.5. Structural analysis of the thiosemicarbazones examined herein.

Structures of the thiosemicarbazones included in the study highlighting the substitutional variations around the imine carbon (blue highlight) and terminal N4 atom (green highlight); as well as the amine substituent at the 3-position of the coordinating pyridyl ring of 3-AP (orange highlight) and methyl substituent at the N2 position of the thiosemicarbazone backbone of Bp2mT (purple highlight).

To initially assess this, cellular proliferation studies were performed using a well characterised pair of cell lines, namely KBV1 (+Pgp) cells which hyper-express Pgp, and KB31 (-Pgp) cells which express only extremely low levels of this protein (Jansson et al., 2015b; Seebacher et al., 2015; Yamagishi et al., 2013). These experiments were performed in the presence or absence of the well characterised Pgp inhibitor, Elacridar (Ela) (Hyafil et al., 1993; Jansson et al., 2015b; Kemper et al., 2004; Yamagishi et al., 2013), to study the effect of Pgp on the anti-proliferative activity of the thiosemicarbazones. Significantly, Ela was implemented as the Pgp

inhibitor of choice, as it gave similar results to Pgp siRNA-treated cells (Jansson et al., 2015b) and is markedly easier to use.

Our previous studies have implemented a range of Pgp expressing cell-types to demonstrate the effect of Dp44mT in terms of its ability to hijack Pgp and overcome drug resistance (Jansson et al., 2015b). We have specifically chosen the KBV1 and KB31 cell lines for this investigation, as: **(1)** the effect of Dp44mT was typical of that found in multiple other Pgp containing cell-types (Jansson et al., 2015b); and **(2)** due to the intensive nature of the studies and the range of thiosemicarbazones utilised, it was experimentally practical to use this pair of well characterised cells (Jansson et al., 2015b; Seebacher et al., 2015; Yamagishi et al., 2013). Finally, these cell-types do not express other common ABC transporters (*e.g.*, MRP1 and ABCG2), and compensatory mechanisms do not lead to resistance to thiosemicarbazones in KB31 cells (Jansson et al., 2015b).

Using KB31 (-Pgp) cells, no significant ($p > 0.05$) difference in cytotoxicity was observed between cells incubated with the thiosemicarbazones, Dp44mT, Bp44mT, DpC, or Ap44mT alone, or these thiosemicarbazones in combination with the Pgp inhibitor, Ela (0.1 µM) after a 24 h/37ºC incubation (Fig. 3.6). Clearly, this is due to the lack of Pgp in these cells, which provides an appropriate negative control and demonstrates that Ela has no intrinsic biological activity in the absence of Pgp, as shown previously (Jansson et al., 2015b; Yamagishi et al., 2013). Bp44mT displayed the most potent anti-proliferative activity of all the thiosemicarbazones in KB31 (-Pgp) cells, with this agent possessing a significantly ($p < 0.001$) lower IC_{50} value than

Dp44mT, DpC and Ap44mT (Fig. 3.6). In contrast, Bp2mT (the negative control agent) and 3-AP demonstrated very poor anti-proliferative activity with IC_{50} values > 800 μM (Fig. 3.6).

In accordance with our previously published results (Jansson et al., 2015b), Dp44mT was 13-fold more cytotoxic towards drug resistant KBV1 (+Pgp) cells than in KB31 (-Pgp) cells (Fig. 3.6). Importantly, in contrast to KB31 (-Pgp) cells, Pgp inhibition with Ela significantly ($p < 0.001$) decreased the cytotoxicity of Dp44mT in KBV1 (+Pgp) cells (Fig. 3.6). This confirmed that the potentiated cytotoxicity of Dp44mT in KBV1 cells was Pgp-dependent. Bp44mT was 13.2-fold more cytotoxic in KBV1 (+Pgp) than KB31 (-Pgp) cells, making it the most cytotoxic of the thiosemicarbazones tested in these cells. Similarly, DpC was 8.1-fold more cytotoxic in KBV1 (+Pgp) cells than in KB31 (-Pgp) cells (Fig. 3.6). As observed with Dp44mT, Pgp inhibition with Ela resulted in a marked and significant ($p < 0.001$) decrease in the cytotoxicity of Bp44mT and DpC in KBV1 cells (Fig. 3.6).

Although Ap44mT was 2.1-fold more cytotoxic in KBV1 (+Pgp) cells compared to KB31 (-Pgp) cells, contrary to the other thiosemicarbazones, Ela had no significant ($p > 0.05$) effect on the cytotoxicity of Ap44mT in KBV1 cells (Fig. 3.6). Similarly to the results using KB31 cells, no appreciable cytotoxicity was observed with either Bp2mT or 3-AP in KBV1 cells, despite both thiosemicarbazones being examined at concentrations up to 800 μM (Fig. 3.6).

The decrease in cytotoxicity (*i.e.,* increased IC_{50} values) of Dp44mT, Bp44mT and DpC observed in KB31 (-Pgp) cells relative to KBV1 (+Pgp) cells suggested that Pgp could potentiate the cytotoxicity of these agents. This was confirmed using the Pgp inhibitor, Ela, which reversed the potentiated cytotoxicity in KBV1 (+Pgp) cells (Fig. 3.6). However, Pgp inhibition using Ela had no significant ($p > 0.05$) effect on the cytotoxicity of Ap44mT (Fig. 3.6). Hence, this observation suggested that in contrast to Dp44mT, Bp44mT and DpC, that Pgp was not involved in potentiating the cytotoxicity of Ap44mT. On the other hand, Bp2mT and 3-AP were not cytotoxic to KBV1 or KB31 cells even at concentrations as high as 800 μM (Fig. 3.6). This is due to the fact that Bp2mT is a negative control, which cannot bind metals that is necessary for these agents to generate ROS and induce cytotoxicity (Chen et al., 2012; Yuan et al., 2004). On the other hand, 3-AP is a thiosemicarbazone that lacks marked anti-proliferative activity (Gutierrez et al., 2014), which could have contributed to its failure in multiple clinical trials (Knox et al., 2007; Merlot et al., 2013; Traynor et al., 2010). The pronounced differences in the observed cytotoxicity of this group of thiosemicarbazones and their differential ability to target Pgp-expressing cells, demonstrated that further assessment of their structure-activity relationships was warranted.

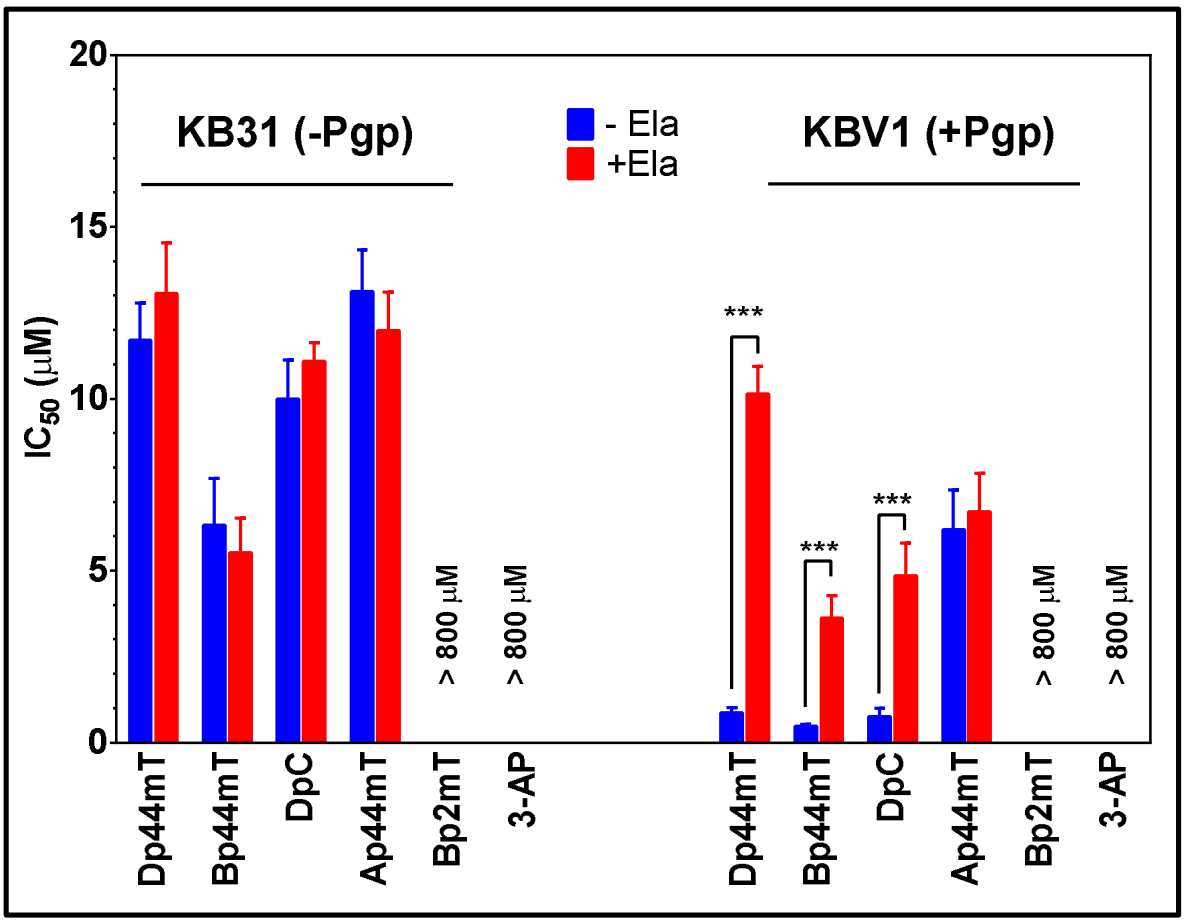

Figure 3.6 MTT assay demonstrates the potentiated cytotoxicity of Dp44mT, Bp44mT and DpC in KBV1 cells

Dp44mT, Bp44mT and DpC exert potentiated cytotoxicity to Pgp-expressing KBV1 cells that can be reversed in the presence the Pgp-inhibitor, Ela. In contrast, the cytotoxicity of the thiosemicarbazones was not significantly ($p > 0.05$) affected by Ela in KB31 cells (-Pgp). KB31 (-Pgp) or KBV1 (+Pgp) were incubated with Dp44mT, Bp44mT, DpC, or Ap44mT alone, or these thiosemicarbazones in combination with the Pgp inhibitor, Ela (0.1 μM) for 24 h/37°C. The MTT assay was then used to examine proliferation. Results are mean ± SD (3 experiments). *** $p < 0.001$ *versus* the respective ligand or complex, as shown.

3.3.5 A Range of Thiosemicarbazones and their Fe(III) and Cu(II) Complexes Increase Pgp-ATPase Activity Suggesting they are Pgp Substrates

Our laboratories have demonstrated that the potentiated cytotoxicity of Dp44mT in MDR cells such as the KBV1 (+Pgp) cell-type is due to Dp44mT acting as a Pgp substrate (Jansson et al., 2015b). Herein, Pgp expression was demonstrated to be a prerequisite for the increased cytotoxicity of Dp44mT, Bp44mT and DpC, but did not markedly affect the cytotoxicity of Ap44mT, especially after incubation with the Pgp inhibitor, Ela (Fig. 3.6). Therefore, the Pgp-ATPase assay was used to assess if the differential cytotoxicity of the thiosemicarbazones towards Pgp-expressing cells could be explained by their ability to act as Pgp substrates.

The ability of the thiosemicarbazones and their Fe(III) and Cu(II) complexes to act as Pgp substrates and increase ATPase activity of Pgp was measured using purified membrane preparations containing high levels of Pgp (Jansson et al., 2015b; Urbatsch et al., 1994). This was vital to assess in order to judge the potential of Pgp to transport thiosemicarbazones across the lysosomal membrane into the lysosome to induce LMP (Jansson et al., 2015b). A compound is considered to be a Pgp substrate if its ATPase activity is above the control activity (> 1), while a Pgp inhibitor decreases Pgp-ATPase activity below the control level (< 1) (Urbatsch et al., 1994). In these experiments, Pgp-enriched membranes (0.5 mg/mL) and Mg(II)-ATP (5 mM) were incubated for 40 min/37°C with thiosemicarbazones and their Fe(III) or Cu(II) complexes (50 ε M), and ATP levels were then measured. The well-characterised Pgp substrate, Verapamil (200 ε M) (Ogihara et al., 2006), was used as a positive control, while sodium orthovanadate (ñVanadateò; 100 ε M) was used as a well

characterised inhibitor of Pgp-activity (Urbatsch et al., 1994). In the current study, the positive control substrate, Verapamil, significantly ($p < 0.001$) increased Pgp-ATPase activity by 5-fold, while the inhibitor, Vanadate, significantly ($p < 0.001$) decreased Pgp-ATPase activity by 11.9-fold relative to the control level (Fig. 3.7). In addition, neither Cu(II) nor Fe(III) alone (*i.e.*, controls for Cu(II) and Fe(III) thiosemicarbazone complexes) had any significant ($p > 0.05$) effect on Pgp-ATPase activity.

All thiosemicarbazones significantly ($p < 0.001$) stimulated Pgp-ATPase activity, indicating that all were Pgp substrates (Fig. 3.7). The three most effective thiosemicarbazones that increased Pgp-ATPase activity were (in descending order): Bp44mT, DpC and Dp44mT, which increased it to 7.9-, 7.4- and 6.6-fold greater than the control, respectively. Both Ap44mT and Bp2mT were less effective and resulted in 5.1- and 5.2-fold increases in Pgp-ATPase activity, respectively (Fig. 3.7). In contrast, 3-AP, a previously reported Pgp substrate (Rappa et al., 1997), resulted in the lowest increase in Pgp activity in this series of thiosemicarbazones (*i.e.*, 4.6-fold *versus* the control; Fig. 3.7).

As observed with the free ligands, all of the Cu(II) thiosemicarbazone complexes were also Pgp substrates (Fig. 3.7). Specifically, [Cu(Dp44mT)] was the best Pgp substrate and mediated a 9.9-fold increase in basal Pgp activity relative to the control, which was significantly ($p < 0.001$) greater than Dp44mT alone. Of note, [Cu(Bp44mT)] resulted in a 7.6-fold increase in Pgp-ATPase activity relative to the control, which was comparable to Bp44mT alone (Fig. 3.7). Both [Cu(DpC)] and [Cu(Ap44mT)] induced a 8.6 and 9.1-fold increase in Pgp activity *versus* the control,

respectively, which were significantly ($p < 0.001$) greater than the respective thiosemicarbazones alone. Upon addition of Cu(II) to Bp2mT, there was no significant ($p > 0.05$) alteration in Pgp-ATPase activity relative to Bp2mT alone (Fig. 3.7), which is consistent with the fact that this compound does not bind metal ions (Chen et al., 2012; Yuan et al., 2004). In contrast, [Cu(3-AP)] significantly ($p < 0.001$) increased Pgp-ATPase activity relative to the 3-AP ligand, with 3-AP and [Cu(3-AP)] increasing Pgp-ATPase activity 4.6- and 5.9-fold relative to the control, respectively (Fig. 3.7).

Similarly to the Cu(II) complexes, all of the Fe(III) complexes also acted as Pgp substrates and mediated significantly ($p < 0.001$) increased Pgp-ATPase activity relative to the control (Fig. 3.7). Notably, [Fe(Dp44mT)$_2$] acted as the best substrate of all of the substrates examined, resulting in a 11.7-fold increase in basal Pgp-ATPase activity relative to the control. In fact, this stimulation of Pgp-ATPase activity by [Fe(Dp44mT)$_2$] was significantly ($p < 0.001$) higher than Dp44mT alone, or the [Cu(Dp44mT)] complex (Fig. 3.7). The fold change in Pgp-ATPase activity mediated by [Fe(Bp44mT)$_2$], [Fe(DpC)$_2$], or [Fe(Ap44mT)$_2$] were similar, resulting in a 9.8-, 10.1- and 10.0-fold change in Pgp activity *versus* the control, respectively. On the other hand, there was no significant ($p > 0.05$) difference in Pgp-ATPase stimulation induced by Bp2mT in the presence of Fe(III) compared to Bp2mT alone, again due to the fact that this agent is a negative control that cannot bind metal ions (Chen et al., 2012; Yuan et al., 2004). The [Fe(3-AP)$_2$] complex mediated a significant ($p < 0.001$) increase in Pgp-ATPase activity in comparison to the control, resulting in a 9.0-fold increase in Pgp activity (Fig. 3.7). The Pgp-ATPase activity of the [Fe(3-

AP)$_2$] complex was significantly ($p < 0.001$) greater than either 3-AP alone or [Cu(3-AP)].

Overall, the fold-change in Pgp-ATPase activity mediated by the thiosemicarbazones and their complexes generally resulted in the following trend: thiosemicarbazone ligand < Cu(II) complex < Fe(III) complex. The only thiosemicarbazones to deviate from this trend were: **(1)** [Cu(Bp44mT)] did not have significantly ($p > 0.05$) greater Pgp-ATPase activity than the ligand; **(2)** [Fe(Ap44mT)$_2$], which did not mediate significantly ($p > 0.05$) greater Pgp-ATPase activity than [Cu(Ap44mT)]; and **(3)** Bp2mT, which did not have significantly ($p > 0.05$) different Pgp-ATPase activity in the presence of Cu(II) or Fe(III) as it is unable to bind metal ions. These results in Figure 3.7 demonstrate that the differences in cytotoxicity observed in Pgp-expressing KBV1 cells (Fig. 3.6) is not entirely dependent on their ability to act as Pgp substrates.

Notably, Pgp substrates are known to be lipophilic in nature (Kimura et al., 2004; Schmid et al., 1999; Seelig and Landwojtowicz, 2000) and this property may explain the differences in the Pgp-ATPase activity mediated by the thiosemicarbazones and their complexes observed herein (Fig. 3.7). For example, upon comparison of the ligands, those with higher lipophilicity, including Bp44mT (calculated log *P*: 2.88) (Broto et al., 1984; Ghose and Crippen, 1987; Viswanadhan et al., 1987) and DpC (calculated log *P*: 4.00) (Broto et al., 1984; Ghose and Crippen, 1987; Viswanadhan et al., 1987), mediated the greatest increase in Pgp-ATPase activity observed (Fig. 3.7). In contrast, those ligands that were relatively less hydrophobic, such as

Ap44mT (calculated log *P*: 1.18) (Broto et al., 1984; Ghose and Crippen, 1987; Viswanadhan et al., 1987) and 3-AP (calculated log *P*: -0.08) (Broto et al., 1984; Ghose and Crippen, 1987; Viswanadhan et al., 1987) were poorer Pgp substrates. Moreover, the markedly increased Pgp-ATPase activity observed with the Cu(II) and Fe(III) complexes relative to the ligand may also be attributed to their lipophilic nature (Richardson et al., 2006). Thus, the overall differences in the ligand/complex lipophilicity may play a role in both their ability to initially enter the cell which is well known for related ligands and thiosemicarbazones of this class (Richardson et al., 1995; Stefani et al., 2011), and also for their subsequent avidity for transport by Pgp across membranes, like other substrates (Kimura et al., 2004; Schmid et al., 1999; Seelig and Landwojtowicz, 2000).

3.3.6 Differential Effects of the Thiosemicarbazones and their Fe(III) or Cu(II) Complexes on Lysosomal Integrity

The potentiated cytotoxicity of Dp44mT in Pgp-expressing cells was previously reported to be due to the Pgp-mediated sequestration of Dp44mT into lysosomes (Jansson et al., 2015b). In fact, once transported into this organelle *via* lysosomal membrane Pgp, Dp44mT can bind endogenous Cu(II) to generate ROS and cause LMP (Jansson et al., 2015b). The lysosome is an active site of Cu(II) recycling in the cell *via* the process of autophagy (Gupte and Mumper, 2009; Kurz et al., 2010; Terman and Kurz, 2013), and hence, it is an important target for this class of ligands (Gutierrez et al., 2014; Jansson et al., 2015b; Lovejoy et al., 2011).

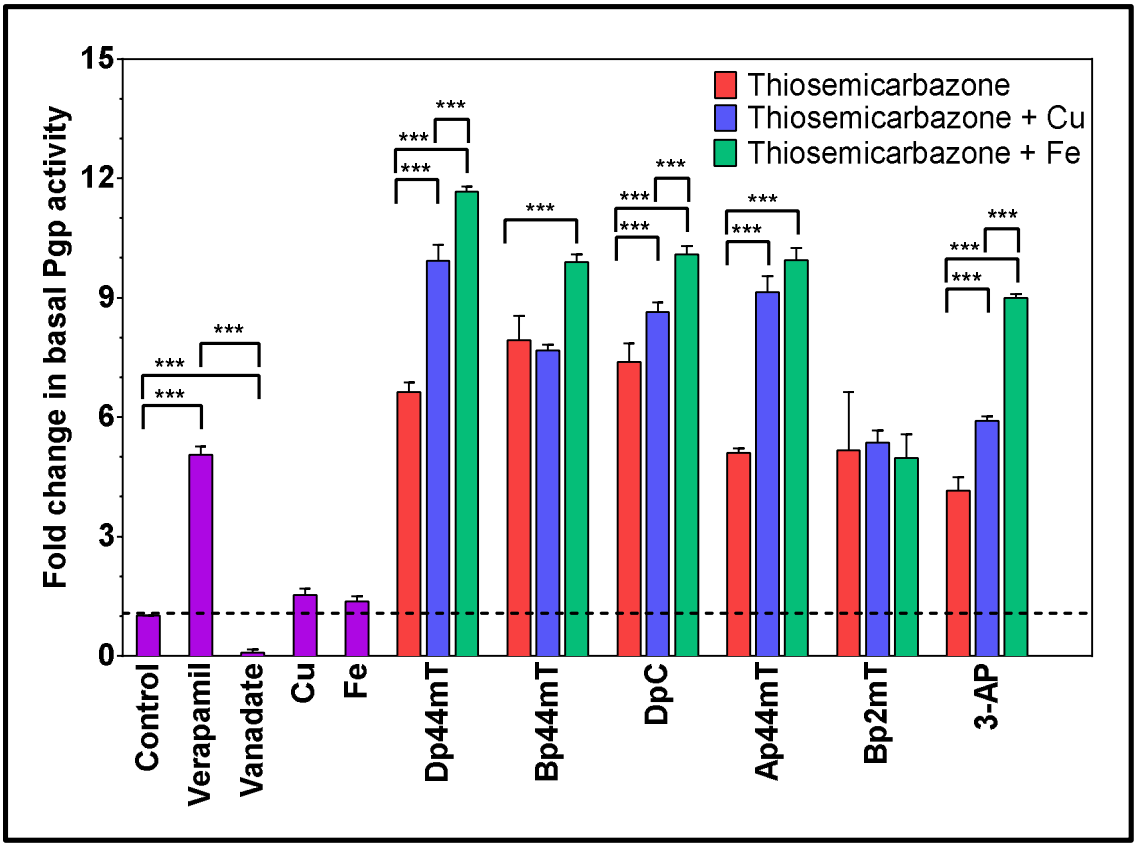

Figure 3.7 Pgp-ATPase assay demonstrates the thiosemicarbazones and their Fe(III) and Cu(II) complexes are all Pgp substrates.

Pgp-enriched membranes (0.5 mg/mL) and Mg(II)-ATP (5 mM) were incubated for 40 min/37°C with thiosemicarbazones and their Fe(III) or Cu(II) complexes (50 ε M), and ATP levels were detected as a luciferase-generated luminescent signal. The well-characterised Pgp substrate, Verapamil (200 ε M) was used as a positive control, while sodium orthovanadate (ñVanadateè; 100 ε M) was used as a well characterised inhibitor of Pgp-activity. Results are mean ± SD (3 experiments). *** $p < 0.001$ relative to the indicated incubation condition in Fig. 3.7.

As all of the thiosemicarbazones in this study and their Fe(III) and Cu(II) complexes were observed to act as Pgp substrates (Fig. 3.7), yet only some resulted in potentiated cytotoxicity in Pgp over-expressing KBV1 cells (Fig. 3.6), we investigated whether lysosomal sequestration and the resultant LMP is affected by thiosemicarbazone structure and/or coordination with Cu(II) or Fe(III) (Fig. 3.8). By using the classical lysosomal marker, acridine orange (AO) (Lovejoy et al., 2011;

Pierzynska-Mach et al., 2014), lysosomal integrity was assessed in KB31 (-Pgp) and KBV1 (+Pgp) cells by fluorescence microscopy (Fig. 3.8A, C) and quantified (Fig. 3.8B, D) as AO intensity/cell. Notably, AO, is well known to accumulate in intact lysosomes to result in red punctate fluorescence, but it exhibits an increase in green fluorescence upon redistribution to the cytosol or nucleus after LMP (Gutierrez et al., 2014; Lovejoy et al., 2011; Nicolini et al., 1979; Nilsson et al., 1997).

After a 30 min/37^{o}C incubation with KB31 (-Pgp) cells, the classical punctuate pattern of orange/red AO-stained lysosomes was observed following incubation with all thiosemicarbazones, in the presence and absence of Cu(II), suggesting that lysosomal damage had not occurred (Fig. 3.8A). This result was corroborated by the quantification of AO intensity/cell, with no significant (p > 0.05) decrease being observed under any of the treatment conditions, compared to vehicle-treated control cells (Fig. 3.8B).

Examining KBV1 (+Pgp) cells, incubation with the thiosemicarbazones alone after 30 min/37^{o}C also did not significantly (p > 0.05) affect lysosomal membrane integrity compared to the respective control (Fig. 3.8Ci, Di). However, following incubation with [Cu(Dp44mT)], [Cu(Bp44mT)] or [Cu(DpC)], the red AO stain dissipated, suggesting that lysosomal membrane integrity was compromised (Fig. 3.8Cii). Indeed, quantification confirmed that the red AO staining significantly (p < 0.001) decreased for [Cu(Dp44mT)], [Cu(Bp44mT)], or [Cu(DpC)] relative to the control (Fig. 3.8Dii). In contrast, following incubation with [Cu(Ap44mT)], Cu and Bp2mT, or [Cu(3-AP)], no significant (p > 0.05) decrease in red AO staining was observed

relative to the control (Fig. 3.8Cii, Dii), which suggested that LMP did not occur. As observed for the thiosemicarbazone ligands alone, none of the Fe(III) complexes affected lysosomal membrane integrity after a 30 min incubation (Fig. 3.8Ciii, Diii).

The decrease in red AO intensity mediated by [Cu(Dp44mT)], [Cu(Bp44mT)] and [Cu(DpC)] was Pgp-dependent, as lysosomal damage was only observed in KBV1 (+Pgp) cells (Fig. 3.8C, D), but not KB31 (-Pgp) cells (Fig. 3.8A, B). These results, like the MTT data (Fig. 3.6), highlighted the importance of Pgp in the anti-proliferative activity of these thiosemicarbazones. At the shorter time point utilised in this AO study (30 min *versus* 24 h used in MTT assays in Figure 3.6), only [Cu(Dp44mT)], [Cu(Bp44mT)] and [Cu(DpC)] mediated a decrease in red AO intensity, suggesting that Cu(II) is involved in mediating Pgp-dependent LMP. In fact, it is notable that previous studies have demonstrated that the Cu(II) complex of Dp44mT is more cytotoxic than its Fe(III) complex.

3.3.7 Ability of the Thiosemicarbazones and their Fe(III) or Cu(II) complexes Complexes to Generate ROS

The generation of ROS by the highly redox-active [Cu(Dp44mT)] complex has been shown to induce LMP (Lovejoy et al., 2011). To assess the role of redox stress in the results obtained for KBV1 (+Pgp) cells in Figures 3.8C and D, we next assessed the ability of all thiosemicarbazones alone and their Cu(II) and Fe(III) complexes to mediate ROS generation in order to determine if their redox activity could explain their efficacy at inducing LMP.

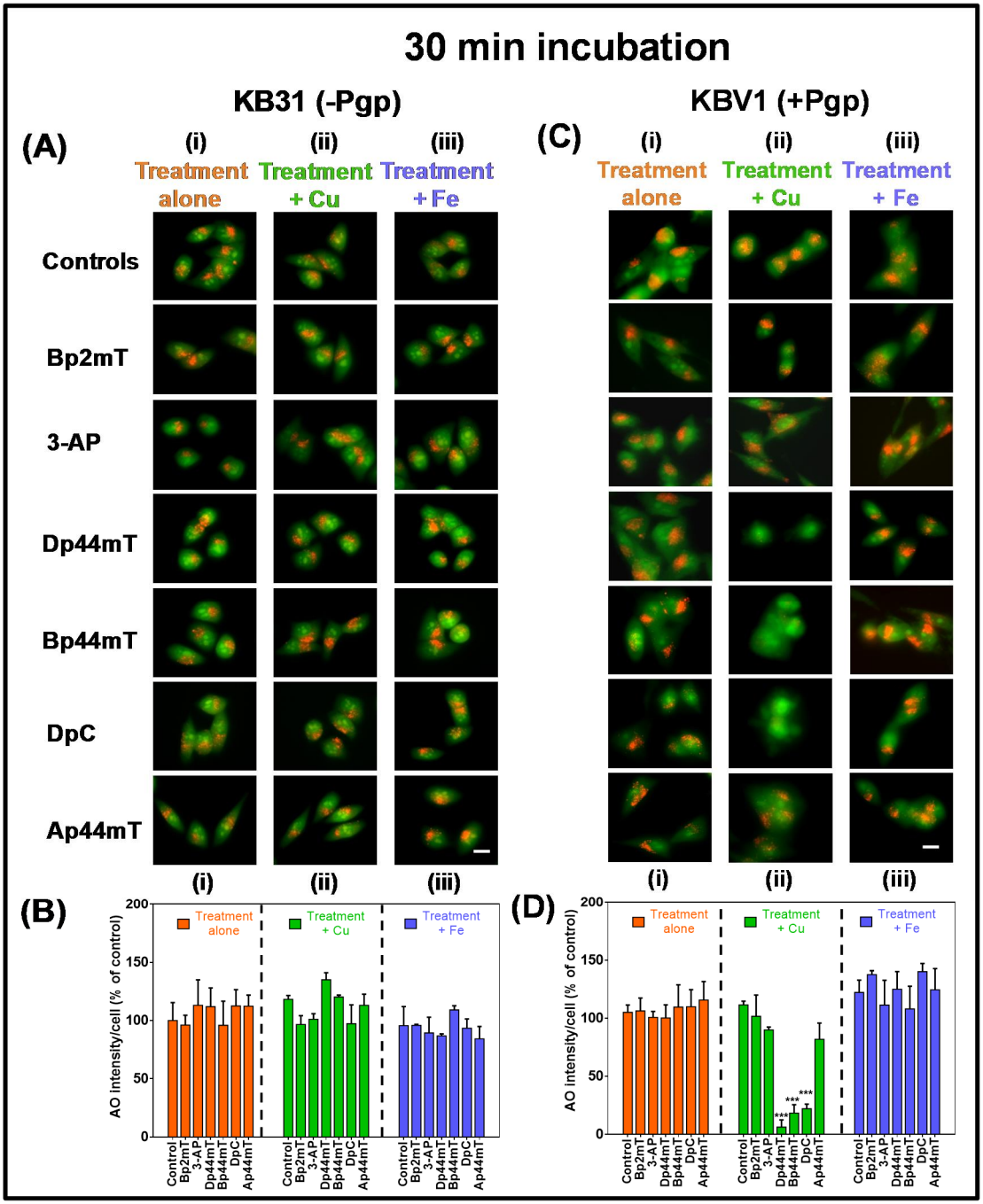

Figure 3.8 Only the Cu(II) complexes of Dp44mT, Bp44mT, or DpC induce lysosomal membrane permeabilisation (LMP) as shown by acridine orange (AO) staining in KBV1 (+Pgp) cells, but not KB31 (-Pgp) cells.

(A, B) Incubation of KB31 (-Pgp) cells with either: **(i)** thiosemicarbazones; **(ii)** thiosemicarbazones (*i.e.*, treatment) and Cu(II); or **(iii)** thiosemicarbazones and Fe(III) (10 ε M, 30 min/37°C) does not significantly ($p > 0.05$) affect LMP relative to the control, as measured by the AO intensity/cell (% of control). **(C, D)** Incubation of KBV1 (+Pgp) cells with either: **(i)** thiosemicarbazones; **(ii)** thiosemicarbazones and Cu(II); or **(iii)** thiosemicarbazones and Fe(III) (10 ε M, 30 min/37°C). Only Dp44mT, Bp44mT or DpC in the presence of Cu(II) mediate significant ($p < 0.001$) LMP relative to the control. Results in **(A, C)** are typical images from 3 experiments. Quantification in **(B, D)** are mean ± SD (3 experiments) *** $p < 0.001$ *versus* the control. Scale bar: 10 ε m.

In these studies, the ability of the agents to mediate cellular ROS generation in KBV1 (+Pgp) cells was evaluated *via* the oxidation of the non-fluorescent, redox-sensitive probe, 2',7'-dichlorodihydrofluorescein (H_2DCF), to the highly fluorescent product, 2',7'-dichlorofluorescein (DCF; Fig. 3.9) (Jansson et al., 2010a; Lovejoy et al., 2011; Yuan et al., 2004).DCF is a well-characterised redox probe and is commonly used for the measurement of ROS generation (Jansson et al., 2010b; Lovejoy et al., 2011; Myhre et al., 2003).

After a 30 min/37ęC incubation of KBV1 (+Pgp) cells with the positive control, H_2O_2 (50 µM), there was a significant ($p < 0.001$) 12.6-fold increase in DCF fluorescence compared to the control cells. Conversely, the $CuCl_2$ and $FeCl_3$ controls did not significantly ($p > 0.05$) affect DCF fluorescence relative to the controls (Fig. 3.9). All of the thiosemicarbazone ligands alone did not significantly ($p > 0.05$) increase DCF fluorescence compared to the control (Fig. 3.9). Therefore, under this short incubation protocol (30 min), significant levels of ROS were not generated by the thiosemicarbazones alone. Examining the effect of adding Cu(II) with the thiosemicarbazones, it was notable that neither [Cu(3-AP)] or Bp2mT in the presence of Cu(II) led to any significant ($p > 0.05$) alteration in DCF fluorescence relative to the control or the thiosemicarbazone alone (Fig. 3.9). However, [Cu(Dp44mT)], [Cu(Bp44mT), [Cu(DpC)] and [Cu(Ap44mT)] significantly ($p < 0.001$) increased intracellular DCF fluorescence relative to the control or their respective thiosemicarbazones alone (Fig. 3.9). Interestingly, [Cu(Dp44mT)] mediated the greatest fold change in intracellular DCF fluorescence, resulting in a 4.0-fold increase in DCF fluorescence relative to Dp44mT alone. Similarly, [Cu(Ap44mT)], [Cu(DpC)] and [Cu(Bp44mT)], increased intracellular DCF fluorescence by 2.6-, 3.0-

and 3.1-fold, respectively, in comparison to their corresponding thiosemicarbazones alone (Fig. 3.9). Of note, [Cu(Ap44mT)] mediated significantly (p < 0.001-0.01) decreased levels of DCF fluorescence relative to [Cu(Dp44mT)], [Cu(Bp44mT) or [Cu(DpC)] (Fig. 3.9).

All of the thiosemicarbazones in the presence of Fe(III) generated comparable levels of DCF fluorescence when compared to the control or their respective thiosemicarbazones alone (Fig. 3.9). In summary, only [Cu(Dp44mT)], [Cu(Bp44mT) and [Cu(DpC)] demonstrated the greatest ability to induce ROS formation (Fig. 3.9) and to cause LMP as judged by using AO (Fig. 3.8 C, D). However, while [Cu(Ap44mT)] also significantly (p < 0.001) increased ROS (Fig. 3.9), it did not lead to LMP (Fig. 3.8C, D). This disparity may be related to the incubation time used, as [Cu(Ap44mT)] is a significantly (p < 0.001) less potent oxidant than [Cu(Dp44mT)], [Cu(Bp44mT), or [Cu(DpC)] (Fig. 3.9), which could be responsible for its lack of effect on LMP after a 30 min incubation (Fig. 3.8C, D).

3.3.8 Lysosomal Membrane Permeabilisation Mediated by Dp44mT, Bp44mT and DpC is Dependent on Pgp, as Shown Using the Pgp Inhibitor, Ela

The LMP observed upon incubation with [Cu(Dp44mT)], [Cu(Bp44mT)], or [Cu(DpC)], occurred only in KBV1 (+Pgp) cells (Figs. 3.8C, D), but not in KB31 (-Pgp) cells (Figs. 3.8A, B).

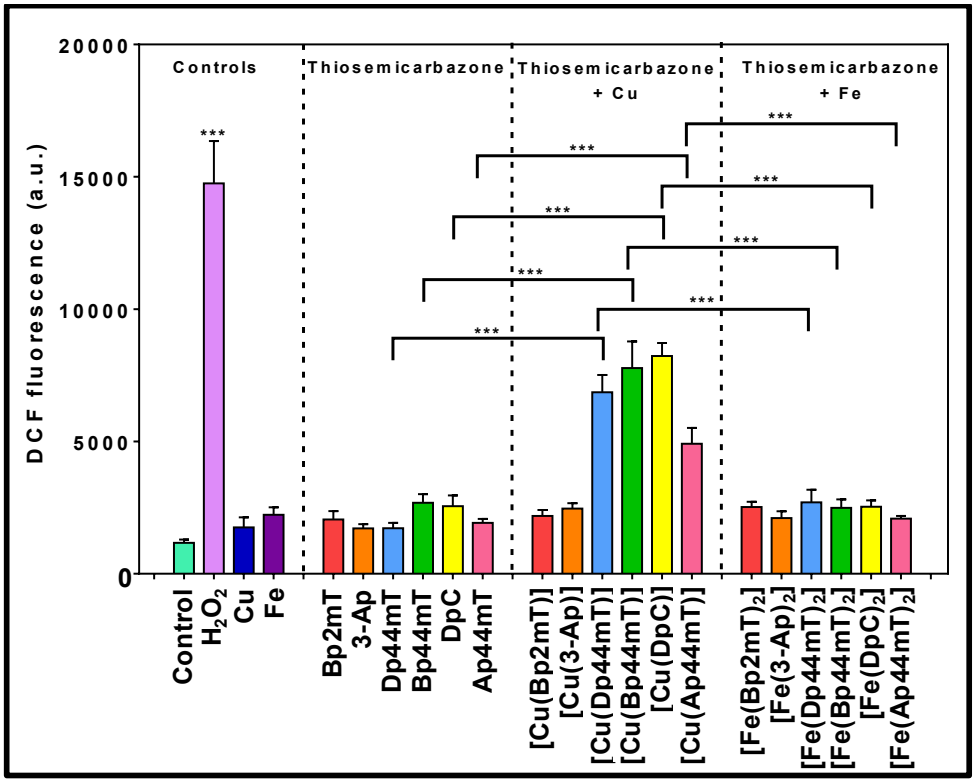

Figure 3.9. The Cu(II) complexes of Dp44mT, Bp44mT and DpC demonstrate marked intracellular redox activity in KBV1 (+Pgp) cells, while the Ap44mT Cu(II) complex demonstrates lower efficacy.

The redox activities of the thiosemicarbazones (10 ε M, 30 min/37°C) were assessed in KBV1 (+Pgp) cells incubated with H_2DCF-DA (30 ε M, 30 min/37°C) with the fluorescence being measured by flow cytometry. The [Cu(Dp44mT)], [Cu(Bp44mT)], [Cu(DpC)] and [Cu(Ap44mT)] complexes are significantly (p < 0.001) more redox-active than the thiosemicarbazones (ligands) alone, or the Fe(III) complexes. Note: H_2O_2 (50 µM) was included as a positive control. Additional controls include $CuCl_2$ and $FeCl_3$ that were used in the preparation of the thiosemicarbazone Fe(III) and Cu(II) complexes. Results are mean ± SD (3 experiments). *** p < 0.001 *versus* the respective ligand or complex, as shown.

Thus, the importance of Pgp in mediating LMP was assessed using KBV1 (+Pgp) cells by implementing the Pgp inhibitor, Ela, and assessing its effects on the activity of the Cu(II) complexes on AO staining (Fig. 3.10A). We also examined the effect of thiosemicarbazone structure on LMP by comparing [Cu(Dp44mT)], [Cu(Bp44mT)]

and [Cu(DpC)], that induced LMP, to [Cu(Ap44mT)] which did not, using KBV1 (+Pgp) cells (Fig. 3.10A).

In these studies, incubation of KBV1 (+Pgp) cells for 30 min/37^{o}C with [Cu(Dp44mT)], [Cu(Bp44mT)], or [Cu(DpC)] resulted in a significant ($p < 0.001$) decrease in AO intensity relative to the control (Fig. 3.10Aiii), consistent with LMP, as demonstrated in Figures 3.8C, D. In contrast, [Cu(Ap44mT)] did not significantly ($p > 0.05$) affect AO intensity compared to the control KBV1 (+Pgp) cells (Fig. 3.10Ai,iii). Interestingly, co-incubation with the Pgp inhibitor, Ela, prevented the decrease in AO intensity mediated by [Cu(Dp44mT)], [Cu(Bp44mT)] and [Cu(DpC)] (Fig. 3.10Aii). Indeed, the red intensity of AO staining was significantly ($p < 0.001$) greater for [Cu(Dp44mT)], [Cu(Bp44mT) and [Cu(DpC)] upon Ela co-incubation compared to these Cu(II) complexes alone (Fig. 3.10Aii,iii). This observation suggested that the LMP mediated by [Cu(Dp44mT)], [Cu(Bp44mT)] or [Cu(DpC)] was Pgp-dependent and could explain the potentiated cytotoxicity of these thiosemicarbazones in Pgp-expressing cells (Fig. 3.6). As [Cu(Ap44mT)] incubation alone did not result in LMP, it is unsurprising that co-incubation with Ela also did not significantly ($p > 0.05$) affect lysosomal integrity (Fig. 3.10Ai,ii,iii).

To further examine the involvement of Pgp in thiosemicarbazone-mediated LMP, lysosomal stability was additionally examined *via* the intracellular distribution of the soluble lysosomal enzyme, Cathepsin D, and its co-localisation with lysosomal-associated membrane protein 2 (LAMP2; Fig. 3.10B), in the presence or absence of the Pgp inhibitor, Ela (Hyafil et al., 1993; Kemper et al., 2004; Yamagishi et al.,

2013). When lysosomal membrane integrity is compromised, intra-lysosomal Cathepsin D staining will decrease due to the release of this soluble enzyme out of the lysosome into the cytosol (Jansson et al., 2015b). In contrast, LAMP2 staining will be less affected, as LAMP2 is an integral part of the damaged lysosomal membrane (Eskelinen, 2006; Kagedal et al., 2001; Roberg et al., 1999) (Fig. 3.10B).

In this study, Dp44mT and Ap44mT, were assessed since the studies above (Figs. 3.8C, D) indicate that their respective Cu(II) complexes do, and do not, induce LMP, respectively. The uncoordinated thiosemicarbazone ligands were used in these studies to determine the role of LMP in the cytotoxicity observed during the proliferation assay, which was performed over a 24 h incubation (Fig. 3.6). Hence, these conditions implementing a 24 h incubation period were utilised, as 30 min incubations with these ligands alone did not have any significant ($p > 0.05$) effect on LMP (Fig. 3.8A, B). Notably, during the longer 24 h incubation period, the activity of the ligand is assessed in terms of its ability to enter KBV1 (+Pgp) cells, bind endogenous Cu(II) to form the redox-active complex, and then induce LMP after transport into the lysosome *via* Pgp.

In these experiments, using KBV1 (+Pgp) cells either under control conditions or cells treated with Ela alone, both Cathepsin D (green; Fig. 3.10Bi) and LAMP2 (red; Fig. 3.10Bii) led to particulate staining typical of lysosomes (Jansson et al., 2015b). Moreover, due to their same lysosomal localisation, this staining was co-localised upon the electronic merge, leading to yellow, punctate fluorescence consistent with intact lysosomes (Fig. 3.10Biii), as observed in previous studies (Jansson et al.,

2015b). After a 24 h incubation with Dp44mT, the fluorescence of Cathepsin D co-localised with LAMP2 was significantly ($p < 0.001$) decreased relative to control KBV1 cells (Fig. 3.10Bi,iii,iv). In contrast, LAMP2 fluorescence was not significantly ($p < 0.05$) affected, as LAMP2 is an integral protein of lysosomal membranes, and unlike Cathepsin D, does not dissipate from lysosomes after LMP (Fig. 3.10Bii) (Eskelinen, 2006; Kagedal et al., 2001; Roberg et al., 1999). In contrast, in cells incubated with Dp44mT in the presence of Ela, the intensity of Cathepsin D and LAMP2 remained unchanged relative to the control (Fig. 3.10Bi,ii). Hence, in the presence of Dp44mT and Ela, there was markedly and significantly ($p < 0.001$) greater co-localisation of Cathepsin D and LAMP2 relative to cells incubated with Dp44mT alone (Fig. 3.10Biii). This led to a yellow punctate pattern consistent with undamaged lysosomes that retained Cathepsin D. In contrast to Dp44mT, no significant ($p > 0.05$) alteration in the co-localisation of Cathepsin D and LAMP2 was observed after incubation of KBV1 (+Pgp) cells with Ap44mT or Ap44mT + Ela when compared to the control (Fig. 3.10B).

Collectively, the results in Figure 3.10B using the Pgp inhibitor, Ela, demonstrated that thiosemicarbazone-induced LMP was dependent on Pgp activity. Furthermore, we showed that LMP was Pgp-dependent for [Cu(Dp44mT)], [Cu(Bp44mT)] and [Cu(DpC)] (Fig. 3.10A), as well as Dp44mT alone (Fig. 3.10B). In contrast, both [Cu(Ap44mT)] (Fig. 3.10A) and Ap44mT (Fig. 3.10B) had no significant ($p > 0.05$) effect on lysosomal membrane stability. Importantly, the use of both the shorter (30 min) time points for the AO studies (Fig. 3.10A) and longer time points (24 h) used for the Cathepsin D/LAMP2 studies (Fig. 3.10B) demonstrate the more potent effect of Dp44mT on LMP relative to Ap44mT.

Clearly, over 24 h there is greater opportunity for the ligand to bind endogenous Cu(II) to form redox-active complexes that can then induce LMP. Finally, it should be noted that both DpC and Bp44mT acted in an analogous manner to Dp44mT, resulting in LMP that was inhibited using Ela (Fig.3.11, 3.12).

3.3.9 Lysosomal Membrane Permeabilisation Mediated by Dp44mT, Bp44mT and DpC is Dependent on Cu(II)

As [Cu(Dp44mT)], [Cu(Bp44mT)] and [Cu(DpC)] mediated LMP (Figs. 3.8, 3.10A) in KBV1 (+ Pgp) cells, we investigated whether Cu(II) coordination was required to induce LMP or not. These experiments were performed using the non-cytotoxic Cu(II) chelator, tetrathiomolybdate (TM; Fig. 3.13) that has been shown to prevent LMP mediated by the Cu(II) complexes of Dp44mT and bis(thiosemicarbazones) by sequestering Cu(II) (Lovejoy et al., 2011; Stefani et al., 2015).

Using the lysosomal stain, AO (Lovejoy et al., 2011; Stefani et al., 2015), we showed that the LMP mediated by [Cu(Dp44mT)], [Cu(Bp44mT) and [Cu(DpC)] over a 30 min incubation was significantly ($p < 0.001$) abrogated in the presence of the Cu chelator, TM, relative to when the Cu(II) complex was added alone (Fig. 3.13Ai,ii,iii). Of note, TM itself did not significantly ($p > 0.05$) affect lysosomal membrane integrity as demonstrated by the presence of intact AO-stained lysosomes (Fig. 3.13Ai,ii,iii), which is consistent with the low cytotoxicity of this Cu chelator (Lovejoy et al., 2011; Stefani et al., 2015). Therefore, these results reveal that Cu(II) chelation by Dp44mT, Bp44mT and DpC was essential in order for LMP to occur. In contrast,

[Cu(Ap44mT)] did not mediate LMP, and thus, co-incubation with TM had no effect on lysosomal integrity (Fig. 3.13Ai,ii,iii).

To further examine the role of Cu(II) chelation and LMP in the cytotoxic effects of the thiosemicarbazones, conditions analogous to that used during the MTT assay (24 h/37^{o}C) were again utilised (Fig. 3.13B). Control KBV1 (+Pgp) cells stained for the lysosomal enzyme, Cathepsin D (green), and lysosomal membrane protein, LAMP2 (red), demonstrated co-localisation upon the merge to form a yellow, punctuate pattern indicative of intact lysosomes (Fig. 3.13Bi, ii, iii). Incubation of cells with TM alone had significant effect on the co-localisation of Cathepsin D and LAMP2. As shown in Figure 3.10B, KBV1 (+Pgp) cells were incubated for 24 h/37^{o}C with the structurally different thiosemicarbazones, Dp44mT and Ap44mT, which demonstrated either marked LMP or no LMP, respectively. After incubation with Dp44mT, the intensity of Cathepsin D fluorescence co-localised with LAMP2 was significantly ($p < 0.001$) reduced relative to control cells, indicating the release of soluble Cathepsin D from this organelle upon LMP (Fig. 3.13Biii).

However, in cells incubated with Dp44mT in the presence of the Cu chelator, TM, Cathepsin D and LAMP2 were co-localised, generating a yellow punctate pattern consistent with undamaged lysosomes (Fig. 3.13Bi,ii,iii). In fact, the level of Cathepsin D and LAMP2 co-localisation upon Dp44mT and TM co-incubation was comparable to control cells (Fig. 3.13Biv).

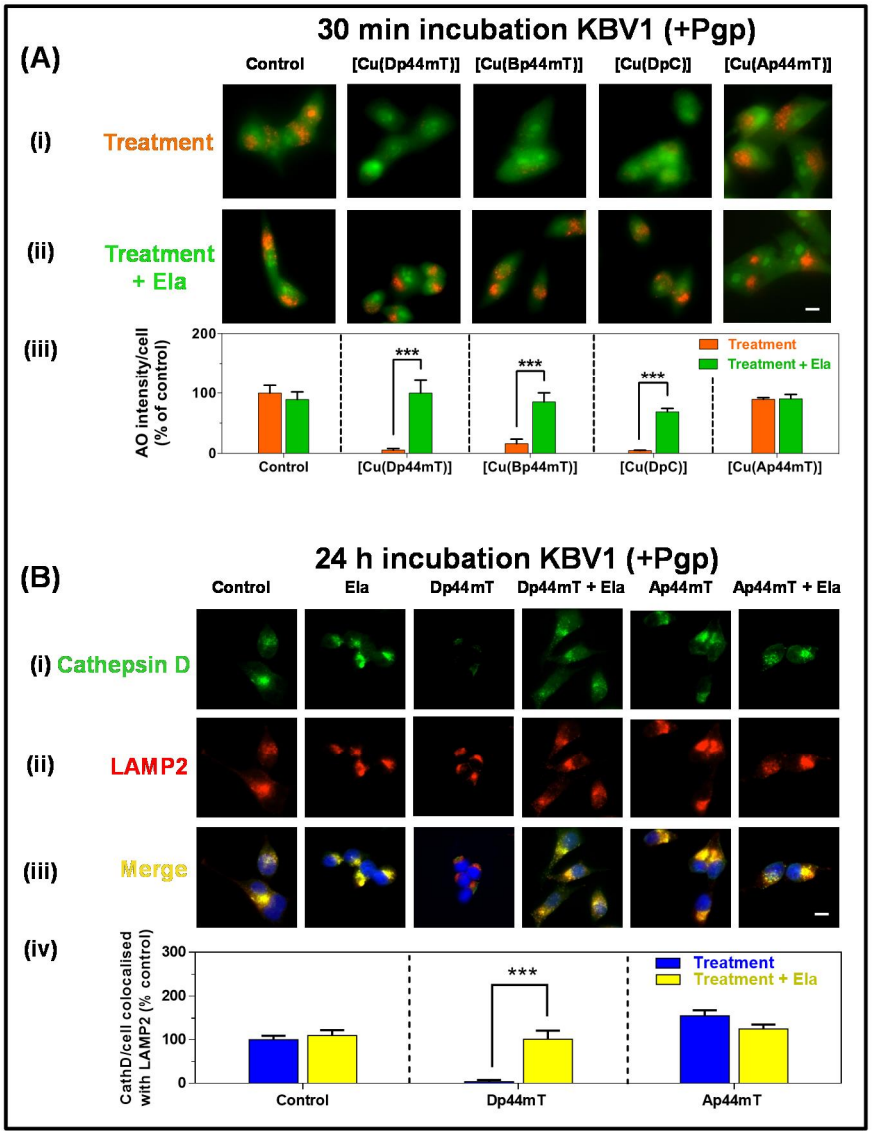

Figure 3.10. The Cu(II) complexes of Dp44mT, Bp44mT and DpC, but not Ap44mT, can induce LMP in Pgp-expressing KBV1 cells.

(A) Incubation of KBV1 (+Pgp) cells with [Cu(Dp44mT)], [Cu(Bp44mT)] or [Cu(DpC)] (10 ε M, 30 min/37°C), but not [Cu(Ap44mT)] (10 ε M, 30 min/37°C), results in a significant (**iii**; $p < 0.001$) increase in LMP, measured with AO as the AO intensity/cell (% control). The LMP was markedly reversed following treatment with the Pgp inhibitor, Ela (0.1 ε M) (**ii**). **(B)** The lysosomal markers, Cathepsin D (**i,** green) and LAMP2 (**ii,** red), co-localise (yellow, **iii**) upon the electronic merge. Only incubation with Dp44mT, but not Ap44mT (25 µM, 24 h/37^{o}C) in KBV1 cells (+Pgp) leads to: (**i**) a significant ($p < 0.001$) loss of lysosomal Cathepsin D; (**ii**) no marked alteration of LAMP2-stained lysosomes; and (**iii**) a decrease in yellow fluorescence upon the merge. Incubation of Dp44mT with Ela (0.1 µM) prevents Cathepsin D redistribution from LAMP2-stained lysosomes. Quantification of Cathepsin D intensity in the fluorescence images is shown in **iv**. The images in **(A and B)** are typical from 3 experiments. The quantification in **(Aiii, Biv)** are mean ± SD (3 experiments). ***, $p < 0.001$ *versus* untreated condition. Scale bar: 10 ε m.

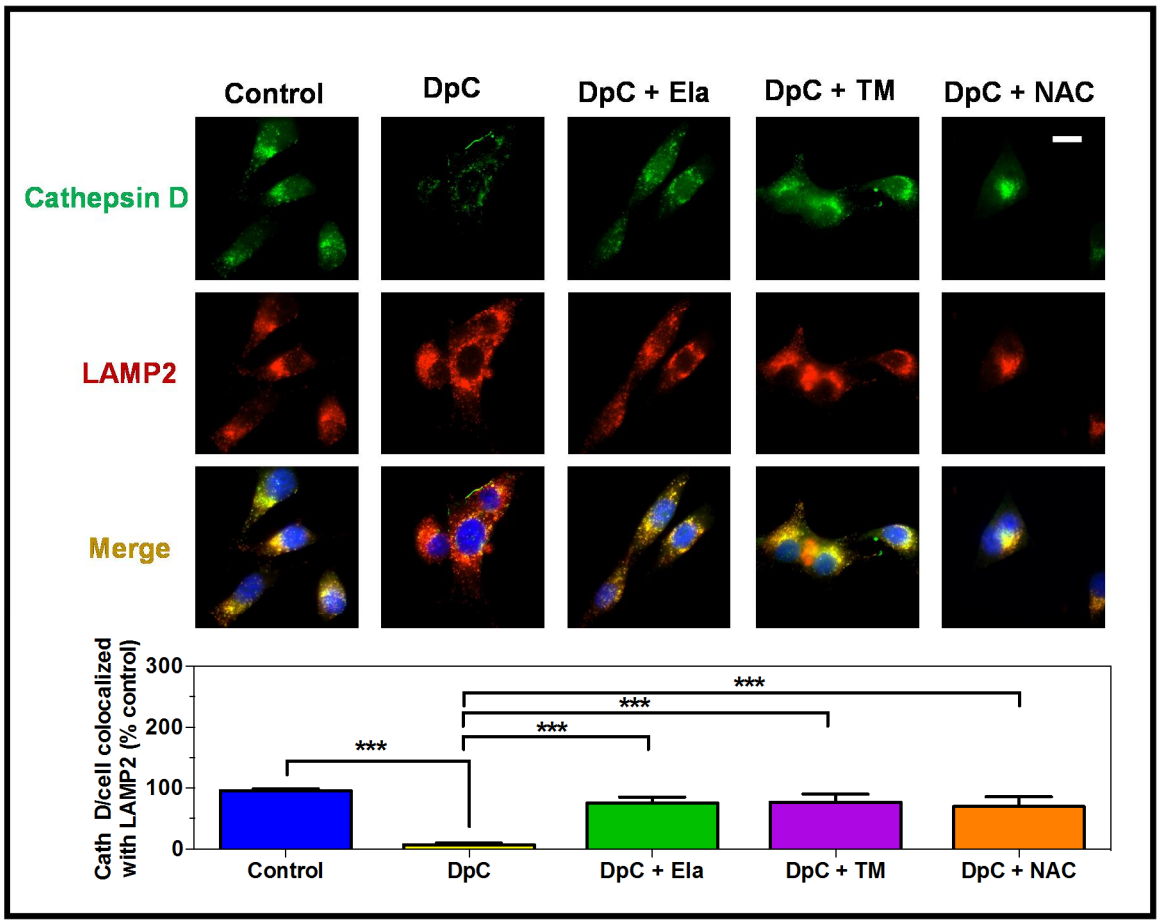

Figure 3.11. DpC-induced lysosomal membrane permeabilisation (LMP) in KBV1 cells (+Pgp) is inhibited by: the Pgp transport inhibitor Elacridar (Ela), copper-chelation using tetrathiomolybdate (TM) and the anti-oxidant, *N*-acetyl-L-cysteine (NAC).

The lysosomal markers, Cathepsin D (**i,** green) and LAMP2 (**ii,** red), co-localise (yellow, **iii**) upon the electronic merge. Only incubation of DpC (25 µM, 24 h/37^{o}C) with KBV1 cells (+Pgp) leads to: (**i**) a significant (p < 0.001) loss of lysosomal Cathepsin D; (**ii**) no marked alteration of LAMP2-stained lysosomes; and (**iii**) a decrease in yellow fluorescence upon the merge. Incubation of DpC with either the Pgp inhibitor Elacridar (Ela; 0.1 µM), the copper chelator tetrathiomolybdate (TM; 10 µM), or the anti-oxidant and cellular GSH precursor, *N*-acetyl-L-cysteine (NAC; 5 mM), prevents Cathepsin D redistribution from LAMP2-stained lysosomes. Quantification of Cathepsin D intensity in the fluorescence images is shown in **iv**. The images are typical from 3 experiments. The quantitation in **iv** is mean ± SD (3 experiments). ***, p < 0.001 *versus* untreated condition. Scale bar: 10 ε m.

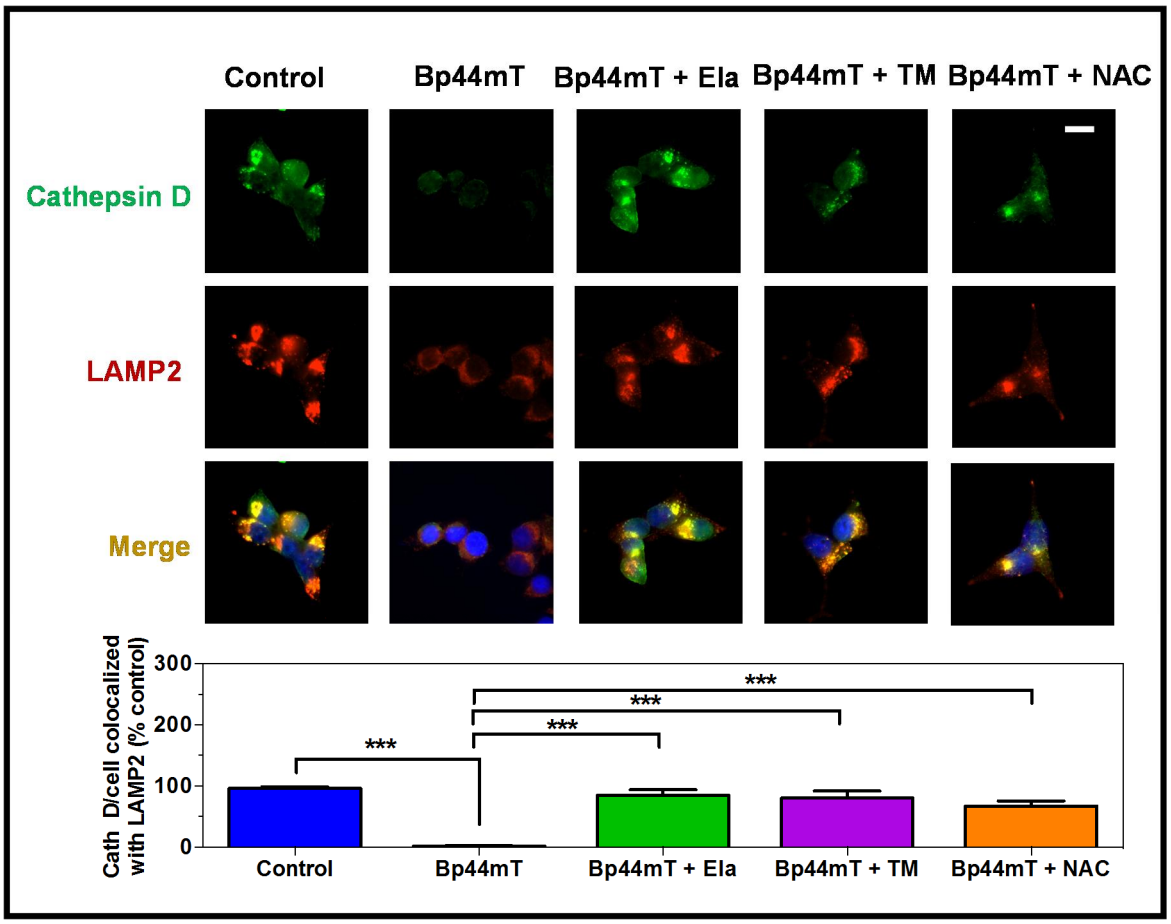

Figure 3.12. Bp44mT-induced lysosomal membrane permeabilisation (LMP) in KBV1 cells (+Pgp) is inhibited by: the Pgp transport inhibitor Elacridar (Ela), copper-chelation using tetrathiomolybdate (TM) and the anti-oxidant, *N*-acetyl-L-cysteine (NAC).

The lysosomal markers, Cathepsin D (**i,** green) and LAMP2 (**ii,** red), co-localise (yellow, **iii**) upon the electronic merge. Only incubation of Bp44mT (25 µM, 24 h/37^{o}C) with KBV1 cells (+Pgp) leads to: (**i**) a significant (p < 0.001) loss of lysosomal Cathepsin D; (**ii**) no marked alteration of LAMP2-stained lysosomes; and (**iii**) a decrease in yellow fluorescence upon the merge. Incubation of Bp44mT with either the Pgp inhibitor Elacridar (Ela; 0.1 µM), the copper chelator tetrathiomolybdate (TM; 10 µM), or the anti-oxidant and cellular GSH precursor, *N*-acetyl-L-cysteine (NAC; 5 mM), prevents Cathepsin D redistribution from LAMP2-stained lysosomes. Quantification of Cathepsin D intensity in the fluorescence images is shown in **iv**. The images are typical from 3 experiments. The quantitation in **iv** is mean ± SD (3 experiments). ***, p < 0.001 *versus* untreated condition. Scale bar: 10 ε m.

In contrast to Dp44mT (Fig. 3.13Biv), no significant ($p > 0.05$) alteration in the co-localisation of Cathepsin D and LAMP2 was observed using KBV1 cells upon incubation with Ap44mT in the presence or absence of TM in comparison to control cells (Fig. 3.13B), suggesting that LMP did not occur. In contrast to Dp44mT (Fig. 3.13Biv), no significant ($p > 0.05$) alteration in the co-localisation of Cathepsin D and LAMP2 was observed using KBV1 cells upon incubation with Ap44mT in the presence or absence of TM in comparison to control cells (Fig. 3.13B), suggesting that LMP did not occur.

It is notable that Ap44mT implemented at a 10-fold lower concentration than that used herein was observed to induce LMP in the presence of Cu(II) in previous studies using human SK-N-MC neuroepithelioma cells (Al-Eisawi et al., 2016). This result suggests that the KBV1 cells used herein were much more resistant to Ap44mT-mediated LMP relative to SK-N-MC cells and indicate that differences in their ability to handle oxidative stress and their overall sensitivity to thiosemicarbazones may contribute to this effect (Al-Eisawi et al., 2016; Jansson et al., 2015a). The important point is that the propensity to induce LMP was far more marked with Dp44mT relative to Ap44mT.

The results in Figure 3.13 illustrated that Cu(II) chelation by Dp44mT, Bp44mT and DpC was necessary for LMP in Pgp-expressing KBV1 cells. This was true for [Cu(Dp44mT)], [Cu(Bp44mT) and [Cu(DpC)], as well as Dp44mT alone. Indeed, the Dp44mT ligand was able to mediate Cu(II)-dependent LMP after a 24 h incubation (Fig. 3.13B) relative to after 30 min when it could not (Fig. 3.8A, B).

This difference likely occurred as Dp44mT must enter the cell, bind endogenous Cu(II) and then form sufficient redox active complex within the lysosome in order to induce LMP. Regardless of the presence of Cu(II) or the incubation period used (*i.e.*, 30 min; Figs. 3.8C, D, 3.10A, 3.13A) or 24 h (Figs. 3.10B, 3.13B), Ap44mT was unable to induce appreciable LMP, suggesting that structural differences in the ligands played an important role in the ability of thiosemicarbazones to mediate Cu(II)-dependent LMP in Pgp-expressing cells. Significantly, DpC and Bp44mT behaved in a similar manner to Dp44mT, resulting in LMP that was inhibited using TM (Figs. 3.11, 3.12).

3.3.10 Lysosomal Membrane Permeabilisation Mediated by Dp44mT, Bp44mT, or DpC is Dependent on Redox Stress

The generation of ROS, due to redox cycling of metal complexes, is known to damage the membrane lipid bilayer, such as the lysosomal membrane (Ollinger and Brunk, 1995; Valko et al., 2007). Notably, [Cu(Dp44mT)], [Cu(Bp44mT) and [Cu(DpC)] mediated H_2DCF oxidation in cells within 30 min, while [Cu(Ap44mT)] showed less activity (Fig. 3.9). Therefore, the role of cellular ROS generated by these [Cu(II)(thiosemicarbazones)] to result in LMP was assessed. These studies were performed using the anti-oxidant and cellular GSH precursor, *N*-acetyl-L-cysteine (NAC), which enhances the production of GSH by cells and prevents LMP mediated by the Cu(II) complexes of Dp44mT and bis(thiosemicarbazones) (Lovejoy et al., 2011; Stefani et al., 2015). While [Cu(Dp44mT)], [Cu(Bp44mT)] and [Cu(DpC)] resulted in a significant ($p < 0.001$) decrease in red fluorescence associated with AO-stained lysosomes relative to the control, co-treatment with NAC prevented [Cu(II)(thiosemicarbazone)]-mediated lysosomal damage (Fig. 3.14A).

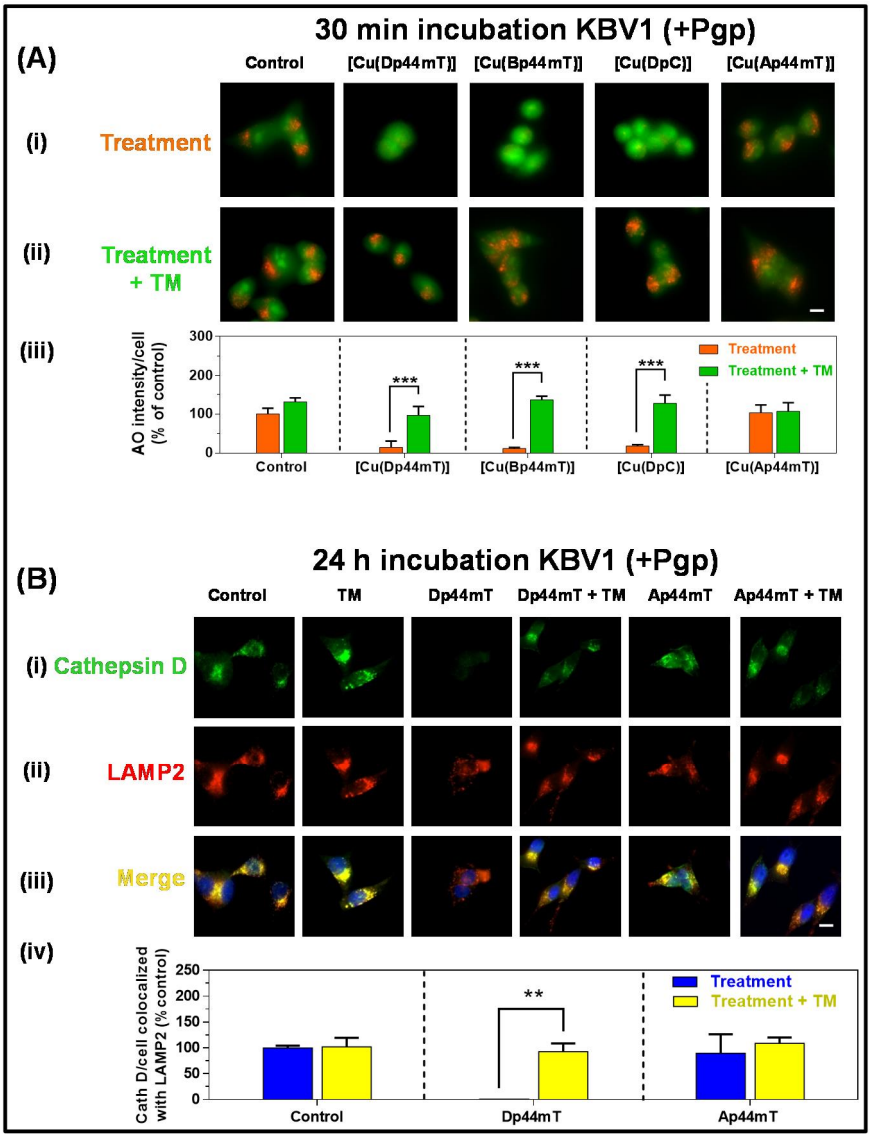

Figure 3.13. Cu(II) chelation by the non-toxic Cu(II) chelator, tetrathiomolybdate (TM), prevents: (A) LMP by Dp44mT; and (B) the release of Cathepsin D from LAMP2-stained lysosomes.

Treatment of KBV1 (+Pgp) cells with [Cu(Dp44mT)], [Cu(Bp44mT)] or [Cu(DpC)] (10 ε M, 30 min/37°C), but not [Cu(Ap44mT)], mediates a significant (**iii**; $p < 0.001$) increase in LMP relative to control cells, measured with AO. The LMP was reversed following treatment with the Cu(II) chelator, TM (10 ε M) (**ii**). **(B)** The lysosomal markers, Cathepsin D (**i,** green) and LAMP2 (**ii,** red), co-localise (yellow, **iii**) upon the electronic merge. Only incubation with Dp44mT, but not Ap44mT (25 µM, 24 h/37^{o}C) in KBV1 cells (+Pgp) leads to: (**i**) a significant ($p < 0.001$) loss of lysosomal Cathepsin D; (**ii**) no marked alteration of LAMP2-stained lysosomes; resulting in (**iii**) decreased yellow fluorescence upon the merge relative to the control. Incubation of Dp44mT with TM (25 µM) prevents Cathepsin D redistribution from LAMP2-stained lysosomes. Quantification of Cathepsin D intensity in the fluorescence images is shown in **iv**. Images in **(A)** and **(B)** are typical of 3 experiments. The quantification in **(Aiii, Biv)** are mean ± SD (3 experiments). ***, $p < 0.001$ *versus* untreated condition. Scale bar: 10 ε m.

In fact, incubation with NAC resulted in a significant ($p < 0.001$) increase in red fluorescence associated with intact AO-stained lysosomes relative to these [Cu(II)(thiosemicarbazones)] alone (Fig. 3.14A). On the other hand, as demonstrated in Figures 3.10A, 11A, [Cu(Ap44mT)] did not result in significant ($p > 0.05$) LMP, and thus, co-incubation with NAC had no significant ($p > 0.05$) effect on lysosomal integrity and was comparable to the control (Fig. 3.14A).

As in Figures 3.10B and 3.14B, lysosomal stability was further studied by observing the intracellular distribution of the soluble lysosomal enzyme, Cathepsin D, and its association with lysosomal LAMP2 (Jansson et al., 2015b), after incubating Pgp-expressing KBV1 cells with Dp44mT or Ap44mT for 24 h/37^{o}C (Fig. 3.14B). The strong co-localisation of Cathepsin D with LAMP2, was observed as a punctate, yellow fluorescence in control cells and was significantly ($p < 0.001$) decreased upon incubation with Dp44mT (Fig. 3.14Biii,iv). However, in cells incubated with Dp44mT in the presence of NAC, the Cathepsin D fluorescence intensity co-localised with LAMP2 was significantly ($p < 0.001$) increased compared to Dp44mT alone. This observation suggested that NAC was able to alleviate Dp44mT-mediated oxidative stress and protect lysosomes from LMP (Fig. 3.14B). In contrast to Dp44mT, no significant ($p > 0.05$) alteration in the co-localisation of Cathepsin D and LAMP2 was observed after incubation of KBV1 (+Pgp) cells with Ap44mT in the presence or absence of NAC (Fig. 3.14B).

This finding is consistent with our previous results (Fig. 3.9), which suggested that the Cu(II) complex of Ap44mT generated significantly lower levels of ROS than

Dp44mT, which may be insufficient to damage the lysosomal membrane and result in LMP. Notably, both DpC and Bp44mT behaved similarly to Dp44mT, resulting in LMP that was inhibited using NAC (Figs. 3.11, 3.12).

The results in Figure 3.14 suggest that, in addition to acting as Pgp substrates and Cu(II) chelators (Figs. 3.6-11), the redox cycling of the [Cu(II)(thiosemicarbazones)] and the resultant formation of ROS was vital in their mechanism of action.

3.4 Conclusions

As described previously, all ligands included in this study were Ŭ-*N*-heterocyclic thiosemicarbazones with each analogue containing substitutional variations at the: **(1)** imine carbon and **(2)** terminal N4 atom. Critically, the identity of the substituent at the imine position proved to be pivotal in determining the ability of the thiosemicarbazone to form Cu(II) complexes that mediated sufficient ROS formation and subsequent LMP in Pgp-expressing cells. Only those analogues derived from di-2-pyridylketone or 2-benzoylpyridine, namely, Dp44mT (Fig. 3.1B), DpC (Fig. 3.1C), or Bp44mT (Fig. 3.1D), contain the inductively electron-withdrawing 2-pyridyl or phenyl moieties (relative to hydrogen) at the imine position which result in marked LMP (Fig. 3.15A) and the death of Pgp-expressing cells (Fig. 3.6). In contrast, Ap44mT (Fig. 3.1E) has the inductively electron-donating methyl substituent (relative to hydrogen) positioned at the imine carbon, while a hydrogen is located at the imine

carbon of 3-AP (Fig. 3.1A), and these substitutions resulted in no LMP (Fig. 3.15B) and led to no enhanced death in Pgp-expressing cells (Fig. 3.6).

Significantly, the Cu(II) complexes of Dp44mT, Bp44mT and DpC were observed to have potent, Pgp-dependent anti-proliferative activity (Fig. 3.6) and mediate LMP in Pgp-over-expressing KBV1 cells (Figs. 3.8C, D). All assessed ligands and their Cu(II) or Fe(III) complexes were found to act as Pgp substrates (Fig. 3.7) and this suggested that their ability to be transported into the lysosome by Pgp was not the only factor that was significant in terms of their ability to mediate LMP (Figs. 3.8, 3.10) or cytotoxicity (Fig. 3.6) in KBV1 cells.

One such additional factor is lipophilicity, which is well known to be involved in the efficacy of these and closely related ligands to transverse membranes and enter cells to chelate metal ions (Richardson et al., 1995; Stefani et al., 2011). Moreover, while all the thiosemicarbazones were Pgp substrates, generally the more lipophilic compounds induced greater Pgp-ATPase activity (*i.e.*, ligands < Cu(II) complexes < Fe(III) complexes; Fig. 3.7), and this is in accordance with the fact that Pgp prefers lipophilic substrates for transport (Kimura et al., 2004; Schmid et al., 1999; Seelig and Landwojtowicz, 2000). Hence, the lower lipophilicity of the ligand, Ap44mT, may have potentially contributed to its reduced entry into the cell, its slightly lower activity as a Pgp substrate (relative to Dp44mT, Bp44mT and DpC; Fig. 3.7), and its decreased ability to induce LMP to overcome resistance.

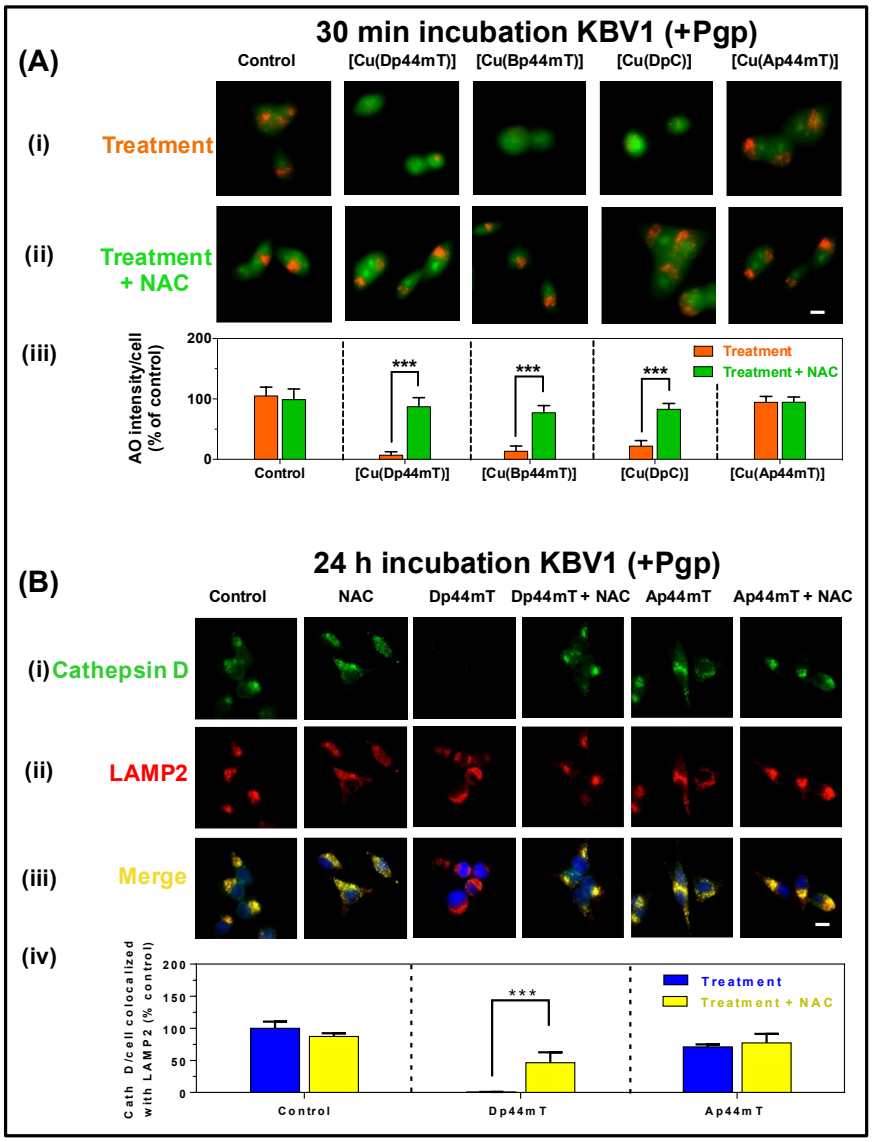

Figure 3.14. The anti-oxidant and glutathione precursor, NAC, prevents the LMP in KBV1 (+Pgp) cells induced by Dp44mT, Bp44mT or DpC or their Cu(II) complexes

(A) Incubation of KBV1 (+Pgp) cells with [Cu(Dp44mT)], [Cu(Bp44mT)] or [Cu(DpC)] (10 ε M, 30 min/37°C), but not [Cu(Ap44mT)], mediates a significant (**iii**; $p < 0.001$) increase in LMP, measured with AO as the AO intensity/cell (% of control). The LMP was reversed following incubation with the anti-oxidant, NAC (5 mM) (**ii**). **(B)** The lysosomal markers Cathepsin D (**i,** green) and LAMP2 (**ii,** red) co-localise (yellow, **iii**) upon merging. Only incubation with Dp44mT, but not Ap44mT (25 μM, 24 h/37^{o} C) in KBV1 cells (+Pgp) leads to: (**i**) a significant ($p < 0.001$) loss of lysosomal Cathepsin D relative to the control; (**ii**) no marked effect on LAMP2-stained lysosomes; and (**iii**) decreased yellow fluorescence upon the electronic merge. Incubation of Dp44mT with NAC (5 mM) prevents Cathepsin D redistribution from LAMP2-stained lysosomes. Quantification of Cathepsin D intensity in the fluorescence images is shown in **iv**. Images in **(A)** and **(B)** are typical of 3 experiments. The quantification in **(Aiii, Biv)** are mean ± SD (3 experiments). ***, $p < 0.001$ *versus* untreated condition. Scale bar: 10 ε m.

Another crucial factor that was identified in this study was the influence of inductive effects of substituents close to the metal-ligating site (Fig. 3.15). Our previous investigations have also demonstrated the ability of the inductive effects of substituents at the imine position of thiosemicarbazones to influence the electrochemistry of their resultant metal complexes (Jansson et al., 2010b; Kalinowski et al., 2007; Richardson et al., 2009). This is undoubtedly due to the close proximity of the imine position to the metal centre (Jansson et al., 2010b; Kalinowski et al., 2007; Richardson et al., 2009). The inclusion of inductively electron-withdrawing groups at the imine position results in Fe(III) or Cu(II) complexes with higher redox potentials (***e.g.,*** metal complexes of Dp44mT, DpC or Bp44mT) relative to the resultant Fe(III) or Cu(II) complexes derived from ligands containing inductively electron-donating substituents at the imine position (***e.g.,*** metal complexes of Ap44mT) (Jansson et al., 2010b; Kalinowski et al., 2007; Richardson et al., 2009). This consequently influences the redox behaviour of their metal complexes.

Our laboratories have also previously demonstrated the increased ability of [Cu(Dp44mT)] to mediate the formation of ROS relative to [Cu(Ap44mT)] both in cells and cell-free systems (Jansson et al., 2010b). Moreover, the [Cu(Dp44mT)] complex mediated increased levels of cellular oxidative stress relative to [Cu(Ap44mT)], as demonstrated by the greater decrease in the GSH/GSSG ratio mediated by [Cu(Dp44mT)] (Jansson et al., 2010b). This effect was consistent with the higher redox potentials of the [Cu(Dp44mT)] complex relative to [Cu(Ap44mT)] (Jansson et al., 2010b). The current study demonstrated the ability of [Cu(Dp44mT)], [Cu(Bp44mT)] and [Cu(DpC)], to catalyse the marked oxidation of H_2DCF to DCF in

cells (Fig. 3.9) and this suggested their ability to generate significant quantities of cytotoxic ROS that can lead to LMP (Figs. 3.8, 3.10-12), and induce cell death.

While [Cu(Ap44mT)] also mediated the oxidation of H_2DCF, it was significantly less redox-active than [Cu(Dp44mT)], [Cu(Bp44mT)], or [Cu(DpC)], suggesting that the lack of LMP in response to [Cu(II)(Ap44mT)] (Figs. 3.8C, D) may be related to the less potent redox activity of the complex. These results are in agreement with previous studies, suggesting that the inductively electron-withdrawing substituents located at the imine position of Dp44mT, Bp44mT and DpC result in the formation of Cu(II) complexes with redox potentials that lie in an optimal window that allow for a redox cycling mechanism to become established (Bernhardt et al., 2009; Jansson et al., 2010b; Lovejoy et al., 2012). This property results in Cu(II) complexes that can catalyse the production of ROS (Fig. 3.9) and the subsequent induction of LMP (Figs. 3.8, 3.9-11). In comparison, the inductively electron-donating effects of the imine methyl group of Ap44mT resulted in a Cu(II) complex with a lower redox potential (Jansson et al., 2010b) that lies outside of this optimal window, preventing sufficient generation of ROS (Fig. 3.9) to mediate LMP (Figs. 3.8, 3.10-12). This redox behaviour, in combination with the lower lipophilicity of Ap44mT, may play an important role in the inability of Ap44mT to mediate LMP relative to Dp44mT, Bp44mT, or DpC, leading to: **(1)** decreased passage of Ap44mT through the cell membrane; **(2)** decreased transport of Ap44mT by Pgp into the lysosome; and **(3)** decreased ROS generation by the Cu(II) complex of Ap44mT in the lysosome (Fig. 3.15B).

It is of interest to note the difference between the Cu(II) and Fe(III) complexes of these thiosemicarbazones in terms of the failure to induce LMP (Fig. 3.8C,D). This occurred despite the fact that the Fe(III) complexes are Pgp substrates (Fig. 3.7) and that at least some of these compounds are redox active and cytotoxic. The difference in their ability to induce LMP is probably related to the efficacy of ROS generation that we demonstrate is far more pronounced for the Cu(II) complexes than the respective (Fe(III) complexes (Fig. 3.9). Hence, the appropriate redox potentials of the Cu(II) complexes of these ligands, relative to the Fe(III) complexes, leads to marked ROS generation that is crucial for inducing LMP. In fact, our laboratory has previously demonstrated that much longer incubations of cells with Fe(III) complexes than Cu(II) complexes are required before LMP is observed, namely 5 min for [Cu(Dp44mT)] relative to 24 h for [Fe(Dp44mT)$_2$]. Importantly, the current studies assessed only short incubations (30 min) of the Fe(III) and Cu(II) complexes, and thus, only the Cu(II) complexes with greatest ROS generating activity (namely those of Dp44mT, Bp44mT and DpC) demonstrated LMP (Figs. 3.8C,D, 3.9).

In summary, in order to induce LMP in Pgp-expressing cells and overcome drug resistance, our studies demonstrate that this general group of thiosemicarbazones must possess five characteristics, namely: **(1)** inductively electron-withdrawing substituents at the imine carbon; **(2)** high relative lipophilicity; **(3)** Pgp substrate activity; **(4)** Cu(II) chelation efficacy; and **(5)** the induction of ROS generation (Fig. 3.15). Based on these studies further ñfine tuningò of thiosemicarbazone structural features could lead to more active agents to overcome multi-drug resistance *via* the

exploitation of lysosomal Pgp to induce LMP and the death of resistant tumour cells that are a major problem for cancer treatment.

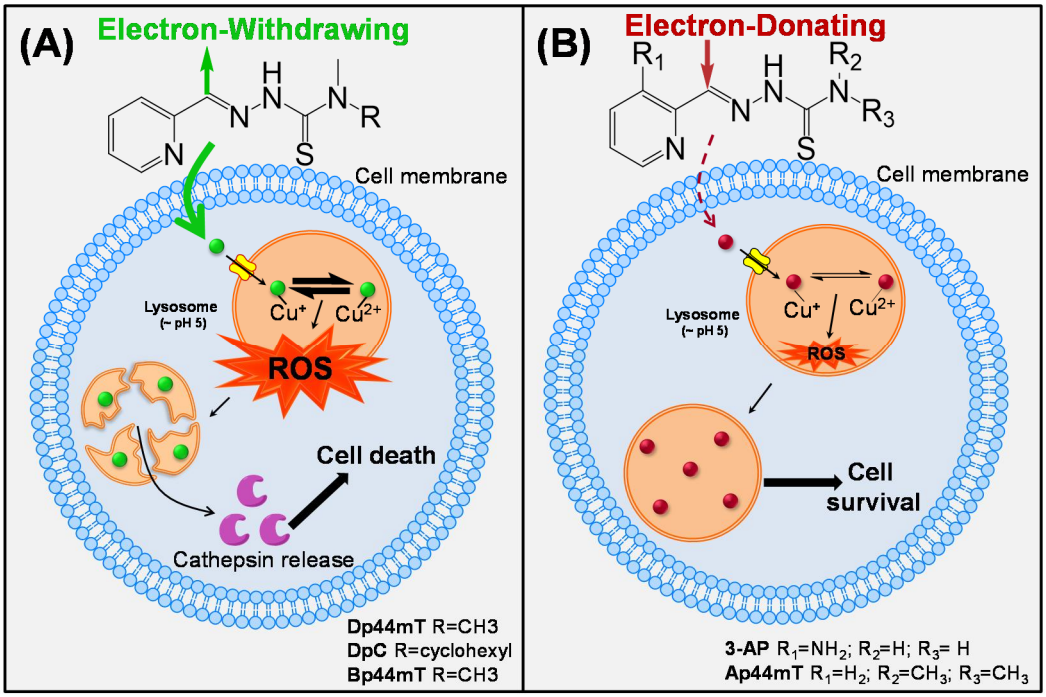

Figure 3.15. Schematic of the differences in structural features of thiosemicarbazones that either have a marked effect in terms of inducing LMP (*e.g.*, as observed for Dp44mT, Bp44mT and DpC; 11A), or not (*i.e.*, Ap44mT, 3-AP; 11B).

Key properties of thiosemicarbazones that enable LMP which is crucial for overcoming Pgp-mediated resistance in tumour cells include: **(1)** electron-withdrawing inductive effects at the imine carbon; **(2)** lipophilicity; **(3)** being a Pgp substrate; **(4)** Cu(II) chelation; and **(5)** the generation of ROS. **(A)** For Dp44mT, Bp44mT and DpC, the presence of two aromatic substituents at the imine carbon leads to an electron-withdrawing inductive effect. This results in higher redox potentials which are within an ñoptimal windowò for oxidising biological substrates and generating ROS. The increased lipophilicity enhances transport through biological membranes and transport *via* Pgp into the lysosome. **(B)** In contrast, for 3-AP or Ap44mT, the presence an aromatic substituent and either a H-atom or an inductively electron-donating methyl, respectively, results in lower redox potentials that are less avid in terms of oxidising biological substrates and generating ROS. At the same time, the decreased relative lipophilicity of 3-AP or Ap44mT relative to Dp44mT, Bp44mT and DpC, results in decreased membrane permeability and lower activity as a Pgp substrate, and thus, decreased ability to induce LMP and overcome resistance. In contrast to all the agents above, Bp2mT, possessed a methyl group at N2 (Fig. 3.1F), preventing its ability to form Cu(II) complexes that inhibits ROS generation essential for LMP.

Chapter 4 - Zinc(II)-Thiosemicarbazone Complexes Are Localised to the Lysosomal Compartment Where They Transmetallate with Copper Ions to Induce Cytotoxicity

(Taken from Stacy *et al* (2016) *J. Med. Chem*.)

4.1 Introduction

Since their origin as potential anti-tuberculosis agents (Domagk et al., 1946; Donovick et al., 1950), thiosemicarbazones and their metal complexes have been found to have a broad range of therapeutic uses (Hamre et al., 1950; Klayman et al., 1979; Liberta and West, 1992). The demonstrated anti-viral activity (Brownlee and Hamre, 1951; Hamre et al., 1950; Shipman et al., 1986) of thiosemicarbazones led researchers to investigate their possible use as anti-cancer agents (Brockman et al., 1956). Indeed, 2-formylpyridine thiosemicarbazone was the first of this class to demonstrate potent anti-cancer activity (Brockman et al., 1956). This property has since led this class of compounds to become the focus of extensive research and development.

The anti-cancer efficacy of thiosemicarbazones was initially described to be due to their action as inhibitors of ribonucleotide reductase (Reichard and Ehrenberg, 1983; Sartorelli et al., 1970), which catalyses the rate-limiting step of DNA synthesis.

Subsequent studies demonstrated that effect represented only a fraction of their activity with the formation of redox-active metal complexes that generate ROS being of considerable significance to their mechanism of action (Richardson et al., 2006; Yu et al., 2009b; Yuan et al., 2004) Furthermore, early research demonstrated that *N*-heterocyclic thiosemicarbazones that utilise the N-N-S donor system (French and Blanz, 1966) in the formation of complexes with transition metals have increased cytotoxicity both *in vitro* (Antholine et al., 1976; Baker et al., 1992; Blanz et al., 1970; Crim and Petering, 1967; Saryan et al., 1979) and *in vivo* (Petering et al., 1967). One such thiosemicarbazone that was developed for cancer treatment was 3-AP, which has entered greater than 20 multi-centre clinical trials (Knox et al., 2007; Merlot et al., 2013; Odenike et al., 2008; Traynor et al., 2010). However, 3-AP has suffered multiple problems, including low efficacy in some tumour-types and serious side effects, including methaemoglobinaemia (Knox et al., 2007; Merlot et al., 2013; Odenike et al., 2008; Traynor et al., 2010).

Over the last 20 years, our laboratory has developed ligands as anti-cancer agents (Baker et al., 1992; Becker et al., 2003; Darnell and Richardson, 1999; Richardson et al., 1995; Richardson and Milnes, 1997). Through extensive structure-activity relationship studies, the DpT series was designed by including the di-2-pyridylketone moiety into a structural backbone derived from previous aroylhydrazones (Becker et al., 2003; Bernhardt et al., 2003; Richardson et al., 2006; Yuan et al., 2004). The DpT analogues showed potent anti-tumour activity and anti-metastatic activity both *in vitro* and *in vivo* (Chen et al., 2012; Liu et al., 2012; Lovejoy et al., 2012; Richardson et al., 2006; Whitnall et al., 2006; Yuan et al., 2004). The best characterised member of the DpT analogues, Dp44mT (Fig. 3.1A), has been demonstrated to target the

lysosome *via* ñhijackingò of the multidrug resistance pump, Pgp (Gutierrez et al., 2014; Jansson et al., 2015b; Lovejoy et al., 2011; Seebacher et al., 2016a). Once inside the lysosome, Dp44mT redox cycles with copper ions to produce ROS that induce LMP and apoptosis (Gutierrez et al., 2014; Jansson et al., 2015b; Lovejoy et al., 2011).

Importantly, the anti-proliferative effects of Dp44mT are significantly greater than 3-AP and demonstrate improved tolerability (Whitnall et al., 2006). However, the cardiac fibrosis induced by high, non-optimal doses of Dp44mT (Whitnall et al., 2006) led to the design and synthesis of novel thiosemicarbazones, including the second generation of DpT analogues and the ApT series, such as Ap44mT (Fig. 4.1A), that also showed marked and selective anti-tumour activity *in vitro* and *in vivo* (Kowol et al., 2007a; Kowol et al., 2007b; Lovejoy et al., 2012; Richardson et al., 2009).

The second generation of DpT analogues, in which the terminal H at N4 was replaced with an alkyl group, showed particular promise (Kovacevic et al., 2011; Lovejoy and Richardson, 2002). Of these ligands, DpC (Fig. 4.1A) was identified as the lead agent (Kovacevic et al., 2011; Lovejoy et al., 2012) and possessed many advantages over Dp44mT, including: **(1)** greater anti-tumour activity than Dp44mT *in vivo* against tumour xenografts (Kovacevic et al., 2011; Lovejoy et al., 2012); (**2)** markedly improved tolerability when administered orally, as well as intravenously compared to Dp44mT that is toxic when given orally (Lovejoy et al., 2012; Yu et al., 2012); **(3)** unlike Dp44mT, DpC does not induce oxidation of oxyhaemoglobin to

methaemoglobin in erythrocytes (Quach et al., 2012); **(4)** DpC demonstrates a markedly greater plasma half-life in the rat, namely 10.7 h *versus* 1.7 h for Dp44mT (Sestak et al., 2015); **(5)** the anti-tumour efficacy of DpC exceeds that of gemcitabine (the ñgold standardò chemotherapy for pancreatic cancer) *in vivo* against pancreatic xenografts (Kovacevic et al., 2011) and **(6)** DpC does not induce cardiac fibrosis in nude mice even when given at markedly higher doses than Dp44mT (Kovacevic et al., 2011; Lovejoy et al., 2012). Significantly, due to these favourable properties, DpC was commercialised and has entered clinical trials in 2016 (ClinicalTrials.gov Identifier NCT02688101) for the treatment of advanced and resistant cancers (Jansson et al., 2015a).

As with other thiosemicarbazones (Antholine et al., 1976; Blanz et al., 1970; Cowley et al., 2005; Crim and Petering, 1967; Kowol et al., 2010; Petering et al., 1967; Saryan et al., 1979; Van Giessen et al., 1973), it was observed that the DpT and ApT series form Zn(II) and Cu(II) complexes, of which the Cu(II) complexes potently mediate cancer cell death (Jansson et al., 2010a; Lovejoy et al., 2011; Richardson et al., 2006; Richardson et al., 2009; Yuan et al., 2004). Indeed, some thiosemicarbazone complexes of transition metals, such as Cu(II) and zinc (Zn(II)) complexes, generally exhibit greater anti-neoplastic activities both *in vitro* and *in vivo* than the thiosemicarbazones alone (Antholine et al., 1976; Blanz et al., 1970; Cowley et al., 2005; Crim and Petering, 1967; Jansson et al., 2010a; Kalinowski et al., 2007; Kowol et al., 2010; Lovejoy et al., 2011; Petering et al., 1967; Richardson et al., 2006; Richardson et al., 2009; Saryan et al., 1979; Van Giessen et al., 1973; Yuan et al., 2004). While the mechanism of action of such thiosemicarbazones have been examined previously (Jansson et al., 2015b; Kovacevic et al., 2011; Lovejoy et

al., 2011; Richardson et al., 2009; Sartorelli et al., 1970), relatively little has been done to unequivocally determine their subcellular distribution (Cowley et al., 2005; Kowol et al., 2010). Recent reports have demonstrated that the Zn(II) complexes of some mono and bis(thiosemicarbazones) possess intrinsic fluorescence, presenting an opportunity to examine their intracellular distribution that enables further insight into their mechanism of action (Cowley et al., 2005; Dayal et al., 2011; Kowol et al., 2010; Lim et al., 2010; Pascu et al., 2007; Pascu et al., 2008). For example, [Zn(3-AP)Cl_2] has been shown to localise to the nucleoli of colon adenocarcinoma SW480 cells (Kowol et al., 2010).

Herein, in order to examine the subcellular distribution of our potent thiosemicarbazones, we synthesised and characterised their Zn(II) complexes based on their previously demonstrated marked and selective anti-cancer activity (Kalinowski et al., 2007; Lovejoy et al., 2012; Richardson et al., 2009; Yuan et al., 2004). Dp44mT and DpC were included as our lead compounds, and Ap44mT was added as a structurally different thiosemicarbazone to enable elucidation of information on structure-activity relationships. Their anti-proliferative effects were examined in several tumour cell-types, and importantly the Zn(II) complexes showed significantly greater cytotoxicity than their thiosemicarbazone ligands alone. For the first time, the subcellular localisation of the [Zn$(DpC)_2$]$(ClO_4)_2$ complex was directly examined and demonstrated a predominantly lysosomal pattern of distribution. Importantly, we also show that [Zn$(Dp44mT\text{-}H)_2$], [Zn$(Ap44mT\text{-}H)_2$] and [Zn$(DpC)_2$]$(ClO_4)_2$ transmetallates with lysosomal copper ions to form redox-active Cu(II) complexes that mediate LMP and cytotoxicity.

4.3 Results and Discussion

4.3.1 Synthesis and Characterisation of Novel Zn(II)-Thiosemicarbazone Complexes

A series of Zn(II) complexes were prepared from Dp44mT, Ap44mT and DpC·HCl at 1:1 (Fig. 4.1B) and 1:2 (Fig. 4.1C) (Zn(II)/ligand) molar ratios. The 1:1 Zn(II) complexes were synthesised *via* the reaction of equimolar amounts of the thiosemicarbazone and $ZnCl_2$ in ethanol, while the 1:2 Zn(II) complexes were obtained by reacting 2 equivalents of the corresponding thiosemicarbazone with 1 equivalent of $Zn(ClO_4)_2 \cdot 6H_2O$ in ethanol in the presence of triethylamine. All complexes were characterised by ^{1}H and ^{13}C NMR, IR, UV and mass spectrometry and their purity was assessed by elemental analysis and determined to be >95%.

As expected, Dp44mT and Ap44mT formed neutral 1:2 (Zn(II)/ligand) complexes with $Zn(ClO_4)_2 \cdot 6H_2O$ upon deprotonation of the NH-C=S moiety in the presence of the base, triethylamine (Fig. 4.1C). In contrast, even in the presence of excess base, DpC·HCl formed a cationic 1:2 (Zn(II)/ligand) complex with perchlorate counter ions (Fig. 4.1C), which is evident from the observation of strong vibrational stretching at 1090 cm^{-1}.

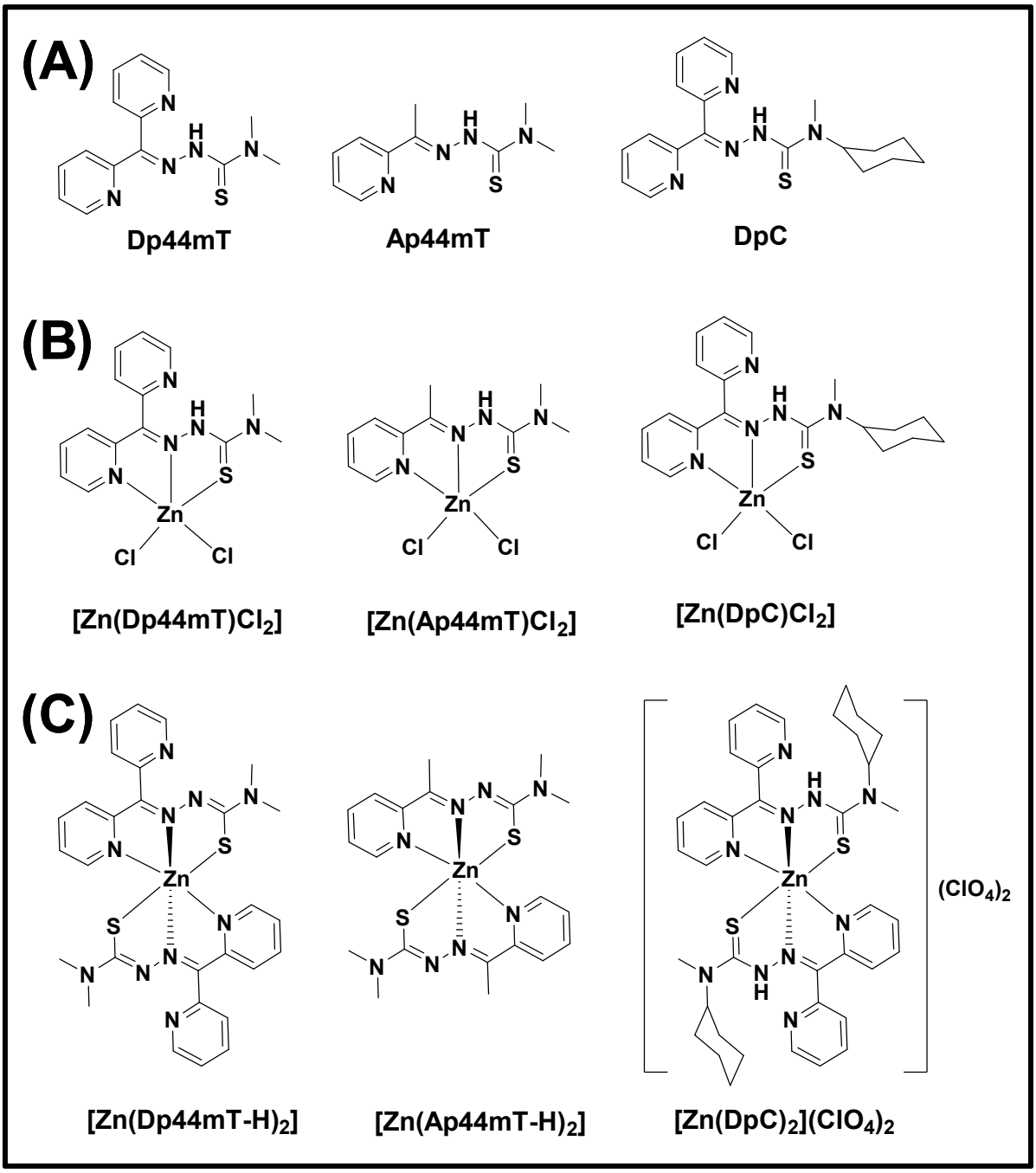

Figure 4.1. Line drawings of the thiosemicarbazones and their 1:1 and 1:2 Zn(II) complexes relevant to this investigation.

(A) From left to right: Dp44mT, Ap44mT, DpC·HCl **(B)** $[Zn(Dp44mT)Cl_2]$, $[Zn(Ap44mT)Cl_2]$, $[Zn(DpC)Cl_2]$ **(C)** $[Zn(Dp44mT\text{-}H_2]$, $[Zn(Dp44mT\text{-}H_2]$, $[Zn(DpC)_2(ClO_4)_2]$

4.3.2 X-ray Crystallography

Four of the Zn(II) complexes were structurally characterised by single crystal X-ray analysis as the structure of these compounds provides important information that can be utilised to understand their biological activity (Jansson et al., 2010a; Lovejoy et al., 2012; Richardson et al., 2006; Richardson et al., 2009). Their thermal ellipsoid plots and the summary of crystallographic data are given in Figure 4.2 and Table 4.2, respectively.

The 1:1 Zn(II)-thiosemicarbazone complex, [Zn(DpC)Cl_2] (Fig. 4.2A) crystallised in ethanol, exhibits a five-coordinate geometry comprising a tridentate coordinated neutral thiosemicarbazone and two chlorido ligands. The geometry was approximately square pyramidal using the structural parameter Űdefined by Addison et al (Addison et al., 1984), (Ű = (Ŭ-ƀ)/60 where Ŭ and ƀ are the two largest coordinate angles; for square pyramidal, Ű= 0; for trigonal bipyramidal, Ű= 1), and in this case, Ű = 0.16. The axially coordinated chlorido ligand (Cl2) was significantly more strongly bound (Zn-Cl2 2.246(1) Å) than the equatorial Zn-Cl1 bond (2.287(1) Å; Fig. 4.2A). The Zn-N bond to the pyridyl ring (2.169(4) Å) was stronger than to the imine N-atom (2.201(4) Å) (Table 4.1).

This lengthening of the Zn-N bond was due to the trans influence of the Zn-Cl1 bond. There are several structurally similar dichloride Zn(II) complexes, and in all cases, the pyridyl thiosemicarbazone was coordinated in its neutral (thioamide) form (Kasuga et al., 2003; Kovala-Demertzi et al., 2006; Kowol et al., 2010; Shao et al., 2014). In [Zn(DpC)Cl_2], there is an intramolecular H-bond between the thioamide

proton attached to N3 and the non-coordinated pyridyl ring (Fig. 4.2A). Given the fact that N3 was protonated, the C=S bond is formally a double bond (1.684(5) Å) and the adjacent C-N(H) bond (C12-N3 1.365(6) Å) was consistent with a thioamide tautomer. The cyclohexyl ring exhibited rotational disorder about the N4-C bond with the two contributors being approximately equal (53%: 47%). The major contributor is shown in Figure 4.2A.

The crystallisation of the analogous Zn(II) complex of Ap44mT in DMSO resulted in the 5-coordinate complex [Zn(Ap44mT-H)(Cl)(DMSO)] (Fig. 4.2B), where the thiosemicarbazone is deprotonated at N3 and only a single chlorido ligand was present. The structure comprises two complexed molecules in the asymmetric unit, both on general positions (Fig. 4.2B). The coordination sphere of each Zn(II) ion was completed by an axially Oï bound DMSO (Fig. 4.2B). Notably, [Zn(Ap44mT-H)(Cl)(DMSO)] adopts a geometry that was more distorted away from square pyramidal (Ű=0.36) than [Zn(DpC)Cl_2] (*cf.* Fig. 4.2A to 4.2B). The equatorial Zn-Cl bond (2.2790(5) Å) was similar to the equatorial Zn-Cl bond in [Zn(DpC)Cl_2]. A notable feature was that the Zn1-N2a bond to the imine N-atom (2.100(2) Å) was much shorter than the bond to the pyridyl N-donor (2.148(2) Å). In fact, both Zn-N bonds in [Zn(Ap44mT-H)(Cl)(DMSO)] (Fig. 4.2B) were significantly shorter than those observed for [Zn(DpC)Cl_2] (Fig. 4.2A) due to the augmented ionic contribution to the coordination bonds involving the anionic thiosemicarbazone (Table 4.1). Deprotonation also affected the internal ligand bond lengths. Relative to the neutral DpC ligand in [Zn(DpC)Cl_2] (Fig. 4.2A), the C8a-S1a bond in the anionic $(Ap44mT-H)^-$ lengthened to 1.738(2) Å, while the adjacent C8-N3 bond contracted (1.327(3) Å), which was indicative of the imine-thiolate form of the ligand (Fig. 4.2B).

The structure of the 1:2 complex [Zn(Ap44mT-H)$_2$]·2CHCl$_3$ revealed a distorted octahedral geometry (Fig. 4.2C). The two thiosemicarbazone ligands coordinate in their deprotonated form *via* the *NNS* donor atoms in a meridional fashion (Fig. 4.2C). The Zn(II) ion occupied a crystallographic two-fold axis of symmetry (Fig. 4.2C). Similar 1:2 Zn(II)-thiosemicarbazone complexes have been previously reported, and in most cases, both ligands are deprotonated at the thioamide N-atom (N3 in this structure) (Bermejo et al., 2007; Bernhardt et al., 2009; Castiñeiras et al., 2002; Kovala-Demertzi et al., 2006; Li Ming et al., 2008; Li et al., 2010; Stanojkovic et al., 2010; Yang et al., 2013b). However, in some cases, the ligands are neutral, rendering the complex dicationic (Cheng et al., 2010; Kasuga et al., 2003). Deprotonation of the ligands in [Zn(Ap44mT-H)$_2$]·2CHCl$_3$ (Fig. 4.2C) leads to the same imine-thiolate form of the ligands observed in [Zn(Ap44mT-H)(Cl)(DMSO)] (Fig. 4.2B) on the basis of their C-S and C=N bond lengths (Table 4.1). The Zn-N and Zn-S coordinate bonds increase relative to [Zn(Ap44mT-H)(Cl)(DMSO)], principally due to the increase in coordination number (Table 4.1). As observed in the structure of [Zn(Ap44mT-H)(Cl)(DMSO)] (Fig. 4.2B), the Zn-N2 (imine) bond was much shorter than the Zn-N1 (pyridine) bond (Fig. 4.2C) (Table 4.1).

As crystals of the 1:2 (Zn(II)/ligand) zinc complex of Dp44mT could not be obtained with the use of Zn(ClO$_4$)$_2$·6H$_2$O in different solvents, an attempt to synthesise the same complex was conducted using ZnSO$_4$.6H$_2$O as the precursor salt. Crystals of [Zn(Dp44mT)$_2$](HSO$_4$)$_2$ were obtained from an ethanol solution and the structure is shown in Figure 4.2D. The complex cation comprised two zwitterionic ligands of Dp44mT that are deprotonated at N3, but protonated at N5 (the non-coordinated pyridine) (Fig. 4.2D). Two hydrogen sulphate anions (each disordered) balance the

charge. The protons on N5A and N5B were clearly seen in difference maps and the C-N3 and C-S1 bond lengths were consistent with the imine-thiolate form of the ligand, as found in $[Zn(Ap44mT\text{-}H)_2].2CHCl_3$ and [Zn(Ap44mT-H)(Cl)(DMSO)] (Table 4.1).

Collectively, these physical studies demonstrate that both 1:1 and 1:2 Zn(II)-thiosemicarbazone complexes can form. Although we know the chemical nature of the zinc complexes at solid state, their actual chemical species in water at pH: 7.4 is not known, but they are biologically-relevant and should be considered in terms of assessing their intracellular distribution (see below).

	Zn-N1	Zn-N2	Zn-S1	C-S1	N3-C
$[Zn(Ap44mT\text{-}H)_2]$	2.205(3)	2.132(3)	2.4607(8)	1.736(3)	1.325(4)
[Zn(Ap44mT-H)Cl(DMSO)]	2.148(2)	2.100(2)	2.4106(6)	1.738(2)	1.327(3)
$[Zn(Dp44mT)_2](HSO_4)_2$	2.205(3)	2.150(3)	2.449(1)	1.727(4)	1.361(5)
$[Zn(DpC)Cl_2]$	2.169(4)	2.201(4)	2.457(2)	1.684(5)	1.365(6)

Table 4.1 Selected bond lengths.

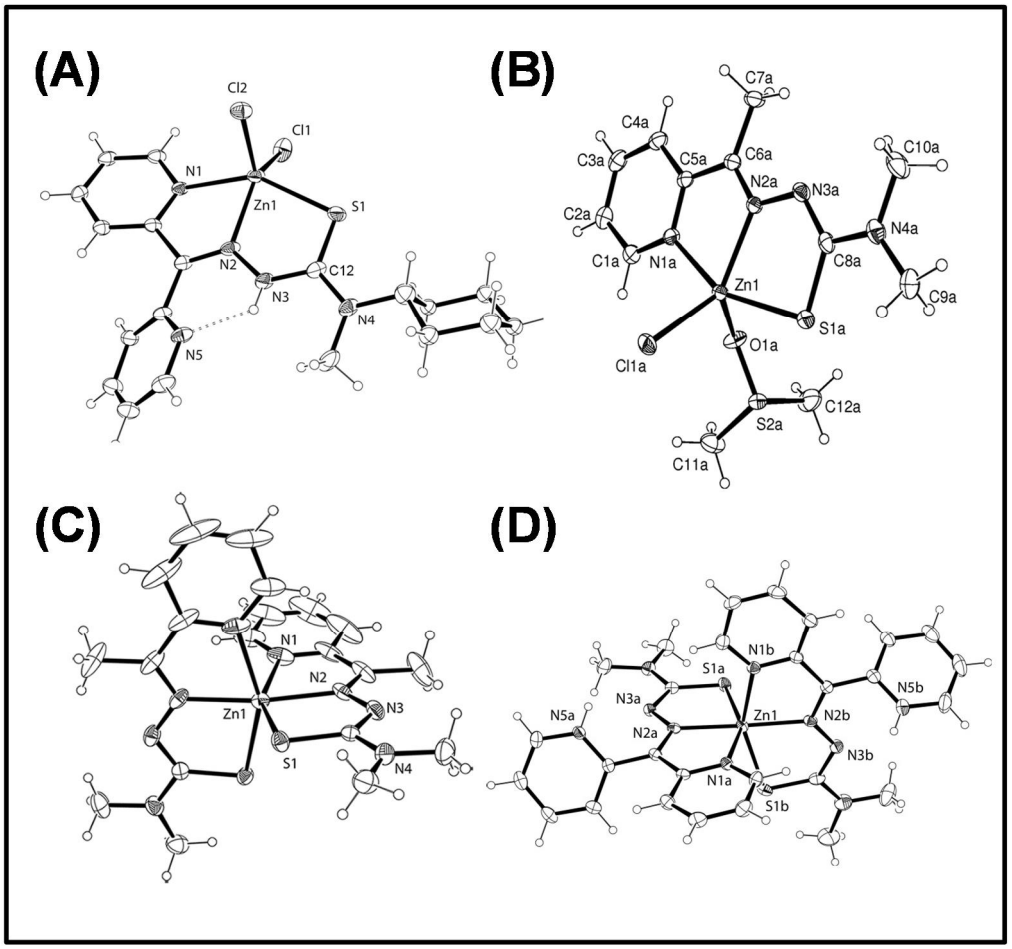

Figure 4.2. ORTEP views of the Zn(II) complexes.

(A) [Zn(DpC)Cl_2]. **(B)** [Zn(Ap44mT-H)(Cl)(DMSO)]. **(C)** [Zn(Ap44mT-H)$_2$]. **(D)** [Zn(Dp44mT-H)(Dp44mT)](HSO_4). Solvents and counter ions, if any, were omitted for clarity.

4.3.3 UV–Vis and Fluorescence Spectral Studies of the Zn(II) complexes

In terms of determining the intracellular localisation of the Zn(II)-thiosemicarbazone complexes by the technique of fluorescence-based cellular imaging (Cowley et al., 2005; Dayal et al., 2011; Kowol et al., 2010; Lim et al., 2010; Pascu et al., 2007; Pascu et al., 2008), it was important to determine their quantum yields in order to utilise appropriate complexes for these investigations.

	[Zn(Ap44mT)(Cl) (DMSO)]	[Zn(DpC)Cl_2]	[Zn(Ap44mT-H)$_2$] ·2$CHCl_3$	[Zn(Dp44mT)(HSO_4)$_2$]
Formula	$C_{12}H_{19}ClN_4OS_2Zn$	$C_{19}H_{23}Cl_2N_5SZn$	$C_{22}H_{28}Cl_6N_8S_2Zn$	$C_{28}H_{32}N_{10}O_8S_4Zn$
weight	400.25	489.75	746.71	830.25
M.W	Monoclinic	Monoclinic	Monoclinic	Triclinic
Crystal system	*C*2/*c*	*P*2$_1$/*c*	*C*2/*c*	$P\bar{1}$
Space group	Yellow	Yellow	Yellow	Yellow
Colour	1.54180	0.71073	0.71073	0.71073
Wavelength (Å)	35.4880(9)	9.2036(3)	12.473(1)	9.2029(5)
a (Å)	7.8212(2)	8.4487(3)	13.502(2)	14.1732(8)
b (Å)	26.1152(6)	27.3261(14)	19.810(2)	15.7067(10)
c (Å)				116.794(6)
α (deg)	108.757(3)	95.267(4)	90.668(9)	101.212(5)
β (deg)				91.723(5)
γ (deg)	6863.5(3)	2115.86(15)	3335.9(6)	1777.54(18)
V (Å^3)	190(2)	190(2)	190(2)	190(2)
T (K)	4	4	4	2
Z	0.0543	0.0428	0.0560	0.0560
R_1 (obsd data)	0.0315	0.1075	0.1100	0.1533
wR_2	0.0799	1.027	1.019	1.022
GOF	1.040			

Table 4.2. Crystal data.

Absorption spectra of [Zn(Dp44mT)Cl_2], [Zn(Ap44mT)Cl_2], [Zn(DpC)Cl_2], [Zn(Dp44mT-H)$_2$], [Zn(Ap44mT-H)$_2$] and [Zn(DpC)$_2$](ClO_4)$_2$ were recorded in DMSO and showed an absorption band observed between 404-425 nm (see Table 4.3 for λ_{max}), which was characteristic of charge transfer transitions from sulphur to Zn(II) (Fig. 4.3A) (Türkkan et al., 2015).

Complexes	Absorbance λ_{max} (nm) ($\varepsilon \times 10^{-4}$ $M^{-1}cm^{-1}$)	Emission[a] λ_{max} (nm)	Quantum yield[b] $\Phi \times 10^{-3}$
$[Zn(Dp44mT\text{-}H)_2]$	309 (2.2), 418 (2.7)	481	0.19
$[Zn(Ap44mT\text{-}H)_2]$	309 (2.2), 403 (3.1)	482	0.16
$[Zn(DpC)_2](ClO_4)_2$	315 (2.3), 423 (3.2)	532	0.36
$[Zn(Dp44mT)Cl_2]$	309 (1.1), 420 (1.5)	479	0.60
$[Zn(Ap44mT)Cl_2]$	307 (1.1), 404 (1.8)	512	1.34
$[Zn(DpC)Cl_2]$	310 (1.2), 423 (1.7)	533	0.54

Table 4.3 Photophysical properties of Zn(II) complexes.

[a]Emission spectra were recorded with 420-nm excitation and 10 nm slit width in DMSO.
[b]The quantum yield was estimated using $[Zn(3\text{-}AP)Cl_2]$ ($\bar{u} = 21 \times 10^{-3}$) as a reference.

Fluorescence spectra of these zinc complexes (Fig. 4.3B) were measured in DMSO following excitation at 420 nm and the quantum yields were estimated (Table 4.3) using $[Zn(3\text{-}AP)Cl_2]$ as a standard (Kowol et al., 2010). It was observed that all 1:1 (Zn(II)/ligand) complexes exhibited higher quantum yields than the corresponding 1:2 (Zn(II)/ligand) complexes (Table 4.3), with a maximum of 1.34×10^{-3} for $[Zn(Ap44mT)Cl_2]$. This value is close to the quantum yield exhibited by the well-known Zn(II) bis(thiosemicarbazone) complex, [Zn(ATSM)], in DMSO (1.25×10^{-3}), which has been used previously for cell imaging studies examining its distribution in cancer cells (Brockman et al., 1956). In addition, all complexes showed fluorescence in the green region of visible spectrum, which is amenable to fluorescence-based cellular imaging (Table 4.3).

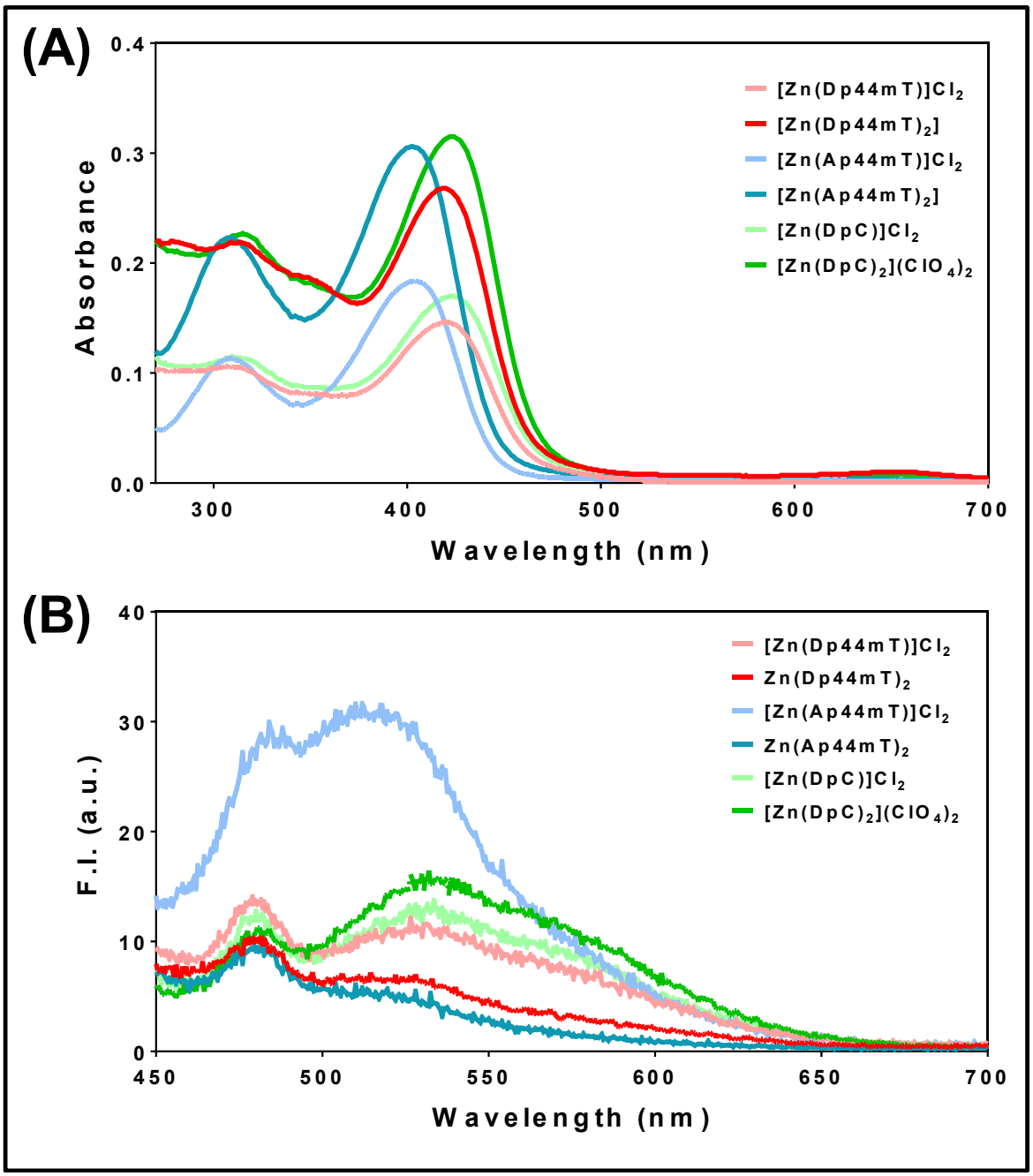

Figure 4.3 Absorption and fluorescence spectra of Zn(II) complexes

(A) Absorption spectra of $[Zn(Dp44mT)Cl_2]$, $[Zn(Ap44mT)Cl_2]$, $[Zn(DpC)Cl_2]$, $[Zn(Dp44mT\text{-}H)_2]$, $[Zn(Ap44mT\text{-}H)_2]$ and $[Zn(DpC)_2](ClO_4)_2$ recorded in DMSO (10 µM). **(B)** Fluorescence spectra of $[Zn(Dp44mT)Cl_2]$, $[Zn(Ap44mT)Cl_2]$, $[Zn(DpC)Cl_2]$, $[Zn(Dp44mT\text{-}H)_2]$, $[Zn(Ap44mT\text{-}H)_2]$ and $[Zn(DpC)_2](ClO_4)_2$ measured in DMSO (10 µM) after excitation at 420 nm.

4.3.4 Zn(II)- Ligand Binding Studies

Since we performed all biological studies in aqueous media containing DMSO, the binding behaviour of ligands with Zn(II) in DMSO alone and in MOPS buffer (pH: 7.4) containing DMSO (10% v/v) was examined using UV-visible spectroscopy. Notably, 10% (v/v) DMSO was necessary due to the limited aqueous solubility of the ligands and resultant complexes over the duration of the experiment.

The thiosemicarbazone, Dp44mT (Fig. 4.4A), displayed an intense peak in the UV region with a maximum at 340 nm in DMSO. However, the addition of Zn(II) induced a new peak in the visible region with a λ_{max} at 422 nm with a clear isosbestic point at 372 nm. Upon incremental addition of Zn(II) (0ï 1.6 equiv.), the intensity of a new peak at 422 nm increased linearly with a simultaneous decrease in absorption at 340 nm, but saturated at approximately 1 equivalent with respect to Dp44mT (Fig. 4.4A). The presence of only 1 distinct isosbestic point confirmed the complete conversion of the ligand into a single Zn(II) complex. Further stoichiometric binding analysis as determined by plotting absorption maximum at 422 nm (A_{422}) *versus* [Zn(II)]/[Dp44mT], confirmed the 1:1 binding ratio of Zn(II)/ligand (Fig. 4.4B).

The binding studies of Dp44mT with Zn(II) were also examined in water containing 10% DMSO and the results are shown in Figures 4.4C and 4.4D. The ligand Dp44mT exhibited a strong absorption band at 325 nm that decreased with a concomitant increase in the intensity of a new peak at 398 nm upon gradual addition of Zn(II) until a 0.5 equivalent with respect to Dp44mT was reached (Fig. 4.4C). However, further addition of Zn(II) did not increase the absorption at 398 nm.

Appearance of a single isosbestic point at 354 nm confirmed the formation of a single species (Fig. 4.4C). Stoichiometric analysis further revealed that Dp44mT formed 1:2 (Zn(II)/ligand) complexes with zinc (Fig. 4.4D).

Similarly, Ap44mT and DpC ligands showed 1:1 binding behaviour with Zn(II) in DMSO, with isosbestic points at 360 and 372 nm, respectively (Fig. 4.5A, 4.6A). The 1:1 binding ratio of ligand/Zn(II) in DMSO was also confirmed for Ap44mT (Fig. 4.5B) and DpC (Fig. 4.6B) *via* binding stoichiometric analysis. The absorption maximum was plotted against [Zn(II)]/[ligand] at 404 (A_{404}) for Ap44mT (Fig. 4.5B) and 424 (A_{424}) for DpC (Fig. 4.6B). Binding studies were also performed in water containing 10% DMSO for Ap44mT (Fig. 4.5C) and DpC (Fig. 4.6C). Similarly to Dp44mT, both ligands prefer to form 2:1 complexes (L/Zn(II)) rather of 1:1 complexes with Zn in an aqueous solution containing 10% DMSO. Strong absorption bands were found at 308 nm for Ap44mT (Fig. 4.5C) and 338 nm for DpC (Fig. 4.6C) which were decreased with a concomitant increase in the intensity of a new peaks at 376 and 444 nm, respectively, upon gradual addition of Zn(II) till 0.5 equiv. w.r. to ligand (Fig. 4.5C, 4.6C). Appearance of isosbestic points at 356 nm for Ap44mT (Fig. 4.5C) and 354 nm for DpC (Fig. 4.6C) confirmed the formation of single species. Further Stoichiometric analysis demonstrated that Ap44mT (Fig. 4.5D) and DpC (Fig. 4.6D) form 2:1 complexes with Zn(II) in water containing 10% DMSO. Similar results were also obtained when the concentration of DMSO in water was decreased to 0.5%, which was the maximum utilised in biological studies (Richardson et al., 2009).

Collectively, these binding studies demonstrate that the ligands, Dp44mT, Ap44mT and DpC, preferred to form 1:1 complexes with Zn(II) in DMSO alone, whereas they preferred to form 1:2 (Zn(II)/ligand) complexes in an aqueous solution containing DMSO. Notably, it is possible that the formation of the 1:2 (Zn(II)/ligand) complexes was inhibited in DMSO as this solvent can also act as a coordinating ligand. In fact, this was observed in the case of [Zn(Ap44mT)Cl_2] in the solid state, where one of the chlorides was found to be replaced by DMSO to form the [Zn(Ap44mT-H)(Cl)(DMSO)] complex when crystallised in DMSO. These ligands could form 1:2 (Zn(II)/ligand) complexes with zinc in aqueous milieu and are the possible active species in cells.

4.3.5 Cytotoxicity of Novel Zn(II)-thiosemicarbazone Complexes Examined in Different Tumour Cell-Types

The ligands, Dp44mT, Ap44mT and DpC, have been shown to be potent cytotoxic agents in a variety of cancer cells and *in vivo* models (Jansson et al., 2010a; Jansson et al., 2015b; Kovacevic et al., 2011; Lovejoy et al., 2011; Lovejoy et al., 2012; Whitnall et al., 2006; Yuan et al., 2004). Moreover, we have shown that the cytotoxicity of Dp44mT and DpC is potentiated when cells express high levels of the drug transporter, Pgp (Jansson et al., 2015a; Jansson et al., 2015b; Seebacher et al., 2016a; Whitnall et al., 2006). This is due to the ability of Pgp to transport the ligands into the lysosome to induce lysosomal rupture and cell death (Jansson et al., 2015a; Jansson et al., 2015b; Seebacher et al., 2016a; Whitnall et al., 2006). Hence, this imparts these agents with the highly beneficial property of being able to effectively overcome Pgp-mediated drug resistance, which is a major problem in the clinics (Jansson et al., 2015a).

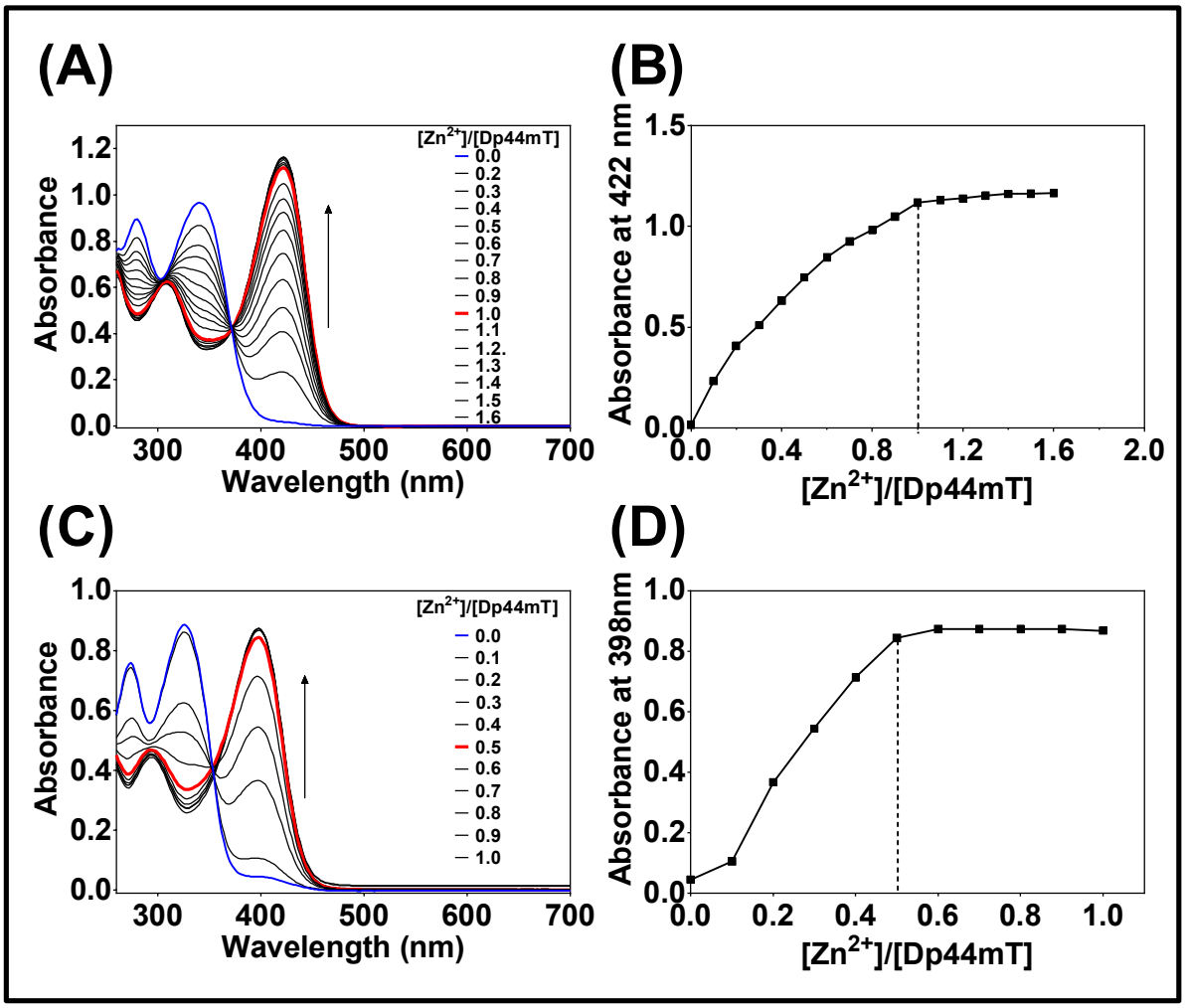

Figure 4.4. Zn(II)-Dp44mT Binding Studies.

(A) Dp44mT (blue line) displayed an intense peak in the UV region with a maximum at 340 nm in DMSO (50 µM). Addition of Zn(II) induced a new peak in the visible region with a λ_{max} at 422 nm with a clear isosbestic point at 372 nm, which saturated at nearly 1 equivalent with respect to Dp44mT (red line). **(B)** Binding stoichiometric analysis as determined by plotting the absorption maximum at 422 (A_{422}) *versus* Zn^{2+}/Dp44mT confirmed the 1:1 binding ratio of Zn(II)/Ligand. **(C)** Dp44mT (blue line, 50 µM) exhibited a strong absorption band at 325 nm that decreased with a concomitant increase in the intensity of a new peak at 398 nm upon gradual addition of Zn(II) until 0.5 equivalents with respect to Dp44mT (red line) in MOPS buffer (pH: 7.4) containing 10% DMSO. Appearance of an isosbestic point at 354 nm confirmed the formation of single species. **(D)** Stoichiometric analysis further revealed that the ligand, Dp44mT, formed 1:2 (Zn(II)/ligand) complexes with zinc in MOPS buffer (pH: 7.4) containing 10% DMSO.

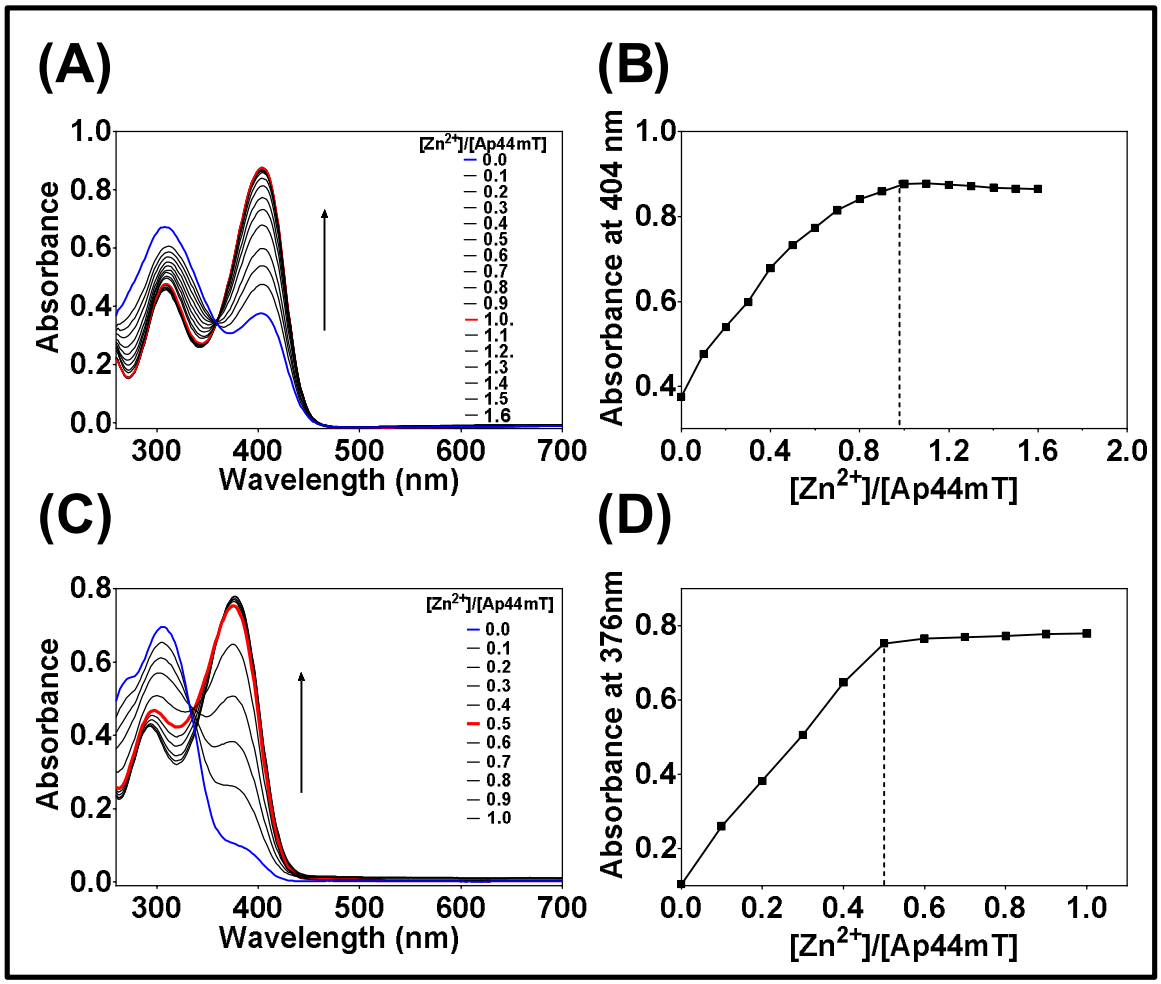

Figure 4.5. Zn(II)-Ap44mT Binding Studies

(A) Ap44mT (blue line) displayed an intense peak in the UV region with a maximum at 308 nm in DMSO. Addition of Zn(II) induced a new peak in the visible region with a λ_{max} at 404 nm with a clear isosbestic point at 360 nm, which saturated at nearly 1 equivalent with respect to Ap44mT (red line) (B) Binding stoichiometric analysis as determined by plotting absorption maximum at 404 (A_{422}) versus [Zn(II)]/[Ap44mT] confirmed 1:1 binding ratio of ligand/Zn(II) (C) Ap44mT (blue line) exhibited a strong absorption band at 308 nm that was decreased with a concomitant increase in the intensity of a new peak at 376 nm upon gradual addition of Zn(II) until 0.5 equiv. w.r. to Ap44mT (red line) in water containing 10% DMSO. Appearance of an isosbestic point at 356 nm confirmed the formation of single species. (D) Stoichiometric analysis further revealed that the ligand Ap44mT form 2:1 complexes with Zn(II) in water containing 10% DMSO.

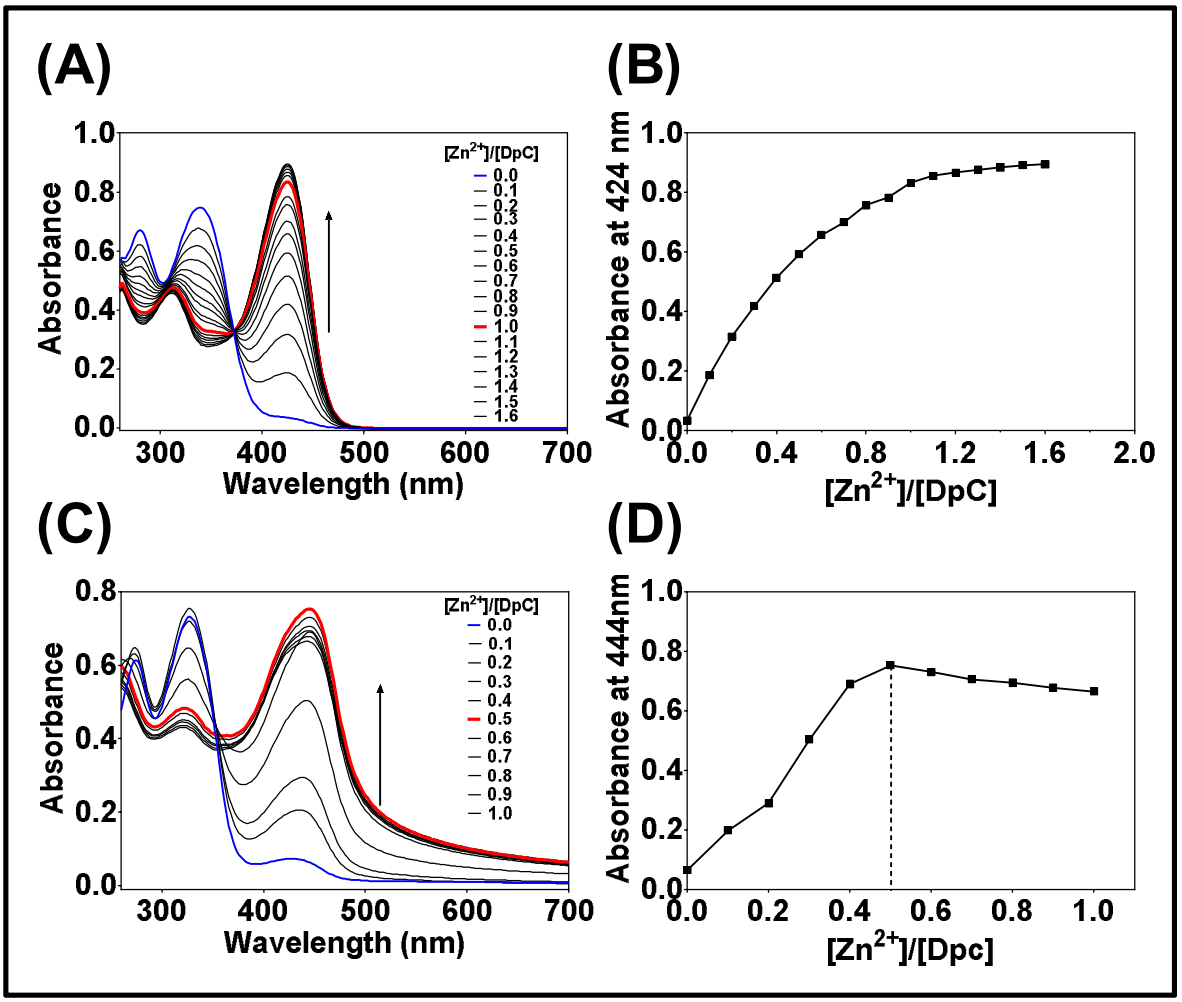

Figure 4.6 Zn(II)-DpC Binding Studies

(A) DpC (blue line) displayed an intense peak in the UV region with a maximum at 338 nm in DMSO. Addition of Zn(II) induced a new peak in the visible region with a λ_{max} at 424 nm with a clear isosbestic point at 372 nm, which saturated at nearly 1 equivalent with respect to DpC (red line) **(B)** Binding stoichiometric analysis as determined by plotting absorption maximum at 424 (A_{422}) versus [Zn(II)]/[DpC] confirmed 1:1 binding ratio of ligand/Zn(II) **(C)** DpC (blue line) exhibited a strong absorption band at 338 nm that was decreased with a concomitant increase in the intensity of a new peak at 444 nm upon gradual addition of Zn(II) until 0.5 equiv. w.r. to DpC (red line) in water containing 10% DMSO. Appearance of an isosbestic point at 354 nm confirmed the formation of single species. **(D)** Stoichiometric analysis further revealed that the ligand DpC form 2:1 complexes with Zn(II) in water containing 10% DMSO.

Moreover, we have established that Cu(II) complexes of the DpT and ApT series are more cytotoxic than the ligand alone (Jansson et al., 2010a). Interestingly, research from other laboratories has demonstrated that Zn(II)-thiosemicarbazone complexes are often more potently cytotoxic than the thiosemicarbazone ligands alone (Atassi et al., 1979; Kovala-Demertzi et al., 2006; Kowol et al., 2010; Petering et al., 1967). Therefore, studies examined the cytotoxicity of Dp44mT, Ap44mT and DpC relative to their respective 1:1 and 1:2 (Zn(II)/ligand) zinc complexes in a pair of cell-types used to assess Pgp-mediated drug resistance, namely, cervical carcinoma cell lines KBV1 (+Pgp; high Pgp expression) compared to KB31 (-Pgp; negligible Pgp expression) (Jansson et al., 2015b; Seebacher et al., 2016a; Seebacher et al., 2015; Yamagishi et al., 2013) (Fig. 4.7). This would provide data on the effectiveness of the Zn(II) complexes of thiosemicarbazones on overcoming Pgp-mediated resistance (Jansson et al., 2015b; Seebacher et al., 2016a) . We have also included the SW480 colon (low Pgp expression) adenocarcinoma cell-type (Miklos et al., 2015; Montazami et al., 2015), which was of interest as it has been used previously to demonstrate that 3-AP entered the nucleus (Kowol et al., 2010). Several cell-types were included as it has been reported that the subcellular distribution of Zn(II)-thiosemicarbazones can vary depending on the tumour cell-type examined (Cowley et al., 2005; Pascu et al., 2008), which could result in differences in cytotoxicity.

(i) Cytotoxicity of Dp44mT and its Zn(II) Complexes: Similar trends in the IC_{50} values of the 1:1 and 1:2 (Zn(II)/ligand) zinc complexes of Dp44mT, compared to Dp44mT alone, were found across the three cell-types (Fig. 4.7). Notably, [Zn(Dp44mT)Cl_2] was 2.5-, 6.2- and 4.9-fold more cytotoxic ($p < 0.01$) than Dp44mT in KBV1 (+Pgp), KB31 (-Pgp) and SW480 (low Pgp) cells, respectively (Fig. 4.7).

Using KB31 cells, [Zn(Dp44mT-H)$_2$] was also significantly ($p < 0.001$) more cytotoxic relative to Dp44mT (Fig. 4.7). However, in both KBV1 and SW480 cells, [Zn(Dp44mT-H)$_2$] was less cytotoxic than Dp44mT, with IC_{50} values that were 3.7- and 5.2-fold ($p < 0.001$) higher than that of Dp44mT (Fig. 4.7). In all three cell-types, [Zn(Dp44mT-H)$_2$] was significantly ($p < 0.001$) less cytotoxic than [Zn(Dp44mT)Cl$_2$] (Fig. 4.7). The general trend for the IC_{50} values of Dp44mT and its Zn(II) complexes were therefore: [Zn(Dp44mT)Cl$_2$] < Dp44mT < [Zn(Dp44mT-H)$_2$]. This indicates that zinc complexes have different cytotoxic properties than the ligand alone.

(ii) Cytotoxicity of Ap44mT and its Zn(II) Complexes: The IC_{50} values of the 1:1 and 1:2 (Zn(II)/ligand) zinc complexes of Ap44mT, compared to the Ap44mT alone, followed a consistent trend across the KBV1, KB31 and SW480 cell-types (Fig. 4.7). In all cells examined, [Zn(Ap44mT)Cl$_2$] was significantly ($p < 0.001$) more cytotoxic than Ap44mT. The IC_{50} values of [Zn(Ap44mT)Cl$_2$] were 13.3-, 12.5- and 14.4-fold lower ($p < 0.001$) than Ap44mT in KBV1, KB31 and SW480 cells, respectively (Fig. 4.7). Similarly, the IC_{50} values of [Zn(Ap44mT-H)$_2$] in KBV1, KB31 and SW480 cells were 5.5-, 11.0- and 16.5-fold ($p < 0.001$) more cytotoxic than Ap44mT, respectively (Fig. 4.7). Notably, there was no significant ($p > 0.05$) difference between the cytotoxicity of [Zn(Ap44mT)Cl$_2$] and [Zn(Ap44mT-H)$_2$] (Fig. 4.7). The trend for the IC_{50} values of Ap44mT and its Zn(II) complexes was [Zn(Ap44mT)Cl$_2$] = [Zn(Ap44mT-H)$_2$] < Ap44mT (Fig. 4.7).

(iii) Cytotoxicity of DpC and its Zn(II) Complexes: The trends in the IC_{50} values of DpC and its 1:1 and 1:2 (Zn(II)/ligand) zinc complexes were not entirely consistent

across the three cell-types (Fig. 4.7). Using KBV1 (+Pgp) cells, [Zn(DpC)Cl_2] was less cytotoxic than DpC with an IC_{50} value 8.3-fold higher ($p < 0.001$) than DpC (Fig. 4.7). However, assessing KB31 (-Pgp) and SW480 (low Pgp) cells, the IC_{50} values of [Zn(DpC)Cl_2] were 1.2- and 2.6-fold lower ($p < 0.05$) than DpC, making [Zn(DpC)Cl_2] more cytotoxic (Fig. 4.7). In KBV1 (+Pgp) cells, there was no significant ($p > 0.05$) difference between [Zn$(DpC)_2$]$(ClO_4)_2$ and DpC. In contrast, in the KB31 and SW480 cell-types, [Zn$(DpC)_2$]$(ClO_4)_2$ was 1.6- and 5.4-fold ($p < 0.01$) more cytotoxic than DpC, respectively (Fig. 4.7). In all cell-types examined in this study, [Zn$(DpC)_2$]$(ClO_4)_2$ was significantly (p < 0.001-0.01) more cytotoxic than [Zn(DpC)Cl_2], with IC_{50} values 7.3-, 1.3- and 2.36-fold less in KBV1, KB31 and SW480 cells, respectively (Fig. 4.7). The general trend in IC_{50} values for DpC and its Zn(II) complexes in KB31 and SW480 cells was [Zn$(DpC)_2$]$(ClO_4)_2$ < [Zn(DpC)Cl_2] < DpC. However in KBV1 cells, the trend in IC_{50} values was [Zn$(DpC)_2$]$(ClO_4)_2$ = DpC < [Zn(DpC)Cl_2] (Fig. 4.7).

Interestingly, the cytotoxicity of Dp44mT, DpC and their 1:1 and 1:2 (Zn(II)/ligand) zinc complexes were greatest in KBV1 (+Pgp) cells compared to the KB31 (-Pgp) and SW480 (low Pgp) cell-types (Fig. 4.7). Indeed, the IC_{50} values of the Zn(II) complexes of Dp44mT and DpC in the KB31 and SW480 cell-types were between 3.5- to 25-fold higher relative to those observed in KBV1 cells (Fig. 4.7). These observations are in good agreement with the fact that Dp44mT, DpC and their Cu(II) complexes exhibit potentiated cytotoxicity in Pgp-expressing cells (Jansson et al., 2015b; Seebacher et al., 2016a; Whitnall et al., 2006), and from the current studies, it appears that the Zn(II) complexes may also be more cytotoxic in Pgp-expressing

cells (KBV1) than in low-Pgp expressing cells (KB31 and SW480) (Fig. 4.7). This would be clearly important for the treatment of Pgp-resistant tumours.

In contrast to the Zn(II) complexes of Dp44mT and DpC, the cytotoxicity of the Zn(II) complexes of Ap44mT did not appear to be as greatly affected by Pgp expression (Fig. 4.7). Notably, the IC_{50} values of the 1:1 and 1:2 (Zn(II)/ligand) zinc complexes of Ap44mT were similar across all 3 cell-types, suggesting that their cytotoxicity was not dependent on Pgp expression (Fig. 4.7). This interesting structure-activity relationship reveals the replacement of the non-coordinating pyridine ring with a methyl substituent leads to the loss of Pgp-potentiated cytotoxicity. Thus, the di-2-pyridyl moiety is an important pharmacophore that mediates the ability of these thiosemicarbazones to overcome Pgp-dependent resistance.

In summary, with the exception of [Zn(Dp44mT-$H)_2$] in KBV1 and SW480 cells, and [Zn(DpC)Cl_2] in KBV1 cells, Zn(II) complexation resulted in more potent cytotoxic effects relative to the free ligand alone (Fig. 4.7). Notably, the Zn(II) complexes of Dp44mT and DpC appeared to exhibit potentiated cytotoxicity against Pgp-expressing KBV1 cells, a property essential for overcoming Pgp-mediated drug resistance in tumours.

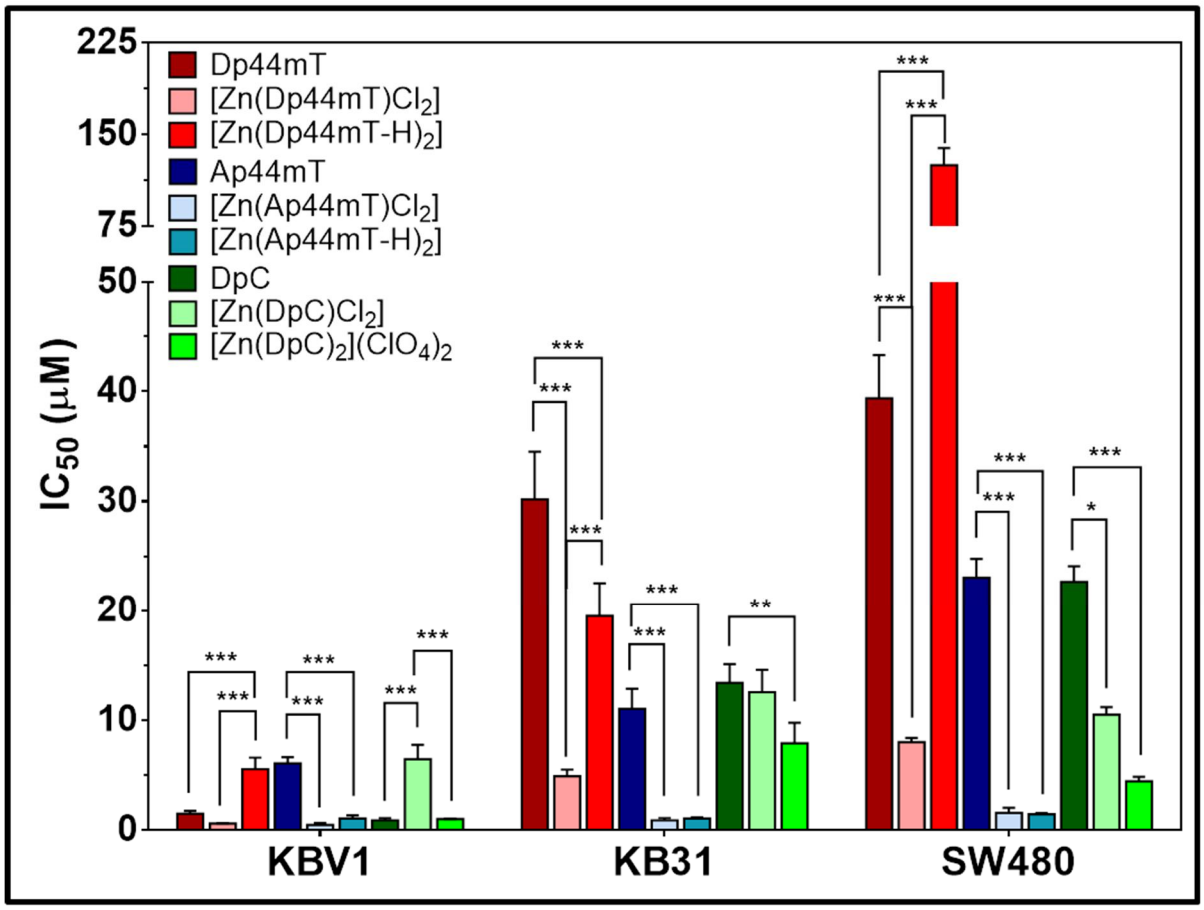

Figure 4.7. MTT assay of Dp44mT, Ap44mT and DpC and their respective 1:1 and 1:2 (Zn(II)/ligand) zinc complexes in KBV1, KB31 and SW480 cells.

The cytotoxicity of the ligands and their respective 1:1 and 1:2 (Zn(II)/ligand) zinc complexes using KBV1, KB31 and SW480 cells after a 24 h/37°C incubation. Results are mean ± SD (3 experiments). * $p < 0.05$, ** $p < 0.01$, *** $p < 0.001$ *versus* the respective ligand or complex, as shown.

4.3.6 The Intracellular Localisation of $[Zn(DpC)_2](Cl_2O_4)$ is Not Nuclear

Previous studies have highlighted the potential application of Zn(II) mono- and bis(thiosemicarbazones) for intracellular imaging (Cowley et al., 2005; Dayal et al., 2011; Kowol et al., 2010; Lim et al., 2010; Pascu et al., 2007; Pascu et al., 2008). Understanding the intracellular localisation of agents can provide valuable

information regarding their potential mechanism(s) of action. There are significant advantages of using Zn(II) complexes over Cu(II) complexes, namely: **(1)** that they are relatively less toxic than Cu(II) complexes (Palanimuthu et al., 2013); and **(2)** they possess intrinsic fluorescence due to intra-ligand excitation, whereas Cu(II) is d^9 and paramagnetic (Pascu et al., 2010) and quenches the fluorescence of adjacent fluorophores (Pascu et al., 2007).

Examples of using Zn(II) complexes as imaging tools for assessing intracellular localisation include the well-known anti-cancer thiosemicarbazone, 3-AP, which was shown to be localised to the nucleolus of SW480 cells (Kowol et al., 2010). However, other Zn(II)bis(thiosemicarbazones) have been reported to be localised to a range of subcellular organelles, including lysosomes and mitochondria (Cowley et al., 2005; Dayal et al., 2011; Pascu et al., 2008). Furthermore, the localisation of Zn(II)bis(thiosemicarbazone) complexes may be cell-type-dependent, as [Zn(ATSM)] has been shown to localise to the nucleus of PC-3 (prostate cancer) cells, while its lysosomal localisation was observed in IRGOV (ovarian cancer) cells (Cowley et al., 2005).

Considering that the subcellular distribution of other Zn(II)bis(thiosemicarbazones) has been shown to vary depending on the cell-type used, we sought to establish directly the intracellular localisation of the Zn(II) complexes of Dp44mT, Ap44mT and DpC in KBV1, KB31 and SW480 cells. The 1:2 (Zn(II)/ligand) complexes were utilised as binding studies suggested that these are the major species formed in aqueous solutions (Fig. 4.4, 4.5, 4.6). Both [Zn(Dp44mT-$H)_2$] and [Zn(Ap44mT-$H)_2$]

exhibited negligible intracellular fluorescence, an issue which has been encountered by others examining the subcellular distribution of different Zn(II)bis(thiosemicarbazones) complexes (Cowley et al., 2005; Pascu et al., 2008). Therefore, we focused our efforts on examining the intracellular distribution of the Zn(II) complex of our lead compound, DpC, which will enter clinical trials in 2016 (ClinicalTrials.gov Identifier NCT02688101) (Jansson et al., 2015a).

As some Zn(II)bis(thiosemicarbazones) (Cowley et al., 2005; Dayal et al., 2011; Kowol et al., 2010) have demonstrated nuclear localisation, their presence in the nucleus was assessed first, using the far red nuclear stain (Nuc), DRAQ5Ê (Figs. 4.8, 4.9, 4.10). After a 10 min/37°C incubation with KBV1 (+Pgp) cells, $[Zn(DpC)_2](ClO_4)_2$ (50 µM) exhibited a punctate pattern of green fluorescence at 405 nm (Fig. 4.8Ai). The Nuc stain assessed at 690 nm produced structurally well-defined staining of the nucleus, with the nuclear membrane and nucleoli clearly delineated (Figs. 4.8Aii). Following co-incubation with $[Zn(DpC)_2](ClO_4)_2$ and Nuc, the green fluorescence of $[Zn(DpC)_2](ClO_4)_2$ did not overlap (Pearsonôs correlation coefficient R = -0.01) with the red fluorescence of the Nuc stain (Figs. 4.8Aiii; see expanded view), as illustrated in the cytofluorogram (Fig. 4.8B). In KB31 (-Pgp) and SW480 cells a punctate pattern of green fluorescence was also observed following incubation with $[Zn(DpC)_2](ClO_4)_2$ (Fig. 4.9Ai, 4.10Ai). Similarly to KBV1 cells (+Pgp; Fig. 4.8Aiii), a total lack of overlap between $[Zn(DpC)_2](ClO_4)_2$ and the Nuc stain was also observed in KB31 (-Pgp) and SW480 cells (Fig. 4.9iii, 4.10iii), which had Pearsonôs correlation coefficients of R = -0.08 and R = -0.01, respectively (Fig. 4.9B, 4.10B). From these results, it was apparent that unlike the Zn(II) complex of 3-AP

(Kowol et al., 2010), $[Zn(DpC)_2](ClO_4)_2$ was not localised to the nucleus/nucleoli of the cell.

4.3.7 The Intracellular Localisation of $[Zn(DpC)_2](Cl_2O_4)$ is Not Mitochondrial

We next assessed whether $[Zn(DpC)_2](ClO_4)_2$ showed any co-localisation with the mitochondrion using MitoTracker® Deep Red (Mito; Fig 4.11, 4.12, 4.13), as some Zn(II)bis(thiosemicarbazones) display partial localisation to mitochondria (Pascu et al., 2008). Of relevance, our laboratory has demonstrated that Dp44mT can induce the release of holo-cytochrome *c* (h-cyt*c*) from the mitochondrial intermembrane space into the cytosol (Yuan et al., 2004), a key step in mitochondrial-dependent apoptosis, suggesting some effect on the mitochondrion (Yang et al., 1997). The punctate pattern of green $[Zn(DpC)_2](ClO_4)_2$ fluorescence at 405 nm was again observed in KBV1, KB31 and SW480 cells (Fig. 4.11Ai, 4.12Ai, 4.13Ai), while a typical, perinuclear punctate staining pattern was observed for Mito at 690 nm (Fig. 4.11Aii, 4.12Aii, 4.13Aii). When the cells were incubated with both $[Zn(DpC)_2](ClO_4)_2$ and Mito, no co-localisation was apparent in any of the cell-types tested (Fig. 4.11Aiii, 4.12Aiii, 4.13Aiii). Pearson's correlation coefficients of R = 0.11, 0.08 and 0.06 were obtained using KBV1, KB31 and SW480 cells, respectively, and support the lack of observable co-localisation (Fig. 4.11B, 4.12B, 4.13B). Hence, it can be concluded that $[Zn(DpC)_2](ClO_4)_2$ does not localise in mitochondria.

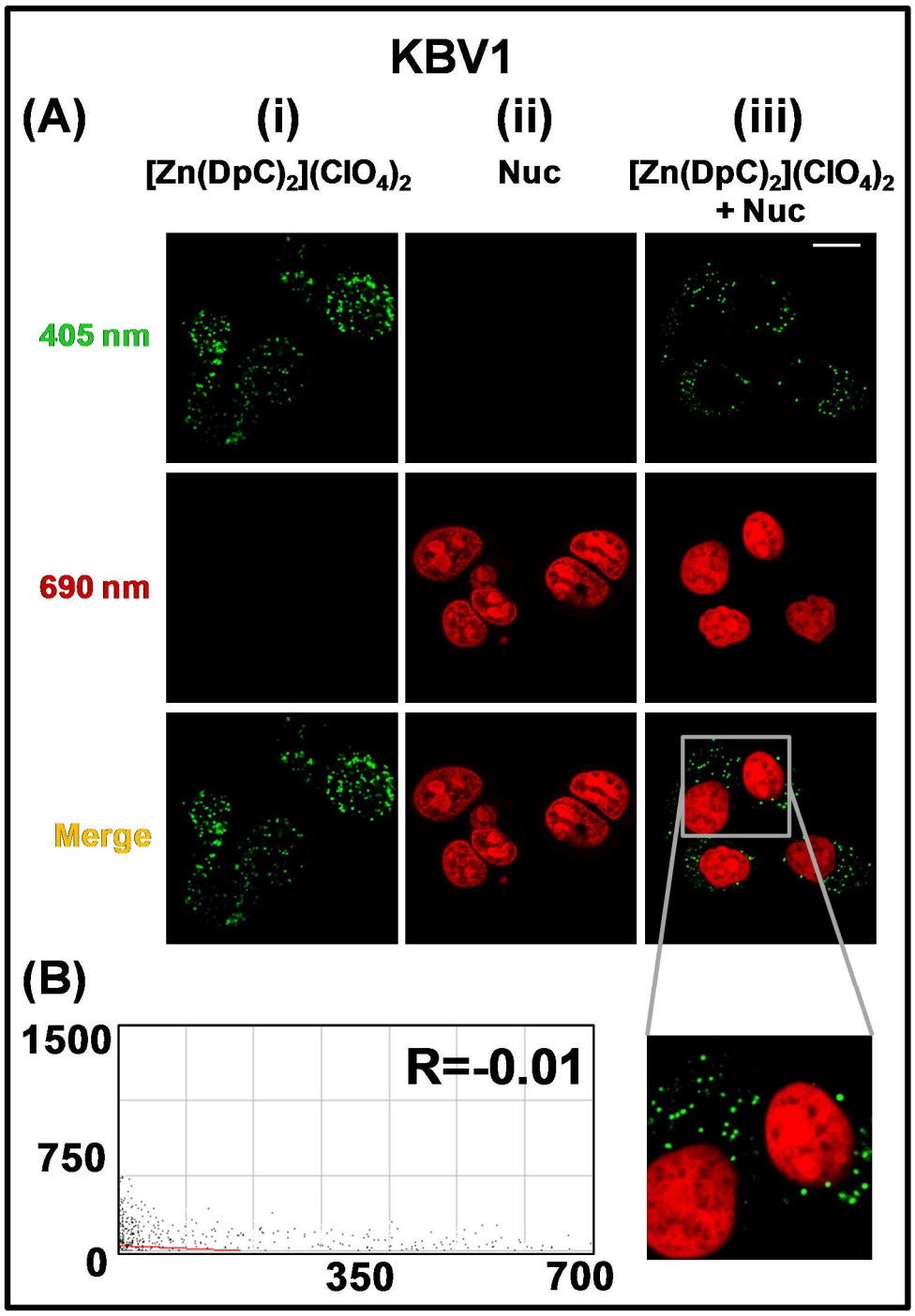

Figure 4.8 The intracellular localisation of $[Zn(DpC)_2](Cl_2O_4)$ is not nuclear in the KBV1 cell line

(A) (i) In the KBV1 cell line, incubation with $[Zn(DpC)_2](Cl_2O_4)$ (50 ε M, 10 min/37°C) resulted in a punctate pattern of green (405 nm) fluorescence **(ii)** Incubation with the far red nuclear stain (690 nm, Nuc), DRAQ5Ê , generated well-defined staining of the nucleus, with the nuclear membrane and nucleoli clearly delineated **(iii)** Co-incubation of KBV1 cells with $[Zn(DpC)_2](Cl_2O_4)$ and Nuc revealed no overlap between $[Zn(DpC)_2](Cl_2O_4)$ and Nuc **(iv)** The lack of co-localisation between $[Zn(DpC)_2](Cl_2O_4)$ and Nuc was confirmed by the Pearsonôs correlation coefficient of R = -0.01. The images are typical from 3 experiments. Scale bar: 10 ε m.

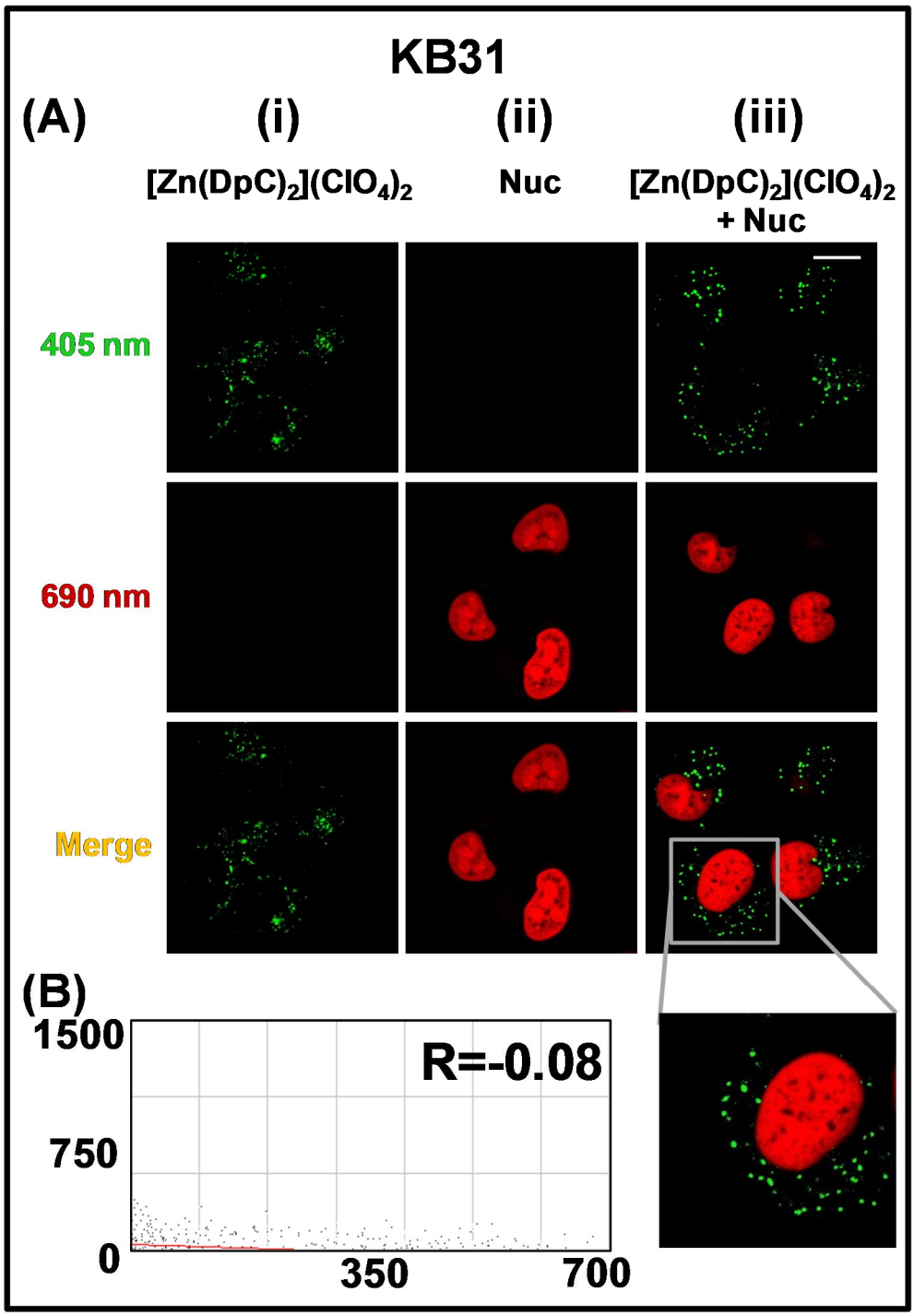

Figure 4.9 The intracellular localisation of $[Zn(DpC)_2](Cl_2O_4)$ is not nuclear in the KB31 cell line

(A) (i) In the KB31 cell line, incubation with $[Zn(DpC)_2](Cl_2O_4)$ (50 ε M, 10 min/37°C) resulted in a punctate pattern of green (405 nm) fluorescence **(ii)** Incubation with the far red nuclear stain (690 nm, Nuc), DRAQ5Ê , generated well-defined staining of the nucleus, with the nuclear membrane and nucleoli clearly delineated **(iii)** Co-incubation of KB31 cells with $[Zn(DpC)_2](Cl_2O_4)$ and Nuc revealed no overlap between $[Zn(DpC)_2](Cl_2O_4)$ and Nuc **(iv)** The lack of co-localisation between $[Zn(DpC)_2](Cl_2O_4)$ and Nuc was confirmed by the Pearsonôs correlation coefficient of R = -0.08. The images are typical from 3 experiments. Scale bar: 10 ε m.

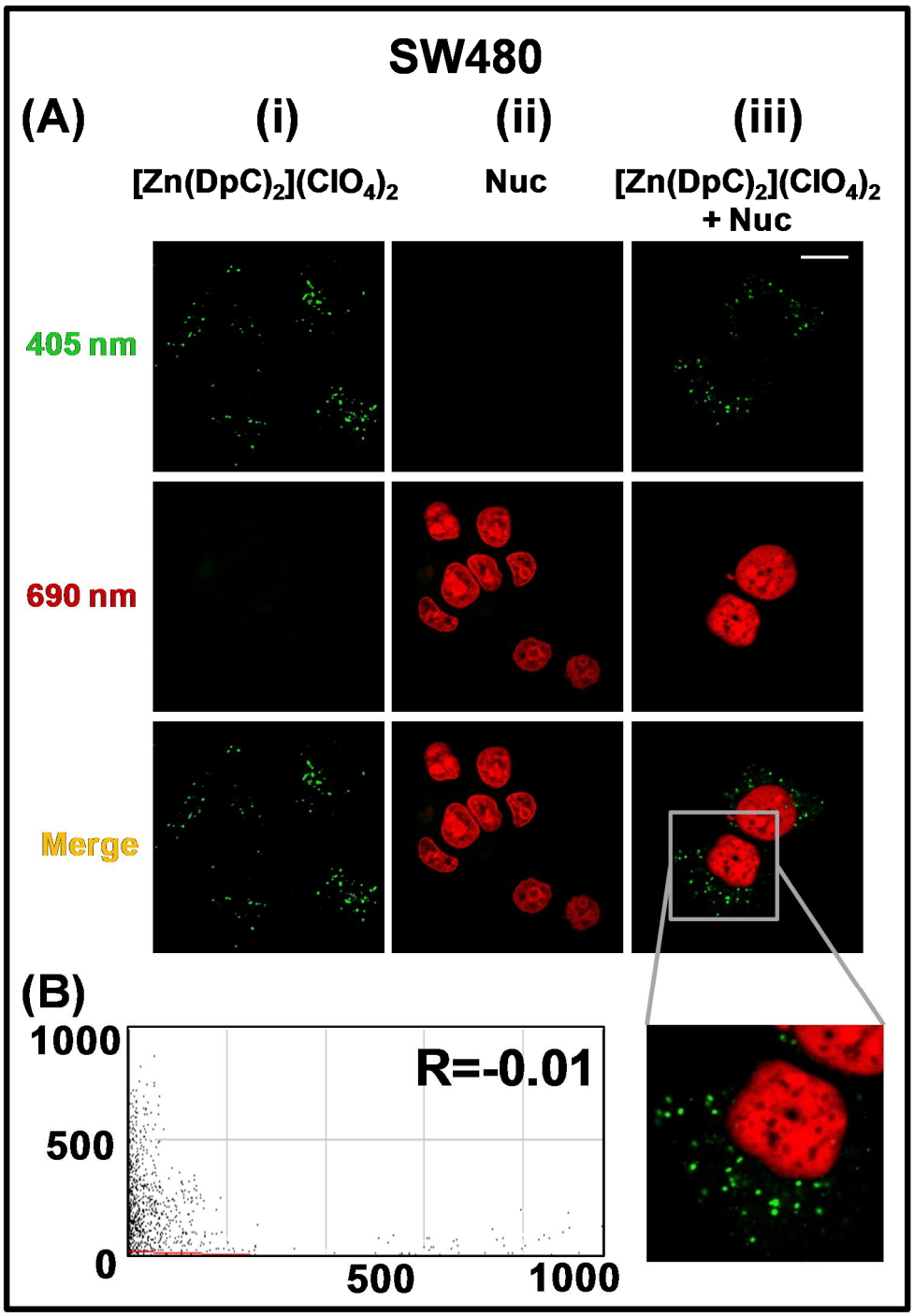

Figure 4.10 The intracellular localisation of $[Zn(DpC)_2](Cl_2O_4)$ is not nuclear in the SW480 cell line

(A) (i) In the SW480 cell line, incubation with $[Zn(DpC)_2](Cl_2O_4)$ (50 ε M, 10 min/37°C) resulted in a punctate pattern of green (405 nm) fluorescence **(ii)** Incubation with the far red nuclear stain (690 nm, Nuc), DRAQ5Ê , generated well-defined staining of the nucleus, with the nuclear membrane and nucleoli clearly delineated **(iii)** Co-incubation of SW480 cells with $[Zn(DpC)_2](Cl_2O_4)$ and Nuc revealed no overlap between $[Zn(DpC)_2](Cl_2O_4)$ and Nuc **(iv)** The lack of co-localisation between $[Zn(DpC)_2](Cl_2O_4)$ and Nuc was confirmed by the Pearsonŝ correlation coefficient of R = -0.01. The images are typical from 3 experiments. Scale bar: 10 ε m.

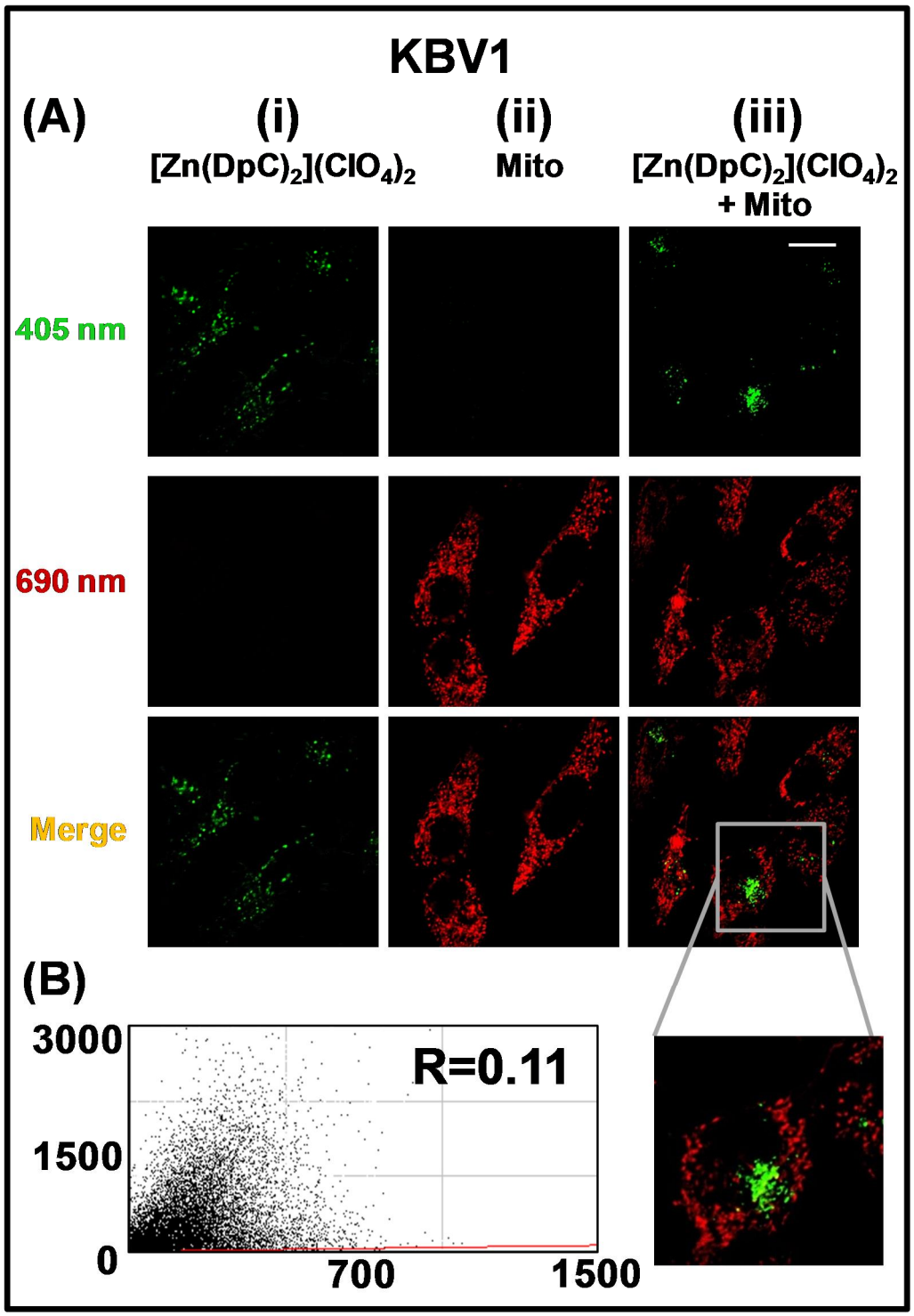

Figure 4.11 The intracellular localisation of $[Zn(DpC)_2](Cl_2O_4)$ is not mitochondrial in the KBV1 cell line

(A) (i) In the KBV1 cell line, incubation with $[Zn(DpC)_2](Cl_2O_4)$ (50 ε M, 10 min/37°C) resulted in a punctate pattern of green (405 nm) fluorescence **(ii)** Incubation with MitoTracker® Deep Red (690 nm, Mito) generated a typical spindle-like pattern **(iii)** Co-incubation of KBV1 cells with $[Zn(DpC)_2](Cl_2O_4)$ and Mito revealed no overlap between $[Zn(DpC)_2](Cl_2O_4)$ and Mito **(iv)** The lack of co-localisation between $[Zn(DpC)_2](Cl_2O_4)$ and Mito was confirmed by the Pearsonς correlation coefficient of R = 0.11. The images are typical from 3 experiments. Scale bar: 10 ε m.

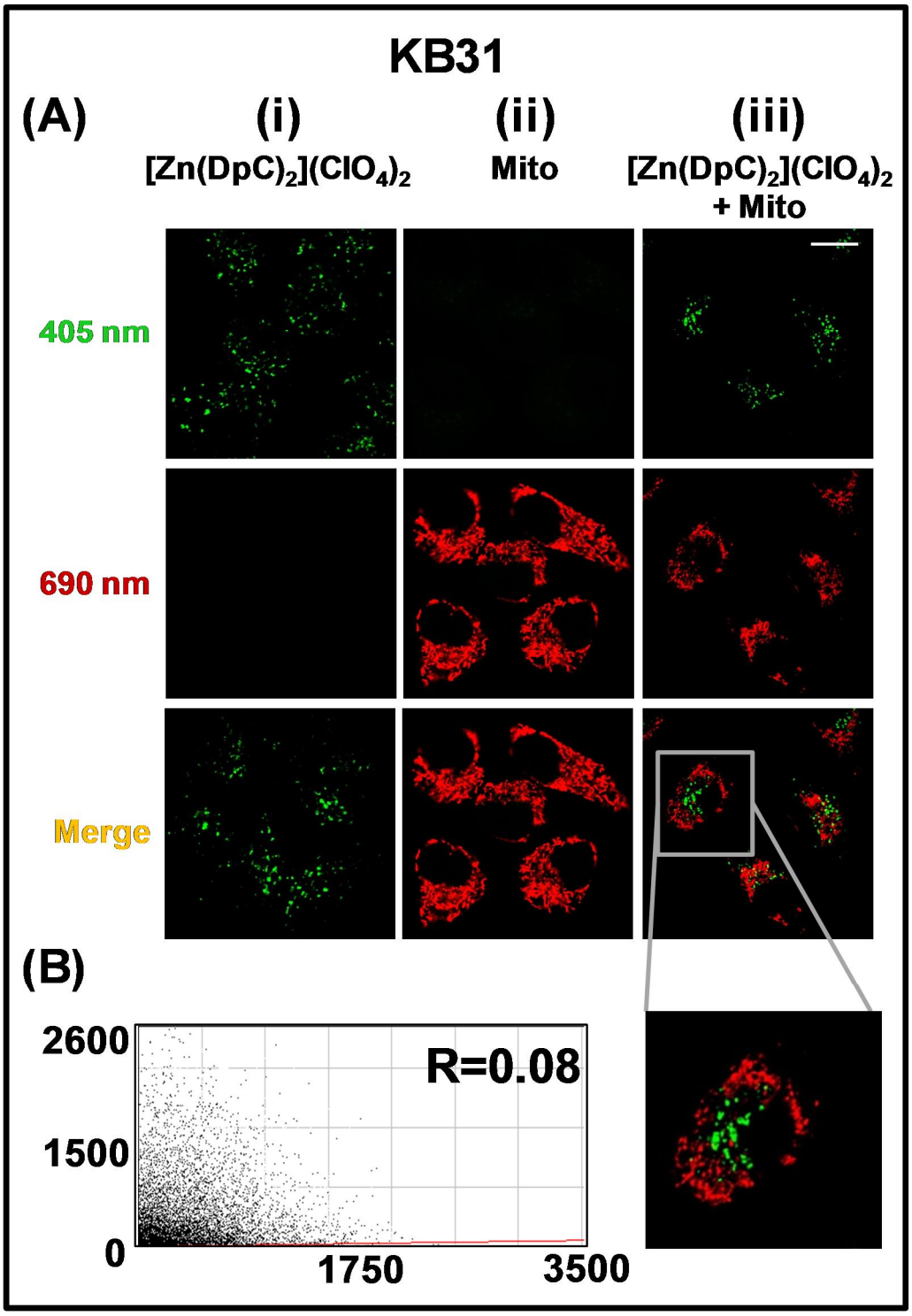

Figure 4.12 The intracellular localisation of $[Zn(DpC)_2](Cl_2O_4)$ is not mitochondrial in the KB31 cell line

(A) (i) In the KB31 cell line, incubation with $[Zn(DpC)_2](Cl_2O_4)$ (50 ε M, 10 min/37°C) resulted in a punctate pattern of green (405 nm) fluorescence **(ii)** Incubation with MitoTracker® Deep Red (690 nm, Mito) generated a typical spindle-like pattern **(iii)** Co-incubation of KB31 cells with $[Zn(DpC)_2](Cl_2O_4)$ and Mito revealed no overlap between $[Zn(DpC)_2](Cl_2O_4)$ and Mito **(iv)** The lack of co-localisation between $[Zn(DpC)_2](Cl_2O_4)$ and Mito was confirmed by the Pearsonς correlation coefficient of R = 0.08. The images are typical from 3 experiments. Scale bar: 10 ε m.

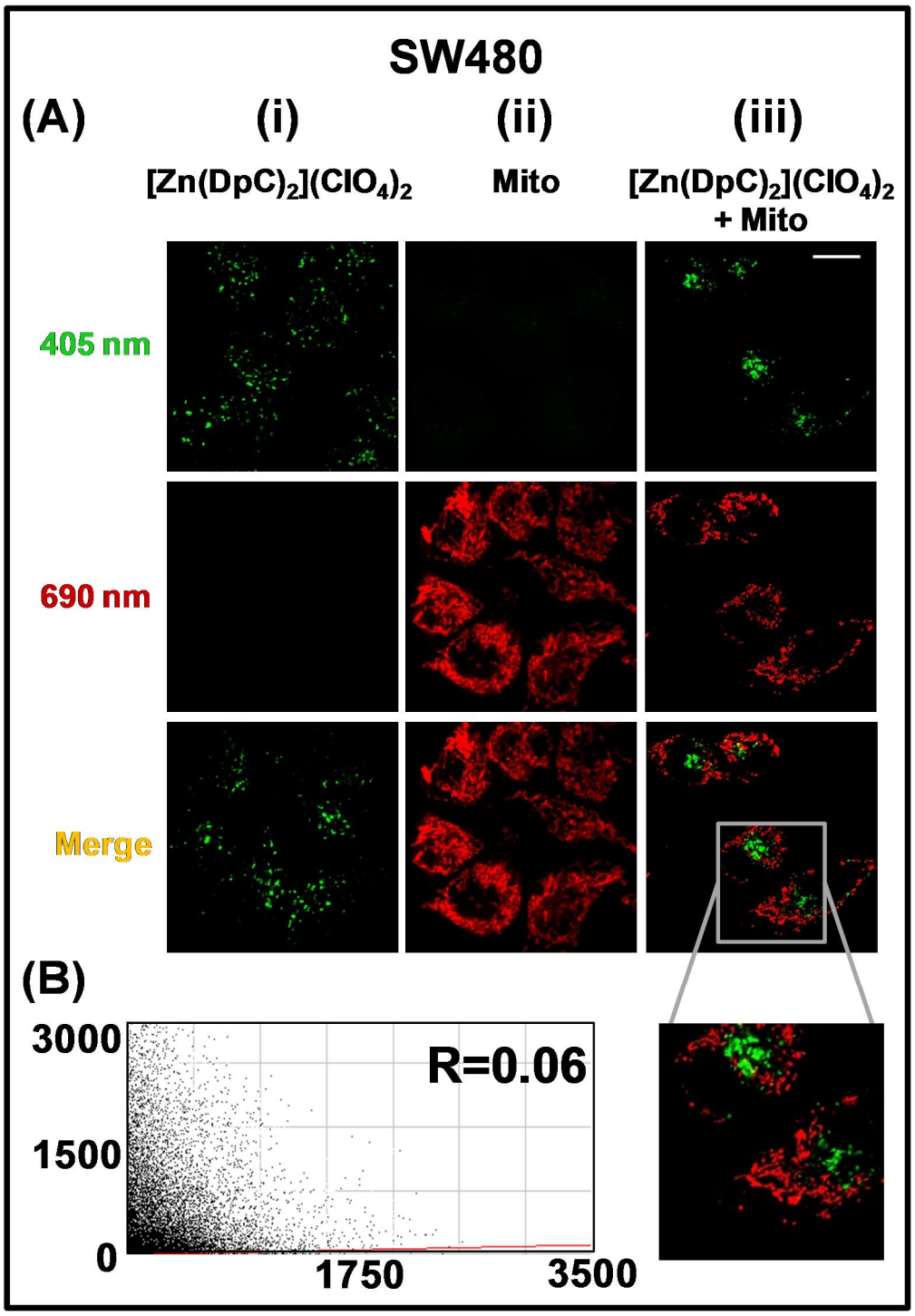

Figure 4.13 The intracellular localisation of $[Zn(DpC)_2](Cl_2O_4)$ is not mitochondrial in the SW480 cell line

(A) (i) In the SW480 cell line, incubation with $[Zn(DpC)_2](Cl_2O_4)$ (50 εM, 10 min/37°C) resulted in a punctate pattern of green (405 nm) fluorescence **(ii)** Incubation with MitoTracker® Deep Red (690 nm, Mito) generated a typical spindle-like pattern **(iii)** Co-incubation of SW480 cells with $[Zn(DpC)_2](Cl_2O_4)$ and Mito revealed no overlap between $[Zn(DpC)_2](Cl_2O_4)$ and Mito **(iv)** The lack of co-localisation between $[Zn(DpC)_2](Cl_2O_4)$ and Mito was confirmed by the Pearsonς correlation coefficient of R = 0.06. The images are typical from 3 experiments. Scale bar: 10 εm.

4.3.8 The Intracellular Localisation of $[Zn(DpC)_2](Cl_2O_4)$ is Lysosomal

Our previous results have indirectly suggested that the lead thiosemicarbazones, Dp44mT and DpC, are sequestered within lysosomes (Gutierrez et al., 2014; Jansson et al., 2015b; Lovejoy et al., 2011). Additionally, lysosomal distribution of the Zn(II)bis(thiosemicarbazone) complex [Zn(ATSM)] has been reported by others (Cowley et al., 2005). In all cell-types examined, incubation with $[Zn(DpC)_2](ClO_4)_2$ produced a punctate pattern of green fluorescence at 405 nm (Fig. 4.14Ai, 4.15Ai, 4.16Ai). In addition, incubation with LysoTrackerÊ Deep Red (Lyso) resulted in a similar punctate pattern of red fluorescence at 690 nm (Fig. 4.14Aii, 4.15Aii, 4.16Aii). Interestingly, incubation with both $[Zn(DpC)_2](ClO_4)_2$ (green) and Lyso (red) resulted in a punctate pattern of yellow fluorescence when the respective channels were merged, suggesting that $[Zn(DpC)_2](ClO_4)_2$ and Lyso were co-localised (Fig. 4.14Aiii, 4.15Aiii, 4.16Aiii). The Pearsonôs correlation coefficients of R = 0.84, 0.86 and 0.84 obtained for KBV1, KB31 and SW480 cells, respectively, also demonstrated that $[Zn(DpC)_2](ClO_4)_2$ was co-localised to the lysosome (Fig. 4.14B, 4.15B, 4.16B).

Previously it has been reported that Dp44mT (Jansson et al., 2015b; Lovejoy et al., 2011; Seebacher et al., 2016a) and DpC (Seebacher et al., 2015) appear to be sequestered in lysosomes, where they redox cycle after complexation with copper ions to induce LMP. For the first time, these results provide direct evidence that the 1:2 (Zn(II)/ligand) zinc complex of our lead compound, DpC, is sequestered in lysosomes. Other reports have shown that the localisation of some bis(thiosemicarbazones) can differ between cell-types (Cowley et al., 2005; Pascu et al., 2008). Nonetheless, the localisation of $[Zn(DpC)_2](ClO_4)_2$ did not vary with

respect to the cells used, despite apparent cell-type dependent differences in cytotoxicity (Fig. 4.7). In addition, we found that $[Zn(DpC)_2](ClO_4)_2$ entered and localised in the lysosome of both Pgp-expressing KBV1 cells and non-Pgp expressing KB31 and SW480 cells. These results demonstrated the ability of $[Zn(DpC)_2](ClO_4)_2$ to localise to the lysosome, independent of Pgp expression.

Collectively, these results in Figures 4.14-16 demonstrate that $[Zn(DpC)_2](ClO_4)_2$ clearly localises to the lysosomal compartment, but not the nucleus, or the mitochondrion in 3 cell lines and supports our previous studies using DpC that indirectly suggested its localisation in the lysosome (Seebacher et al., 2015).

4.3.9 Effects of $[Zn(Dp44mT\text{-}H)_2]$, $[Zn(Ap44mT\text{-}H)_2]$ and $[Zn(DpC)_2](ClO_4)_2$ on Lysosomal Integrity and the Induction of Lysosomal Membrane Permeabilisation

Our previous results have suggested that the Cu(II) complexes of Dp44mT and DpC can be sequestered in lysosomes, where they generate ROS and cause LMP (Jansson et al., 2015b; Lovejoy et al., 2011). As $[Zn(DpC)_2](ClO_4)_2$ is localised to lysosomes, we next assessed the effects of all 1:2 complexes, $[Zn(Dp44mT\text{-}H)_2]$, $[Zn(Ap44mT\text{-}H)_2]$ and $[Zn(DpC)_2](ClO_4)_2$ on lysosomal integrity, compared to the ligands, Dp44mT, Ap44mT and DpC (Fig. 4.17). The 1:2 (Zn(II)/ligand) zinc complexes were again used as binding studies suggest that the ligands prefer to form 1:2 (Zn(II)/ligand) complexes with zinc under aqueous conditions (Figs. 4.4, 4.5, 4.6).

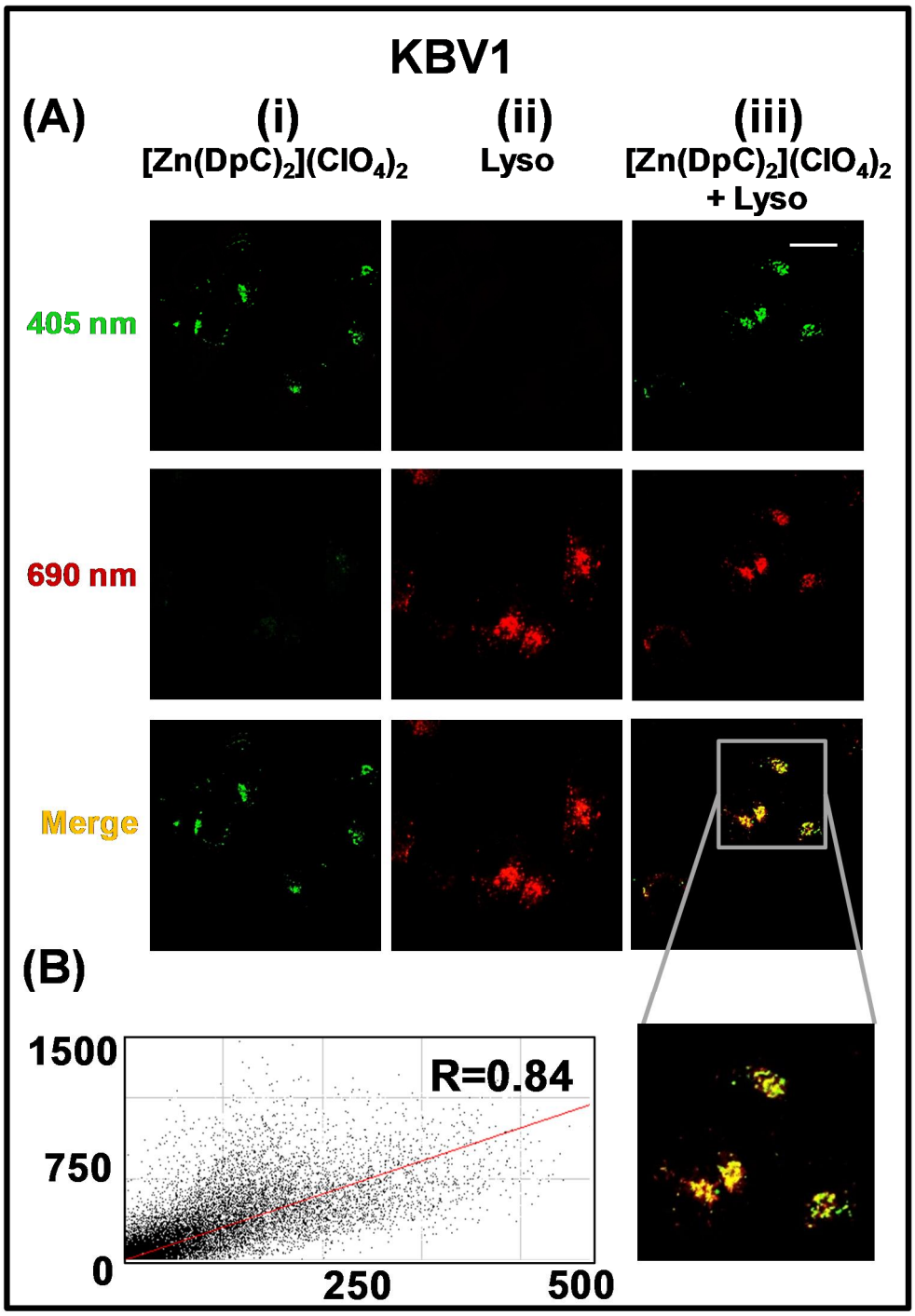

Figure 4.14 The intracellular localisation of $[Zn(DpC)_2](Cl_2O_4)$ is lysosomal in the KBV1 cell line

(A) (i) In the KBV1 cell line, incubation with $[Zn(DpC)_2](Cl_2O_4)$ (50 ε M, 10 min/37°C) resulted in a green (405 nm), punctate pattern **(ii)** Incubation with LysoTracker® Deep Red (Lyso) resulted in a typical, punctate pattern of red (690 nm) fluorescence **(iii)** Co-incubation of the KBV1 cell line with both $[Zn(DpC)_2](Cl_2O_4)$ (green) and Lyso (red) resulted in a yellow, punctate pattern of fluorescence on merge **(iv)** The co-localisation of $[Zn(DpC)_2](Cl_2O_4)$ and Lyso was confirmed by the strong Pearsonûs correlation coefficient of R = 0.84. The images are typical from 3 experiments. Scale bar: 10 ε m.

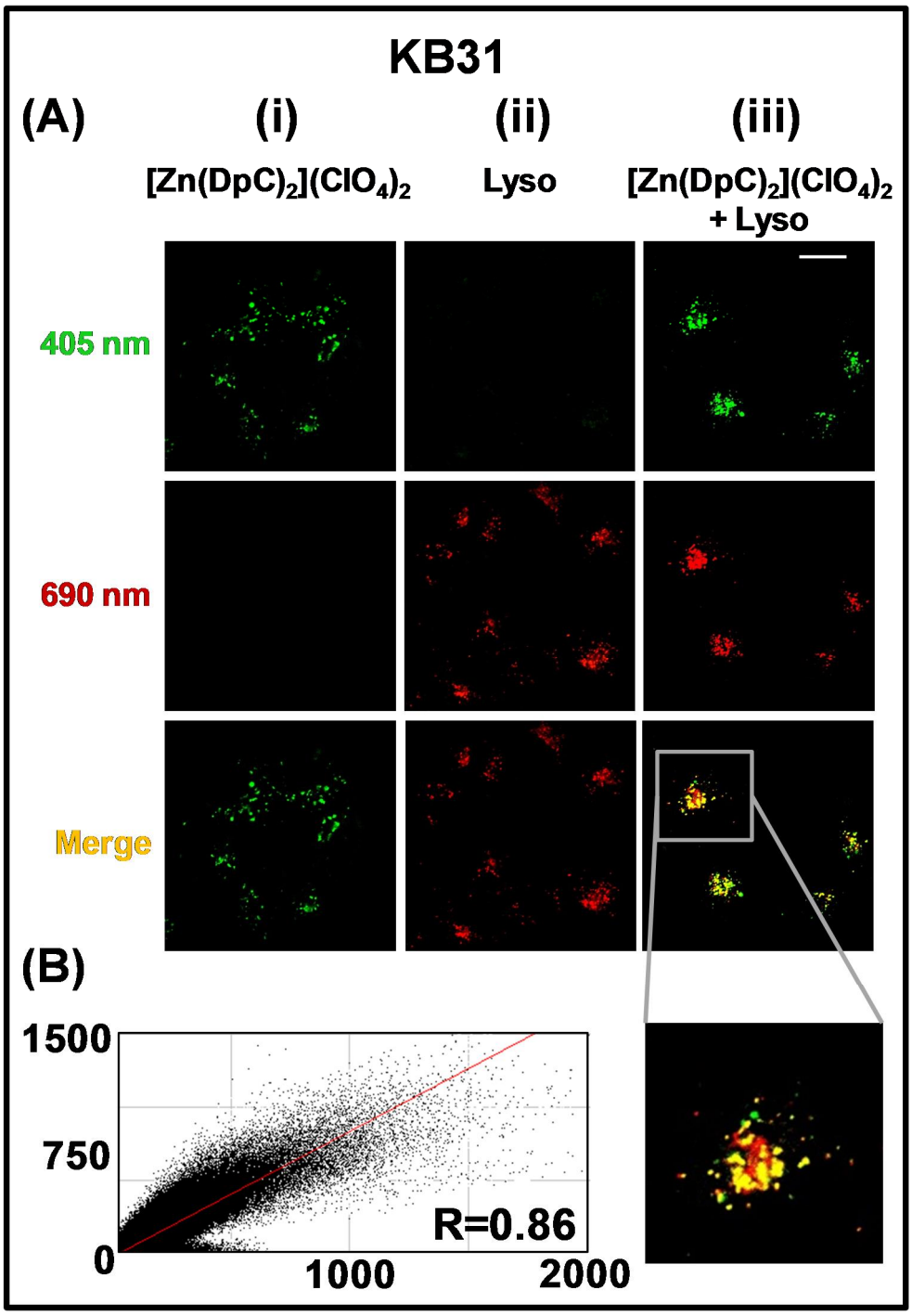

Figure 4.15 The intracellular localisation of $[Zn(DpC)_2](Cl_2O_4)$ is lysosomal in the KB31 cell line

(A) (i) In the KB31 cell line, incubation with $[Zn(DpC)_2](Cl_2O_4)$ (50 ε M, 10 min/37°C) resulted in a green (405 nm), punctate pattern **(ii)** Incubation with LysoTracker® Deep Red (Lyso) resulted in a typical, punctate pattern of red (690 nm) fluorescence **(iii)** Co-incubation of the KB31 cell line with both $[Zn(DpC)_2](Cl_2O_4)$ (green) and Lyso (red) resulted in a yellow, punctate pattern of fluorescence on merge **(iv)** The co-localisation of $[Zn(DpC)_2](Cl_2O_4)$ and Lyso was confirmed by the strong Pearsonûs correlation coefficient of R = 0.86. The images are typical from 3 experiments. Scale bar: 10 ε m.

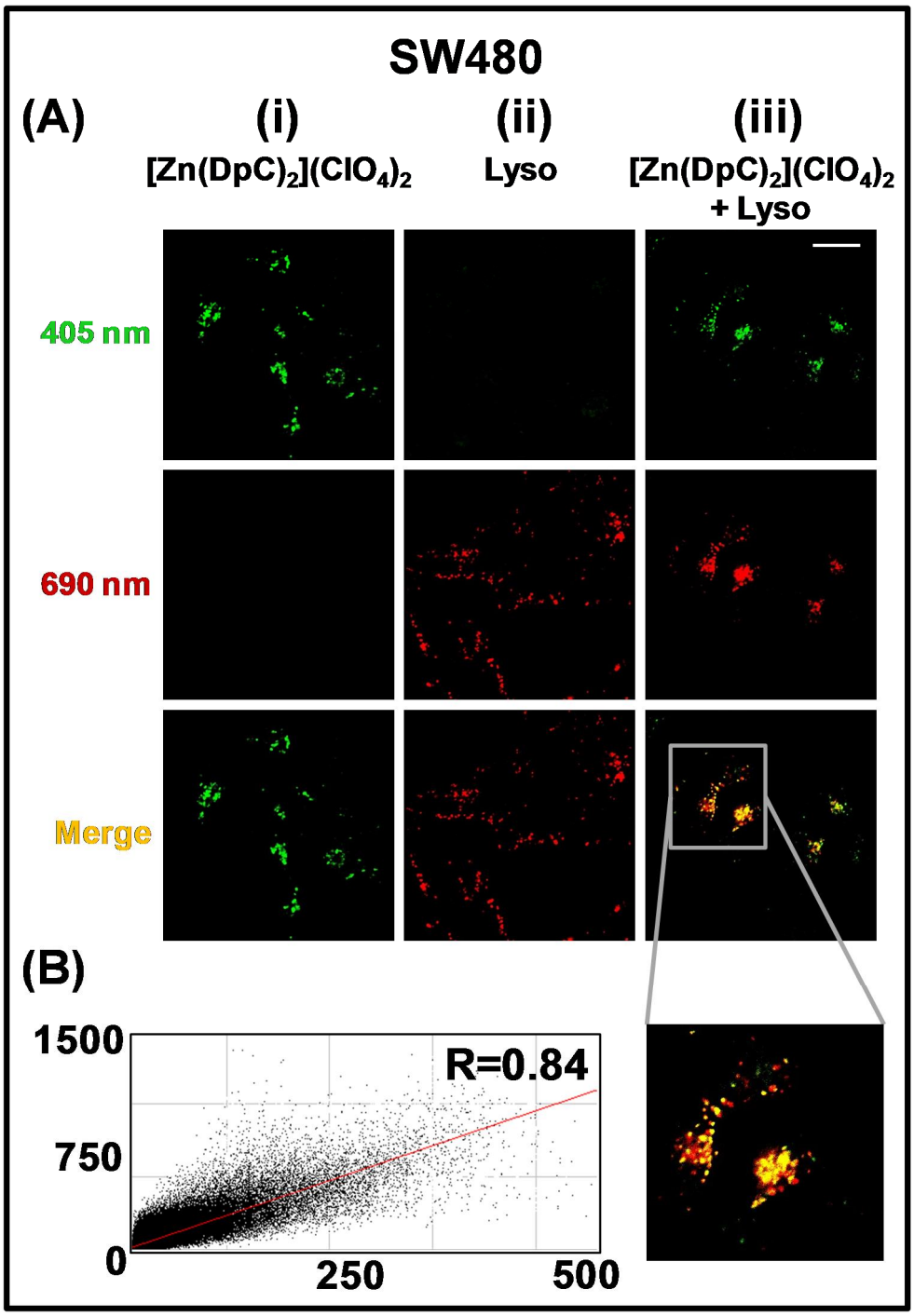

Figure 4.16 The intracellular localisation of $[Zn(DpC)_2](Cl_2O_4)$ is lysosomal in the SW480 cell line

(A) (i) In the SW480 cell line, incubation with $[Zn(DpC)_2](Cl_2O_4)$ (50 ε M, 10 min/37°C) resulted in a green (405 nm), punctate pattern (ii) Incubation with LysoTracker® Deep Red (Lyso) resulted in a typical, punctate pattern of red (690 nm) fluorescence (iii) Co-incubation of the SW480 cell line with both $[Zn(DpC)_2](Cl_2O_4)$ (green) and Lyso (red) resulted in a yellow, punctate pattern of fluorescence on merge (iv) The co-localisation of $[Zn(DpC)_2](Cl_2O_4)$ and Lyso was confirmed by the strong Pearsonς correlation coefficient of R = 0.84. The images are typical from 3 experiments. Scale bar: 10 ε m.

In these studies, lysosomal integrity was assessed by fluorescence microscopy using the classical lysosomal marker, AO (Gutierrez et al., 2014; Jansson et al., 2010a; Lovejoy et al., 2011; Nicolini et al., 1979; Pierzynska-Mach et al., 2014), in KBV1, KB31 and SW480 cells (Fig. 4.17). Notably, AO, is well known to accumulate in intact lysosomes to result in red punctate fluorescence, but exhibits an increase in green fluorescence upon redistribution to the cytosol or nucleus after LMP (Gutierrez et al., 2014; Lovejoy et al., 2011; Nicolini et al., 1979; Nilsson et al., 1997; Pierzynska-Mach et al., 2014).

In KBV1 (+Pgp), KB31 (-Pgp) and SW480 cells, the classical punctuate pattern of orange/red AO-stained lysosomes (Gutierrez et al., 2014; Jansson et al., 2015b; Lovejoy et al., 2011; Nicolini et al., 1979; Pierzynska-Mach et al., 2014) was observed following 1 h/37^{o}C incubation with Dp44mT, Ap44mT and DpC (Fig. 4.17). However, using this very brief incubation with the ligand, the cells did not show a decrease in orange/red AO staining compared to the controls, indicating that lysosomal membrane integrity was intact and LMP had not occurred (Fig. 4.17). This has been shown previously for Dp44mT, where incubations of up to 24 h were required to demonstrate lysosomal permeabilisation (Lovejoy et al., 2011) and indicates a marked kinetic delay. In contrast, following incubation with [Zn(Dp44mT-H)$_2$], [Zn(Ap44mT-H)$_2$] and [Zn(DpC)$_2$](ClO$_4$)$_2$, the red AO stain dissipated in all cell-types, suggesting that lysosomal membrane integrity was compromised and LMP had occurred (Fig. 4.17). Clearly, relative to the ligand alone, the Zn(II) complex appears more facile in terms of inducing lysosomal rupture.

This may be explained by the increased lipophilicity of the Zn(II) complexes (Richardson et al., 2006), which facilitates their passage across the cellular and lysosomal membranes, relative to the ligands alone, leading to enhanced uptake, cytotoxicity (Fig. 4.7) and ability to induce LMP (Fig. 4.17).At the shorter time point utilised in this AO study (1 h) *versus* the longer incubation period used in MTT assays (24 h) in Fig. 4.7, only [Zn(Dp44mT-H)$_2$], [Zn(Ap44mT-H)$_2$] and [Zn(DpC)$_2$](ClO$_4$)$_2$ mediated a decrease in orange/red AO intensity (Fig. 4.17). Indeed, these Zn(II) complexes were generally more cytotoxic than their respective ligands (Fig. 4.7). Hence, these results suggested that the increased cytotoxicity of the Zn(II) complexes may be due to their ability to decrease the integrity of lysosomal membranes (Fig. 4.17).

4.3.10 [Zn(Dp44mT-H)$_2$], [Zn(Ap44mT-H)$_2$] and [Zn(DpC)$_2$](ClO$_4$)$_2$ Can Transmetallate with Copper Ions to Generate Redox-Active Cu(II) Complexes

The redox activity of the Cu(II) complexes of Dp44mT, Ap44mT and DpC has been demonstrated to be highly important for their mechanism of action as anti-tumour agents (Jansson et al., 2010a; Lovejoy et al., 2011). In agreement with the Irving-Williams series (Irving and Williams, 1953), Dp44mT has a preference for binding Cu(II) over Zn(II) (Gaal et al., 2014). Furthermore, it has been demonstrated that Zn(II)bis(thiosemicarbazone) complexes can transmetallate with copper ions (Pascu et al., 2007).

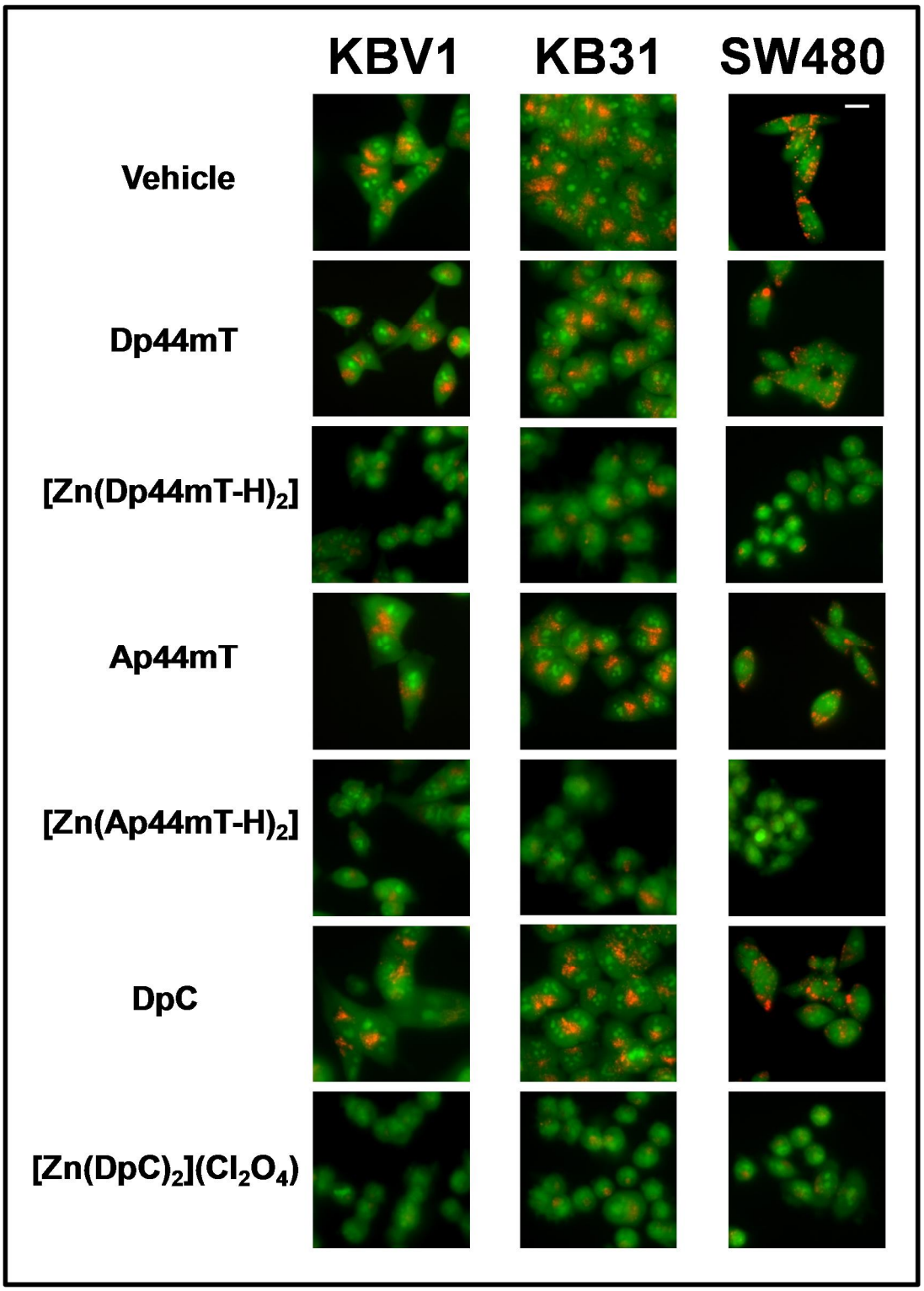

Figure 4.17 $[Zn(Dp44mT\text{-}H)_2]$, $[Zn(Ap44mT\text{-}H)_2]$ and $[Zn(DpC)_2](ClO_4)$ induce LMP

In KBV1, KB31 and SW480 cells, $[Zn(Dp44mT\text{-}H)_2]$, $[Zn(Ap44mT\text{-}H)_2]$, and $[Zn(DpC)_2](ClO_4)_2$ appear to cause LMP, as demonstrated by the loss of the typical, red, punctate pattern of AO staining seen in control cells. The images are typical from 3 experiments. Scale bar: 10 ε m.

Considering that the 1:2 (Zn(II)/ligand) zinc complex of Dp44mT is not redox-active (Berg and Shi, 1996; Bernhardt et al., 2009), yet the Zn(II) complexes exhibit enhanced cytotoxicity (Fig. 4.7) and lysosomal damage (Fig. 4.17) relative to the ligands alone, we next investigated whether the cytotoxicity of the Zn(II) complexes could be due to transmetallation involving exchange of Zn(II) for Cu(II).

4.3.10 $[Zn(Dp44mT\text{-}H)_2]$, $[Zn(Ap44mT\text{-}H)_2]$ and $[Zn(DpC)_2](ClO_4)_2$ Can Transmetallate with Copper Ions to Generate Redox-Active Cu(II) Complexes

The redox activity of the Cu(II) complexes of Dp44mT, Ap44mT and DpC has been demonstrated to be highly important for their mechanism of action as anti-tumour agents (Jansson et al., 2010a; Lovejoy et al., 2011). In agreement with the Irving-Williams series (Irving and Williams, 1953), Dp44mT has a preference for binding Cu(II) over Zn(II) (Gaal et al., 2014). Furthermore, it has been demonstrated that Zn(II)bis(thiosemicarbazone) complexes can transmetallate with copper ions (Pascu et al., 2007). Considering that the 1:2 (Zn(II)/ligand) zinc complex of Dp44mT is not redox-active (Berg and Shi, 1996; Bernhardt et al., 2009), yet the Zn(II) complexes exhibit enhanced cytotoxicity (Fig. 4.7) and lysosomal damage (Fig. 4.17) relative to the ligands alone, we next investigated whether the cytotoxicity of the Zn(II) complexes could be due to transmetallation involving exchange of Zn(II) for Cu(II). In these studies, the ability of the agents to mediate ROS generation was evaluated *via* the oxidation of the non-fluorescent, redox-sensitive probe, H_2DCF, to the highly fluorescent product, DCF (Jansson et al., 2010a; Lovejoy et al., 2011; Yuan et al., 2004). Notably, DCF is a well-characterised redox probe that is commonly used for

the measurement of ROS generation (Jansson et al., 2010a; Lovejoy et al., 2011; Myhre et al., 2003) .

The oxidation of H_2DCF to DCF was assessed in a cell-free system at both cytosolic pH 7.4 and lysosomal pH 5, as in previous studies (Fig. 4.18) (Jansson et al., 2010a; Lovejoy et al., 2011). At both cytosolic or lysosomal pH, $CuCl_2$, $Zn(ClO_4)_2$ or the well characterised copper ion chelator, TM (Lovejoy et al., 2011; Stefani et al., 2015), did not generate DCF fluorescence, indicating that they were not redox-active (Fig. 4.18). Similarly, Dp44mT alone did not result in an increase in DCF fluorescence and was not redox-active, which was in agreement with previous results (Fig. 4.18) (Lovejoy et al., 2011). As expected (Bernhardt et al., 2009), [Zn(Dp44mT-$H)_2$] did not cause a significant ($p > 0.05$) increase in DCF fluorescence compared to the controls (Fig. 4.18).

However, in accordance with previously published results (Lovejoy et al., 2011), [Cu(Dp44mT)] was highly redox-active resulting in a significant ($p < 0.001$) increase in DCF fluorescence relative to Dp44mT or [Zn(Dp44mT-$H)_2$] (Fig. 4.18). Interestingly, the addition of Cu(II) to [Zn(Dp44mT-$H)_2$] also resulted in significantly ($p < 0.001$) greater DCF fluorescence relative to Dp44mT or [Zn(Dp44mT-$H)_2$] (Fig. 4.18). This redox activity was abrogated by the addition of the Cu(II) chelator, TM, to [Zn(Dp44mT-$H)_2$]+Cu(II), which caused a significant ($p < 0.001$) decrease in DCF fluorescence compared to [Cu(Dp44mT)] or [Zn(Dp44mT-$H)_2$] + Cu(II) (Fig. 4.18).

These data suggest that although [Zn(Dp44mT-H)$_2$] itself was not redox-active, in the presence of copper ions, transmetallation can occur, resulting in a redox-active [Cu(Dp44mT)] complex that can mediate the oxidation of H_2DCF to DCF (Fig. 4.18). Similarly, [Zn(Ap44mT-H)$_2$] and [Zn(DpC)$_2$](ClO_4) followed the same trend as [Zn(Dp44mT-H)$_2$], where the Zn(II) complexes did not generate DCF fluorescence, but in the presence of Cu(II), exhibited a significant ($p < 0.001$) increase in DCF fluorescence relative to the Zn(II) complexes alone (Fig. 4.18). The increased DCF fluorescence of [Zn(Ap44mT-H)$_2$] and [Zn(DpC)$_2$](ClO_4) in the presence of Cu(II) could also be negated upon addition of the copper ion chelator, TM (Fig. 4.18).

These data again suggested that transmetallation may occur at both cytosolic or lysosomal pH, whereby [Zn(Ap44mT-H)$_2$] and [Zn(DpC)$_2$](ClO_4) exchange Zn(II) for Cu(II) and form redox-active Cu(II) complexes that can mediate the oxidation of H_2DCF (Fig. 4.18)These results may explain the effect of [Zn(Dp44mT-H)$_2$], [Zn(Ap44mT-H)$_2$] and [Zn(DpC)$_2$](ClO_4)$_2$ on lysosomal membrane integrity (Fig. 4.17), as it has been previously demonstrated that Dp44mT and DpC can form redox-active Cu(II) complexes which are sequestered in lysosomes (Jansson et al., 2010a; Lovejoy et al., 2011; Seebacher et al., 2016a). The redox activity of these Cu(II) complexes results in the formation of ROS, which induce LMP and lead to cell death (Jansson et al., 2010a; Lovejoy et al., 2011; Seebacher et al., 2016a). This is a key mechanism by which these agents exert their cytotoxic effects, and could account for the cytotoxicity and LMP observed in the presence of the Zn(II) complexes (Fig. 4.7,4.17). The ability of the Zn(II) complexes to undergo transmetallation with copper ions and mediate the oxidation of H_2DCF at lysosomal pH 5 (Fig. 4.18) is important, as [Zn(DpC)$_2$](ClO_4)$_2$ is localised to lysosomes. This

finding suggests that transmetallation with copper ions and subsequent redox cycling could explain the LMP observed in Figure 4.17.

4.3.11 Lysosomal Membrane Permeabilisation Mediated by $[Zn(Dp44mT\text{-}H)_2]$, $[Zn(Ap44mT\text{-}H)_2]$ and $[Zn(DpC)_2](ClO_4)_2$ is Dependent on Copper Ions

Previous results have demonstrated that the redox activity of [Cu(Dp44mT)] and [Cu(DpC)] mediates LMP (Jansson et al., 2015a; Lovejoy et al., 2011; Seebacher et al., 2016a). The transmetallation of $[Zn(Dp44mT\text{-}H)_2]$, $[Zn(Ap44mT\text{-}H)_2]$ and $[Zn(DpC)_2](ClO_4)_2$ with copper ions to generate redox-active Cu(II) complexes at both cytosolic (pH 7.4) and lysosomal pH (pH 5; Fig. 4.18), may explain their ability to mediate LMP (Fig. 4.17). Furthermore, it is unlikely that LMP occurs due to transmetallation of Zn(II) with Fe(III), as we previously demonstrated that the Fe(III)-Dp44mT complex does not induce LMP (Lovejoy et al., 2011). To investigate whether copper ion transmetallation was required to induce LMP by $[Zn(Dp44mT\text{-}H)_2]$, $[Zn(Ap44mT\text{-}H)_2]$ and $[Zn(DpC)_2](ClO_4)_2$, we examined lysosomal rupture in the presence and absence of the non-cytotoxic Cu(II) chelator, TM. TM has been shown to prevent LMP-mediated by the Cu(II) complexes of Dp44mT and bis(thiosemicarbazones) by sequestering copper ions (Lovejoy et al., 2011; Stefani et al., 2015).

Using the lysosomal integrity stain, AO (Gutierrez et al., 2014; Lovejoy et al., 2011; Nicolini et al., 1979; Pierzynska-Mach et al., 2014; Stefani et al., 2015), we assessed lysosomal membrane integrity in the KBV1, KB31 and SW480 cell-types.

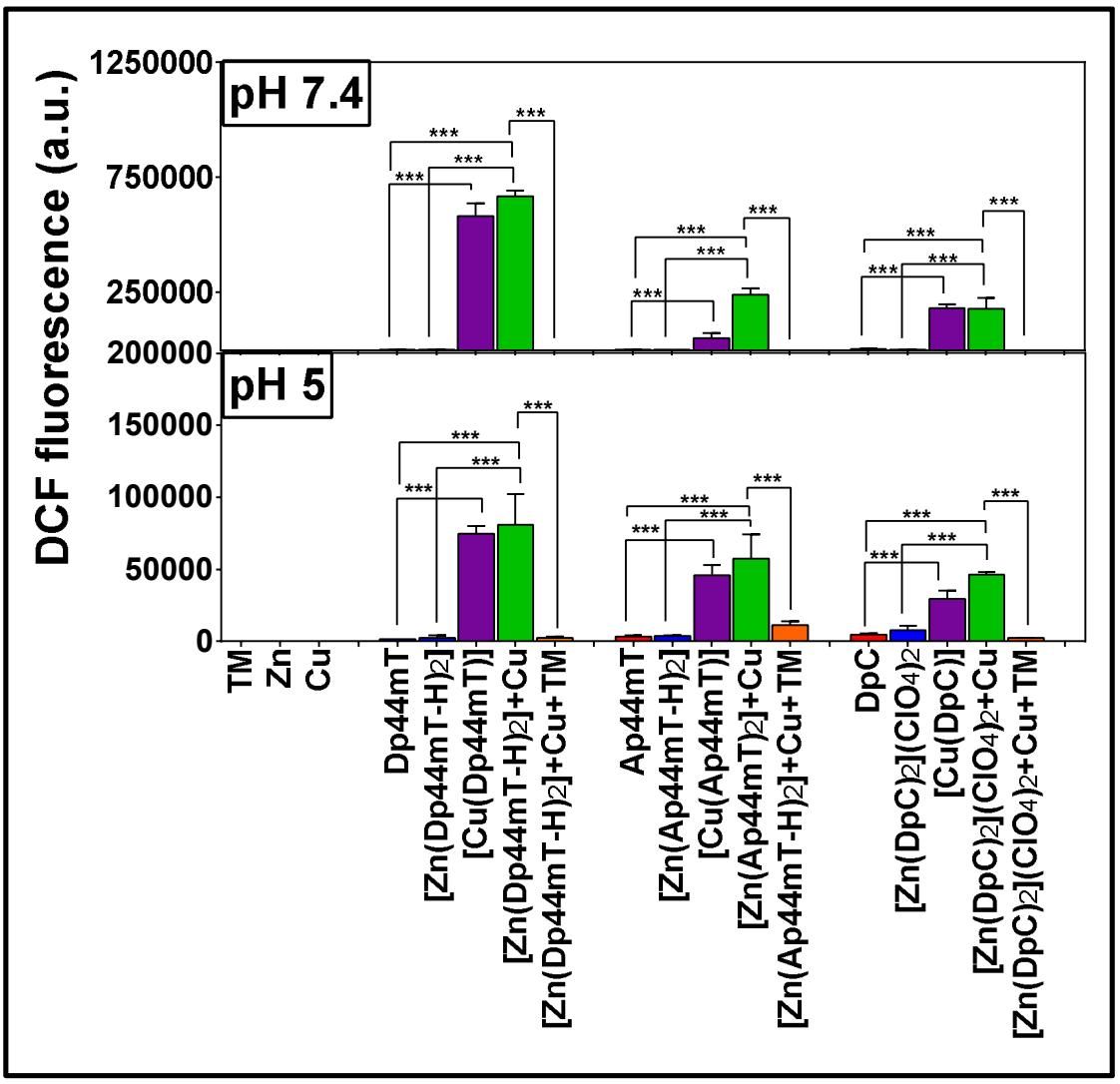

Figure 4.18. The redox activity of $[Zn(Dp44mT\text{-}H)_2]$, $[Zn(Ap44mT\text{-}H)_2]$ and $[Zn(DpC)_2](ClO_4)_2$ is dependent on transmetallation with copper ions.

At cytosolic pH (pH 7.4) and cytosolic pH (pH 5.0), Dp44mT, Ap44mT and DpC and their respective 1:2 (Zn(II)/ligand) zinc complexes show minimal redox activity. However, the Cu(II) complexes and the Zn(II) complexes + Cu(II) show significantly ($p < 0.001$) greater redox activity than their respective thiosemicarbazones or Zn(II) complex counterparts alone. The addition of the Cu(II) chelator, TM, to the Zn(II) complexes + Cu(II) reaction mixture, resulted in significantly ($p < 0.001$) decreased redox activity comparable to Zn(II) complexes + copper ions. Results are mean ± SD (3 experiments). *** $p < 0.001$.

[$Zn(Dp44mT\text{-}H)_2$], [$Zn(Ap44mT\text{-}H)_2$] and [$Zn(DpC)_2$](ClO_4)$_2$ mediated apparent lysosomal membrane disruption, shown by the absence of the red, punctate pattern of AO staining, over a 1 h/37^oC incubation (Fig. 4.19). However, the LMP mediated by [$Zn(Dp44mT\text{-}H)_2$], [$Zn(Ap44mT\text{-}H)_2$] and [$Zn(DpC)_2$](ClO_4)$_2$ was abrogated in the presence of the copper ion chelator, TM in all cell-types, as the punctate pattern of red AO staining was comparable to control cells (Fig. 4.19). Of note, TM itself did not significantly ($p > 0.05$) affect lysosomal membrane integrity (data not shown), which is consistent with the low cytotoxicity of this copper ion chelator.(Lovejoy et al., 2011; Stefani et al., 2015)

These results revealed that copper ions are involved in the induction of LMP observed following treatment with [$Zn(Dp44mT\text{-}H)_2$], [$Zn(Ap44mT\text{-}H)_2$] and [$Zn(DpC)_2$](ClO_4)$_2$ (Fig. 4.19). This is likely due to transmetallation with copper ions within the lysosomes (where [$Zn(DpC)_2$](ClO_4)$_2$ is sequestered; Fig. 4.14, 4.15, 4.16), which are known to have relatively high concentrations of copper ions, derived from autophagy of copper-containing proteins (Gupte and Mumper, 2009; Kurz et al., 2010; Terman and Kurz, 2013). In fact, we have demonstrated that it is possible for [$Zn(Dp44mT\text{-}H)_2$], [$Zn(Ap44mT\text{-}H)_2$] and [$Zn(DpC)_2$](ClO_4)$_2$ to form redox-active Cu(II) complexes under lysosomal conditions (Fig. 4.18).

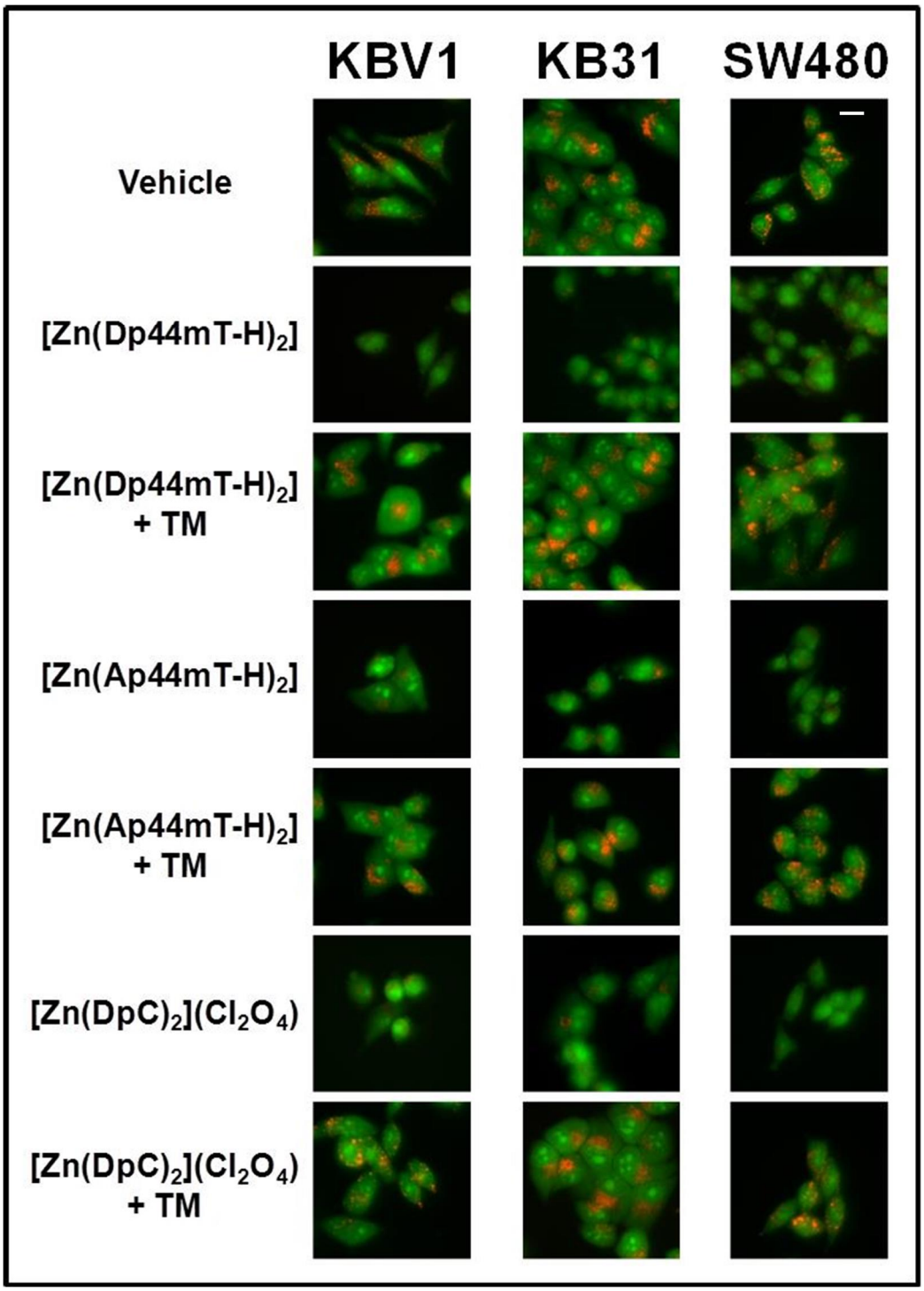

Figure 4.19. LMP mediated by [Zn(Dp44mT-H_2)], [Zn(Ap44mT-$H)_2$] and [$Zn(DpC)_2$]($(ClO_4)_2$ is dependent on copper ions.

Incubation of KBV1, KB31 and SW480 cells with [Zn(Dp44mT-H_2)], [Zn(Ap44mT-$H)_2$] and [$Zn(DpC)_2$]($(ClO_4)_2$ results in the loss of red, punctate staining that is indicative of intact lysosomes in control cells. However, co-incubation with [Zn(Dp44mT-H_2)], [Zn(Ap44mT-$H)_2$] and [$Zn(DpC)_2$]($(ClO_4)_2$ and the copper ion chelator, TM, prevents the loss of lysosomal membrane integrity observed with the Zn(II) complexes alone as the cells contain comparable amounts of red, AO-stained lysosomes as the control cells. The images are typical from 3 experiments. Scale bar: 10 ε m.

4.3.12 Involvement of Copper Ions in the Cytotoxicity of $[Zn(Dp44mT\text{-}H)_2]$, $[Zn(Ap44mT\text{-}H)_2]$ and $[Zn(DpC)_2](ClO_4)_2$

Previous studies have shown that the binding of copper ions by TM can markedly inhibit the cytotoxicity of Cu(II)-Dp44mT and other Cu(II)-thiosemicarbazone complexes (Lovejoy et al., 2011; Stefani et al., 2015). As the Zn(II) complexes were demonstrated to transmetallate to form redox-active Cu(II) complexes (Fig. 4.18), MTT assays were conducted in order to assess the effect of copper ions on the cytotoxicity of the Zn(II) complexes (Lovejoy et al., 2011; Stefani et al., 2015).

These MTT assays were carried out in the presence or absence of the non-toxic copper ion chelator, TM (Lovejoy et al., 2012; Stefani et al., 2015), in the KBV1, KB31 and SW480 cell-types. In the KBV1 cells, the addition of TM to $[Zn(Dp44mT\text{-}H)_2]$ caused a significant ($p < 0.01$), 2.1-fold increase in the IC_{50} relative to $[Zn(Dp44mT\text{-}H)_2]$ (Fig. 4.20). TM also significantly ($p < 0.05$) decreased the cytotoxicity of $[Zn(Ap44mT\text{-}H)_2]$ by 3.8-fold (Fig. 4.20). Similarly, the addition of TM to $[Zn(DpC)_2](ClO_4)_2$, significantly ($p < 0.001$) increased the IC_{50} of $[Zn(DpC)_2](ClO_4)_2$ by 44-fold (Fig. 4.20).

The results in the KB31 and SW480 cell-types followed a similar trend as in the KBV1 cell-type. In the KB31 cells, TM caused a significant ($p < 0.001$), 2.5-fold increase in the IC_{50} of $[Zn(Dp44mT\text{-}H)_2]$ (Fig. 4.20). However, in the SW480 cells, the IC_{50} of $[Zn(Dp44mT\text{-}H)_2]$ was not significantly ($p > 0.05$) affected by the addition of TM (Fig. 4.20).

The IC_{50} values of $[Zn(Ap44mT\text{-}H)_2]$ and $[Zn(DpC)_2](ClO_4)_2$ in both KB31 and SW480 cells were significantly (p < 0.001-0.01) increased by TM between 3.4- to 6.8-fold (Fig. 4.20). These results demonstrated that the cytotoxicity of the Zn(II) complexes involved transmetallation with copper ions, as the copper ion chelator TM decreased the cytotoxicity of the Zn(II) complexes. This cytotoxicity was a result of lysosomal membrane disruption (Figs. 4.17, 4.19), caused by transmetallation and formation of ROS-generating Cu(II) complexes within lysosomes (Fig. 4.18). Indeed, it has been demonstrated previously that the Cu(II) complexes of Dp44mT and DpC (Jansson et al., 2015b; Lovejoy et al., 2011; Seebacher et al., 2016a) cause LMP *via* redox cycling within lysosomes.

4.4 Conclusions

For over a decade, the *in vitro* and *in vivo* anti-cancer activity of a range of thiosemicarbazone ligands derived from ApT, DpT and BpT series has been explored (Gutierrez et al., 2014; Jansson et al., 2010a; Jansson et al., 2015a; Jansson et al., 2015b; Kalinowski et al., 2007; Kovacevic et al., 2011; Lovejoy and Richardson, 2002; Lovejoy et al., 2012; Richardson et al., 2006; Richardson et al., 2009). In spite of potent activity as Fe(III) and Cu(II) chelators, their intracellular localisation has been poorly understood. However, it appeared from indirect evidence that Dp44mT and DpC could be sequestered in lysosomes, where they could form redox-active Cu(II) complexes to induce LMP (Gutierrez et al., 2014; Jansson et al., 2010a; Jansson et al., 2015b; Lovejoy et al., 2011).

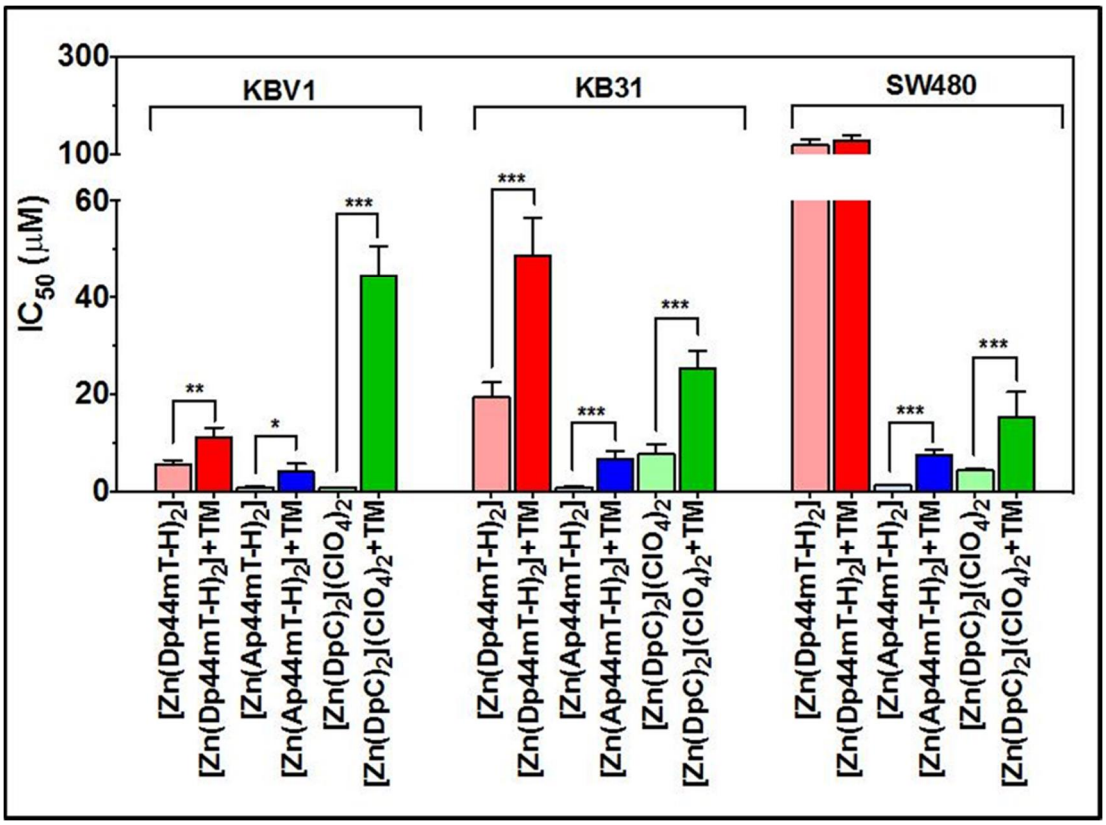

Figure 4.20 Copper ion chelation decreases the cytotoxicity of Zn(Dp44mT-H)2], [Zn(Ap44mT-H)2] and [Zn(DpC)2](ClO4)2.

In the KBV1, KB31 and SW480 cell-types, 24 h/37°C incubation of cells with $[Zn(Dp44mT\text{-}H)_2]$, $[Zn(Ap44mT\text{-}H)_2]$ and $[Zn(DpC)_2](ClO_4)_2$ in the presence of the copper ion chelator, TM, resulted in significantly higher ($p < 0.01$) IC_{50} values relative to $[Zn(Dp44mT\text{-}H)_2]$, $[Zn(Ap44mT\text{-}H)_2]$ and $[Zn(DpC)_2](ClO_4)_2$ alone. Results are mean ± SD (3 experiments). *$p < 0.05$; ** $p < 0.01$; *** $p < 0.001$.

Precise determination of the subcellular distribution of the ligands, Dp44mT, Ap44mT and DpC, were limited by the lack of inherent fluorescence exhibited by the thiosemicarbazones. In order to circumvent this limitation, we have designed and synthesised a series of Zn(II)-thiosemicarbazone complexes of our lead compounds, Dp44mT and DpC. Further, we have also prepared Zn(II)-thiosemicarbazone complexes of Ap44mT, which was added as a structurally different thiosemicarbazone to enable elucidation of structure-activity relationships.

Previous studies have highlighted the application of Zn(II) mono- and bis(thiosemicarbazones) for intracellular imaging by utilising the intrinsic fluorescence of Zn(II) (Cowley et al., 2005; Dayal et al., 2011; Lim et al., 2010; Pascu et al., 2007; Pascu et al., 2008). We sought to take advantage of this useful property to examine the localisation of our Zn(II) complexes in different cancer cell-types, which could provide information regarding mechanism(s) of action.

Our studies demonstrated the ability of Dp44mT, Ap44mT and DpC to form both 1:1 and 1:2 (Zn(II)/ligand) zinc complexes with distorted square pyramidal or octahedral geometry, respectively (Fig. 4.2). Interestingly, Zn(II)/ligand binding studies demonstrated the preference for the formation of 1:1 and 1:2 (Zn(II)/ligand) zinc complexes in DMSO and in aqueous solution (MOPS; pH: 7.4), respectively (Fig. 4.4, 4.5, 4.6). Moreover, our fluorescence studies of the Zn(II) complexes in DMSO characterised their energy emission profile, which were utilised further for fluorescence-based cellular imaging experiments (Fig. 4.3).

Proliferation assays evaluating the cytotoxicity of the 1:1 and 1:2 (Zn(II)/ligand) zinc complexes demonstrated that, in general, the majority of Zn(II) complexes were more cytotoxic than their corresponding free ligands in KBV1, KB31 and SW480 cells (Fig. 4.7). Furthermore, the 1:1 and 1:2 (Zn(II)/ligand) complexes of Dp44mT and DpC were more cytotoxic in Pgp-expressing KBV1 cells relative to KB31 and SW480 cells that have low levels of Pgp expression (Jansson et al., 2015b; Miklos et al., 2015; Montazami et al., 2015; Seebacher et al., 2016a; Seebacher et al., 2015; Yamagishi et al., 2013) (Fig. 4.7). On the other hand, the cytotoxicity of the 1:1 and

1:2 (Zn(II)/ligand) complexes of Ap44mT were similar between all three cell-types, suggesting that Pgp expression did not affect its activity (Fig. 4.7). In terms of structure-activity relationships, the replacement of the non-coordinating pyridine ring of Dp44mT and DpC with the methyl substituent present in Ap44mT leads to the loss of Pgp-potentiated cytotoxicity and highlights the importance of the di-2-pyridyl pharmacophore in overcoming Pgp-dependent resistance. Previous reports have demonstrated that Dp44mT and DpC exhibit potentiated cytotoxicity in Pgp-expressing cells (Jansson et al., 2015b; Seebacher et al., 2016a; Whitnall et al., 2006) and the current data support these results (Fig. 4.7).

Previous imaging studies involving Zn(II) thiosemicarbazone complexes demonstrated that the distribution of Zn(II)bis(thiosemicarbazones) varies depending on the cancer cell-type used (Cowley et al., 2005; Pascu et al., 2008). We therefore used three cell-types (*i.e.*, KBV1, KB31 and SW480) to assess the localisation of our Zn(II) complexes. We assessed co-localisation with the nucleus (Fig. 4.8, 4.9, 4.10), mitochondria (Fig. 4.11, 4.12, 4.13) and lysosomes (Fig. 4.14, 4.15, 4.16), as similar Zn(II) thiosemicarbazone complexes have been reported to localise to these organelles (Cowley et al., 2005; Dayal et al., 2011; Kowol et al., 2010; Pascu et al., 2008; Pascu et al., 2010). Our cell-based experiments utilised the 1:2 (Zn(II)/ligand) zinc complexes as binding studies demonstrated that this was the major species to form in aqueous solution (Fig. 4.4, 4.5, 4.6). In particular, we examined $[Zn(DpC)_2](ClO_4)_2$, which exhibited good intracellular fluorescence and was also of special interest as DpC will enter clinical trials in 2016 (ClinicalTrials.gov Identifier NCT02688101) (Jansson et al., 2015a). The results of our co-localisation studies revealed that $[Zn(DpC)_2](ClO_4)_2$ was localised to lysosomes in all three cell-types

(Fig. 4.14, 4.15, 4.16), rather than the nucleus (Fig. 4.8, 4.9, 4.10), or mitochondrion (4.11, 4.12, 4.13).

Further mechanistic studies illustrated the role of intracellular copper ions on the cytotoxicity of the Zn(II) complexes. While the Zn(II) complexes were not redox-active, as Zn(II) is unable to redox cycle (Berg and Shi, 1996), the addition of Cu(II) to the Zn(II) complexes caused a significant increase in DCF fluorescence (Fig. 4.18). This increase in DCF fluorescence could be abrogated by the addition of the non-toxic copper ion chelator, TM, which suggested that the Zn(II) complexes could transmetallate with copper ions and form redox-active Cu(II) complexes (Fig. 4.18). Furthermore, TM could also reverse the LMP (Fig. 4.19) and cytotoxicity (Fig. 4.20) induced by the Zn(II) complexes. These studies with TM suggested that transmetallation with copper ions was integral to the anti-cancer activity observed with the Zn(II) complexes.

Collectively, the results presented herein demonstrated that the mechanism of action of our Zn(II) complexes involved: **(1)** sequestration within lysosomes; **(2)** transmetallation with the intra-lysosomal copper ions (Gupte and Mumper, 2009; Kurz et al., 2010; Terman and Kurz, 2013) which produced redox-active complexes; and **(3)** induction of LMP-mediated cytotoxicity by ROS (Fig. 21).

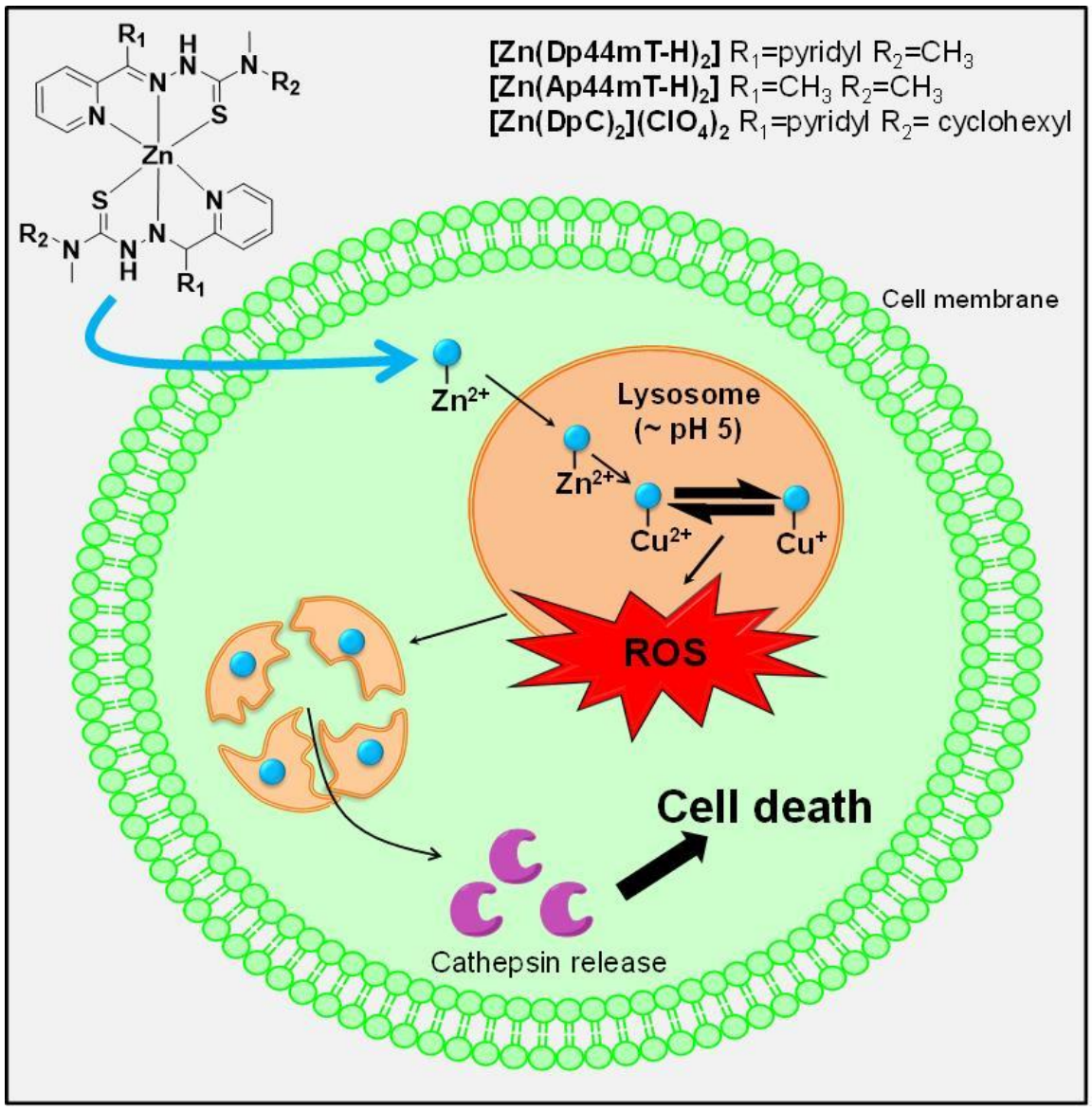

Figure 4.21. Schematic illustrating the mechanism of action of Zn(II)-thiosemicarbazone complexes.

The mechanism of the Zn(II) complexes involves uptake into the cell followed by sequestration within lysosomes. The Zn(II) complexes transmetallate with copper ions present in the lysosomes to form redox-active complexes. The redox cycling of these newly formed Cu(II) complexes generates ROS, which causes LMP-mediated cytotoxicity.

Chapter 5 - DpC, but not Dp44mT, Overcomes Bcl-2-Mediated Multidrug Resistance in Melanoma

5.1 Introduction

The Bcl-2 family of proteins act as master regulators of the intrinsic pathway of apoptosis (Cory and Adams, 2002; Czabotar et al., 2014; Youle and Strasser, 2008). The family consists of three classes of proteins: **(1)** Bcl-2 homology 3 (BH3)-only proteins ("Initiators") that exert pro-apoptotic effects; **(2)** multi-domain anti-apoptotic ("Guardians"), which include Bcl-2 (Tsujimoto et al., 1985); and **(3)** multi-domain pro-apoptotic ("Effectors"), which includes Bcl-2-associated X protein (Bax) (Oltvai et al., 1993). An interplay between the pro-apoptotic and anti-apoptotic Bcl-2 family members regulates the release of cytochrome *c* from the mitochondria, and subsequent activation of the effector caspases that induce apoptosis (Cory and Adams, 2002; Czabotar et al., 2014; Danial, 2007). In addition to their role in regulating apoptosis, Bcl-2 family members have been found to regulate autophagy (Chang et al., 2010; Kihara et al., 2001; Pattingre et al., 2005). A key protein involved in autophagy initiation, Beclin 1, is in fact a novel BH3-only protein that is inhibited by Bcl-2 (Chang et al., 2010; Kihara et al., 2001; Pattingre et al., 2005).

Dysregulated expression of the Bcl-2 family members is an underlying cause or contributor in many different types of cancer, as impairment of apoptosis is fundamental to carcinogenesis (Thomas et al., 2013). Over-expression of Bcl-2 occurs in a diverse range of cancers (Bincoletto et al., 1999; Gazzaniga et al., 1996; Hermine et al., 1996; Jiang et al., 1995; Joensuu et al., 1994; McDonnell et al., 1992; Sinicrope et al., 1995; Tothova et al., 2002; Weiss et al., 1987; Weller et al., 1995); including metastatic melanoma (Grover and Wilson, 1996), which is resistant to all standard chemotherapies (Soengas and Lowe, 2003). In many of these cancers, including melanoma, Bcl-2 has been linked to severity of malignancy, poor clinical response and poor prognosis (Bincoletto et al., 1999; Grover and Wilson, 1996; Hermine et al., 1996; Joensuu et al., 1994; McDonnell et al., 1992; Tothova et al., 2002). Indeed, the Bcl-2 antisense oligonucleotide, oblimersen, was clinically trialled in advanced melanoma (Bedikian et al., 2006; Bedikian et al., 2014).

Bcl-2 exerts its anti-apoptotic function by binding to the pro-apoptotic family members, Bax and Bak, which prevents them from causing mitochondrial outer membrane permeabilisation (Certo et al., 2006). Over-expression of Bcl-2 allows cancer cells to ñignoreò apoptotic signals generated in response to chemotherapeutics, in the form of increased levels and activation of pro-apoptotic Bcl-2 family members (Amundson et al., 2000; Dole et al., 1994; Miyashita and Reed, 1993; Schmitt et al., 2000; Shibata et al., 1999; Strasser et al., 1993; Thomas et al., 1996; Vaux et al., 1988; Wang et al., 2013). Bcl-2 over-expression has consequently been found to contribute to MDR (Amundson et al., 2000; Dole et al., 1994; Miyashita and Reed, 1993; Schmitt et al., 2000; Shibata et

al., 1999; Strasser et al., 1993; Thomas et al., 1996; Vaux et al., 1988; Wang et al., 2013), making it an important drug target (Thomas et al., 2013). Indeed, inhibiting Bcl-2 sensitises cells to standard chemotherapies in MDR cancers, such as melanoma (Nemati et al., 2014; Raisova et al., 2001; Watanabe et al., 2013; Wroblewski et al., 2013). This has resulted in the development of several promising small molecule inhibitors of Bcl-2, such as ABT-199 (venetoclax), that have progressed to clinical trials (Roberts et al., 2016; Stilgenbauer et al., 2016).

Over the last 20 years, our laboratory has developed a range of novel anti-cancer agents (Baker et al., 1992; Becker et al., 2003; Darnell and Richardson, 1999; Richardson et al., 1995; Richardson and Milnes, 1997). Extensive structure-activity relationship studies led to the development of the DpT series, designed by incorporating the di-2-pyridylketone moiety into a structural backbone derived from aroylhydrazones (Becker et al., 2003; Bernhardt et al., 2003; Richardson et al., 2006; Yuan et al., 2004). The DpT analogues exhibit potent anti-tumour activity and anti-metastatic activity both *in vitro* and *in vivo* (Chen et al., 2012; Liu et al., 2012; Lovejoy et al., 2012; Richardson et al., 2006; Whitnall et al., 2006; Yuan et al., 2004). The best-characterised member of the DpT analogues, Dp44mT, targets the lysosome, where it redox cycles with copper ions (Figs. 3.6, 3.8, 3.9, 3.10, 4.17, 4.18, 4.19) (Gutierrez et al., 2014; Jansson et al., 2015b; Lovejoy et al., 2011). The redox activity of the [Cu(Dp44mT)] complex produces ROS that induce LMP and apoptosis (Figs. 3.4, 3.6, 3.8, 3.9, 3.10, 4.17, 4.18, 4.19) (Gutierrez et al., 2014; Jansson et al., 2015b; Lovejoy et al., 2011). Dp44mT also affects the expression of Bcl-2 family members by increasing the ratio of pro-apoptotic

Bax to anti-apoptotic Bcl-2, causing the release of holocytochrome *c* from the mitochondria (Gutierrez et al., 2014; Yuan et al., 2004). Dp44mT is notable for the multiple ways in which it is able to ñhijackò mechanisms of cellular resistance, namely, the Pgp drug efflux transporter and the autophagy pathway, to target lysosomes and induce apoptosis (Gutierrez et al., 2014; Jansson et al., 2015b; Seebacher et al., 2016a; Whitnall et al., 2006).

Unfortunately, high, non-optimal doses of Dp44mT induced cardiac fibrosis (Whitnall et al., 2006), which led to the design and synthesis of the second generation of DpT analogues, in which the terminal H at N4 was replaced with an alkyl group. This group showed particular promise, and of these ligands, DpC was identified as the lead agent (Kovacevic et al., 2011; Lovejoy and Richardson, 2002; Lovejoy et al., 2012). Favourable properties such as greater anti-tumour activity *in vivo* (Kovacevic et al., 2011; Lovejoy et al., 2012), and markedly improved tolerability (Lovejoy et al., 2012; Quach et al., 2012; Yu et al., 2012) compared to Dp44mT, resulted in DpC being commercialised. DpC has entered clinical trials in 2016 (ClinicalTrials.gov Identifier NCT02688101) for the treatment of advanced and resistant cancers (Jansson et al., 2015a).

Herein, we examined for the first time the effects of Dp44mT and DpC in cells over-expressing Bcl-2. Interestingly, we demonstrated that DpC decreased Bcl-2 expression, while Dp44mT did not. Moreover, silencing of Bcl-2 only affected the cytotoxicity of

Dp44mT, but not DpC. Furthermore, we showed that the mechanism by which DpC and Dp44mT exerted their cytotoxicity in melanoma cells did not involve copper ion binding or ROS generation, which are characteristics that thiosemicarbazones must possess in order to cause LMP.

This latter effect was starkly different in melanoma cells compared to other neoplastic cell types (Gutierrez et al., 2014; Jansson et al., 2010b; Jansson et al., 2015b; Lovejoy et al., 2011; Seebacher et al., 2016a), indicating a remarkably different mechanism. In fact, DpC induced autophagosome formation and increased the accumulation of acidic vesicles (***e.g.***, autolysosomes), regardless of Bcl-2 expression. Dp44mT, on the other hand, did not increase the formation of autophagosomes in Bcl-2 expressing cells, and only increased the number of acidic vesicles in the absence of Bcl-2 expression. We propose the mechanism by which DpC is able to overcome Bcl-2-mediated resistance involves decreasing the expression of Bcl-2, which increases autophagosome formation and the accumulation of autolysosome-like acidic vesicles.

5.3 Results and Discussion

5.3.1 DpC, but Not Dp44mT, Overcomes Bcl-2-mediated MDR

Targeting Bcl-2 expression is of interest as over-expression of Bcl-2 confers MDR by allowing cells to ignore cytotoxic stimuli and evade apoptosis (Amundson et al., 2000;

Dole et al., 1994; Miyashita and Reed, 1993; Schmitt et al., 2000; Shibata et al., 1999; Strasser et al., 1993; Thomas et al., 1996; Vaux et al., 1988; Wang et al., 2013). This is significant in a wide range of cancers, including melanoma (Grover and Wilson, 1996), where Bcl-2 is commonly up-regulated (Bincoletto et al., 1999; Gazzaniga et al., 1996; Hermine et al., 1996; Jiang et al., 1995; Joensuu et al., 1994; McDonnell et al., 1992; Sinicrope et al., 1995; Tothova et al., 2002; Weller et al., 1995). High Bcl-2 expression enables cancer cells to survive exposure to chemotherapy, thus contributing to MDR (Skommer et al., 2006; Wang et al., 2013; Wu et al., 2015). It has been demonstrated that Dp44mT causes an increase in the Bax:Bcl-2 ratio, suggesting that Dp44mT may act, at least in part, by regulating the ratio of pro- and anti-apoptotic Bcl-2 family members (Gutierrez et al., 2014; Yuan et al., 2004). Furthermore, Dp44mT induces the release of holocytochrome ***c*** from mitochondria and activates caspases, due to the increase in the Bax:Bcl-2 ratio (Yuan et al., 2004). However, the effect of Bcl-2 expression on the cytotoxicity of Dp44mT or DpC has not previously been examined.

Notably, Dp44mT and DpC are able to overcome Pgp-mediated MDR (Jansson et al., 2015a; Seebacher et al., 2016a) (Figs. 3.4, 3.6, 3.8). Therefore, it is of interest to examine whether Dp44mT or DpC are also able to overcome Bcl-2-mediated MDR. We investigated this using the M14 melanoma cell line (Chambers, 2009; Rae et al., 2007), as melanoma is known to be prone to Bcl-2-mediated MDR, and there is a pressing need for new therapies (Grover and Wilson, 1996; Soengas and Lowe, 2003).

M14 Bcl-2 (Bcl-2 over-expressing) and M14 PC (control) cells were incubated with Dp44mT or DpC for 24 h/37°C. Dp44mT was 1.5-fold less ($p < 0.001$) cytotoxic in M14 Bcl-2 cells than in M14 PC cells, demonstrating a 20 μM difference in IC_{50} values between the cell lines (Fig. 5.1). In contrast, there was no significant difference ($p > 0.05$) in cytotoxicity mediated by DpC between the M14 Bcl-2 and M14 PC cell lines (Fig. 5.1).

The results from Figure 5.1 suggested that DpC, but not Dp44mT, was capable of overcoming Bcl-2-mediated MDR. That is, Bcl-2 provided a survival advantage against Dp44mT-mediated cell killing, but not DpC-mediated cell killing. Regardless of whether cells expressed Bcl-2, the IC_{50} value of DpC did not change. However, in cells that expressed Bcl-2 (M14 Bcl-2), Dp44mT was significantly less cytotoxic than in cells that did not express Bcl-2 (M14 PC). This is an interesting result, as targeting Bcl-2 has long been investigated as a method of improving the efficacy of cancer treatments (Czabotar et al., 2014; Lessene et al., 2008; Thomas et al., 1996). Unlike overcoming Pgp-mediated MDR, in which DpC and Dp44mT act in a similar manner, these agents differ in their mechanism to overcoming Bcl-2 MDR, at least in M14 melanoma cells (Figs. 3.4, 3.6, 3.8). These results warranted further investigation in order to determine the mechanism by which DpC overcame Bcl-2-mediated MDR.

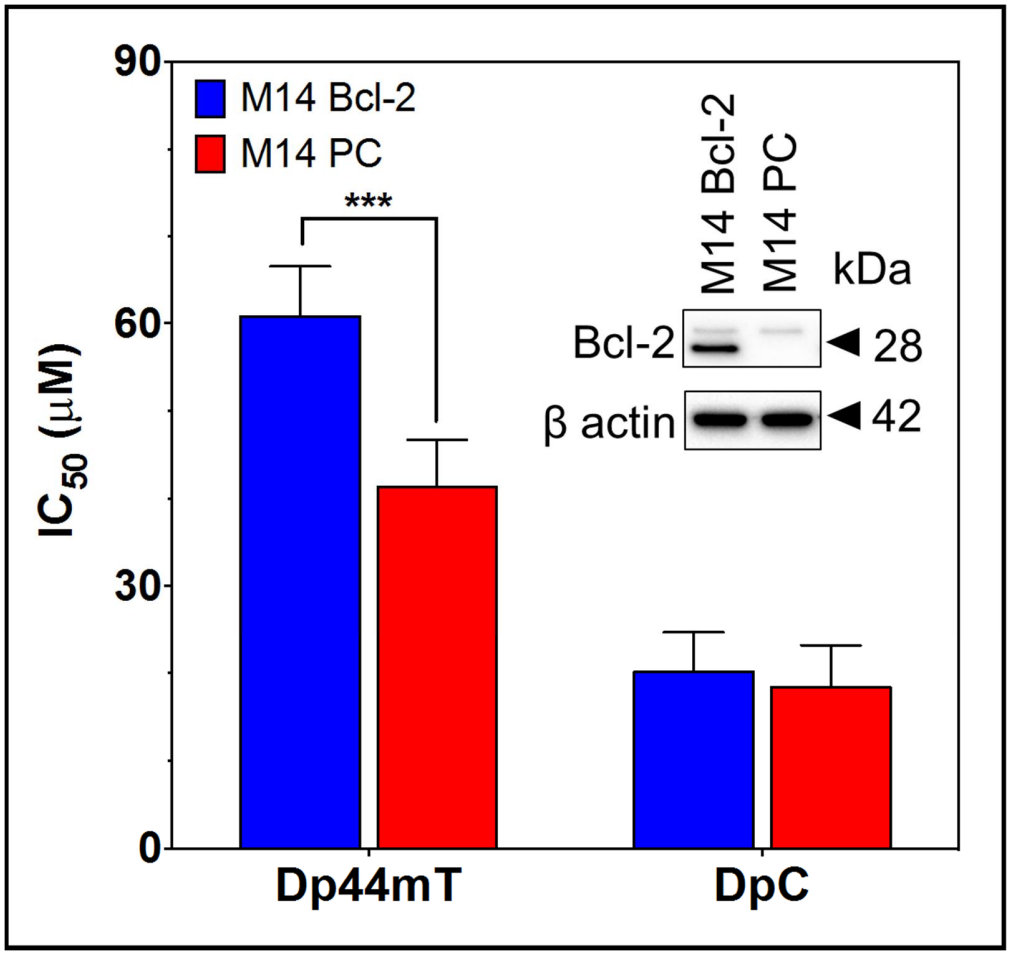

Figure 5.1 DpC, but not Dp44mT, overcomes Bcl-2-mediated drug resistance.

The cytotoxicity of Dp44mT was significantly (p < 0.001) less in M14 Bcl-2 over-expressing cells than in M14 PC (control) cells following a 24 h/37°C incubation. Bcl-2 expression did not affect the cytotoxicity of DpC. *Inset* Western blot of Bcl-2 expression in M14 bcl-2 and M14 PC cells. Results are mean ± SD (3 experiments). *** p < 0.001

5.3.2 DpC Decreases the Expression of Bcl-2, Relative to Dp44mT and Control

Dp44mT has been reported to cause an increase in the ratio of pro-apoptotic Bax to anti-apoptotic Bcl-2 (Gutierrez et al., 2014; Yuan et al., 2004). This indicates that

Dp44mT increases the sensitivity of cells to apoptosis (Raisova et al., 2001), and suggests that Dp44mT may regulate Bcl-2 family members (Gutierrez et al., 2014; Yuan et al., 2004). Herein, we have shown that DpC, but not Dp44mT, is capable of overcoming Bcl-2-mediated MDR in the M14 cell lines, M14 Bcl-2 and M14 PC (Fig. 5.1). Therefore, we assessed the effects of Dp44mT and DpC on Bcl-2 protein expression *via* Western blotting in the Bcl-2 over-expressing M14 Bcl-2 cell line.

A 24 h/37°C incubation with Dp44mT (30 μM) induced a non-significant ($p > 0.05$) 15% decrease in Bcl-2 expression, relative to control (Fig. 5.2A,B). Interestingly, a similar incubation with DpC (30 μM) resulted in a statistically significant ($p < 0.01$) 57% decrease in Bcl-2 expression, relative to control (Fig. 5.2A,B). Furthermore, incubation with DpC induced a 50% ($p < 0.05$) decrease in Bcl-2 expression, relative to Dp44mT (Fig. 5.2B).

The results in Figure 5.2 show that DpC, but not Dp44mT, significantly ($p < 0.01$) decreased the expression of Bcl-2 in M14 Bcl-2 cells, relative to control. The decrease in Bcl-2 expression following treatment with DpC could explain its ability to overcome Bcl-2-mediated MDR (Fig. 5.1), as cells could be expected to become more sensitive to the apoptotic signals generated by DpC (Raisova et al., 2001). Unlike DpC, Dp44mT did not cause a significant ($p > 0.05$) decrease in Bcl-2 expression (Fig. 5.2A,B). Hence, as Dp44mT did not decrease Bcl-2 expression compared to DpC, this could explain why Dp44mT was significantly ($p < 0.001$) less cytotoxic in M14 Bcl-2 cells (*i.e.*, higher IC_{50})

than in M14 PC cells (Fig. 5.1). The effect of Dp44mT on Bcl-2 expression appears to be dependent on the cell line used, as Dp44mT did not affect Bcl-2 expression in the MCF-7 cell line (Gutierrez et al., 2014), but did decrease Bcl-2 expression in the SK-N-MC cell line (Yuan et al., 2004). Importantly, these studies highlight the potential of DpC to overcome Bcl-2-mediated MDR and treating melanoma. Although some have focused on inhibiting Bcl-2 (Lessene et al., 2008; Thomas et al., 2013), DpC instead decreases the expression of Bcl-2, similar to the clinically trialled drug, oblimersen (Bedikian et al., 2006; Bedikian et al., 2014; O'Brien et al., 2009).

5.3.3 Bcl-2 Silencing Affects the Cytotoxicity of Dp44mT, but not DpC

Bcl-2 expression is known to cause MDR by preventing apoptosis in response to chemotherapy treatment in cancer cells (Amundson et al., 2000; Dole et al., 1994; Miyashita and Reed, 1993; Schmitt et al., 2000; Shibata et al., 1999; Strasser et al., 1993; Thomas et al., 1996; Vaux et al., 1988). Bcl-2 silencing and inhibition has been investigated, with some success, as an important drug discovery target (Lessene et al., 2008; Thomas et al., 2013). DpC induced a significant decrease in Bcl-2 expression (Fig 5.2), which may account for its ability to overcome Bcl-2-mediated MDR (Fig. 5.1). This is in contrast to Dp44mT, which did not reduce Bcl-2 expression (Fig. 5.2), and did not overcome Bcl-2-mediated MDR (Fig. 5.1). Given the different effects of DpC and Dp44mT on cytotoxicity and Bcl-2 expression (Figs. 5.1, 5.2), it was of interest to examine the effects of silencing the *BCL2* gene, using siRNA.

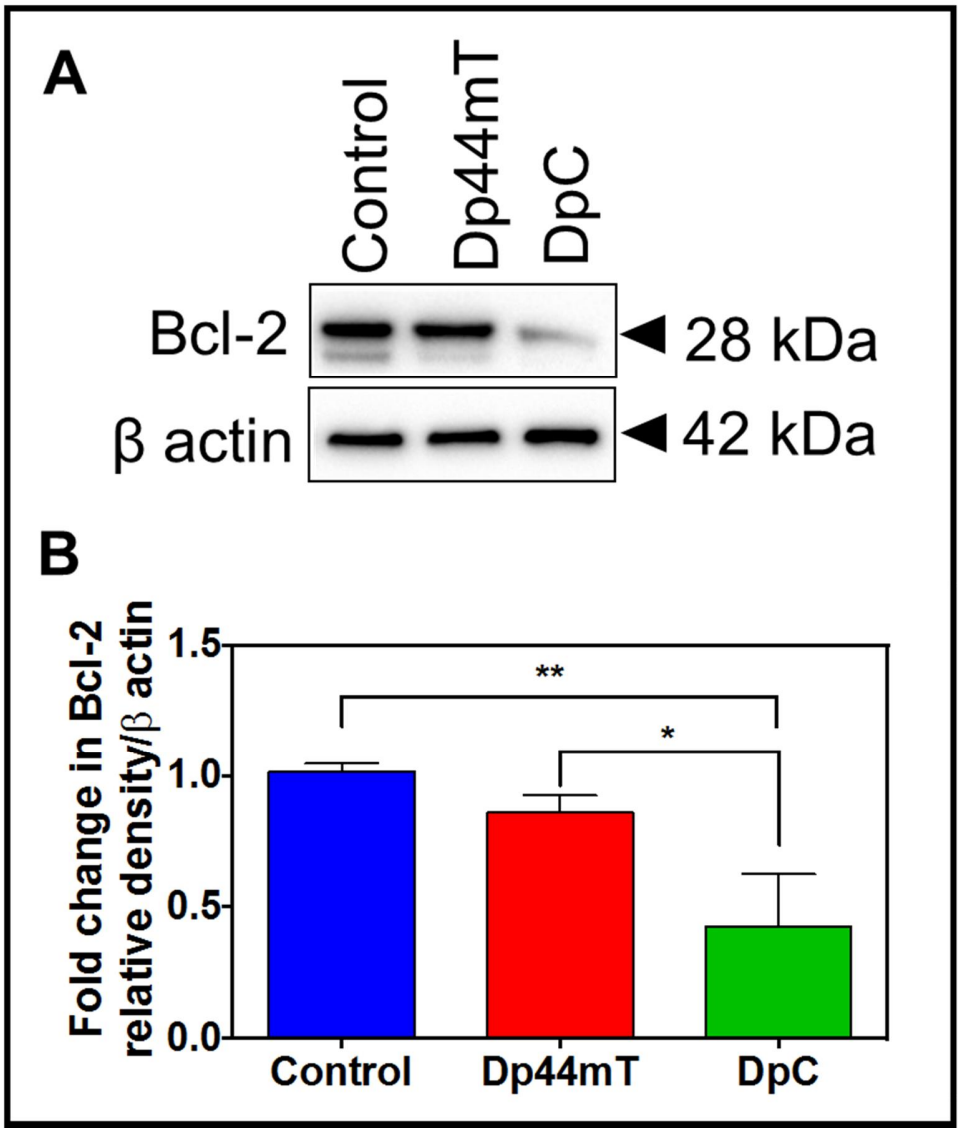

Figure 5.2 DpC significantly decreases Bcl-2 expression, relative to control or Dp44mT.

(A) M14 Bcl-2 cells were treated with control medium or medium containing Dp44mT (30 ε M) or DpC (30 ε M), and incubated for 24 h/ 37°C. Western blotting was performed to determine Bcl-2 expression. DpC, but not Dp44mT, decreased the expression of Bcl-2. **(B)** Densitometric analysis (arbitrary units) of **(A)**. DpC significantly decreased Bcl-2 expression, relative to control ($p < 0.01$) and Dp44mT ($p < 0.05$). Blots shown are representative of three experiments. Densitometric analysis is the mean of 3 ± S.D. * $p < 0.05$, ** $p < 0.01$.

M14 Bcl-2 cells were incubated with Dp44mT or DpC for 24 h/37°C, following a pre-incubation with siRNA targeting *BCL2* (Fig. 5.3). Silencing of Bcl-2 protein expression caused a significant ($p < 0.01$) decrease in the cytotoxicity of Dp44mT compared to control (Fig. 5.3). However, siRNA-mediated Bcl-2 silencing did not significantly ($p > 0.05$) affect the cytotoxicity of DpC (Fig. 5.5).

Bcl-2 silencing and inhibition using drugs such as oblimersin or ABT-199, respectively, has been shown to increase the clinical efficacy of commonly used chemotherapies (Bedikian et al., 2006; Skommer et al., 2006; Tse et al., 2008). Therefore, it is unsurprising that Dp44mT, which did not alter Bcl-2 expression (Fig 5.2), became more cytotoxic following silencing of Bcl-2 (Fig. 5.3). It could be expected that because DpC alone so effectively decreases Bcl-2 expression (Fig. 5.3), Bcl-2 silencing has no effect on its cytotoxicity (Fig. 5.3). These results demonstrate that Dp44mT-mediated cytotoxicity is more sensitive to Bcl-2 expression than DpC (Figs. 5.1, 5.3), which is likely due to the fact that DpC can decrease the expression of Bcl-2 much more effectively than Dp44mT (Fig. 5.2). Furthermore, these studies highlight the potential of DpC to overcome Bcl-2-mediated MDR, as DpC-mediated cytotoxicity was unaffected by Bcl-2 expression (Figs. 5.1, 5.3).

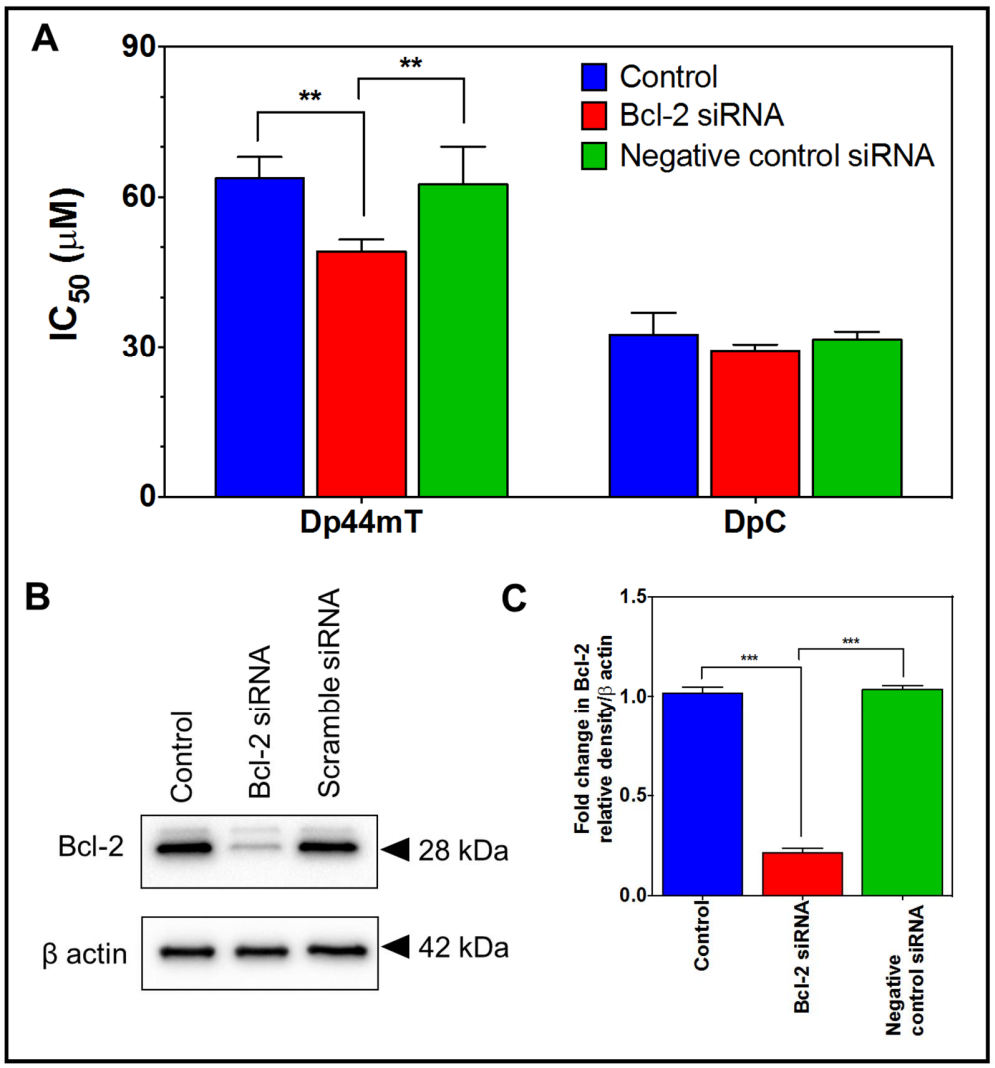

Figure 5.5. The cytotoxicity of Dp44mT, but not DpC, is increased by Bcl-2 silencing.

(A) The IC_{50} value of Dp44mT is significantly ($p < 0.01$) decreased following transfection of M14 Bcl-2 cells with *BCL2* siRNA for 96 h/ 37°C. The cytotoxicity of DpC was not significantly affected by Bcl-2 silencing ($p > 0.05$). The negative control siRNA did not affect the cytotoxicity of Dp44mT or DpC. **(B)** M14 Bcl-2 cells were transfected with *BCL2* siRNA or negative control scramble siRNA, and Western blotting performed to examine Bcl-2 expression. **(C)** Densitometric analysis (arbitrary units) of **(B)**. Blots shown are representative of three experiments. Densitometric analysis is the mean of 3 ± S.D. ** $p < 0.01$, *** $p < 0.001$

5.3.4 The Cytotoxicity Mediated by Dp44mT and DpC is Not Dependent on Copper Ions

The importance of Cu(II) binding in the mechanism of Dp44mT (Jansson et al., 2010b; Lovejoy et al., 2011) and DpC (Figs. 3.6, 3.9, 4.18-4.20) has been previously demonstrated. Studies have shown that the binding of copper ions by the copper ion chelator, TM, can markedly inhibit the cytotoxicity of [Cu(Dp44mT)] and other Cu(II)-thiosemicarbazone complexes (Figs. 3.9, 4.19, 4.20) (Jansson et al., 2015b; Lovejoy et al., 2011; Stefani et al., 2015). Furthermore, elesclomol, a structurally-related thiosemicarbazone that has been clinically trialled in melanoma (O'Day et al., 2013), is a potent and redox-active Cu(II) chelator (Yadav et al., 2013). We next assessed whether copper ion binding was involved in the cytotoxicity mediated by Dp44mT and DpC, in the M14 Bcl-2 and M14 PC melanoma cell lines.

After a 24 h/37°C co-incubation with control medium or the copper ion chelator, TM, no significant ($p > 0.05$) difference in the cytotoxicity of Dp44mT or DpC was observed (Fig. 5.4).

These results clearly demonstrate that the cytotoxicity mediated by Dp44mT and DpC in the M14 Bcl-2 and M14 PC cell lines was not related to their ability to bind Cu(II) (Fig. 5.4). This is in contrast to previous results that have shown that Cu(II) binding is required to induce potent cytotoxicity (Figs. 3.9, 4.19, 4.20) (Jansson et al., 2015b; Lovejoy et al., 2011; Stefani et al., 2015). Furthermore, DpC appears to overcome Bcl-

2-mediated MDR in melanoma *via* a novel mechanism that does not involve Cu(II) binding (Fig. 5.4). In contrast, Cu(II) binding is a requirement for DpC to overcome Pgp-mediated MDR (Figs. 3.6, 3.7, 3.9).

Notably, the copper-binding proteins, metallothioneins, have been shown to be highly expressed in melanoma, and are negative prognostic indicators (Krauter et al., 1989; Weinlich et al., 2006; Zelger et al., 1993). The probable lack of free, unbound, intracellular Cu(II) in the M14 melanoma cell lines could account for the results in Figure 5.4, as there may have been very low levels of free copper ions present within the cell for Dp44mT or DpC to bind (Krauter et al., 1989; Weinlich et al., 2006; Zelger et al., 1993). High expression of metallothionein also may account for the failure of the structurally-related elesclomol in clinical trials for advanced melanoma (O'Day et al., 2013), as Cu(II) binding is involved in its mechanism (Kirshner et al., 2008; Yadav et al., 2013). Indeed, elesclomol was shown to bind Cu(II) outside of cells and enter the cytoplasm as a Cu(II) complex, as opposed to binding Cu(II) intracellularly (Blackman et al., 2012; Nagai et al., 2012). Indeed, in order to examine the redox activity of elesclomol *in vitro* in melanoma cells, Cu(II) was added to the culture medium (Blackman et al., 2012; Nagai et al., 2012), which would circumvent the physiologically low levels of unbound copper ions in melanoma (Krauter et al., 1989; Weinlich et al., 2006; Zelger et al., 1993). However, DpC was able to overcome Bcl-2-mediated MDR (Fig. 5.1) in melanoma regardless of the presence of copper ions (Fig. 5.4), demonstrating its potential as a novel therapy for melanoma.

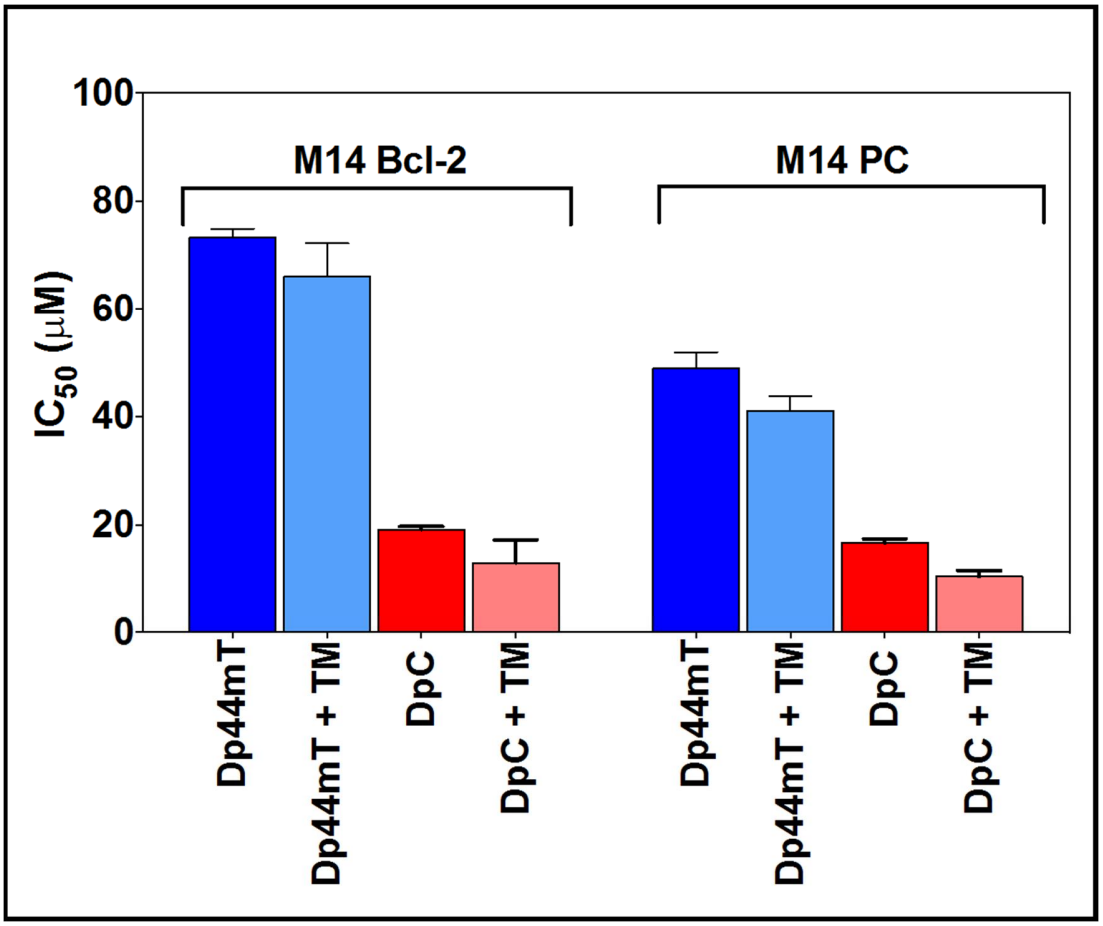

Figure 5.3 The cytotoxicity of Dp44mT and DpC is not dependent on copper ions.

The IC_{50} values of Dp44mT and DpC were not significantly different ($p > 0.05$) following a 24 h/ 37°C incubation with the copper ion chelator, TM (150 ε M). Results are mean ± SD (3 experiments).

5.3.5 Cytotoxicity Mediated by Dp44mT and DpC is Not Dependent on Redox Stress

Apart from acting as a crucial regulator of apoptosis, Bcl-2 has been reported to affect cellular redox state (Voehringer and Meyn, 2000). Evidence suggests that Bcl-2 exerts

anti-oxidant effects that cause cells to be resistant to oxidative injury (Ellerby et al., 1996; Hochman et al., 1998; Voehringer and Meyn, 2000; Zimmermann et al., 2007). The cytotoxicity of Dp44mT (Jansson et al., 2010b; Lovejoy et al., 2011) and DpC has been shown to be dependent on the ability of their metal complexes to redox cycle and generate ROS, leading to apoptotic cell death (Figs. 3.4, 3.7, 3.10). Indeed, redox cycling with Cu(II) and ROS generation was a requirement for Dp44mT and DpC to overcome Pgp-mediated MDR in KBV1 cervical cancer cells (Figs. 3.6-3.10). Interestingly, despite the reported anti-oxidant effects of Bcl-2 (Voehringer and Meyn, 2000), Dp44mT and DpC were cytotoxic in M14 Bcl-2 cells, although Dp44mT did not overcome Bcl-2-mediated MDR like DpC (Fig. 5.1). DpC also caused a significant decrease in Bcl-2 expression (Fig. 5.2), which could alter the anti-oxidant effects of Bcl-2. We therefore next investigated whether the observed cytotoxicity of Dp44mT and DpC could be related to their redox activity using the membrane-permeant anti-oxidant, NAC (Lovejoy et al., 2011; Stefani et al., 2015).

Following a 24 h/37°C co-incubation with the anti-oxidant, NAC, no significant ($p > 0.05$) difference in cytotoxicity was observed as compared to Dp44mT and DpC alone (Fig. 5.5). This is in contrast to previous results in other cell types, which have demonstrated that the redox activity of Dp44mT (Jansson et al., 2010b; Lovejoy et al., 2011) and DpC, is a key requirement in their anti-proliferative mechanism of action (Figs. 3.6-3.10).

Indeed, despite inducing a significant decrease in the expression of Bcl-2 (Fig 2), which has been shown to act as an anti-oxidant by regulating levels of the anti-oxidant protein, GSH, and by affecting mitochondrial ROS production (Ellerby et al., 1996; Hochman et al., 1998; Voehringer and Meyn, 2000; Zimmermann et al., 2007), DpC does not demonstrate evidence of redox cycling (Figs. 5.4). This could be due to the probable lack of free, unbound copper ions due to high metallothionein expression in the melanoma cell lines (Krauter et al., 1989; Weinlich et al., 2006; Zelger et al., 1993); as the Cu(II) complex of DpC is more potently redox-active than the ligand alone (Figs. 3.7, 3.10, 4.17). Intriguingly, these results suggested that DpC overcame Bcl-2-mediated MDR *via* a novel mechanism that did not involve the generation of ROS.

5.3.6 DpC, but Not Dp44mT, Increases Expression of the Classical Marker of Autophagosome Formation, LC3-II

Dp44mT has been shown to target the pro-survival autophagy pathway (Gutierrez et al., 2014). The formation of the double membrane vesicle, the autophagosome, involves a complex interplay of proteins such as the PI3K·Beclin 1 complex, ATG5·ATG12, and LC3-phosphatidylethanolamine conjugation system (Kondo et al., 2005).

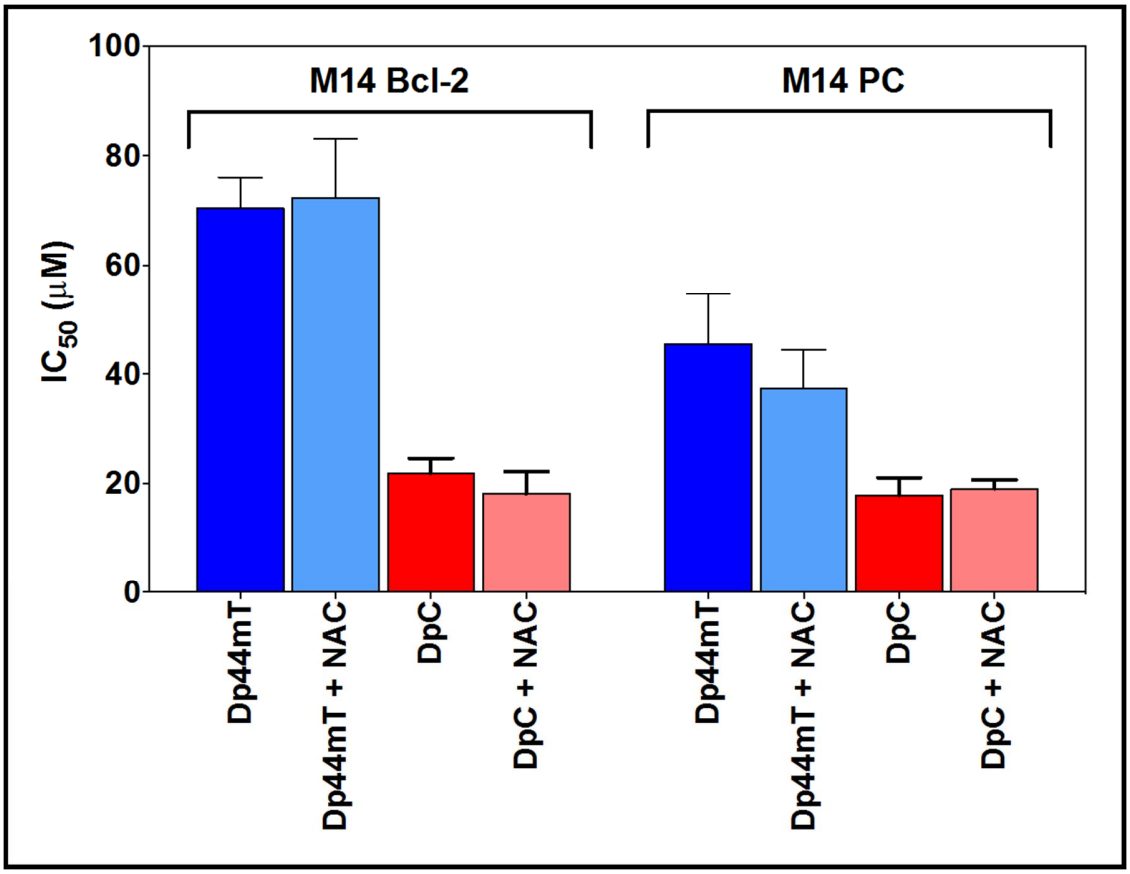

Figure 5.4 The cytotoxicity of Dp44mT and DpC were not dependent on redox activity.

The IC_{50} values of Dp44mT and DpC were not significantly different ($p > 0.05$) following a 24 h/ 37°C co-incubation with the anti-oxidant, NAC (10 mM). Results are mean ± SD (3 experiments).

The fusion of autophagosomes with lysosomes results in the degradation of the cytoplasmic contents of the newly-formed autolysosome, which can then be recycled to protect the cell against apoptotic stressors, such as nutrient deprivation and cytotoxic signals (Kondo et al., 2005). However, the disruption of lysosomal membranes by Dp44mT inhibits the development of functional autolysosomes, preventing the fusion of

the autophagosomes with lysosomes (Gutierrez et al., 2014). Dp44mT converts the pro-survival autophagy pathway into a mechanism of cytotoxicity, resulting in a build-up of cellular debris, and inducing LMP that results in apoptosis due to the release of degradative lysosomal cathepsins into the cytosol (Gutierrez et al., 2014).

Bcl-2 is a known inhibitor of autophagy, as it suppresses the activity of the key autophagy protein, Beclin 1 (Chang et al., 2010; Pattingre et al., 2005). Beclin 1 forms an integral part of the complex that participates in the initiation of autophagosome formation, mediating the localisation of other autophagy proteins to the pre-autophagosomal membrane (Kihara et al., 2001). Interestingly, silencing of Beclin 1 has been demonstrated to inhibit Dp44mT-induced autophagy (Gutierrez et al., 2014). Herein, we have demonstrated that DpC inhibited Bcl-2 (Fig. 5.2) and was capable of overcoming Bcl-2-mediated MDR (Fig. 5.1), whereas Dp44mT was not (Figs. 5.1, 5.2). We therefore investigated the effects of Dp44mT and DpC on the autophagic pathway in the Bcl-2 expressing M14 Bcl-2 cell line, using the classical marker of autophagosome formation, LC3-II (Klionsky et al., 2016; Mizushima et al., 2010).

The conversion of LC3-I, the cytosolic form of the protein, to LC3-II, the autophagosome membrane-bound form, was examined in response to a 24 h/37°C incubation with Dp44mT (30 μM) or DpC (30 μM) in the M14 Bcl-2 cell line. LC3-II expression was quantified densitometrically, as it is a classical marker of autophagosome formation (Klionsky et al., 2016; Mizushima et al., 2010). Dp44mT did not induce a significant ($p >$

0.05) increase in the expression of LC3-I or LC3-II, relative to the control (Fig. 5.6). However, DpC markedly and significantly ($p < 0.001$) increased LC3-I and LC3-II expression, compared to the control and Dp44mT (Fig. 5.6). The expression of LC3-II was increased 3.4-fold ($p < 0.001$) in response to incubation with DpC, whereas Dp44mT only increased LC3-II expression 1.1-fold ($p > 0.05$) (Fig. 5.6)

Previous studies in the MCF-7 breast cancer cell line demonstrated that Dp44mT increases the expression of the marker of autophagosome formation, LC3-II (Gutierrez et al., 2014). Herein, we found that only DpC, but not Dp44mT, induced an increase in LC3-II, in the Bcl-2 over-expressing cell line, M14 Bcl-2. This result may be related to the ability of DpC, but not Dp44mT, to decrease the expression of Bcl-2 (Fig 5.2). Bcl-2 is a known autophagy inhibitor, as it binds to Beclin 1, a BH3-only domain protein, and prevents it from participating in the formation of the autophagy-initiation complex (Chang et al., 2010; Liang et al., 1998; Pattingre et al., 2005). As DpC decreases the expression of Bcl-2 (Fig. 5.2), more Beclin 1 may be free to participate in autophagy initiation, resulting in the induction of autophagosome formation and an increase in LC3-II expression (Fig. 5.6). Dp44mT, on the other hand, does not decrease the expression of Bcl-2 (Fig. 5.2). Beclin 1 may be bound to Bcl-2 and inhibited, preventing the initiation of autophagy and increase in autophagosome formation, as is seen with DpC (Fig. 5.6). Therefore, the differing effects of Dp44mT in the MCF-7 and M14 Bcl-2 cell lines may be related to the over-expression of Bcl-2 in the M14 Bcl-2 cell line.

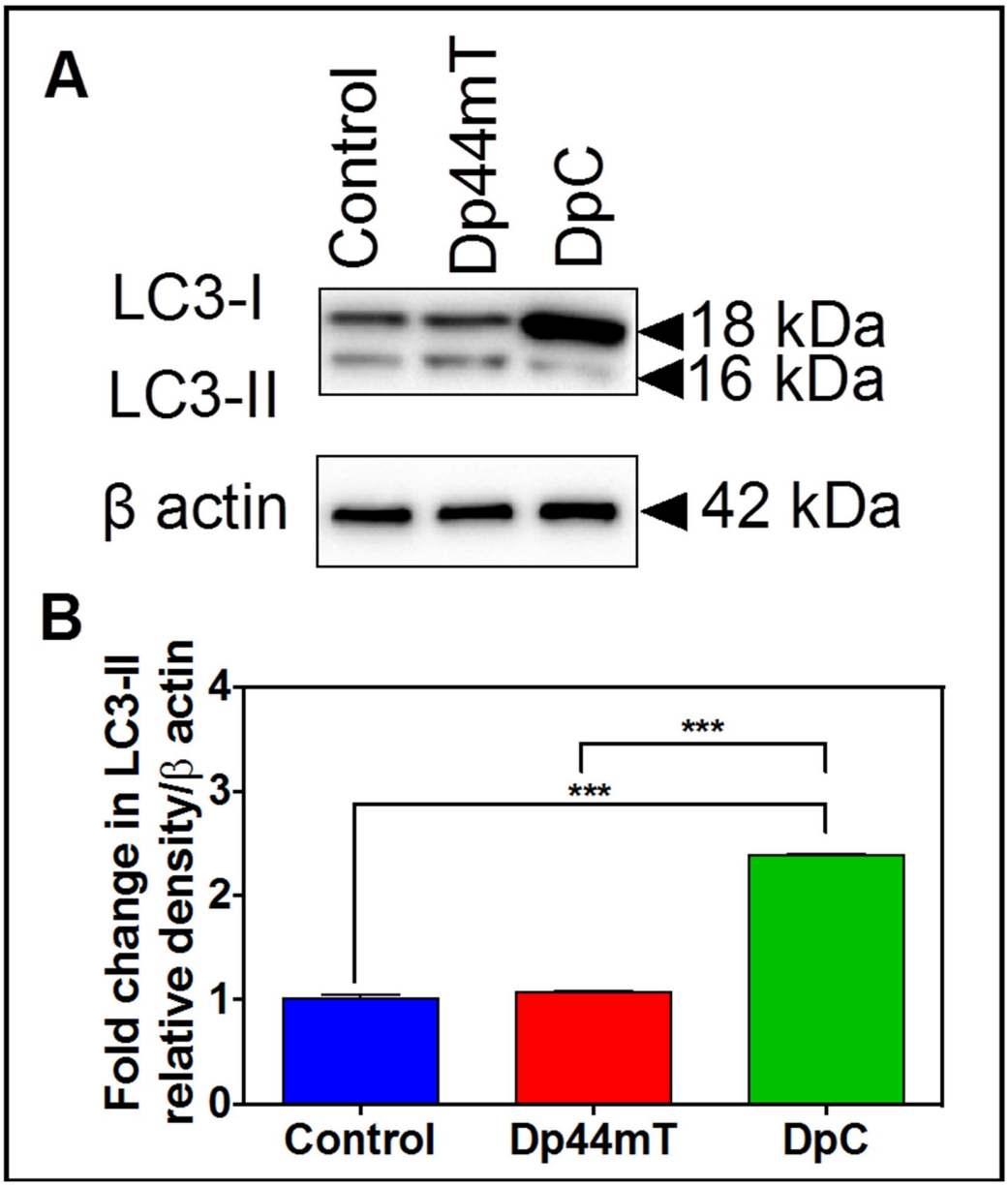

Figure 5.6 DpC, but not Dp44mT, induces an increase in the expression of the autophagy marker, LC3-II.

(A) M14 Bcl-2 cells were treated with control medium or medium containing Dp44mT (30 ε M) or DpC (30 ε M) and incubated for 24 h/ 37°C. Western blotting was performed to determine LC3 expression. DpC, but not Dp44mT, increased the expression of LC3-I and LC3-II. **(B)** Densitometric analysis (arbitrary units) of LC3-II expression in **(A)**. DpC significantly increased LC3-II expression, relative to control ($p < 0.001$) and Dp44mT ($p < 0.001$) Blots shown are representative of three experiments. Densitometric analysis is the mean of 3 ± S.D (3 experiments). *** $p < 0.001$.

5.3.7 Formation of Acidic Vesicles Mediated by Dp44mT and DpC

Dp44mT has multiple mechanisms for targeting lysosomes to induce cytotoxicity (Gutierrez et al., 2014; Jansson et al., 2010b; Jansson et al., 2015b; Lovejoy et al., 2011). Firstly, Dp44mT and DpC have been shown to localise to the lysosomal compartment, where they induce LMP by redox cycling with Cu(II) to generate ROS (Figs. 3.6, 3.7, 3.9, 3.10) (Gutierrez et al., 2014; Jansson et al., 2010b; Jansson et al., 2015b; Lovejoy et al., 2011).

This mechanism also enables the targeting of Pgp-mediated MDR (Figs. 3.4- 3.10) (Jansson et al., 2015b). Additionally, Dp44mT has been shown to target the pro-survival autophagy pathway by inducing the formation of autophagosomes, but prevents their fusion with lysosomes by inducing LMP, resulting in apoptosis (Gutierrez et al., 2014). Herein, we showed that in M14 melanoma cells that over-express Bcl-2, DpC, but not Dp44mT, can increase the expression of the classical autophagy marker, LC3-II (Fig. 5.6). This may be related to the superior ability of DpC to decrease the expression of Bcl-2, which is an inhibitor of autophagy (Fig. 5.2). We next investigated the effects of Dp44mT and DpC on the stability of lysosomal membranes in the Bcl-2 expressing M14 Bcl-2 cell line, compared to the control M14 PC cell line. We utilised the lysosomal marker, AO, which stains acidic vesicles, (*i.e.* lysosomes, red/orange) and other, more alkaline cellular compartments as green.

Both M14 Bcl-2 and M14 PC cells exhibited comparable amounts of the classical, punctate pattern of orange/red AO-stained acidic vesicles, under control conditions (Fig. 5.7). Following a 24 h/37°C incubation with Dp44mT (30 μM), the number of acidic vesicles remained unchanged compared to the control in M14 Bcl-2 cells (Fig. 5.7). However, in M14 PC cells, incubation with Dp44mT induced a significant ($p < 0.001$) increase in the number of red, AO-stained acidic vesicles, relative to both the control and Dp44mT-treated M14 Bcl-2 cells (Fig. 5.7). In contrast to Dp44mT, in M14 Bcl-2 cells, DpC induced a significant ($p < 0.001$) increase (Fig. 5.7) in the number of red, AO-stained vesicles relative to both Dp44mT and the control (Fig. 5.7). Similarly, incubation with DpC induced a significant ($p < 0.001$) increase in the number of acidic vesicles in M14 PC cells, compared to control. The increase in the number of acidic, lysosomal-like vesicles induced by incubation with DpC was also significantly ($p < 0.001$) greater in M14 PC cells, compared to M14 Bcl-2 cells.

The accumulation of acidic vesicles observed in the M14 cell lines is a novel effect of Dp44mT and DpC, as in other, diverse cell lines such as MCF-7, KBV1, KB31 and SK-N-MC, both these agents cause high levels of LMP (Figs. 3.6, 3.7, 3.9, 3.10) (Gutierrez et al., 2014; Jansson et al., 2010b; Lovejoy et al., 2011). However, induction of LMP in other cell lines was dependent on redox cycling with Cu(II) to produce ROS that peroxidise, and so disrupt, the lysosomal membrane (Figs. 3.6, 3.7, 3.9, 3.10) (Gutierrez et al., 2014; Jansson et al., 2010b; Lovejoy et al., 2011). Herein, we have demonstrated that the cytotoxicity of Dp44mT and DpC in the M14 cell lines is not

dependent on Cu(II) binding or ROS generation, therefore, it is unsurprising that LMP does not occur.

These results showed that DpC was more effective than Dp44mT at inducing an increase in the number of acidic lysosomal vesicles in cells that express Bcl-2 (Fig. 5.7). However, in cells that did not express Bcl-2, Dp44mT and DpC were equally effective at inducing an increase in the number of acidic vesicles. Bcl-2 inhibits autophagy as it is an inhibitor of the autophagy initiator, Beclin 1 (Chang et al., 2010; Pattingre et al., 2005). It is possible that the increased number of acidic vesicles seen in M14 Bcl-2 cells following treatment with DpC (Fig. 5.7) was a result of DpC decreasing the expression of Bcl-2 (Fig. 5.2). Consequently, Beclin 1 activity would be de-repressed, so autophagy would increase. Indeed, the formation of autophagosomes, which requires Beclin 1, was increased by DpC (Fig. 5.6). Autophagosomes ultimately fuse with lysosomes to form autolysosomes, so it is possible that the acidic vesicles in Figure 5.7 were in fact autolysosomes that had formed as a result of increased autophagy (Kondratskyi et al., 2014; Mizushima et al., 2010). Dp44mT, on the other hand, was not capable of significantly decreasing Bcl-2 (Fig. 5.2), so Beclin 1 would have been inhibited. Due to the inhibition of Beclin 1 by Bcl-2, the formation of autophagosomes may also have been inhibited, as was demonstrated (Fig. 5.6). Therefore, Dp44mT would not induce increase in autolysosome number in Bcl-2 expressing cells (Fig. 5.7). In the M14 PC cell line, which do not express Bcl-2, both Dp44mT and DpC may have induced autolysosome formation because, in contrast to the M14 Bcl-2 cell line, Beclin 1 would not have been inhibited by Bcl-2 (Fig. 5.2).

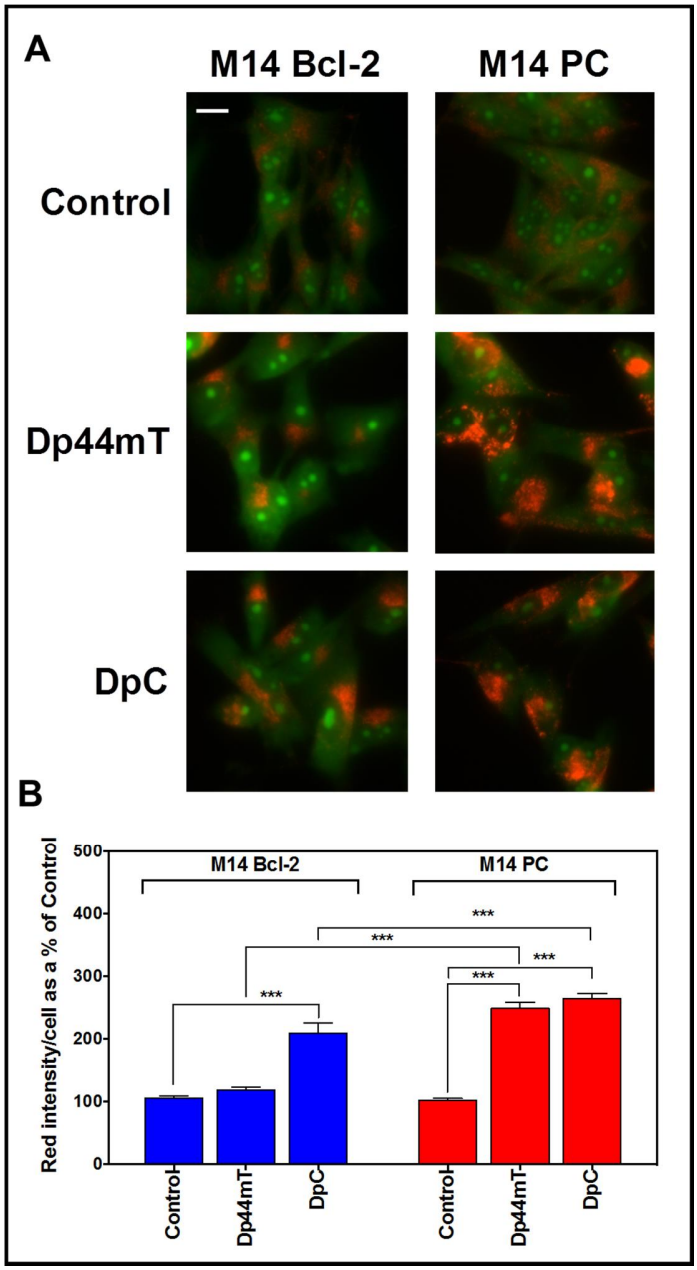

Figure 5.7. Increase in the number of acidic vesicles induced by Dp44mT and DpC is affected by Bcl-2 expression.

(A,B) Dp44mT does not induce a significant increase in the number of red/orange-stained acidic vesicles in M14 Bcl-2 cells. However, in M14 PC cells, Dp44mT does induce an increase in the number of red/orange-stained acidic vesicles. In contrast, DpC induces a significant increase in the number of red/orange-stained acidic vesicles in both the M14 Bcl-2 and M14 PC cell lines. Results in **(A)** are representative images from 3 experiments. Quantification in **(B)** is mean ± SD (3 experiments); *** $p < 0.001$ Scale bar: 10 ε m.

5.4 Conclusions

Our laboratory has developed novel thiosemicarbazones as anti-cancer agents for the past 20 years, of which the DpT series of thiosemicarbazone analogues has been the most successful (Jansson et al., 2015a; Kalinowski and Richardson, 2005; Kalinowski et al., 2007; Merlot et al., 2013). The best characterised agents from this series, Dp44mT and DpC, target lysosomes to induce potent cytotoxicity (Figs. 3.4- 3.10, 4.17- 4.20) (Gutierrez et al., 2014; Jansson et al., 2010b; Lovejoy et al., 2011; Stefani et al., 2015). Furthermore, Dp44mT and DpC have a propensity for co-opting cell survival mechanisms and utilising them to induce marked and selective cytotoxicity. Notably, Dp44mT and DpC overcome Pgp-mediated MDR by ñhijackingò Pgp to increase their lysosomal accumulation (Figs. 3.4-3.10) (Jansson et al., 2015b; Seebacher et al., 2016a).

Dp44mT has also been shown to take advantage of the pro-survival autophagy pathway by increase autophagy, while at the same time preventing autophagosomes fusing with lysosomes by destabilising lysosomal membranes (Gutierrez et al., 2014). This has the effect of potentiating Dp44mT-induced cytotoxicity in two ways: **(1)** due to the build-up of cellular debris that can no longer be recycled *via* the autophagic pathway; and (2) through induction of LMP, resulting in the release of degradative cathepsins into the cytosol (Gutierrez et al., 2014). Given the ability of Dp44mT and DpC to overcome various mechanisms of MDR, and that DpC has entered clinical trials for advanced solid tumours in 2016 (ClinicalTrials.gov Identifier NCT02688101), investigating their activity

against other mechanisms of resistance is crucial. As Dp44mT has been shown to alter the ratio of anti-apoptotic Bcl-2 and pro-apoptotic Bax expression (Gutierrez et al., 2014; Yuan et al., 2004), we investigated the efficacy of Dp44mT and DpC in the M14 Bcl-2 cell line, which over-expresses Bcl-2, and the M14 PC cell line, which does not express Bcl-2. Importantly, these cell lines are melanoma cell lines (Chambers, 2009; Rae et al., 2007). Metastatic melanoma is inherently MDR, making it notoriously difficult to develop treatments for (Grover and Wilson, 1996; Soengas and Lowe, 2003).

Our studies showed that DpC, but not Dp44mT, was able to overcome Bcl-2-mediated MDR in melanoma (Fig. 5.1). In both M14 Bcl-2 cells, which over-express Bcl-2, and M14 PC cells, which express negligible amounts of Bcl-2, the IC_{50} value of DpC was not significantly ($p > 0.05$) different. However, Dp44mT was significantly less cytotoxic in the M14 Bcl-2 cell line, than in the M14 PC cell line (Fig. 5.1). Therefore, Dp44mT acted more like a traditional chemotherapy drug in the M14 melanoma cell line, as Bcl-2 over-expression has been shown to decrease the sensitivity of cancer cells to chemotherapy agents (Amundson et al., 2000; Dole et al., 1994; Miyashita and Reed, 1993; Schmitt et al., 2000; Shibata et al., 1999; Strasser et al., 1993; Thomas et al., 1996; Vaux et al., 1988; Wang et al., 2013). Interestingly, DpC and Dp44mT behaved differently in Bcl-2-mediated MDR, which only DpC could overcome; whereas their activity is indistinguishable in Pgp-mediated MDR, which both could overcome (Figs. 3.4-3.10).

The over-expression of anti-apoptotic Bcl-2 mediates resistance to apoptosis by binding to pro-apoptotic family members, preventing them from initiating the intrinsic, mitochondrial pathway of apoptosis (Cory and Adams, 2002; Czabotar et al., 2014; Youle and Strasser, 2008). Inhibition of Bcl-2 has been targeted with small molecule inhibitors that are BH3-only protein mimetics, that bind Bcl-2 and release pro-apoptotic proteins so that they may induce apoptosis (Souers et al., 2013; Tse et al., 2008; van Delft et al., 2006; Wroblewski et al., 2013). However, we demonstrated that, rather than inhibiting the Bcl-2 protein, DpC instead significantly ($p < 0.01$) decreased Bcl-2 expression, compared to control (Fig. 5.2). Dp44mT, on the other hand, did not decrease expression significantly ($p > 0.05$), relative to control (Fig. 5.2). The ability of DpC to decrease Bcl-2 expression, relative to Dp44mT, may explain why DpC overcame Bcl-2-mediated MDR, but Dp44mT did not. Although Dp44mT has consistently been shown to increase the Bax:Bcl-2 ratio, its efficacy in decreasing Bcl-2 expression appears to depend on the cell line used (Gutierrez et al., 2014; Yuan et al., 2004).

In addition to Bcl-2 over-expression having no effect on the cytotoxicity of DpC (Fig. 5.1), we also demonstrated that silencing of Bcl-2 has no effect on DpC-mediated cytotoxicity (Fig. 5.3). As DpC is already efficient at decreasing Bcl-2 expression (Fig. 5.2), it can be suggested that further silencing of Bcl-2 has no effect (Fig. 5.3). In contrast, the cytotoxicity of Dp44mT was significantly ($p < 0.01$) increased by Bcl-2 silencing (Fig. 5.3). Compared to DpC, Dp44mT did not affect Bcl-2 expression (Fig. 5.2), therefore, silencing of Bcl-2 increased the cytotoxicity of Dp44mT (Fig. 5.3).

Moreover, silencing of Bcl-2 increased the cytotoxicity of Dp44mT, which has also been demonstrated for common chemotherapy agents that are ineffective against Bcl-2-mediated MDR (Nemati et al., 2014; Raisova et al., 2001; Watanabe et al., 2013; Wroblewski et al., 2013). Indeed, Bcl-2 silencing using oligonucleotides (oblimersen) was investigated as a method of targeting Bcl-2-mediated MDR, although this approach failed at clinical trials (Bedikian et al., 2006; Bedikian et al., 2014). DpC may offer significant improvements over oblimersen, as it is more like the successful small molecule inhibitors in terms of structure (Lessene et al., 2008; Thomas et al., 2013), as opposed to an oligonucleotide. Indeed, the clinical use of antisense oligonucleotides will always be limited due to their susceptibility to DNAse-mediated degradation and undesirable side effects (Dai et al., 2005). Other advantages of DpC include its ability to be given orally, and that it can overcome Pgp-mediated MDR as well as its polypharmacological mechanism that targets and inhibits multiple key biological processes, *e.g.* cell cycle progression, DNA synthesis, metastasis, *etc* (Jansson et al., 2015a).

Dp44mT and DpC bind to Cu(II) and redox cycle to generate ROS that induce LMP (Figs. 3.6-3.10, 4.17-4.20) (Gutierrez et al., 2014; Jansson et al., 2010b; Lovejoy et al., 2011; Stefani et al., 2015). However, we showed that in the M14 melanoma cell lines, prevention of Cu(II) binding using the copper ion chelator, TM, had no effect on the cytotoxicity of either Dp44mT or DpC (Fig. 5.4). Furthermore, prevention of ROS generation using the anti-oxidant, NAC, did not affect the cytotoxicity of Dp44mT or DpC (Fig. 5.5). Studies have shown that melanoma cells express abnormally high levels of

the copper ion binding proteins, metallothioneins, which reduces the level of unbound copper ions in cells (Krauter et al., 1989; Weinlich et al., 2006; Zelger et al., 1993). This could account for the lack of effect TM (Fig. 5.5) and NAC (Fig. 5.6) had on the cytotoxicity of Dp44mT and DpC, as the levels of free copper ions for Dp44mT and DpC to bind and redox cycle with may have been exceedingly small. These results suggested that Dp44mT and DpC were acting *via* an alternative mechanism to induce cytotoxicity in the M14 PC melanoma cell line, and in the case of DpC, the M14 Bcl-2 cell line.

The effects of Dp44mT and DpC on the formation of autophagosomes in the M14 Bcl-2 cell line were investigated using the classical marker of autophagosome formation, LC3-II. DpC significantly ($p < 0.001$) increased the expression of LC3-II compared to control (Fig. 5.6). Dp44mT, on the other hand, did not increase LC3-II expression (Fig. 5.6). This is in contrast to previous results, which have shown that Dp44mT induces LC3-II expression (Gutierrez et al., 2014). However, Bcl-2 is a known inhibitor of Beclin 1, a key protein involved in autophagy initiation (Kihara et al., 2001; Liang et al., 1998; Pattingre et al., 2005). In the M14 Bcl-2 cell line, which over-expresses Bcl-2, the inhibition of Beclin 1 may have prevented the formation of autophagosomes in response to Dp44mT (Fig. 5.6). In contrast, DpC induced a significant decrease in the expression of Bcl-2 (Fig. 5.2). Therefore, the formation of autophagosomes could have occurred in response to DpC treatment because Beclin 1 was not inhibited by Bcl-2 (Fig. 5.6).

Dp44mT and DpC mediate potent cytotoxicity by targeting lysosomes and inducing LMP (Figs. 3.4-3.10, 4.17-4.20) (Gutierrez et al., 2014; Jansson et al., 2010b; Lovejoy et al., 2011). However, in the M14 melanoma cell lines used in this study, neither Dp44mT nor DpC induced LMP (Fig. 5.7). This may be related to their inability to bind Cu(II) and redox cycle in the M14 melanoma cell lines (Figs. 5.4, 5.5); characteristics which are required in order to induce LMP (Figs. 3.4-3.10, 4.17-4.20) (Gutierrez et al., 2014; Jansson et al., 2010b; Lovejoy et al., 2011; Stefani et al., 2015). In fact, Dp44mT and DpC increased the number of acidic vesicles in a Bcl-2 dependent manner (Fig. 5.7). Dp44mT increased the number of acidic vesicles in the control M14 PC cell line, but not the Bcl-2 expressing M14 Bcl-2 cell line (Fig. 5.7). DpC, on the other hand, increased the number of acidic vesicles in both the M14 Bcl-2 and M14 PC cell lines (Fig. 5.7).

We suggest that the acidic vesicles are in fact autolysosomes, formed by the fusion of autophagosomes and lysosomes (Fig. 5.8) (Kondo et al., 2005). The inhibition of Beclin 1 by Bcl-2 in the M14 Bcl-2 cell line would have prevented the initiation of autophagy, thus there would be no increase in the number of autophagosomes, as observed, following incubation with Dp44mT (Fig. 5.6). This could explain the decreased in the number of acidic vesicles, which may be autolysosomes seen in response to Dp44mT treatment (Figs. 5.7, 5.8) (Chang et al., 2010; Pattingre et al., 2005). Indeed, when Bcl-2 was not expressed in the M14 PC cell line, Dp44mT did increase the number of acidic vesicles (Figs. 5.7, 5.8). In contrast, the ability of DpC to decrease Bcl-2 expression, thus decreasing Beclin 1 inhibition, could have resulted in increased autophagosome formation in M14 Bcl-2 cells (Fig. 5.6). In agreement with this hypothesis, DpC was able

to increase the number of acidic vesicles, which may be autolysosomes, in both cell lines (Figs. 5.7, 5.8).

However, further studies, using specific vesicular markers, are needed to confirm the specific identity of the acidic vesicles formed in Figure 5.7, and whether there is a relationship between the increase in acidic vesicle formation and induction of cytotoxicity. However, the trends in cytotoxicity were similar to the trends in acidic vesicle formation. DpC was equally cytotoxic in the M14 Bcl-2 and M14 PC cell lines, and induced similar increases in the number of acidic vesicles. Dp44mT, on the other hand, was less cytotoxic in the M14 Bcl-2 cell line than in the M14 PC cell line. Dp44mT also did not induce an increase in acidic vesicles in the M14 Bcl-2 cell line, although did in the M14 PC cell line. These results suggest that there may be a causal relationship between acidic vesicle formation and cytotoxicity induced by Dp44mT and DpC, which is related to Bcl-2 expression.

Evasion of apoptosis mediated by Bcl-2 over-expression is not only a hallmark of carcinogenesis; it also contributes to MDR by allowing cancer cells to ignore apoptotic signals generated in response to cytotoxic drugs (Lessene et al., 2008; Thomas et al., 2013). Bcl-2 is therefore an important drug target (Lessene et al., 2008; Thomas et al., 2013). While small molecule inhibitors of Bcl-2, such as ABT-199, have been developed and progressed to clinical trials (Roberts et al., 2016; Stilgenbauer et al., 2016), none have gained Federal Drug Administration approval to date. Based on these studies,

further investigation into the mechanism of Dp44mT and DpC in both Bcl-2-mediated MDR and inherently resistant melanoma, are warranted. Importantly, we have demonstrated the potent ability of DpC, has entered clinical trials in 2016 (ClinicalTrials.gov Identifier NCT02688101), to overcome Bcl-2-mediated MDR by decreasing the expression of Bcl-2. Furthermore, we have shown that in melanoma cells, Dp44mT and DpC, act in a novel, Bcl-2-dependent, Cu(II)-independent manner to increase the formation of acidic vesicles, as opposed to causing LMP which has been demonstrated in other cancer cell types (Figs. 3.6-3.10, 4.17-4.20) (Gutierrez et al., 2014; Jansson et al., 2010b; Lovejoy et al., 2011; Seebacher et al., 2016a). We suggest that the increase in the formation of acidic vesicles may be related to the ability of Dp44mT and DpC to increase autophagy in a Bcl-2-dependent fashion. Investigations to determine whether the outcome of the increase in acidic vesicles is related to induction of cytotoxicity should be conducted. It is important to elucidate the mechanism by which Dp44mT and DpC exert their cytotoxic effects in melanoma, a cancer for which novel treatments are desperately needed as it is resistant to standard chemotherapies (Grover and Wilson, 1996; Soengas and Lowe, 2003).

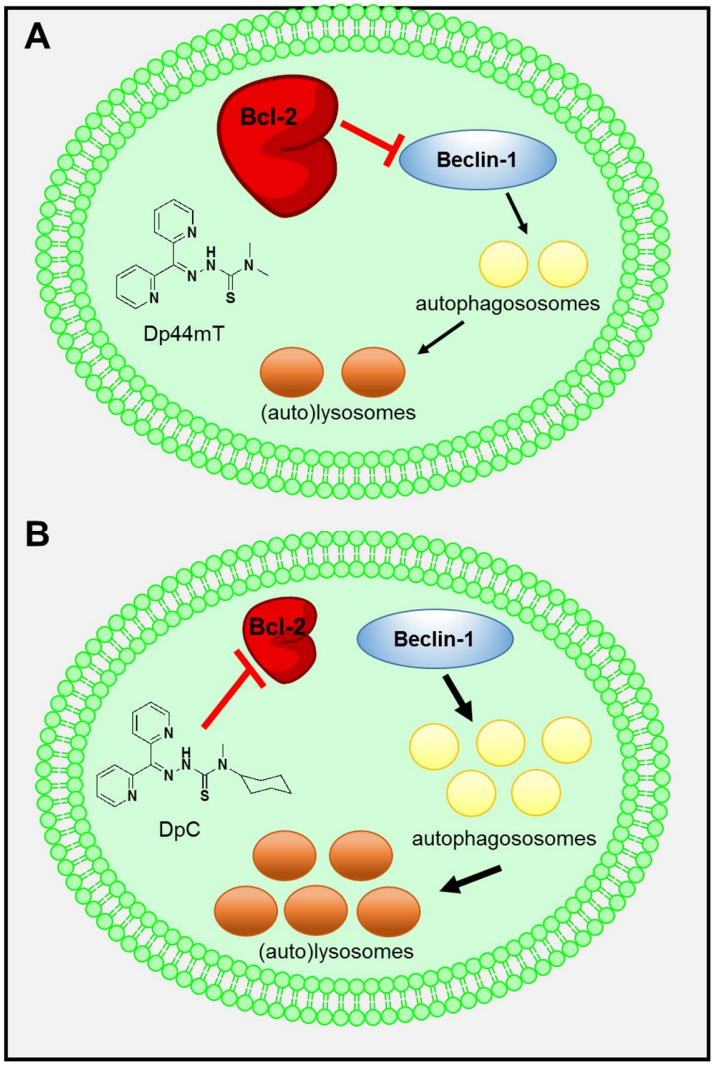

Figure 5.8 Schematic illustrating the possible mechanisms of Dp44mT and DpC in Bcl-2 over-expressing cells.

A Dp44mT, which did not overcome Bcl-2-mediated MDR, did not decrease the expression of Bcl-2. Dp44mT also did not increase the formation of autophagosomes in Bcl-2 over-expressing cells. This could be due to the inhibition of the autophagy initiation protein, Beclin 1, by Bcl-2. The prevention of autophagy by Bcl-2 could have accounted for the decreased number of acidic vesicles induced by Dp44mT treatment, relative to control. We suspect these acidic vesicles were autolysosomes, formed by the fusion of autophagosomes and autolysosomes. **B** DpC, which did overcome Bcl-2-mediated MDR, decreased the expression of Bcl-2 and increased the formation of autophagosomes. This may have been due to decreased inhibition of the autophagy initiation protein, Beclin 1, by Bcl-2. The fusion of the increased numbers of autophagosomes with lysosomes could account for the increased number of acidic vesicles, which may in fact be autolysosomes, in Bcl-2 over-expressing cells following DpC treatment.

Chapter 6 – Discussion

6.1 Prelude to Discussion

Although chemotherapy is the standard treatment for metastatic and haematological malignancies, drug resistance represents a major clinical obstacle to successful treatment (Gottesman, 2002). Drug resistance can be mediated through a number of mechanisms, including: efflux of chemotherapeutic substrates by ABC transporters, such as Pgp (Gottesman et al., 2002); failure to respond to apoptotic signals induced by chemotherapeutics due to over-expression of Bcl-2 family members (Lessene et al., 2008), and lysosomal drug sequestration (Zhitomirsky and Assaraf, 2016). To date, no treatments targeting any of these mechanisms have successfully progressed past Stage III clinical trials (Fletcher et al., 2010). Therefore, the development of novel therapeutic strategies to target MDR is crucial.

In our laboratory, thiosemicarbazones have been developed which display high potency, both *in vitro* and *in vivo* (Jansson et al., 2015a; Jansson et al., 2015b; Kalinowski and Richardson, 2005; Kovacevic et al., 2011; Lovejoy et al., 2012; Whitnall et al., 2006; Yuan et al., 2004). The thiosemicarbazone, Dp44mT, has the notable ability to ñhighjackò lysosomal Pgp and utilise this MDR mechanism to enhance its targeting and effectiveness by increasing apoptosis (Gutierrez et al., 2014; Jansson et al., 2015b; Seebacher et al., 2016a). Given the unique properties of Dp44mT, this thesis examined the anti-cancer efficacy of thiosemicarbazones, and their ability to overcome MDR.

Specifically, in Chapter 3, structural features required by thiosemicarbazones in order to overcome Pgp-mediated MDR were elucidated, and the mechanism by which certain thiosemicarbazones overcome Pgp-mediated MDR were demonstrated. Although thiosemicarbazones have traditionally been thought of as Fe(III) chelators, recent studies have demonstrated the anti-cancer activity of Zn(II)-thiosemicarbazone complexes (Cowley et al., 2005; Kovala-Demertzi et al., 2006; Kowol et al., 2010). Therefore, in Chapter 4, we synthesised Zn(II) complexes of several of our potently anti-neoplastic thiosemicarbazones, and investigated their mechanism of action. Furthermore, Dp44mT has been shown to alter the ratio of the Bcl-2 family members, Bax and Bcl-2, which regulate apoptosis (Gutierrez et al., 2014; Yuan et al., 2004). In Chapter 5, the effect of Bcl-2 expression on the anti-cancer efficacy of Dp44mT and DpC was investigated in mechanistic studies.

6.2 Targeting MDR with Thiosemicarbazones

6.2.1 Overcoming Pgp-Mediated MDR with Thiosemicarbazones

Both Dp44mT (Jansson et al., 2015b; Whitnall et al., 2006) and its Cu(II) (Gutierrez et al., 2014; Jansson et al., 2015b) complex induce potent and selective cytotoxicity in MDR cancer cells expressing Pgp, relative to their non-Pgp expressing counterparts. Pgp expressed in lysosomal membranes transports Dp44mT into lysosomes, where it is

protonated (Jansson et al., 2015a; Lovejoy et al., 2011). Upon protonation of Dp44mT, the agent is no longer able to diffuse out of lysosomes (Jansson et al., 2015a; Lovejoy et al., 2011). With the high amounts of copper available in the lysosomes (Gupte and Mumper, 2009), Dp44mT can form redox-active Cu(II) complexes which generate ROS inside lysosomes (Jansson et al., 2015a; Lovejoy et al., 2011). These ROS damage lysosomal membranes, resulting in LMP and apoptosis in MDR cancer cells (Jansson et al., 2015a; Lovejoy et al., 2011). In order to examine the requirements for overcoming Pgp-mediated MDR *via* the unique mechanism of action exhibited by Dp44mT, a group of structurally-related thiosemicarbazones were examined in the first 5 chapters of this thesis, namely: Dp44mT, DpC, Bp44mT, Ap44mT, 3-AP and Bp2mT. These thiosemicarbazones were chosen based on their marked and selective anti-cancer activity, while Bp2mT was chosen as a negative control that does not bind Fe(III) or Cu(II) (Kalinowski et al., 2007; Knox et al., 2007; Lovejoy et al., 2012; Richardson et al., 2009; Traynor et al., 2010; Yu et al., 2012; Yuan et al., 2004).

All of the panel of thiosemicarbazones screened in this study (Dp44mT, Bp44mT, DpC, Ap44mT, 3-AP and Bp2mT), and their Fe(III) and Cu(II) complexes, induced Pgp ATPase activity, indicating that the ligands alone and when they are bound to Fe(III) or Cu(II) are transported by Pgp drug transporter (Fig. 3.7). Notably, the more lipophilic compounds induced greater Pgp-ATPase activity (*i.e.*, ligands < Cu(II) complexes < Fe(III) complexes; Fig. 3.7). This is in accordance with the observation that Pgp prefers lipophilic substrates for transport (Kimura et al., 2004; Schmid et al., 1999; Seelig and Landwojtowicz, 2000). Although all of the thiosemicarbazones were Pgp substrates,

only Dp44mT, DpC and Bp44mT caused potentiated, Pgp-dependent cytotoxicity and LMP (Figs. 3.6, 3.8, 3.10). The cytotoxicity and LMP induced by Ap44mT was not affected by Pgp expression or Pgp inhibition with a Pgp inhibitor (Figs. 3.6, 3.8, 3.10). Moreover, Bp2mT and 3-AP did not induce cytotoxicity at concentrations of Ó800 ε M, nor did they induce LMP (Figs. 3.6, 3.8). The lack of efficacy 3-AP demonstrated in MDR cancer cells could have contributed to its failure in multiple clinical trials (Knox et al., 2007; Merlot et al., 2013; Traynor et al., 2010). Clearly, being a Pgp substrate was not the only feature a thiosemicarbazone was required to possess in order to induce potentiated cytotoxicity and LMP in Pgp-expressing cells (Figs. 3.6-3.8).

While thiosemicarbazones are traditionally thought of as Fe(III) chelators (Kalinowski et al., 2007), their Cu(II) complexes also exhibit pronounced anti-proliferative effects (Jansson et al., 2010b; Jansson et al., 2015b; Lovejoy et al., 2011). Herein, we demonstrated that Pgp-mediated LMP induced by Dp44mT, Bp44mT and DpC was dependent on their ability to bind Cu(II) (Figs. 3.8, 3.13). Indeed, [Cu(Dp44mT)], [Cu(Bp44mT)] and [Cu(DpC)] were potent inducers of LMP following a 30 min/37°C incubation; whereas the thiosemicarbazones alone did not induce LMP at this time point (Fig. 3.8). However, using a longer time point (24 h), we demonstrated that Dp44mT, Bp44mT and DpC could also induce Pgp-dependent LMP, which was found to be Cu(II) dependent, as the potent copper chelator, TM, prevented LMP induced by these agents (Figs. 3.8, 3.13). Although the thiosemicarbazones alone did not induce LMP at the 30 min time point (Fig. 3.8), over 24 h, there is greater opportunity for the ligand to bind endogenous Cu(II) to form complexes that can then induce LMP (Figs. 3.8-3.14). None

of the other thiosemicarbazones (Bp2mT, 3-AP and Ap44mT) induced Pgp- or Cu(II)-dependent LMP at any of the time points examined in these studies (Figs. 3.6, 3.8, 3.13) As a substitution of a methyl group at N2 in Bp2mT prevents Cu(II) binding (Chen et al., 2012; Yuan et al., 2004), this could explain the lack of efficacy of Bp2mT in inducing LMP. Interestingly, Ap44mT and 3-AP can bind Cu(II) (Jansson et al., 2010b) like Dp44mT, Bp44mT and DpC, yet do not induce LMP or potentiated cytotoxicity in Pgp-expressing KBV1 cells (Figs. 3.6, 3.8, 3.10-3.14). As Cu(II) only potentiated the cytotoxic effects of some of the thiosemicarbazones examined in these studies, this suggested that there were further requirements for inducing Pgp-mediated LMP and cytotoxicity.

Further investigations revealed that the generation of ROS by the Cu(II)-thiosemicarbazone complexes was another characteristic required for the induction of Pgp-dependent LMP and cytotoxicity (Figs. 3.9, 3.14). None of the thiosemicarbazones alone or their Fe(III) complexes generated significant ROS an *in vitro* plate assay (as measured with H_2DCF fluorescence), compared to the control (Fig. 3.9). However, [Cu(Dp44mT)], [Cu(Bp44mT) and [Cu(DpC)] demonstrated the greatest ability to induce ROS formation (Fig. 3.9). Although [Cu(Ap44mT)] was significantly ($p < 0.001$) more redox-active than controls, it was also significantly ($p < 0.001$) less redox-active than [Cu(Dp44mT)], [Cu(Bp44mT) and [Cu(DpC)] (Fig. 3.9). The redox activity of Bp2mT and 3-AP in the presence of Cu(II) did not significantly differ from the controls (Fig. 3.9). In the case of Bp2mT, this could be accounted to its inability to form Cu(II) complexes (Chen et al., 2012; Yuan et al., 2004), which resulted in lack of redox activity (Fig 3.9).

However, 3-AP can form Cu(II) complexes. This suggested that there were characteristics that made 3-AP and Ap44mT less effective at redox cycling with Cu(II), compared to Dp44mT, Bp44mT and DpC.

The differences in the redox activity of [Cu(Dp44mT)], [Cu(Bp44mT) and [Cu(DpC)], compared to [Cu(Ap44mT)] and [Cu(3-AP)] can be explained by structural characteristics of the thiosemicarbazones. For Dp44mT, Bp44mT and DpC, the presence of an inductively electron-withdrawing phenyl or pyridyl moiety at the imine carbon results in Cu(II) complexes with higher redox potentials (Jansson et al., 2010a; Kalinowski et al., 2007; Richardson et al., 2009), suitable for ROS generation (Fig. 3.9) and inducing LMP (Figs 3.8, 3.10-3.14). In contrast, for 3-AP or Ap44mT, the presence of a hydrogen or an inductively electron-donating methyl group at the imine carbon, respectively, results in Cu(II) complexes with lower redox potentials (Jansson et al., 2010a; Kalinowski et al., 2007; Richardson et al., 2009), thus making these agents less avid in generating ROS (Fig. 3.9), resulting in failure to induce LMP (Fig. 3.8, 3.10-3.14) and overcome MDR (Figs. 3.6, 3.10). At the same time, the decreased lipophilicity of 3-AP or Ap44mT relative to Dp44mT, Bp44mT and DpC, results in decreased membrane permeability and lower Pgp substrate activity (Fig. 3.7). This is consistent with the fact that Pgp prefers lipophilic substrates for transport (Kimura et al., 2004; Schmid et al., 1999; Seelig and Landwojtowicz, 2000). Hence, the lower lipophilicity of the ligand, Ap44mT, may have contributed to its reduced entry into the cell, its slightly lower activity as a Pgp substrate (Fig. 3.7) and its decreased ability to induce LMP (Figs. 3.8, 3.10-3.14) and to overcome resistance (Figs. 3.6, 3.10).

In summary, the principal findings of these studies were that in order for thiosemicarbazones to overcome MDR, they must possess five characteristics, namely: **(1)** have inductively electron-withdrawing substituents at the imine carbon (Fig. 3.1); **(2)** have high relative lipophilicity; **(3)** have Pgp substrate activity (Figs. 3.4, 3.5, 3.8); **(4)** have potent Cu(II) chelation efficacy (Figs. 3.6, 3.9); and **(5)** induce ROS generation (Figs. 3.7, 3.10).

6.2.1 Overcoming Bcl-2 Mediated MDR with Thiosemicarbazones

The Bcl-2 family of proteins act as master regulators of the intrinsic pathway of apoptosis (Cory and Adams, 2002; Czabotar et al., 2014; Youle and Strasser, 2008). As impairment of apoptosis is fundamental to carcinogenesis, dysregulated expression of the Bcl-2 family members is an underlying cause or contributor to many different types of cancer (Thomas et al., 2013). Furthermore, overexpression of Bcl-2 contributes to MDR by allowing cancer cells to evade apoptotic signals in response to chemotherapeutics (Amundson et al., 2000; Dole et al., 1994; Miyashita and Reed, 1993; Schmitt et al., 2000; Shibata et al., 1999; Strasser et al., 1993; Thomas et al., 1996; Vaux et al., 1988; Wang et al., 2013). Previously, Dp44mT was demonstrated to increase the ratio of pro-apoptotic Bax to anti-apoptotic Bcl-2 (Gutierrez et al., 2014; Yuan et al., 2004), thereby making cells more sensitive to apoptosis (Raisova et al., 2001). The ability of Dp44mT to regulate the expression of Bcl-2 family members and overcome Pgp-mediated MDR, led us to investigate the anti-cancer efficacy of Dp44mT and our lead agent, DpC, against cells over-expressing Bcl-2. For these studies we utilised M14 Bcl-2 melanoma cell line, endogenously Bcl-2 expressing M14 melanoma

cell line, and the control cell line, M14 PC (Chambers, 2009; Del Bufalo et al., 1997; Rae et al., 2007).

Interestingly, DpC, but not Dp44mT, overcame Bcl-2 mediated MDR following a 24 h/37°C incubation (Fig. 5.1). While the IC_{50} of DpC was the same in both cell lines, Dp44mT was 1.5-fold ($p < 0.001$) less cytotoxic in the Bcl-2 expressing, M14 Bcl-2 cell line, than in the control, M14 PC cell line (Fig. 5.1). Moreover, as Dp44mT has been shown to increase the Bax:Bcl-2 ratio (Gutierrez et al., 2014; Yuan et al., 2004), the effect of Dp44mT and DpC on the expression of Bcl-2 was examined. Dp44mT did not significantly ($p > 0.05$) decrease Bcl-2 expression, relative to the control (Fig. 5.2). DpC, on the other hand, induced a 57% decrease ($p < 0.01$) in Bcl-2 expression, relative to the control (Fig. 5.2). Moreover, incubation with DpC induced a 50% ($p < 0.05$) decrease in Bcl-2 expression, relative to Dp44mT (Fig. 5.2B). The ability of DpC to overcome Bcl-2 mediated MDR may have been related to the significantly greater ($p < 0.05$) decrease in Bcl-2 expression that was induced by DpC, compared to Dp44mT (Fig. 5.2).

Importantly, silencing of Bcl-2 expression affected Dp44mT-induced cytotoxicity, but not DpC-induced cytotoxicity (Fig. 5.3). This could be due to DpC being significantly ($p < 0.05$) more effective at decreasing Bcl-2 expression compared to Dp44mT (Fig. 5.2). Hence, it could be expected that silencing of Bcl-2 would not affect induction of cytotoxicity by DpC to the same extent that it would affect Dp44mT (Fig. 5.3). As

observed with Dp44mT (Fig. 5.3), decreasing Bcl-2 expression has been shown to be effective in increasing the anti-cancer efficacy of standard chemotherapies that are sensitive to Bcl-2-mediated MDR (Bedikian et al., 2006; Skommer et al., 2006; Tse et al., 2008). Importantly, unlike standard chemotherapies or Dp44mT, the cytotoxicity of DpC was unaffected by Bcl-2 over-expression or silencing (Figs. 5.1, 5.3), illustrating the potential of DpC as a novel drug candidate.

Induction of cytotoxicity by Dp44mT and DpC is dependent the formation of redox-active Cu(II) complexes that generate ROS (Figs. 3.9, 4.19, 4.20) (Jansson et al., 2010b; Lovejoy et al., 2011). Cu(II) binding is also involved in the cytotoxicity of other thiosemicarbazones (Stefani et al., 2015), and structurally-related drugs, such as elesclomol (Kirshner et al., 2008; Nagai et al., 2012; Yadav et al., 2013), which has been clinically trialled in melanoma (O'Day et al., 2013). However, in both the M14 Bcl-2 and M14 PC cell lines, chelation of copper ions (Fig. 5.4) and adding the GSH precursor, NAC, to prevent ROS generation (Fig. 5.5) had no effect on the cytotoxicity of Dp44mT or DpC. These results demonstrated that DpC may overcome Bcl-2 mediated MDR in melanoma *via* a novel mechanism.

We investigated the interplay between Bcl-2 over-expression and induction of autophagy mediated by Dp44mT and DpC in the M14 Bcl-2 cell line. Bcl-2 inhibits the pro-survival autophagy pathway, as it is an inhibitor of the autophagy initiator protein, Beclin 1 (Chang et al., 2010; Kihara et al., 2001; Pattingre et al., 2005). Interestingly,

silencing of Beclin 1 has been found to inhibit Dp44mT-induced autophagy (Gutierrez et al., 2014). Herein, we found that DpC, but not Dp44mT, increased the expression of the classical marker of autophagosome formation, LC3-II (Fig. 5.5). We hypothesise that this is related to the ability of DpC, but not Dp44mT, to decrease Bcl-2 expression (Fig. 5.2). The decrease in Bcl-2 expression induced by DpC (Fig. 5.2), may result in the de-repression of Beclin 1. Free Beclin 1 could then participate in autophagy initiation, resulting in an increase in LC3-II expression (Fig. 5.6). Dp44mT, on the other hand, does not decrease the expression of Bcl-2 (Fig. 5.2). Beclin 1 may be bound to Bcl-2 and inhibited (Chang et al., 2010; Pattingre et al., 2005), preventing the initiation of autophagy and increase in autophagosome formation, as observed (Fig. 5.6). Indeed, Dp44mT has been shown to induce LC3-II in cells that do not over-express Bcl-2 (Gutierrez et al., 2014).

Dp44mT, DpC and other thiosemicarbazones, have been shown to target lysosomes by inducing LMP due to the generation of ROS (Figs. 3.6, 3.7, 3.9, 3.10) (Gutierrez et al., 2014; Jansson et al., 2010b; Jansson et al., 2015b; Lovejoy et al., 2011; Stefani et al., 2015). We investigated the effects of Dp44mT and DpC on lysosomal membrane stability, using the acidic vesicle stain, AO. Herein, in the Bcl-2 over-expressing cell line, M14 Bcl-2, Dp44mT did not induce a significant ($p > 0.05$) increase in the number of acidic vesicles, compared to control, following a 24 h/37°C incubation (Fig. 5.7). However, in the control M14 PC cell line, Dp44mT induced a significant increase in the number of acidic vesicles ($p < 0.001$) (Fig. 5.7).

In contrast, DpC induced a significant increase ($p < 0.001$) in the number of acidic vesicles in both the M14 Bcl-2 and M14 PC cell lines (Fig. 5.7). Dp44mT increased the number of acidic vesicles in a Bcl-2 dependent fashion, whereas DpC increased lysosomal number regardless of Bcl-2 expression. These results may be linked to the ability of DpC, but not Dp44mT, to decrease the expression of Bcl-2. We hypothesised that the acidic vesicles may in fact be autolysosomes, which form as a result of the fusion between autophagosomes and lysosomes (Kondo et al., 2005). Dp44mT did not decrease Bcl-2 expression (Fig. 5.2) or increase autophagosome formation (Fig. 5.6), possibly due to the inhibition of the autophagy initiator, Beclin 1, by Bcl-2. Therefore, Dp44mT would not induce increase in autolysosome number in Bcl-2 expressing cells, as observed (Fig. 5.7). DpC, on the other hand, decreased Bcl-2 expression (Fig. 5.2), and thus increased autophagosome formation (Fig. 5.6), possibly due to de-repression of Beclin 1. Consequently, DpC would induce an increase in the formation of autolysosomes (Fig. 5.7). In agreement with this hypothesis, in cells which did not express Bcl-2, both Dp44mT and DpC increased the formation of acidic vesicles (Fig. 5.7). This may have occurred as, in contrast to the M14 Bcl-2 cell line, Beclin 1 would not have been inhibited by Bcl-2 (Fig. 5.2).

The principle findings of these studies showed that DpC was superior to Dp44mT in overcoming Bcl-2-mediated resistance (Fig. 5.1). The mechanism by which DpC targets Bcl-2 cells appears to be one that involves decreasing the expression of Bcl-2 (Fig. 5.2), and may involve induction autophagy (Fig. 5.6) and autolysosome formation (Fig. 5.7). Unusually, DpC and Dp44mT did not exert their anti-cancer effects in the M14

melanoma cell lines *via* the well-established mechanism observed in other cancer cell lines, involving Cu(II) binding, ROS generation and induction of LMP (Figs. 3.6- 3.10) (Gutierrez et al., 2014; Gutierrez et al., 2016; Jansson et al., 2015b; Lovejoy et al., 2011; Seebacher et al., 2016a). The remarkable ability of DpC to overcome Bcl-2 mediated MDR warrants further mechanistic and structure-activity studies to further elucidate the mechanism and structural requirements for overcoming Bcl-2 mediated MDR by thiosemicarbazones, similar to what has already been carried out for Pgp-mediated MDR.

6.2.3 Comparison of the Mechanisms of Overcoming Pgp and Bcl-2 Mediated MDR by Thiosemicarbazones

Thiosemicarbazones that possess the five characteristics identified in this thesis were able to target Pgp-mediated MDR. The five characteristics identified were: **(1)** inductively electron-withdrawing substituents at the imine carbon (Fig. 3.1); **(2)** high relative lipophilicity; **(3)** Pgp substrate activity (Figs. 3.5, 3.6, 3.8); **(4)** Cu(II) chelation efficacy (Figs. 3.6, 3.9); and **(5)** induction of ROS generation (Figs. 3.7, 3.10). Dp44mT, DpC and Bp44mT, fulfilled these requirements, and so were able to selectively and potently induce cytotoxicity in Pgp-expressing cells (Fig. 3.6). The mechanism by which they do so involves passive diffusion across the plasma membrane followed by active transport into lysosomes by Pgp (Jansson et al., 2015b).

Inside lysosomes, Dp44mT, Bp44mT and DpC are protonated by the acidic pH of lysosomal lumens, effectively trapping the thiosemicarbazones inside as they can no longer passively diffuse out across lysosomal membranes (Jansson et al., 2010b; Jansson et al., 2015b; Lovejoy et al., 2011). Dp44mT, Bp44mT and DpC are able to bind Cu(II), which is found at high concentrations within lysosomal lumens (Gupte and Mumper, 2009; Kurz et al., 2006; Yu et al., 2003). Once bound to Cu(II), Dp44mT, Bp44mT and DpC redox cycle and generate ROS that permeabilise lysosomal membranes (Figs. 3.6-3.10) (Jansson et al., 2010b; Jansson et al., 2015b; Lovejoy et al., 2011). LMP ultimately leads to apoptosis (Fig. 3.4) due to the release of degradative lysosomal caspases into the cytosol (Jansson et al., 2010b; Jansson et al., 2015b; Lovejoy et al., 2011; Ollinger and Brunk, 1995). Dp44mT, Bp44mT and DpC met the five requirements identified herein, therefore, were able to utilise Pgp so that rather than reducing their cytotoxicity, the presence of Pgp instead potentiates their cytotoxicity by promoting their lysosomal accumulation.

There are numerous differences between the mechanisms Dp44mT and DpC used to target Pgp, and the mechanism they used to target Bcl-2 over-expression. Overall, Dp44mT and DpC acted in a similar manner to selectively target Pgp-mediated MDR (Figs. 3.4-3.10); however, only DpC, but not Dp44mT, could overcome Bcl-2 mediated MDR (Fig. 5.1). In order to overcome Bcl-2-mediated MDR (Fig. 5.1), DpC decreased the expression of Bcl-2 (Fig. 5.2). Dp44mT, on the other hand, did not decrease Bcl-2 expression (Fig. 5.2), thus, did not overcome Bcl-2-mediated MDR (Fig. 5.1).

Dp44mT appeared to act similarly to common chemotherapeutics, which fail to induce apoptosis in Bcl-2-expressing cells (Amundson et al., 2000; Dole et al., 1994; Miyashita and Reed, 1993; Schmitt et al., 2000; Shibata et al., 1999; Strasser et al., 1993; Thomas et al., 1996; Vaux et al., 1988; Wang et al., 2013). Additionally, silencing of Bcl-2 increased the cytotoxicity (*i.e.* decreased the IC_{50}) of Dp44mT (Fig. 5.3), which has also been demonstrated to increase the efficacy of chemotherapeutics (Wang et al., 2013). However, DpC was potently effective at decreasing Bcl-2 expression, therefore, silencing of Bcl-2 did not further affect its cytotoxicity (Fig. 5.3). Notably, DpC decreased the expression of the Bcl-2 protein. However, in Pgp-mediated MDR, Dp44mT and DpC utilise Pgp to increase their lysosomal sequestration, which consequently increases their cytotoxicity (Figs. 3.4, 3.6, 3.8-3.10).

While Cu(II) binding and ROS generation were required characteristics in order for thiosemicarbazones to induce potentiated, Pgp-mediated cytotoxicity (Figs. 3.6, 3.8, 3.9), neither Cu(II) binding nor ROS generation were required for DpC to overcome Bcl-2 mediated MDR (Figs. 5.4, 5.5). Furthermore, while both Dp44mT and DpC induced LMP to cause cytotoxicity in Pgp-mediated MDR (Figs. 3.4, 3.6-3.10), and also induce LMP in a variety of other cell lines (Gutierrez et al., 2014; Jansson et al., 2010b; Jansson et al., 2015b; Lovejoy et al., 2011; Seebacher et al., 2016a); this was not the case in the M14 melanoma cell lines used to assess the effects of Bcl-2 expression on Dp44mT- and DpC-mediated cytotoxicity (Fig. 5.7). DpC induced an accumulation of acidic vesicles regardless of Bcl-2 expression, however, Dp44mT only induced a

significant increase in acidic vesicles in the control M14 PC cell line that did not express Bcl-2 (Fig. 5.6).

We suggest that the accumulated acidic vesicles were autolysosomes, formed by the fusion of autophagosomes and lysosomes (Fig. 5.7) (Kondo et al., 2005). The accumulation of acidic vesicles, rather than LMP, may be due to the potentially high levels of the copper binding proteins, metallothioneins, which is commonly found in melanoma and is used as a negative prognostic indicator (Krauter et al., 1989; Weinlich et al., 2006; Zelger et al., 1993). High metallothionein levels in the M14 cell lines would prevent the binding of copper ions by Dp44mT and DpC, thus, preventing the generation of ROS and induction of LMP (Figs. 3.6, 3.7, 3.9, 3.10, 4.17-4.20, 5.7). The failure of Dp44mT and DpC to induce LMP (Fig. 5.7), in addition to the ability of DpC to mediate the formation of autophagosomes (Fig. 5.6), underpinned our suggestion that accumulated acidic vesicles were autolysosomes.

There are significant differences in the mechanisms by which certain thiosemicarbazones overcome Pgp-mediated and Bcl-2 mediated MDR. Targeting Pgp required thiosemicarbazones to possess characteristics that included Cu(II) binding, redox cycling and induction of LMP as characteristics the thiosemicarbazones must possess (Figs. 3.6-3.10). However, DpC required none of these characteristics to overcome Bcl-2-mediated MDR (Figs. 5.4, 5.5, 5.7), and rather than induction of LMP, there is instead an accumulation of acidic vesicles (Fig. 5.7). Moreover, whereas

targeting Pgp involves ñhijackingò the transporter and using it to selectively target Pgp expressing cells (Figs. 3.5, 3.8), DpC overcame Bcl-2 mediated MDR by decreasing the expression of the Bcl-2 protein (Figs. 5.1-5.3).

6.3 Targeting Lysosomes and Cu(II) with Thiosemicarbazones

A major mechanism utilised by thiosemicarbazones to induce cytotoxicity involves the formation of redox-active Cu(II) complexes that target lysosomes (Gutierrez et al., 2014; Gutierrez et al., 2016; Jansson et al., 2010b; Jansson et al., 2015b; Lovejoy et al., 2011; Seebacher et al., 2016a; Stefani et al., 2015). Copper is an essential metal that is required for cell survival as it acts as a co-factor in a diverse array of enzymes (Antholine et al., 1976; Gaggelli et al., 2006; Petering et al., 1967; Van Giessen et al., 1973). However, free copper ions are also damaging to the cell, due to their ability to catalyse redox reactions to generate cytotoxic ROS (Gaggelli et al., 2006). Upon uptake into the cell, Cu(II) can be found bound to chaperones, metallothionein, or in the active sites of enzymes (Denoyer et al., 2015). Additionally, lysosomes contain a large proportion of intracellular Cu(II) as a result of the degradation of Cu(II)-containing metalloproteins by lysosomal cathepsins (Gupte and Mumper, 2009; Kurz et al., 2010; Terman and Kurz, 2013).

The high proliferation rate of cancer cells means that they require greater amounts of Cu(II) than non-neoplastic cells (Al-Eisawi et al., 2016). As such, cancer cells are more susceptible to the damaging consequences of Cu(II) sequestration than normal cells (Kalinowski et al., 2016). Some thiosemicarbazones, such as Dp44mT, are able to exploit the higher levels of Cu(II) found in neoplastic cells by forming redox-active Cu(II) complexes inside lysosomes (Gutierrez et al., 2014; Jansson et al., 2010b; Jansson et al., 2015b; Kalinowski et al., 2016; Lovejoy et al., 2011; Stefani et al., 2015). Generally, lysosomal sequestration negatively impacts on the efficacy of chemotherapeutics and contributes to MDR (Gong et al., 2003; Hurwitz et al., 1997; Schindler et al., 1996; Zhitomirsky and Assaraf, 2015a). However, Dp44mT induces apoptosis by accumulating in lysosomes, as the redox activity of the Cu(II)-thiosemicarbazone complexes generates cytotoxic ROS (Gutierrez et al., 2014; Gutierrez et al., 2016; Jansson et al., 2010b; Jansson et al., 2015b; Johansson et al., 2010; Lovejoy et al., 2011; Seebacher et al., 2016a; Stefani et al., 2015; Turk and Turk, 2009). This destabilises the membrane and results in the leaking of degradative lysosomal enzymes into the cytoplasm (Gutierrez et al., 2014; Gutierrez et al., 2016; Jansson et al., 2010b; Jansson et al., 2015b; Johansson et al., 2010; Lovejoy et al., 2011; Seebacher et al., 2016a; Stefani et al., 2015; Turk and Turk, 2009).

Although Pgp is not always required in order for some thiosemicarbazones to target lysosomes (Gutierrez et al., 2014; Gutierrez et al., 2016; Lovejoy et al., 2011; Stefani et al., 2015), it does potentiate their ability to do so (Jansson et al., 2015b; Seebacher et al., 2016a). We showed that inhibition of Pgp prevented LMP and cytotoxicity induced

by Dp44mT, Bp44mT and DpC (Figs. 3.4, 3.8). Furthermore, LMP did not occur in the non-Pgp expressing, KB31 cell line at the concentration and time point used in these studies (Fig. 3.6). Pgp potentiates the cytotoxicity of Dp44mT by actively transporting Dp44mT into lysosomal lumens, where it is protonated and sequestered (Jansson et al., 2015b; Lovejoy et al., 2011). The enhanced lysosomal sequestration of Dp44mT due to Pgp expression in lysosomal membranes results in selective cytotoxicity in Pgp-expressing, MDR cells (Jansson et al., 2015b; Seebacher et al., 2016a).

Whereas lysosomal accumulation has previously been demonstrated using indirect techniques, such as examining the destabilisation of lysosomal membranes following incubation with thiosemicarbazones (Figs. 3.6, 3.8-3.10) (Gutierrez et al., 2014; Gutierrez et al., 2016; Jansson et al., 2010b; Jansson et al., 2015b; Lovejoy et al., 2011; Seebacher et al., 2016a; Stefani et al., 2015); importantly, for the first time, we were also able to definitively localise the Zn(II) complex of our lead thiosemicarbazone, DpC, to lysosomes (Figs. 4.14-4.16), and not nuclei (Figs. 4.8-4.10) or mitochondria (Figs. 4.11-4.13). We synthesised 1:1 and 1:2 Zn(II) complexes of Dp44mT, Ap44mT and DpC·HCl, which were more potently cytotoxic than the ligands alone (Fig. 4.7). The inherent fluorescence of Zn(II) allowed us to conduct confocal microscopy studies, and we demonstrated that the Zn(II) complex of our lead agent, $[Zn(DpC)_2](ClO_4)_2$, accumulated in lysosomes in the KBV1, KB31 and SW480 cell lines (Figs. 4.14- 4.16). This is in contrast to the Zn(II) complex of 3-AP, which was localised to the nucleus/nucleoli of the cell (Kowol et al., 2010). The free ligand, 3-AP, did not cause LMP in our studies (Fig. 3.6), which may be related to its nuclear localisation (Kowol et

al., 2010). We have demonstrated the importance of LMP to the cytotoxicity generated by thiosemicarbazones, so this may have contributed to the failure of 3-AP in clinical trials (Knox et al., 2007; Merlot et al., 2013; Traynor et al., 2010).

In this thesis, we identified characteristics that are required for thiosemicarbazones to target lysosomes, which highlighted the importance of the formation of avidly redox-active Cu(II) complexes (Figs. 3.6-3.10). The formation of Cu(II) complexes may facilitate the trapping of Dp44mT, Bp44mT and DpC inside lysosomes, as the Cu(II) complexes are more lipophilic than the ligands alone, therefore, are better Pgp substrates (Fig. 3.5) (Kimura et al., 2004; Schmid et al., 1999; Seelig and Landwojtowicz, 2000). Indeed, the Cu(II) complexes, but not the Fe(III) complexes or ligands alone of Dp44mT, Bp44mT and DpC, potently induced LMP in Pgp-expressing, KBV1 cells (Fig. 3.6). Moreover, Bp2mT, which cannot bind copper ions due to the substitution of a methyl group at N2, did not induce LMP (Fig. 3.6). Cu(II) chelation also prevented LMP mediated by [Cu(Dp44mT)], [Cu(Bp44mT)] and [Cu(DpC)] (Fig. 3.9). Although [Cu(Dp44mT)], [Cu(Bp44mT)] and [Cu(DpC)] were more potent inducers of LMP than the thiosemicarbazones alone, longer incubations and higher concentrations of Dp44mT, Bp44mT and DpC did induce LMP (Figs. 3.6, 3.8-3.10). Furthermore, we showed that the LMP induced by Dp44mT, Bp44mT and DpC was also dependent on their ability to bind Cu(II) (Fig. 3.9).

It was not enough for thiosemicarbazones to simply bind Cu(II); the Cu(II)-thiosemicarbazone complexes were also required to be highly redox active. This was illustrated by 3-AP and Ap44mT, which can form Cu(II) complexes, yet did not induce LMP like Dp44mT, Bp44mT and DpC (Fig. 3.6). 3-AP was not sufficiently redox-active to induce LMP, as the Cu(II) complex, Fe(III) complex and ligand alone of 3-AP did not mediate the oxidation of the well-characterised redox probe, H_2DCF (Fig. 3.7). However, [Cu(Ap44mT)], like [Cu(Dp44mT)], [Cu(Bp44mT) and [Cu(DpC)], mediated a significant increase in H_2DCF oxidation, relative to control (Fig. 3.7). While [Cu(Ap44mT)] mediated the oxidation of H_2DCF, it was significantly less redox-active than [Cu(Dp44mT)], [Cu(Bp44mT)], or [Cu(DpC)] (Fig. 3.7) and did not induce LMP (Figs. 3.6, 3.8-11). This suggested that the failure of [Cu(Ap44mT)] to induce LMP was, in part, related to its decreased ability to generate ROS (Fig. 3.7).

The inability of [Cu(Ap44mT)] to induce LMP was due to the inductively electron-donating effects of the imine methyl group of Ap44mT which resulted in a Cu(II) complex with a lower redox potential (Jansson et al., 2010a) that lies outside of the optimal window, preventing sufficient generation of ROS (Fig. 3.7) to mediate LMP (Figs. 3.6, 3.8-11). In contrast, the inductively electron-withdrawing substituents located at the imine position of Dp44mT, Bp44mT and DpC resulted in the formation of Cu(II) complexes with redox potentials that lie in an optimal window that allow for a redox cycling mechanism to become established (Bernhardt et al., 2009; Jansson et al., 2010a; Lovejoy et al., 2012). The inability of any of the ligands alone and the Fe(III) complexes to induce H_2DCF oxidation further illustrated the importance of Cu(II)

binding, in order to form highly redox-active complexes that generate LMP-inducing ROS.

Moreover, additional studies highlighted the importance of the formation of avidly redox-active Cu(II) complexes in order to target lysosomes in Pgp-expressing cells, as co-incubation with the antioxidant NAC prevented LMP induced by Dp44mT, Bp44mT, DpC, and their Cu(II) complexes (Fig. 3.10). Clearly, for thiosemicarbazones to induce potent and selective apoptosis in Pgp-expressing cells (Fig. 3.5, 3.8), they were required to be sequestered in lysosomes and bind Cu(II) (Fig. 3.6, 3.8) to form highly redox-active complexes that generate ROS (Fig. 3.7, 3.10) and induce LMP (Fig. 3.6, 3.8-3.10).

Similarly to the Cu(II) complexes of Dp44mT, DpC and Bp44mT, the Zn(II) complexes of Dp44mT, Ap44mT and DpC, targeted lysosomes and induced LMP (Fig. 4.17). Interestingly, despite the fact that Zn(II) complexes of our thiosemicarbazones were not redox-active, they were able to induce LMP (Fig. 4.17) (Berg and Shi, 1996; Bernhardt et al., 2009). However, we had previously demonstrated that thiosemicarbazones must generate ROS when bound to transition metals in order to induce LMP (Fig. 3.10). This accounts for the potency of the Cu(II) complexes, as Cu(II) is highly redox-active and enables the generation of large quantities of ROS (Jansson et al., 2010b; Lovejoy et al., 2011). In agreement with the Irving-Williams series (Irving and Williams, 1953), Dp44mT has a preference for binding Cu(II) over Zn(II) (Gaal et al., 2014). Furthermore, it has

been demonstrated that Zn(II)bis(thiosemicarbazone) complexes can transmetallate with copper ions (Pascu et al., 2007). Herein, we demonstrated that [Zn(Dp44mT-H)$_2$], [Zn(Ap44mT-H)$_2$] and [Zn(DpC)$_2$](ClO$_4$)$_2$, which were not redox-active, were able to transmetallate *in vitro* with copper ions to generate redox-active Cu(II) complexes (Fig. 4.17). This ability of [Zn(Dp44mT-H)$_2$], [Zn(Ap44mT-H)$_2$] and [Zn(DpC)$_2$](ClO$_4$)$_2$ to transmetallate with copper ions (Fig. 4.17) enabled them to mediate LMP (Fig. 4.19), as co-incubation with the copper chelator, TM, prevented induction of LMP (Fig. 4.19). Moreover, co-incubation of [Zn(Dp44mT-H)$_2$], [Zn(Ap44mT-H)$_2$] and [Zn(DpC)$_2$](ClO$_4$)$_2$ with TM decreased the cytotoxicity of the Zn(II) complexes (Fig. 4.20), illustrating the importance of Cu(II) binding, redox cycling and LMP induction in the mechanism of these thiosemicarbazones.

These studies demonstrated in order to target copper and lysosomes to induce LMP thiosemicarbazones a required to possess several characteristics, namely: **(1)** high lipophilicity for ease of diffusion across both plasma and lysosomal membranes; **(2)** multiple ionisable hydrogen atoms, enabling protonation at pH 5 and sequestration within lysosomes; **(3)** a preference for binding copper over other transition metals (Gaal et al., 2014); and **(4)** high redox potentials enabling the generation of significant quantities of cytotoxic ROS. Furthermore, thiosemicarbazones are able to induce potentiated cytotoxicity in Pgp-expressing, MDR cancer cells due to their **(5)** Pgp substrate activity.

Targeting lysosomes by inducing LMP is a mechanism of cytotoxicity that Dp44mT exhibits in a variety of cancer cell lines, including KBV1 (cervical cancer), SK-N-MC (neuroblastoma), MCF-7 (breast cancer) and SW480 (colorectal adenocarcinoma) (Gutierrez et al., 2014; Gutierrez et al., 2016; Jansson et al., 2010b; Jansson et al., 2015b; Lovejoy et al., 2011; Seebacher et al., 2016a; Stefani et al., 2015). However, in the M14 melanoma cell line, there was no evidence of LMP following incubation with Dp44mT or DpC (Fig. 5.7). Thiosemicarbazones are required to bind copper and redox cycle to generate ROS, which peroxidise the lipid bilayer of lysosomal membranes to induce LMP (Fig. 3.6, 3.8-3.10, 4.17- 4.20) (Gutteridge et al., 1979; Ollinger and Brunk, 1995). However, we demonstrated that in the M14 melanoma cell lines, chelation of copper ions with TM had no effect on the cytotoxicity of Dp44mT or DpC (Fig. 5.4).

Moreover, no ROS were generated by Dp44mT or DpC in the M14 melanoma cell lines, as the antioxidant, NAC, had not effect on their cytotoxicity (Fig. 5.5). We propose that this was due to the high levels of metallothionein that melanoma cells express, which could prevent the formation of Cu(II) complexes due to a lack of unbound Cu(II) (Krauter et al., 1989; Weinlich et al., 2006; Zelger et al., 1993). This is in accordance with previous results that have demonstrated the markedly greater redox activity of the Cu(II) complexes of Dp44mT and DpC compared to the ligands alone (Fog. 3.7). Without the ability to bind Cu(II) and generate ROS, Dp44mT and DpC would not be expected to induce LMP.

In fact, we found that Dp44mT and DpC increased the number of acidic vesicles in the M14 cell lines in a manner that was dependent on Bcl-2 expression (Fig. 5.7), possibly by affecting the autophagy pathway (Fig. 5.6). DpC, but not Dp44mT, induced an increase in the expression of the classical marker of autophagosome formation, LC3-II, and in the number of acidic vesicles in Bcl-2 over-expressing M14 Bcl-2 cells (Fig. 5.6, 5.7). We believe that the increase in LC3-II expression induced by DpC is due to the ability of DpC to decrease the expression of Bcl-2 (Fig. 5.2), as Bcl-2 is an inhibitor of the autophagy initiator, Beclin 1 (Chang et al., 2010; Kihara et al., 2001; Pattingre et al., 2005).

We propose that the acidic vesicles may be autolysosomes, formed by the fusion of autophagosomes with lysosomes; therefore, the increase in autophagosome formation induced by DpC would lead to the increase in acidic vesicle/autolysosome number, as observed (Fig. 5.7). While Dp44mT had been found to induce autophagy in the MCF-7 breast cancer cell line (Gutierrez et al., 2014), in the M14 Bcl-2 melanoma cell line, Dp44mT does not induce an decrease in Bcl-2 expression (Fig. 5.2); therefore, Beclin 1 would likely be inhibited (Chang et al., 2010; Liang et al., 1998; Pattingre et al., 2005). Autophagy would not be initiated and no induction of autophagosome formation would be expected following incubation with Dp44mT, as observed (Fig. 5.6). Additionally, Dp44mT did not induce an increase in the number of acidic vesicles formed in M14 Bcl-2 cells, although did induce a significant increase in M14 PC cells (Fig. 5.7). The prevention of autophagy due to Beclin 1 inhibition by Bcl-2 would prevent an increase in

autolysosome formation in M14 Bcl-2 cells, evidenced herein by the lack of increase in the number of acidic vesicles (Fig. 5.7).

In M14 PC cells, on the other hand, Beclin 1 would not be inhibited, thus autophagy could be induced by Dp44mT and the number of acidic vesicles/autolysosomes would increase, as observed (Fig. 5.7). The relationship between the increase in acidic vesicles and cytotoxicity induced by Dp44mT and DpC in the M14 melanoma cell lines is yet to be be determined. However, the trends in cytotoxicity were similar to the trends in acidic vesicle formation. That is, DpC was equally cytotoxic in M14 Bcl-2 and M14 PC cells, and also induced similar increases in the number of acidic vesicles. Dp44mT was less cytotoxic in M14 Bcl-2 cells than in M14 PC cells, and did not induce an increase in acidic vesicles in M14 Bcl-2 cells, although did in M14 PC cells. These results suggest that there may be a causal relationship between acidic vesicle formation and cytotoxicity induced by Dp44mT and DpC, which is related to Bcl-2 expression.

Herein, we have highlighted importance of lysosomal targeting in the mechanism of thiosemicarbazone-induced cytotoxicity. We explored requirements that enabled thiosemicarbazones to potently target lysosomes in Pgp-expressing MDR cells, by ñhighjackingò lysosomal Pgp to increase their accumulation in lysosomes. In accordance with previously published results, these studies highlighted the importance of the ability to bind Cu(II) and generate ROS, in order to induce LMP and apoptosis. The importance of Cu(II) binding and ROS generation was also demonstrated using novel

Zn(II) complexes of Dp44mT, Ap44mT and DpC. Interestingly, the increased cytotoxicity of the Zn(II) complexes of Dp44mT, Ap44mT and DpC, relative to the free ligands, was due to their ability to transmetallate with Cu(II) and generate ROS to induce LMP.

Additionally, for the first time, we directly observed accumulation of the Zn(II) complexes of our lead drug candidate, DpC, in lysosomes. It also appears that Dp44mT and DpC target lysosomes in melanoma, albeit *via* a different mechanism to what is observed in other cancer cell lines. Rather than inducing LMP which results in apoptosis, in melanoma, Dp44mT and DpC induced an increase in the number of acidic vesicles, which we proposed to be autolysosomes. Regardless of the mechanism by which they do so, a common feature of thiosemicarbazones that possess potent anti-cancer activity is the ability to target lysosomes.

6.4 Future Directions

6.4.1 Future Directions for Chapter 3

Chapter 3 confirmed the mechanism by which thiosemicarbazones target Pgp-mediated MDR. Furthermore, we determined five characteristics that thiosemicarbazones were required to possess in order to selectively target Pgp-expressing cancer cells. Considering our results, further studies could involve the synthesis of novel thiosemicarbazones in order to develop more active agents that overcome multi-drug

resistance *via* the exploitation of lysosomal Pgp. Particular emphasis should be placed on developing thiosemicarbazones that fulfil the five criteria identified, namely: **(1)** inductively electron-withdrawing substituents at the imine carbon; **(2)** high relative lipophilicity; **(3)** Pgp substrate activity; **(4)** Cu(II) chelation efficacy; and **(5)** the induction of ROS generation.

The relative importance of these properties for overcoming resistance is unclear, and these agents have not been optimised to overcome MDR. This is demonstrated by the fact that only 16% of our lead agents e.g., Dp44mT are charged & trapped at lysosomal pH (Lovejoy et al., 2011). Thus, this is far from optimal. We will assess a broad library of our thiosemicarbazones with differing substitutions at the imine C and terminal N4 atom (Jansson et al., 2010b; Kalinowski et al., 2007). These studies will identify the best agent and its Fe(III) or Cu(II) complex for further studies later. An established series of analogues is initially utilised, as >10 years of research have already carefully refined the properties vital for anti-cancer activity ***e.g.***, tumour cell selectivity, appropriate pharmacokinetics, safety, ***etc*** (Kovacevic et al., 2011; Lovejoy et al., 2012). We will also develop a second library of agents to enhance their lysosomotropic activity and Pgp substrate properties to result in greater lysosomal accumulation. These new agents (Fig. 6.1B,C) maintain the basic active pharmacophore (Fig. 9A) with the 3 key molecular signatures described above (*i.e.*, (1) being a Pgp substrate; (2) charged and trapped in lysosomes; and (3) binding Cu and inducing LMP) that are vital for the marked activity of the established library (Jansson et al., 2015b; Seebacher et al., 2016c; Yamagishi et al., 2013). New Series 1 (Fig. 6.1B) will feature substituents with

electron-donating effects (*i.e.*, 2-Me, 2,2ôMe, 4-MeO), added to the pyridine rings. This will be done to increase the basicity and protonation of the pyridine rings (Comba et al., 2013) to enhance lysosomal trapping at lysosomal pH 5.

New Series 2 will incorporate of molecular fragments of known lysosomotropic agents such as chloroquine and AO that also have the crucial property of being Pgp substrates (Crowe et al., 2006; Kessel et al., 1991) and are trapped in lysosomes (Abok et al., 1984; de Duve et al., 1974; Jansson et al., 2015b) (Fig. 6.1C). Chemically combining the structures of Dp44mT and chloroquine enables potent trapping in lysosomes, as chloroquine possesses multiple positive charges *even* after lysosomal neutralisation (Al-Bari, 2015). Hence, these multiple positive charges markedly prevent escape across lysosomal membranes and will induce effective lysosomal trapping that we know is vital for thiosemicarbazone anti-tumour efficacy (Jansson et al., 2015b; Lovejoy et al., 2011). Additionally, since chloroquine and Dp44mT are both Pgp substrates (Giles et al., 2003; Jansson et al., 2015b) this should enable highly effective entry into lysosomes *via* lysosomal Pgp. Furthermore, both chloroquine and AO have good tolerability *in vivo* (Al-Bari, 2015). Another beneficial property of the AO or chloroquine analogues is that they can be directly imaged due to their fluorescence, enabling tracking of their intracellular location (Abok et al., 1984; Amador-Hernandez et al., 2001; Jansson et al., 2015b).

The studies below will assess the 3 key molecular signatures in our analogues (Fig. 6.1) that are vital to overcome Pgp resistance and will identify the most effective agent and its metal complex (Fe(III) or Cu(II)) for *in vivo* studies:

6.4.1.1. Role of Agent Ionisation Characteristics in Lysosomal Trapping

Lysosomal trapping occurs if the agents become protonated at lysosomal pH (pH~5) (Lovejoy et al., 2011). This leads to decreased passage of the positively charged ligand across the lysosomal membrane (Lovejoy et al., 2011). To determine if our agents are charged at lysosomal pH, we will assess their ionisation and Cu(II)-binding affinity as a function of pH *via* spectrophotometric/pH titrations. Thus, these experiments will identify the agents/complexes with optimal lysosomotropic properties leading to lysosomal trapping.

6.4.1.2 Thiosemicarbazone Selectivity Against Pgp-Expressing Cells

Considering that Pgp plays a crucial role in potentiating Dp44mT cytotoxicity (Jansson et al., 2015b), we will elucidate if Pgp is involved in the cytotoxic mechanisms of our thiosemicarbazones (Fig. 6.1) and/or their metal complexes. Initial studies will assess if the selective Pgp inhibitors, available in our lab (Jansson et al., 2015b; Yamagishi et al., 2013), namely: Valspodar (Val; 5 ε M) (Jachez et al., 1993) (Novartis) and Ela (0.1 ε M) (Hyafil et al., 1993) (Sigma), or silencing of Pgp with siRNA (2 siRNAs to be tested vs. control-siRNA) (Jansson et al., 2015b; Yamagishi et al., 2013) will decrease cytotoxicity.

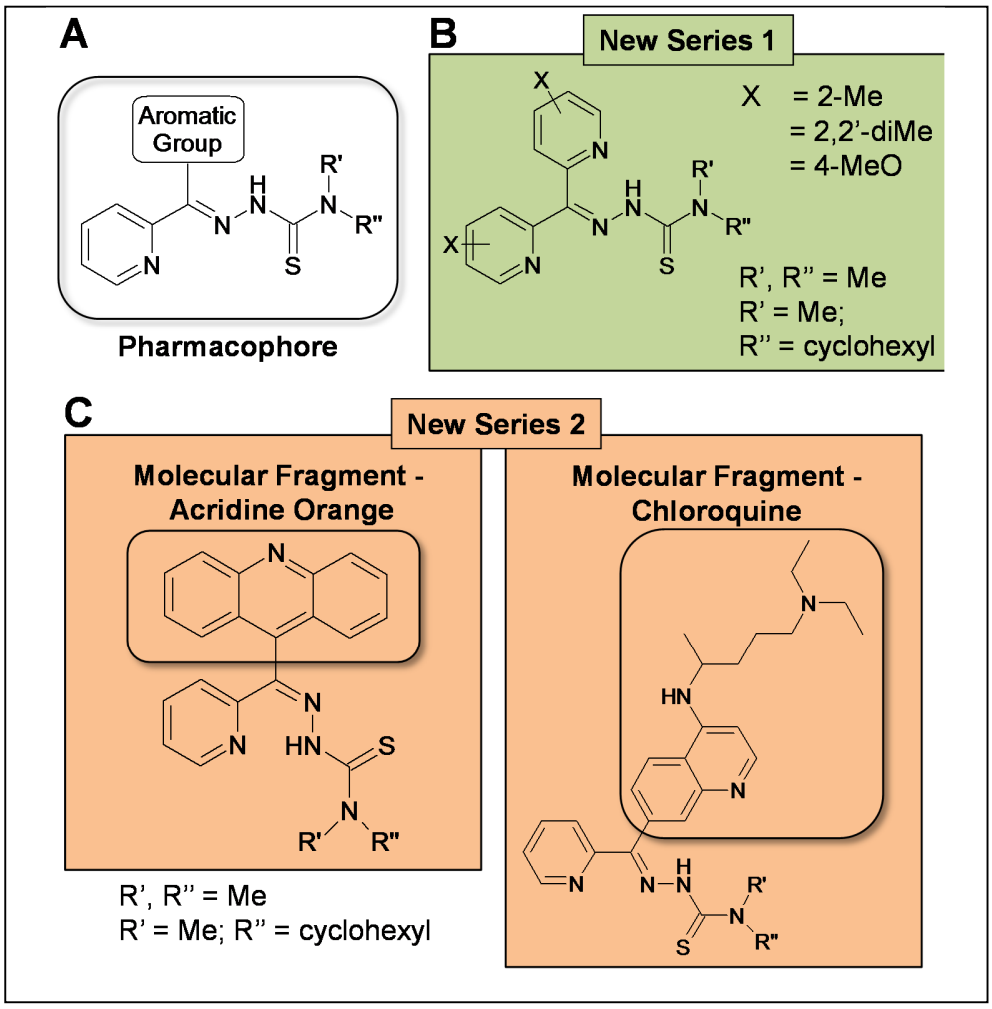

Fig. 6.1 Pharmacophores for Development of Optimised Novel Thiosemicarbazones

Optimised Optimised thiosemicarbazone pharmacophore backbone for Cu(II) binding and redox activity. **(B)** New series 1: Substitutions (X) to increase lysosomal targeting. **(C)** New series 2: Circled moieties designed to increase lysosomal-targeting and Pgp substrate activity.

We hypothesise these Pgp inhibitors will reduce the uptake of thiosemicarbazones into lysosomes via lysosomal Pgp, and thus, will prevent LMP and cell death. To assess this, MTT assays validated by viable cell counts (Kalinowski et al., 2007; Yu et al., 2011) will be performed using our range of cells with high and low Pgp levels. Cellular Pgp levels will be monitored by Western blot (Dixon et al., 2013; Jansson et al., 2015b; Lovejoy et al., 2011; Yamagishi et al., 2013). We will compare the thiosemicarbazones and their Cu(II) and Fe(III) complexes (Fig. 6.1B,C) to Dp44mT (Kovacevic et al., 2010). These studies will determine which thiosemicarbazones and their complexes are best at overcoming Pgp resistance.

6.4.1.3 Examination of Thiosemicarbazone Drugs and their Metal Complexes in Terms of Transport via the Pgp Pump

To assess if our thiosemicarbazone analogues (Fig 9B,C), and their Cu(II)- and Fe(III)-complexes are transported by Pgp, we will initially use the cell-free, Pgp-Glo ATPase Assay system (Promega) (Jansson et al., 2015b) and compare our agents to known Pgp substrates (*e.g.*, doxorubicin, *etc.*). Moreover, to confirm if thiosemicarbazones/complexes are Pgp substrates in a cell system, we will use our standard radiolabelling and efflux protocols (Lovejoy et al., 2011; Richardson and Milnes, 1997; Yuan et al., 2004). These studies will track ^{67}Cu- (Oak Ridge National Labs, TN) or ^{59}Fe- (Perkin-Elmer) labelled complexes in cells and the ^{14}C-labelled thiosemicarbazones (*i.e.*, ^{14}C-Dp44mT, ^{14}C-DpC *etc.* available in our lab (Merlot et al., 2010; Merlot et al., 2013)). Retention/efflux of the labelled (^{67}Cu or ^{59}Fe) metal-ligand complexes will be assessed in Pgp- *vs.* non-Pgp-expressing cells above. We will also

assess Pgpôs role in the retention/efflux of drugs by using the potent Pgp inhibitors, Val (5 ε M) (Jachez et al., 1993) and Ela (0.1 ε M) and Pgp siRNA (Hyafil et al., 1993; Yamagishi et al., 2013). These studies will identify the best structural features necessary for effective trafficking by Pgp.

6.4.1.4 Thiosemicarbazone Selectivity Against Other ABC-Expressing Cells

Other ABC transporters that have been implicated in MDR include ABCG2 and MRP1, which have substantially overlapping substrate specificities with Pgp. It has been suggested that expression of multiple ABC transporters in a tumour cell population may account for the failure of strategies that have only targeted a single ABC transporter. Due to the overlapping substrate specificities, it is possible that the thiosemicarbazones may be substrates of ABCG2 and MRP1, in addition to Pgp. We will examine whether ABCG2 or MRP1 are involved in the cytotoxic mechanisms of the thiosemicarbazones, and/or their metal complexes. Initial studies will assess the effect of the specific ABCG2 inhibitor, KO143 (Allen et al., 2002), and the specific MRP1 inhibitor, MK571 (Jones et al., 1989), or silencing of ABCG2 or MRP1 with siRNA, on the cytotoxicity of the thiosemicarbazones. Lysosomal localisation of ABCG2 and MRP1 has been reported (Rajagopal and Simon, 2003a), so if the thiosemicarbazones are substrates of these transporters, they may act in a manner similar to what has been reported for Dp44mT and DpC in Pgp-expressing cells. MTT assays will assess the cytotoxicity of the thiosemicarbazones in ABCG2 positive/ABCG2 negative and MRP1 positive/MRP1 negative cell line counterparts, such as A549-MX100/A549 and MCF7-VP/MCF7,

respectively. These studies will demonstrate whether the thiosemicarbazones can overcome resistance mediated by ABCG2 or MRP1.

6.4.1.5 Examination of the Importance of the Pgp Drug Pump in Sub-Cellular Distribution of Thiosemicarbazone Complexes

Cu-Dp44mT accumulates in and damages lysosomes (Jansson et al., 2015b; Lovejoy et al., 2011). Furthermore, Pgp is found in lysosomal membranes (Jansson et al., 2015b; Yamagishi et al., 2013), leading to accumulation of Pgp substrates in this organelle (Yamagishi et al., 2013). However, Pgp has also been reported to co-localise with other organelles e.g., endosomes, Golgi, mitochondria and nuclei (Merlot et al., 2010; Molinari et al., 2002; Munteanu et al., 2006) Therefore, we will also assess if Pgp modulates targeting of thiosemicarbazones and their Cu(II) complexes to destabilise these organelles in Pgp- versus non-Pgp-expressing cells. Organelle integrity will be studied using: EEA1-CY3 (early endosome); Golgin-97-CY3 (Golgi); AO; Lysotracker Red/Green; Lamp-2 (lysosomes); TMRE/MitoTracker red (mitochondria); and DAPI staining (nuclei), using confocal microscopy and quantification by flow cytometry (Jansson et al., 2015b; Lovejoy et al., 2011; Yamagishi et al., 2013). If Pgp correlates with drug-induced damage to these organelles, then the Pgp inhibitors or Pgp siRNA (2 siRNAs to be tested vs. control-siRNA) (Yamagishi et al., 2013) will be used to rescue organelle destabilisation. Also, accumulation of radioactive ligands/complexes will be quantified in isolated organelles by density gradient centrifugation (Graham et al., 1994) and assessing retention of 14C-ligands (e.g., 14C-Dp44mT (Lovejoy et al., 2011), ^{67}Cu- and ^{59}Fe-complex) (Lovejoy et al., 2011). Fraction purity & morphology will be checked

by marker analysis (Lovejoy et al., 2011) and electron microscopy, respectively. These studies will examine if Pgp affects organelle targeting/trafficking of thiosemicarbazones to comprehensively understand their subcellular mechanism of action

6.4.1.6 Investigation of Synergism of Thiosemicarbazones with Standard Chemotherapies

Many common, first-line chemotherapies are substrates of Pgp, thus are ineffective against Pgp-expressing, MDR cancer (Gillet and Gottesman, 2010; Gottesman et al., 2002). Examples include doxorubicin, paclitaxel, vinblastine and etoposide (Gillet and Gottesman, 2010; Gottesman et al., 2002). Tumour cell populations are not homogenous, but rather exist as heterogeneous clonal populations of neoplastic cells that express varying levels of proteins, such as Pgp (Burrell and Swanton, 2014). Therefore, in tumours where some cells express Pgp, there will be cells which express little or no Pgp. This heterogeneous population will exhibit different sensitivities to cytotoxic drugs, inhibiting treatment efficacy (Burrell and Swanton, 2014). Indeed, standard treatments often kill only the drug sensitive cells, leaving behind the drug resistant cells to survive and re-populate the tumour. The rational for using combination chemotherapy in such instances is clear: different chemotherapies can target different clonal populations within the tumour, resulting in improved efficacy. Herein, we will examine whether combining our thiosemicarbazones with the common first line chemotherapy, doxorubicin, enhances cytotoxicity in Pgp-expressing tumour cell populationss. Cells derived from Pgp-expressing tumours will be treated with thiosemicarbazones first, in order to kill drug resistant cells. The drug sensitive cells will

then be targeted with doxorubicin. The results of combination therapy will be compared to the thiosemicarbazone alone and doxorubicin alone. Cytotoxicity will be assessed in MTT assays. These studies will determine whether combination therapy with our thiosemicarbazones can improve treatment efficacy in heterogeneous tumour cell populations.

6.4.2 Future Directions for Chapter 4

The ability to examine the intracellular distribution and accumulation of novel drug candidates is useful in order to determine their mechanism of action. Indeed, we were able to demonstrate the lysosomal localisation of the Zn(II) complex of our lead candidate, DpC (Fig. 4.14-16). This supports previous results, which indirectly showed lysosomal accumulation of DpC, and the structurally related thiosemicarbazone, Dp44mT (Gutierrez et al., 2014; Jansson et al., 2010b; Jansson et al., 2015b; Lovejoy et al., 2011; Seebacher et al., 2016a). Herein, we demonstrated that the mechanism of the Zn(II) complexes involves transmetallation with Cu(II) within lysosomes, which forms redox-active complexes that generate ROS and induce apoptosis (Fig. 4.17-4.19). Zn(II) appears to be an ideal transition metal for preparing new compounds as it increases lipophilicity (Richardson et al., 2006), which facilitates their passage across the cellular and lysosomal membranes, relative to the ligands alone, leading to enhanced uptake, cytotoxicity and ability to induce LMP.

However, the pharmacokinetic profile of the Zn(II)-thiosemicarbazone complexes must be assessed. A favourable pharmacokinetic profile would lead to *in vivo* assessment of anti-cancer efficacy, which must also be compared to that of the Fe(III) and Cu(II) complexes which have been assessed to date (Jayakumar et al., 2014; Kovacevic et al., 2011; Yuan et al., 2004). Furthermore, the ability of the Zn(II)-thiosemicarbazone complexes to overcome Pgp-mediated MDR warrants further investigation, as the Zn(II) complexes of Dp44mT and DpC appeared to exhibit potentiated cytotoxicity against Pgp-expressing KBV1 cells, a property essential for overcoming Pgp-mediated drug resistance in tumours (Fig. 4.7). The properties of the Zn(II)-thiosemicarbazone complexes outlined above will be assessed in the following studies:

6.4.2.1 Pharmacokinetic profiles

To assess pharmacokinetic profiles, we will implement our well-characterised UHPLC-MS/MS-based method that we used to assess similar thiosemicarbazones (Sestak et al., 2015). Groups of pre-catheterised (jugular vein) rats (6/group) will be given 2 mg/kg doses (*i.v.*) of the most effective agent, its best metal complex and the vehicle control (Sestak et al., 2015). During a time range of 5ï 1800 min, 500 ε L blood will be taken and the plasma assayed by UHPLC-MS/MS (Sestak et al., 2015). This analysis will yield: max. concentration (c_{max}); time to achieve c_{max} (t_{max}); apparent vol. of distribution (V_z); total plasma clearance (CL); area under curve of concentrationï time profile (AUC); elimination half-life ($t_{1/2}$) (Sestak et al., 2015). This will provide useful pre-clinical data that will facilitate their clinical development.

6.4.2.2 Examination of the Most Effective Transition Metal-Thiosemicarbazone Complex in Terms of Anti-Cancer Efficacy in Cancer Xenografts *In Vivo*

The anti-cancer activity of the best thiosemicarbazone and its metal complex in vivo will be assessed by bioluminescent tumour imaging via injecting either resistant or non-resistant (i.e., passage matched) luciferase (luc)-labelled cells (1×10^5/mouse) into nude mice.

Once the tumour reaches 100 mm^3 (assessed by bioluminescent tumour imaging), treatment will begin (Kovacevic et al., 2011). Groups of 10 mice will be randomly chosen and treated with: **(1)** vehicle control (saline) (Dykes et al., 1995); **(2)** the reference cytotoxic; **(3)** vehicle control for the thiosemicarbazone or its Zn(II) Fe(III) or Cu(II) complex (30% propylene glycol/saline (Kovacevic et al., 2011; Lovejoy et al., 2011); **(4)** the most effective thiosemicarbazone (5 days/week); and **(5)** its metal complex (Zn(II) Cu(II) or Fe(III) complex, whichever is most effective - identified in SO1). These 5 groups will be used for each cell line at their maximum tolerated dose (MTD). Animal numbers and dosing protocols are based on our *in vivo* studies (Kovacevic et al., 2011; Whitnall et al., 2006) and the power is >90% based on (Kovacevic et al., 2011; Whitnall et al., 2006). The agents or vehicles will be injected i.v. (tail vein) 5 days/week (Kovacevic et al., 2011; Lovejoy et al., 2011); or every 4 days for Docetaxel or its vehicle (Dykes et al., 1995). Our specifically developed *i.v*. injection method (Kovacevic et al., 2011) does not lead to tail necrosis.

We will assess MTDs in nude mice using an initial i.v. starting dose (0.4 mg/kg) once/day (5 days/week; Mon-Fri) (Lovejoy et al., 2011) for 4 weeks. This dose/administration route is based on our work with Dp44mT (Kovacevic et al., 2011; Lovejoy et al., 2011). If the MTD is not met, this dose will be adjusted up/down by 10% (generally <5 dose iterations are needed to reach MTD) (Yuan et al., 2004). In these studies, each group consists of 5 mice. Initial studies will use Docetaxel at its MTD (i.v. 20 mg/kg/every 4 days (Dykes et al., 1995)) over 4 weeks. Tumour growth will be assessed by bioluminescent imaging using the Perkin Elmer IVIS Spectrum/CT system, as the 22RV1-luc cells express luciferase. When the tumours have reached 1 cm^3, blood will be collected for comprehensive haematology, biochemistry and blood smears for morphologic and differential analysis (i.e., safety and tolerability assessment) (Kovacevic et al., 2011; Lovejoy et al., 2011; Yuan et al., 2004). Mice will be sacrificed and the major organs & tumour weighed & assessed by histopathology (Kovacevic et al., 2011; Lovejoy et al., 2012; Whitnall et al., 2006; Yuan et al., 2004). Zn(II), Fe(III) and Cu(II) will be assessed by inductive coupled plasma mass spectrometry (ICP-MS) (Lovejoy et al., 2011) These studies will determine which of the Zn(II), Fe(III) or Cu(II) complexes possess the greatest anti-cancer activity, which can guide the future development of novel transition metal-thiosemicarbazone complexes.

6.4.2.3 Examination of Zn(II) Complexes in Terms of Transport via the Pgp Pump

To assess if our Zn(II)-thiosemicarbazone complexes of Dp44mT and DpC are transported by Pgp, we will initially use the cell-free, Pgp-Glo ATPase Assay system (Promega) (Jansson et al., 2015b) and compare our agents to known Pgp substrates

(*e.g.*, doxorubicin, *etc.*). These studies will identify the best structural features necessary for effective trafficking by Pgp.

6.4.2.4 Zn(II)-Thiosemicarbazone Complexes Selectivity Against Pgp-Expressing Cells

Considering that Pgp plays a crucial role in potentiating Dp44mT and [Cu(Dp44mT)] cytotoxicity (Jansson et al., 2015b), we will elucidate if Pgp is involved in the cytotoxic mechanisms of our Zn(II)-thiosemicarbazones, [Zn(Dp44mT)$_2$] and [Zn(DpC)$_2$]. Initial studies will assess if the selective Pgp inhibitors, available in our lab (Jansson et al., 2015b; Yamagishi et al., 2013), namely: Valspodar (Val; 5 ε M) (Jachez et al., 1993) (Novartis) and Ela (0.1 ε M) (Hyafil et al., 1993) (Sigma), or silencing of Pgp with siRNA (2 siRNAs to be tested vs. control-siRNA) (Jansson et al., 2015b; Yamagishi et al., 2013) will decrease cytotoxicity. We hypothesise these Pgp inhibitors will reduce the uptake of Zn(II)-thiosemicarbazones into lysosomes via lysosomal Pgp, and thus, will prevent LMP and cell death. To assess this, MTT assays validated by viable cell counts (Kalinowski et al., 2007; Yu et al., 2009b) will be performed using our range of cells with high and low Pgp levels. Cellular Pgp levels will be monitored by Western blot (Dixon et al., 2013; Jansson et al., 2015b; Lovejoy et al., 2011; Yamagishi et al., 2013). These studies will determine whether Zn(II)-thiosemicarbazones overcome Pgp-mediated resistance.

6.4.2.5 Examination of the Importance of the Pgp Drug Pump in Sub-Cellular Distribution of Zn(II)-Thiosemicarbazone Complexes

Cu-Dp44mT accumulates in and damages lysosomes (Jansson et al., 2015b; Lovejoy et al., 2011). Furthermore, Pgp is found in lysosomal membranes (Jansson et al., 2015b; Yamagishi et al., 2013), leading to accumulation of Pgp substrates in this organelle (Yamagishi et al., 2013). We found that [Zn(DpC)2] was localised to the lysosomes of both KBV1 (+Pgp) and KB31 (-Pgp) cells, and that [Zn(Dp44mT)2] and [Zn(DpC)2] cause lysosomal membrane destabilisation. However, cytotoxicity data (Fig. 4.7) suggested that the cytotoxicity of $[Zn(Dp44mT)_2]$ and $[Zn(DpC)_2]$ may be potentiated by Pgp. Therefore, we will assess if Pgp modulates targeting of Zn(II)-thiosemicarbazones to destabilise lysosomes in Pgp- *versus* non-Pgp-expressing cells. Lysosomal integrity will be studied using alternative methods to AO, such as LysoTracker Deep Red and Lamp-2, using confocal microscopy and quantification by flow cytometry (Jansson et al., 2015b; Lovejoy et al., 2011; Yamagishi et al., 2013). If Pgp correlates with drug-induced damage to these organelles, then the Pgp inhibitors or Pgp siRNA (2 siRNAs to be tested vs. control-siRNA) (Yamagishi et al., 2013) will be used to rescue organelle destabilisation. These studies will examine if Pgp affects organelle targeting/trafficking of Zn(II)-thiosemicarbazones to comprehensively understand their subcellular mechanism of action

6.4.3 Future Directions for Chapter 5

In Chapter 5, we demonstrated that DpC, but not Dp44mT, overcomes Bcl-2 mediated MDR in melanoma cells. DpC appears to do so *via* a novel mechanism, which unlike the

mechanism for overcoming Pgp-mediated MDR, does not involve Cu(II) binding or ROS generation. Furthermore, neither Dp44mT nor DpC induced LMP in melanoma cells. In contrast, DpC induced a Bcl-2 independent increase in acidic vesicles, while Dp44mT only induced an increase in acidic vesicles in non-Bcl-2 expressing melanoma cells.

Several hypotheses were put forward in Chapter 5 and must be examined in greater depth. Firstly, we suggested that Cu(II) chelation using TM had no effect on the cytotoxicity of Dp44mT or DpC due to high levels of metallothionein, which is commonly found in melanoma. Secondly, we suggested that the accumulation of acidic vesicles, which both Dp44mT and DpC induced in the M14 PC cell line but only DpC induced in the M14 Bcl-2 cell line, were autolysosomes. We also suggested that the ability of DpC, but not Dp44mT, to induce the accumulation of acidic vesicles was due to the ability of DpC to decrease the expression of Bcl-2. Finally, while there is reason to believe that the accumulation of acidic vesicles was implicated in the cytotoxicity of Dp44mT and DpC in the M14 melanoma cell lines, this was not confirmed.

6.4.3.1 Comparative Measurements of Intracellular Cu(II) in Neoplastic Cell Lines

In M14 melanoma cells, the copper ion chelator, TM, did not significantly ($p > 0.05$) affect the cytotoxicity of Dp44mT or DpC (Fig. 5.4). In contrast, in KBV1, KB31 and SW480 cell lines (Figs. 3.13, 4.19, 4.20), intracellular Cu(II) chelation by TM decreases both cytotoxicity and prevents induction of LMP. We hypothesised that the M14 melanoma cell line has lower levels of intracellular copper than other cell lines in which

Dp44mT and DpC have been tested. The basal intracellular Cu(II) levels of the M14 melanoma cell lines can be determined by inductively coupled plasma mass spectrometry (Kim et al., 2012). The Cu(II) levels in M14 cells will then be compared to other cell lines in which Dp44mT and DpC have been shown to bind intracellular Cu(II), such as KBV1, KB31, SW480 (Figs. 3.13, 4.19, 4.20). The expression of copper ion binding proteins, metallothioneins, in the M14 cell lines will be compared to KBV1, KB31 and SW480 by Western blot. Furthermore, expression of Cu(II) uptake transporter, CRT1, and the copper ion efflux transporters, ATP7A and ATP7B (Denoyer et al., 2015; Kim et al., 2012), will also be examined by Western blot in M14, KBV1, KB31 and SW480 cell lines. Addiionally, the functionality of the copper transporters will be using our standard radiolabelling and efflux protocols (Lovejoy et al., 2011; Richardson and Milnes, 1997; Yuan et al., 2004). These studies will track the retention/efflux of ^{67}Cu metal in the cell lines listed above. The results of these studies will determine whether low intracellular Cu(II) accounts for the inability of TM to decrease the cytotoxicity of Dp44mT or DpC in M14 melanoma cells.

6.4.3.2 Identification of Acidic Vesicles

We suggested that the identity of the acidic, AO-stained vesicles induced by DpC in M14 Bcl-2 cells, and by DpC and Dp44mT in M14 PC cells, might be autolysosomes (Fig. 5.7). To determine whether these acidic vesicles are autolysosomes, co-localisation of the autophagosome marker, LC3-II, with the lysosomal markers, LAMP2 and Cathepsin D, will be assessed by confocal microscopy (Jansson et al., 2015b). We will also track the formation autolysosomes induced by Dp44mT or DpC using flow

cytometry, by transfecting M14 melanoma cells with the mCherry-GFP-LC3 construct, which measures autolysosome formation from autophagosomes (Hundeshagen et al., 2011; Pankiv et al., 2007). Vesicles which are acidic and express LC3 (*i.e.* autolysosomes) will exhibit red fluorescence only, while those which are neutral (*i.e.* autophagosomes) will appear green (Pankiv et al., 2007). If the acidic vesicles are neither autolysosomes or lysosomes, endolysosomes will also be examined by confocal microscopy through co-localisation of Rab7 with LAMP2 and Cathepsin D (Jager et al., 2004); and by flow cytometry using M14 cells transfected with the GFP-Rab7 construct (Pankiv et al., 2007). These studies will determine the identity of the acidic, vesicular, organelle induced in M14 melanoma cells by DpC (M14 Bcl-2 and M14 PC) and Dp44mT (M14 PC only).

6.4.3.4 Role of Bcl-2 in DpC-Mediated Increase in Acidic Vesicles

DpC induced the formation of acidic vesicles in both M14 Bcl-2 cells and M14 PC cells (Fig. 5.7). However, Dp44mT only induced the formation of acidic vesicles in M14 PC cells (Fig. 5.7). We proposed that Dp44mT did not increase the formation of acidic vesicles, as, unlike DpC, it did not decrease the expression of Bcl-2 (Fig. 5.2). Bcl-2 is an inhibitor of the autophagy initiator, Beclin 1 (Chang et al., 2010; Pattingre et al., 2005), which is required for the formation of autolysosomes, which we believe the acidic vesicles to be. Indeed, silencing of Beclin 1 has been shown to prevent autophagy initiation by Dp44mT (Gutierrez et al., 2014). The role of Bcl-2 in the formation of acidic vesicles in M14 Bcl-2 cells will be confirmed using Bcl-2 siRNA, and examining the formation of acidic vesicles. Beclin 1 siRNA will also be used to determine whether

inhibition of Beclin 1 by Bcl-2 (Chang et al., 2010; Pattingre et al., 2005), prevents the formation of acidic vesicles, *i.e.* autolysosomes. These studies will determine the role of Bcl-2 and Beclin 1 in the formation of acidic vesicles mediated by Dp44mT and DpC in M14 melanoma cells.

6.4.3.5 Importance of Induction of Acidic Vesicle Formation to Cytotoxicity of Dp44mT and DpC in M14 Melanoma Cells

DpC was equally cytotoxic in the M14 Bcl-2 and M14 PC cell lines, and induced similar increases in the number of acidic vesicles. Dp44mT, on the other hand, was less cytotoxic in the M14 Bcl-2 cell line than in the M14 PC cell line. To determine whether there is a relationship between the acidic vesicles induced by Dp44mT (in M14 PC cells) and DpC (in M14 Bcl-2 and M14 PC cells) (Fig. 5.7) and induction of cytotoxicity, the formation of acidic vesicles will be prevented. Depending on the identity of the acidic vesicles, there are several methods that could be employed prevent their accumulation, in order to ascertain their effect on cytotoxicity. For example, if the acidic vesicles were autolysosomes, autophagy could be inhibited using bafilomycin A1, and the effect on the prevention of the formation of autolysosomes on cytotoxicity examined in MTT assays (Gutierrez et al., 2014). Similarly, if the acidic vesicles were lysosomes, lysosomes could be inhibited using chloroquine or ammonium chloride, and the effect on the cytotoxicity of Dp44mT or DpC assessed in MTT assays (Seguin et al., 2014).

6.4.3.6 Effect of Bcl-2 Over-Expression in Other Neoplastic Cell Types

Studies will investigate the effect of DpC in other Bcl-2-expressing cell lines that express endogenously high levels of Bcl-2, such as the leukaemia cell line RS11846, the renal cancer cell line ACHN, or the CNS cancer cell line LN-229 (Placzek et al., 2010), compared to the M14 Bcl-2 melanoma cell line, which was transfected to over-express Bcl-2. The ability of DpC to overcome Bcl-2 mediated MDR will be assessed in MTT assays, and effect of Dp44mT and DpC on lysosomal stability will be assessed using AO. The endogenously Bcl-2 over-expressing 501-MEL cell line (Placzek et al., 2010), will also be included, as will other melanoma cell lines such as SK-MEL-28 and WM-35, to evaluate whether the novel mechanism of Dp44mT and DpC observed in M14 cells was melanoma-specific. These studies will assess whether the important ability of DpC to overcome Bcl-2 mediated MDR is ubiquitous in cancer cell lines, or limited to melanoma cell lines.

6.5 Concluding Remarks

As discussed previously in this thesis, MDR is a major contributing factor to treatment failure (Gottesman et al., 2002). Past strategies to target MDR have not led to successful therapies in the clinic (Gottesman et al., 2002). Therefore, there is a demand for further research in order to develop novel therapies that overcome MDR. This thesis has expanded current knowledge through investigations of the structure-activity

relationships of thiosemicarbazones in MDR models. This research is crucial to the development of new therapeutic strategies.

Herein, we showed that thiosemicarbazones overcome Pgp-mediated MDR *via* a mechanism that involves transport into lysosomes by Pgp, lysosomal sequestration, Cu(II) binding, ROS generation, LMP, and apoptosis. We demonstrated the importance of substitutions at the imine carbon of the thiosemicarbazone backbone. Specifically, in order to overcome Pgp-mediated MDR, inductively electron-withdrawing 2-pyridyl or phenyl moieties at the imine position are required to generate adequate ROS to induce LMP. Importantly, we showed that in addition to Dp44mT, Bp44mT and our lead agent, DpC, also overcome Pgp-mediated MDR *via* this mechanism, expanding our arsenal of potential drug candidates. Based on these studies, further ñfine tuningò of thiosemicarbazone structural features could lead to more active agents to overcome multi-drug resistance *via* the exploitation of lysosomal Pgp to induce LMP and the death of resistant tumour cells.

This thesis also demonstrated the potential of Zn(II)-thiosemicarbazone complexes as anti-cancer agents. These agents have improved lipophilicity compared to the thiosemicarbazones alone, or their Cu(II) complexes (Richardson et al., 2006), which facilitates their passage across the cellular and lysosomal membranes, leading to enhanced uptake, cytotoxicity and ability to induce LMP. Furthermore, we utilised the fluorescence of the Zn(II) complexes to definitively show that the Zn(II) complex of our

lead agent, DpC, is localised to lysosomes. Interestingly, we also demonstrated that the Zn(II) complexes of our thiosemicarbazones transmetallate with Cu(II) to induce LMP and apoptosis, highlighting the importance of Cu(II) in the mechanism of action of these thiosemicarbazones. These studies could pave the way for the development of Zn(II)-thiosemicarbazone complexes with improved anti-cancer efficacy, that take exploit lysosomal drug sequestration and the higher intracellular copper levels found in neoplastic cells (Goodman et al., 2004; Gupte and Mumper, 2009).

Finally, we also investigated the ability of Dp44mT and DpC to overcome an additional, important cellular resistance mechanism: Bcl-2 mediated MDR. Interestingly, we demonstrated that DpC, but not Dp44mT, could overcome Bcl-2 mediated MDR. Further mechanistic studies are required; however, DpC appears to overcome Bcl-2 mediated MDR by decreasing the expression of Bcl-2. This attribute of DpC is clinically important, as Bcl-2 mediated MDR is, like Pgp-mediated MDR, a significant obstacle to the successful treatment of cancer (Kroemer, 1997; Lessene et al., 2008).

The results presented herein clearly demonstrated the polypharmacological activity of thiosemicarbazones (Jansson et al., 2015a). Importantly, we showed that our lead candidate, DpC, is capable of not only coming Pgp-mediated MDR, but Bcl-2 mediated MDR as well. The ability to target two major mechanisms of MDR is clinically significant, and these studies form the basis for future studies that investigate the development of

novel, anti-cancer agents with improved efficacy against MDR, for which treatments are currently desperately lacking.

Appendix

Supporting Information Available

Crystal structure of [Cu(Bp44mT-H)Cl]. This material is available free of charge *via* the Internet at http://pubs.acs.org.

Author Contributions

Chapter 3: Alexandra E. Stacy, Duraippandi Palanimuthu, Paul V. Bernhardt, Danuta S. Kalinowski, Patric J. Jansson and Des R. Richardson

A.E.S. designed studies, performed studies, analysed data, prepared figures, and wrote the manuscript; D.P. and P.V.B. performed some studies and wrote the manuscript; P.J.J. and D.R.R. designed studies and wrote the manuscript; D.S.K. and D.R.R. wrote the manuscript. D.R.R. provided funding. P.J.J. and D.R.R. contributed equally as senior authors.

Chapter 4: Alexandra E. Stacy, Duraippandi Palanimuthu, Paul V. Bernhardt, Danuta S. Kalinowski, Patric J. Jansson and Des R. Richardson

A.E.S. designed studies, performed studies, analysed data, prepared figures, and wrote the manuscript; D.P. and P.V.B. performed some studies and wrote the manuscript; P.J.J. and D.R.R. designed studies and wrote the manuscript; D.S.K. and D.R.R. wrote the manuscript. D.R.R. provided funding.

Chapter 5: Alexandra E. Stacy, Patric J. Jansson and Des R. Richardson

A.E.S designed studies, performed studies, analysed data, prepared figures and wrote the manuscript. P.J.J. and D.R.R. designed studies and contributed to manuscript preparation, D.R.R. provided funding.

References

Abok K, Rundquist I, Forsberg B and Brunk U (1984) Dimethylsulfoxide increases the survival and lysosomal stability of mouse peritoneal macrophages exposed to low-LET ionizing radiation and/or ionic iron in culture. *Virchows Archiv B, Cell pathology including molecular pathology* **46**(4): 307-320.

Abolhoda A, Wilson AE, Ross H, Danenberg PV, Burt M and Scotto KW (1999) Rapid activation of MDR1 gene expression in human metastatic sarcoma after in vivo exposure to doxorubicin. *Clin Cancer Res* **5**(11): 3352-3356.

Adar Y, Stark M, Bram EE, Nowak-Sliwinska P, van den Bergh H, Szewczyk G, Sarna T, Skladanowski A, Griffioen AW and Assaraf YG (2012) Imidazoacridinone-dependent lysosomal photodestruction: a pharmacological Trojan horse approach to eradicate multidrug-resistant cancers. *Cell Death Dis* **3**: e293.

Addison AW, Rao TN, Reedijk J, van Rijn J and Verschoor GC (1984) Synthesis, structure, and spectroscopic properties of copper(II) compounds containing nitrogen-sulphur donor ligands; the crystal and molecular structure of aqua[1,7-bis(N-methylbenzimidazol-2[prime or minute]-yl)-2,6-dithiaheptane]copper(II) perchlorate. *Dalton Trans*(7): 1349-1356.

Advani R, Saba HI, Tallman MS, Rowe JM, Wiernik PH, Ramek J, Dugan K, Lum B, Villena J, Davis E, Paietta E, Litchman M, Sikic BI and Greenberg PL (1999) Treatment of refractory and relapsed acute myelogenous leukemia with combination chemotherapy plus the multidrug resistance modulator PSC 833 (Valspodar). *Blood* **93**(3): 787-795.

Al-Bari MA (2015) Chloroquine analogues in drug discovery: new directions of uses, mechanisms of actions and toxic manifestations from malaria to multifarious diseases. *The Journal of antimicrobial chemotherapy* **70**(6): 1608-1621.

Al-Eisawi Z, Stefani C, Jansson PJ, Arvind A, Sharpe PC, Basha MT, Iskander GM, Kumar N, Sahni S, Bernhardt PV, Richardson DR and Kalinowski DS (2016) Novel mechanism of cytotoxicity for the selective selenosemicarbazone, 2-acetylpyridine 4,4-dimethyl-3-selenosemicarbazone (Ap44mSe): lysosomal membrane permeabilization. *J Med Chem* **59**(1): 294-312.

Allen JD, van Loevezijn A, Lakhai JM, van der Valk M, van Tellingen O, Reid G, Schellens JH, Koomen G-J and Schinkel AH (2002) Potent and Specific Inhibition of the Breast Cancer Resistance Protein Multidrug Transporter in Vitro and in Mouse Intestine by a Novel Analogue of Fumitremorgin C 1 This work was supported in part by grant NKI 97-1433 from the Dutch Cancer Society (to AHS). Synthesis investigations by A. v. L. and GJ. K. were supported by the Netherlands Research Council for Chemical Sciences (NWO/CW) and the Netherlands Technology Foundation (STW). 1. *Molecular Cancer Therapeutics* **1**(6): 417-425.

Aller SG, Yu J, Ward A, Weng Y, Chittaboina S, Zhuo R, Harrell PM, Trinh YT, Zhang Q, Urbatsch IL and Chang G (2009) Structure of P-glycoprotein reveals a molecular basis for poly-specific drug binding. *Science* **323**(5922): 1718-1722.

Altan N, Chen Y, Schindler M and Simon SM (1998) Defective acidification in human breast tumor cells and implications for chemotherapy. *J Exp Med* **187**(10): 1583-1598.

Alvarez M, Paull K, Monks A, Hose C, Lee JS, Weinstein J, Grever M, Bates S and Fojo T (1995) Generation of a drug resistance profile by quantitation of mdr-1/P-glycoprotein in the cell lines of the National Cancer Institute Anticancer Drug Screen. *J Clin Invest* **95**(5): 2205-2214.

Amador-Hernandez J, Fernandez-Romero JM and Luque de Castro MD (2001) Continuous determination of chloroquine in plasma by laser-induced photochemical reaction and fluorescence. *Fresenius' journal of analytical chemistry* **369**(5): 438-441.

Amundson SA, Myers TG, Scudiero D, Kitada S, Reed JC and Fornace AJ, Jr. (2000) An informatics approach identifying markers of chemosensitivity in human cancer cell lines. *Cancer Res* **60**(21): 6101-6110.

Antholine WE, Knight JM and Petering DH (1976) Inhibition of tumor cell transplantability by iron and copper complexes of 5-substituted 2-formylpyridine thiosemicarbazones. *J Med Chem* **19**(2): 339-341.

Appelmans F, Wattiaux R and De Duve C (1955) Tissue fractionation studies. 5. The association of acid phosphatase with a special class of cytoplasmic granules in rat liver. *Biochem J* **59**(3): 438-445.

Appelqvist H, Waster P, Kagedal K and Ollinger K (2013) The lysosome: from waste bag to potential therapeutic target. *J Mol Cell Biol* **5**(4): 214-226.

Atassi G, Dumont P and Harteel JC (1979) Potentiation of the antitumour activity of 2-formylpyridine thiosemicarbazone by metal chelation : 2-formylpyridine thiosemicarbazone zinc sulphate (NSC 294721). *Eur J Cancer* **15**(4): 451-459.

Bae DH, Jansson PJ, Huang ML, Kovacevic Z, Kalinowski D, Lee CS, Sahni S and Richardson DR (2013) The role of NDRG1 in the pathology and potential treatment of human cancers. *J Clin Pathol* **66**(11): 911-917.

Baer MR, George SL, Dodge RK, O'Loughlin KL, Minderman H, Caligiuri MA, Anastasi J, Powell BL, Kolitz JE, Schiffer CA, Bloomfield CD and Larson RA (2002) Phase 3 study of the multidrug resistance modulator PSC-833 in previously untreated patients 60 years of age and older with acute myeloid leukemia: Cancer and Leukemia Group B Study 9720. *Blood* **100**(4): 1224-1232.

Baker E, Richardson D, Gross S and Ponka P (1992) Evaluation of the iron chelation potential of hydrazones of pyridoxal, salicylaldehyde and 2-hydroxy-1-naphthylaldehyde using the hepatocyte in culture. *Hepatology* **15**(3): 492-501.

Bakhshi A, Jensen JP, Goldman P, Wright JJ, McBride OW, Epstein AL and Korsmeyer SJ (1985) Cloning the chromosomal breakpoint of t(14;18) human lymphomas: clustering around JH on chromosome 14 and near a transcriptional unit on 18. *Cell* **41**(3): 899-906.

Becattini B, Kitada S, Leone M, Monosov E, Chandler S, Zhai D, Kipps TJ, Reed JC and Pellecchia M (2004) Rational design and real time, in-cell detection of the proapoptotic activity of a novel compound targeting Bcl-X(L). *Chem Biol* **11**(3): 389-395.

Becker EM, Lovejoy DB, Greer JM, Watts R and Richardson DR (2003) Identification of the di-pyridyl ketone isonicotinoyl hydrazone (PKIH) analogues as potent iron chelators and anti-tumour agents. *Br J Pharmacol* **138**(5): 819-830.

Bedikian AY, Millward M, Pehamberger H, Conry R, Gore M, Trefzer U, Pavlick AC, DeConti R, Hersh EM, Hersey P, Kirkwood JM and Haluska FG (2006) Bcl-2 antisense

(oblimersen sodium) plus dacarbazine in patients with advanced melanoma: the Oblimersen Melanoma Study Group. *J Clin Oncol* **24**(29): 4738-4745.

Bedikian AY, Garbe C, Conry R, Lebbe C and Grob JJ (2014) Dacarbazine with or without oblimersen (a Bcl-2 antisense oligonucleotide) in chemotherapy-naive patients with advanced melanoma and low-normal serum lactate dehydrogenase: 'The AGENDA trial'. *Melanoma Res* **24**(3): 237-243.

Bell DR, Gerlach JH, Kartner N, Buick RN and Ling V (1985) Detection of P-glycoprotein in ovarian cancer: a molecular marker associated with multidrug resistance. *J Clin Oncol* **3**(3): 311-315.

Bengsch F, Buck A, Gunther SC, Seiz JR, Tacke M, Pfeifer D, von Elverfeldt D, Sevenich L, Hillebrand LE, Kern U, Sameni M, Peters C, Sloane BF and Reinheckel T (2014) Cell type-dependent pathogenic functions of overexpressed human cathepsin B in murine breast cancer progression. *Oncogene* **33**(36): 4474-4484.

Benson AB, 3rd, Trump DL, Koeller JM, Egorin MI, Olman EA, Witte RS, Davis TE and Tormey DC (1985) Phase I study of vinblastine and verapamil given by concurrent iv infusion. *Cancer Treat Rep* **69**(7-8): 795-799.

Berg JM and Shi Y (1996) The galvanization of biology: a growing appreciation for the roles of zinc. *Science* **271**(5252): 1081-1085.

Bermejo MR, González-Noya AM, Martínez-Calvo M, Pedrido R, Maneiro M, Fernández MI and Gómez-Fórneas E (2007) New neutral metal complexes from the 4-N-Phenylthiosemicarbazone-2-pyridinecarboxaldehyde ligand ï 113Cd and 207Pb NMR Studies. *Z Anorg Allg Chem* **633**(11-12): 1911-1918.

Bernhardt PV, Caldwell LM, Chaston TB, Chin P and Richardson DR (2003) Cytotoxic iron chelators: characterization of the structure, solution chemistry and redox activity of ligands and iron complexes of the di-2-pyridyl ketone isonicotinoyl hydrazone (HPKIH) analogues. *J Biol Inorg Chem* **8**(8): 866-880.

Bernhardt PV, Sharpe PC, Islam M, Lovejoy DB, Kalinowski DS and Richardson DR (2009) Iron chelators of the dipyridylketone thiosemicarbazone class: precomplexation and transmetalation effects on anticancer activity. *J Med Chem* **52**(2): 407-415.

Bincoletto C, Saad ST, da Silva ES and Queiroz ML (1999) Haematopoietic response and bcl-2 expression in patients with acute myeloid leukaemia. *Eur J Haematol* **62**(1): 38-42.

Blackman RK, Cheung-Ong K, Gebbia M, Proia DA, He S, Kepros J, Jonneaux A, Marchetti P, Kluza J, Rao PE, Wada Y, Giaever G and Nislow C (2012) Mitochondrial electron transport is the cellular target of the oncology drug elesclomol. *PLoS One* **7**(1): e29798.

Blanz EJ, Jr., French FA, DoAmaral JR and French DA (1970) Carcinostatic activity of thiosemicarbazones of formyl heteroaromatic compounds. VII. 2-Formylpyridine derivatives bearing additional ring substituents. *J Med Chem* **13**(6): 1124-1130.

Bohley P and Seglen PO (1992) Proteases and proteolysis in the lysosome. *Experientia* **48**(2): 151-157.

Boise LH, Gonzalez-Garcia M, Postema CE, Ding L, Lindsten T, Turka LA, Mao X, Nunez G and Thompson CB (1993) bcl-x, a bcl-2-related gene that functions as a dominant regulator of apoptotic cell death. *Cell* **74**(4): 597-608.

Bond CS, Clements PR, Ashby SJ, Collyer CA, Harrop SJ, Hopwood JJ and Guss JM (1997) Structure of a human lysosomal sulfatase. *Structure* **5**(2): 277-289.

Bourhis J, Benard J, Hartmann O, Boccon-Gibod L, Lemerle J and Riou G (1989a) Correlation of MDR1 gene expression with chemotherapy in neuroblastoma. *J Natl Cancer Inst* **81**(18): 1401-1405.

Bourhis J, Goldstein LJ, Riou G, Pastan I, Gottesman MM and Benard J (1989b) Expression of a human multidrug resistance gene in ovarian carcinomas. *Cancer Res* **49**(18): 5062-5065.

Boyd JM, Gallo GJ, Elangovan B, Houghton AB, Malstrom S, Avery BJ, Ebb RG, Subramanian T, Chittenden T, Lutz RJ and et al. (1995) Bik, a novel death-inducing protein shares a distinct sequence motif with Bcl-2 family proteins and interacts with viral and cellular survival-promoting proteins. *Oncogene* **11**(9): 1921-1928.

Brockman RW, Thomson JR, Bell MJ and Skipper HE (1956) Observations on the antileukemic activity of pyridine-2-carboxaldehyde thiosemicarbazone and thiocarbohydrazone. *Cancer Res* **16**(2): 167-170.

Broto P, Moreau G and Vandycke C (1984) Molecular structures: perception, autocorrelation descriptor and sar studies: system of atomic contributions for the calculation of the n-octanol/water partition coefficients. *Eur J Med Chem* **19**(1): 71-78.

Brown WJ, Goodhouse J and Farquhar MG (1986) Mannose-6-phosphate receptors for lysosomal enzymes cycle between the Golgi complex and endosomes. *J Cell Biol* **103**(4): 1235-1247.

Brownlee KA and Hamre D (1951) Studies on chemotherapy of vaccinia virus. I. An experimental design for testing antiviral agents. *J Bacteriol* **61**(2): 127-134.

Burrell RA and Swanton C (2014) Tumour heterogeneity and the evolution of polyclonal drug resistance. *Molecular oncology* **8**(6): 1095-1111.

Callaghan R, Ford RC and Kerr ID (2006) The translocation mechanism of P-glycoprotein. *FEBS letters* **580**(4): 1056-1063.

Carstea ED, Morris JA, Coleman KG, Loftus SK, Zhang D, Cummings C, Gu J, Rosenfeld MA, Pavan WJ, Krizman DB, Nagle J, Polymeropoulos MH, Sturley SL, Ioannou YA, Higgins ME, Comly M, Cooney A, Brown A, Kaneski CR, Blanchette-Mackie EJ, Dwyer NK, Neufeld EB, Chang TY, Liscum L, Strauss JF, 3rd, Ohno K, Zeigler M, Carmi R, Sokol J, Markie D, O'Neill RR, van Diggelen OP, Elleder M, Patterson MC, Brady RO, Vanier MT, Pentchev PG and Tagle DA (1997) Niemann-Pick C1 disease gene: homology to mediators of cholesterol homeostasis. *Science* **277**(5323): 228-231.

Castiñeiras A, García I, Bermejo E, Ketcham KA, West DX and El-Sawaf AK (2002) Coordination of ZnII, CdII, and HgII by 2-Pyridineformamide-3-piperidyl-thiosemicarbazone. *Z Anorg Allg Chem* **628**(2): 492-504.

Certo M, Del Gaizo Moore V, Nishino M, Wei G, Korsmeyer S, Armstrong SA and Letai A (2006) Mitochondria primed by death signals determine cellular addiction to antiapoptotic BCL-2 family members. *Cancer Cell* **9**(5): 351-365.

Chambers AF (2009) MDA-MB-435 and M14 cell lines: identical but not M14 melanoma? *Cancer Res* **69**(13): 5292-5293.

Chan HS, Haddad G, Thorner PS, DeBoer G, Lin YP, Ondrusek N, Yeger H and Ling V (1991) P-glycoprotein expression as a predictor of the outcome of therapy for neuroblastoma. *N Engl J Med* **325**(23): 1608-1614.

Chan HS, Grogan TM, Haddad G, DeBoer G and Ling V (1997) P-glycoprotein expression: critical determinant in the response to osteosarcoma chemotherapy. *J Natl Cancer Inst* **89**(22): 1706-1715.

Chang NC, Nguyen M, Germain M and Shore GC (2010) Antagonism of Beclin 1-dependent autophagy by BCL-2 at the endoplasmic reticulum requires NAF-1. *EMBO J* **29**(3): 606-618.

Chapuy B, Koch R, Radunski U, Corsham S, Cheong N, Inagaki N, Ban N, Wenzel D, Reinhardt D, Zapf A, Schweyer S, Kosari F, Klapper W, Truemper L and Wulf GG (2008) Intracellular ABC transporter A3 confers multidrug resistance in leukemia cells by lysosomal drug sequestration. *Leukemia* **22**(8): 1576-1586.

Chen CJ, Chin JE, Ueda K, Clark DP, Pastan I, Gottesman MM and Roninson IB (1986) Internal duplication and homology with bacterial transport proteins in the mdr1 (P-glycoprotein) gene from multidrug-resistant human cells. *Cell* **47**(3): 381-389.

Chen L, Willis SN, Wei A, Smith BJ, Fletcher JI, Hinds MG, Colman PM, Day CL, Adams JM and Huang DC (2005) Differential targeting of prosurvival Bcl-2 proteins by their BH3-only ligands allows complementary apoptotic function. *Mol Cell* **17**(3): 393-403.

Chen Q, Fei J, Wu L, Jiang Z, Wu Y, Zheng Y and Lu G (2011) Detection of cathepsin B, cathepsin L, cystatin C, urokinase plasminogen activator and urokinase plasminogen activator receptor in the sera of lung cancer patients. *Oncol Lett* **2**(4): 693-699.

Chen Z, Zhang D, Yue F, Zheng M, Kovacevic Z and Richardson DR (2012) The iron chelators Dp44mT and DFO inhibit TGF-beta-induced epithelial-mesenchymal transition via up-regulation of N-Myc downstream-regulated gene 1 (NDRG1). *J Biol Chem* **287**(21): 17016-17028.

Cheng EH, Wei MC, Weiler S, Flavell RA, Mak TW, Lindsten T and Korsmeyer SJ (2001) BCL-2, BCL-X(L) sequester BH3 domain-only molecules preventing BAX- and BAK-mediated mitochondrial apoptosis. *Mol Cell* **8**(3): 705-711.

Cheng L, Zhang L-M and Wang J-Q (2010) Bis(pyridine-2-carbaldehyde thiosemicarbazone)zinc(II) dinitrate dihydrate. *Acta Crystallog Sect E* **66**(10): m1340.

Chipuk JE, Bouchier-Hayes L and Green DR (2006) Mitochondrial outer membrane permeabilization during apoptosis: the innocent bystander scenario. *Cell Death Differ* **13**(8): 1396-1402.

Chittenden T, Harrington EA, O'Connor R, Flemington C, Lutz RJ, Evan GI and Guild BC (1995) Induction of apoptosis by the Bcl-2 homologue Bak. *Nature* **374**(6524): 733-736.

Cleary ML, Smith SD and Sklar J (1986) Cloning and structural analysis of cDNAs for bcl-2 and a hybrid bcl-2/immunoglobulin transcript resulting from the t(14;18) translocation. *Cell* **47**(1): 19-28.

Coffey JW and De Duve C (1968) Digestive activity of lysosomes. I. The digestion of proteins by extracts of rat liver lysosomes. *J Biol Chem* **243**(12): 3255-3263.

Cole SP, Bhardwaj G, Gerlach JH, Mackie JE, Grant CE, Almquist KC, Stewart AJ, Kurz EU, Duncan AM and Deeley RG (1992) Overexpression of a transporter gene in a multidrug-resistant human lung cancer cell line. *Science* **258**(5088): 1650-1654.

Cole SP (2014) Multidrug resistance protein 1 (MRP1, ABCC1), a "multitasking" ATP-binding cassette (ABC) transporter. *J Biol Chem* **289**(45): 30880-30888.

Coley HM (2010) Overcoming multidrug resistance in cancer: clinical studies of p-glycoprotein inhibitors. *Methods Mol Biol* **596**: 341-358.

Colone M, Calcabrini A, Toccacieli L, Bozzuto G, Stringaro A, Gentile M, Cianfriglia M, Ciervo A, Caraglia M, Budillon A, Meo G, Arancia G and Molinari A (2008) The multidrug transporter P-glycoprotein: a mediator of melanoma invasion? *J Invest Dermatol* **128**(4): 957-971.

Comba P, Morgen M and Wadepohl H (2013) Tuning of the properties of transition-metal bispidine complexes by variation of the basicity of the aromatic donor groups. *Inorg Chem* **52**(11): 6481-6501.

Cordon-Cardo C, O'Brien JP, Boccia J, Casals D, Bertino JR and Melamed MR (1990) Expression of the multidrug resistance gene product (P-glycoprotein) in human normal and tumor tissues. *J Histochem Cytochem* **38**(9): 1277-1287.

Cory JG, Cory AH, Rappa G, Lorico A, Liu MC, Lin TS and Sartorelli AC (1994) Inhibitors of ribonucleotide reductase. Comparative effects of amino- and hydroxy-substituted pyridine-2-carboxaldehyde thiosemicarbazones. *Biochem Pharmacol* **48**(2): 335-344.

Cory S and Adams JM (2002) The Bcl2 family: regulators of the cellular life-or-death switch. *Nat Rev Cancer* **2**(9): 647-656.

Cowley AR, Davis J, Dilworth JR, Donnelly PS, Dobson R, Nightingale A, Peach JM, Shore B, Kerr D and Seymour L (2005) Fluorescence studies of the intra-cellular distribution of zinc bis(thiosemicarbazone) complexes in human cancer cells. *Chem Commun (Camb)*(7): 845-847.

Crim JA and Petering HG (1967) The antitumor activity of Cu(II)KTS, the copper (II) chelate of 3-ethoxy-2-oxobutyraldehyde bis(thiosemicarbazone). *Cancer Res* **27**(7): 1278-1285.

Cripe LD, Li X, Litzow M, Paietta E, Rowe JM, Luger S and Tallman M (2006) A Randomized, Placebo-Controlled, Double Blind Trial of the MDR Modulator, Zosuquidar, during Conventional Induction and Post-Remission Therapy for Pts> 60 Years of Age with Newly Diagnosed Acute Myeloid Leukemia (AML) or High-Risk Myelodysplastic Syndrome (HR-MDS): ECOG 3999, in *ASH Annual Meeting Abstracts* p 423.

Crowe A, Ilett KF, Karunajeewa HA, Batty KT and Davis TM (2006) Role of P glycoprotein in absorption of novel antimalarial drugs. *Antimicrob Agents Chemother* **50**(10): 3504-3506.

Czabotar PE, Lessene G, Strasser A and Adams JM (2014) Control of apoptosis by the BCL-2 protein family: implications for physiology and therapy. *Nat Rev Mol Cell Biol* **15**(1): 49-63.

Dai G, Wei X, Liu Z, Liu S, Marcucci G and Chan KK (2005) Characterization and quantification of Bcl-2 antisense G3139 and metabolites in plasma and urine by ion-pair reversed phase HPLC coupled with electrospray ion-trap mass spectrometry. *J Chromatogr B Analyt Technol Biomed Life Sci* **825**(2): 201-213.

Dai H, Ding H, Meng XW, Lee SH, Schneider PA and Kaufmann SH (2013) Contribution of Bcl-2 phosphorylation to Bak binding and drug resistance. *Cancer Res* **73**(23): 6998-7008.

Dale IL, Tuffley W, Callaghan R, Holmes JA, Martin K, Luscombe M, Mistry P, Ryder H, Stewart AJ, Charlton P, Twentyman PR and Bevan P (1998) Reversal of P-glycoprotein-mediated multidrug resistance by XR9051, a novel diketopiperazine derivative. *Br J Cancer* **78**(7): 885-892.

Dalton WS, Grogan TM, Meltzer PS, Scheper RJ, Durie BG, Taylor CW, Miller TP and Salmon SE (1989) Drug-resistance in multiple myeloma and non-Hodgkin's lymphoma: detection of P-glycoprotein and potential circumvention by addition of verapamil to chemotherapy. *J Clin Oncol* **7**(4): 415-424.

Damiani D, Michieli M, Ermacora A, Russo D, Fanin R, Zaja F, Baraldo M, Pea F, Furlanut M and Baccarani M (1998) Adjuvant treatment with cyclosporin A increases the toxicity of chemotherapy for remission induction in acute non-lymphocytic leukemia. *Leukemia* **12**(8): 1236-1240.

Danial NN (2007) BCL-2 family proteins: critical checkpoints of apoptotic cell death. *Clin Cancer Res* **13**(24): 7254-7263.

Darnell G and Richardson DR (1999) The potential of iron chelators of the pyridoxal isonicotinoyl hydrazone class as effective antiproliferative agents III: the effect of the ligands on molecular targets involved in proliferation. *Blood* **94**(2): 781-792.

Dash R, Azab B, Quinn BA, Shen X, Wang XY, Das SK, Rahmani M, Wei J, Hedvat M, Dent P, Dmitriev IP, Curiel DT, Grant S, Wu B, Stebbins JL, Pellecchia M, Reed JC, Sarkar D and Fisher PB (2011) Apogossypol derivative BI-97C1 (Sabutoclax) targeting Mcl-1 sensitizes prostate cancer cells to mda-7/IL-24-mediated toxicity. *Proc Natl Acad Sci USA* **108**(21): 8785-8790.

Dayal D, Palanimuthu D, Shinde SV, Somasundaram K and Samuelson AG (2011) A novel zinc bis(thiosemicarbazone) complex for live cell imaging. *J Biol Inorg Chem* **16**(4): 621-632.

de Bruin M, Miyake K, Litman T, Robey R and Bates SE (1999) Reversal of resistance by GF120918 in cell lines expressing the ABC half-transporter, MXR. *Cancer Lett* **146**(2): 117-126.

De Duve C, Pressman BC, Gianetto R, Wattiaux R and Appelmans F (1955) Tissue fractionation studies. 6. Intracellular distribution patterns of enzymes in rat-liver tissue. *Biochem J* **60**(4): 604-617.

De Duve C (1965) The separation and characterization of subcellular particles. *Harvey Lect* **59**: 49-87.

de Duve C, de Barsy T, Poole B, Trouet A, Tulkens P and Van Hoof F (1974) Commentary. Lysosomotropic agents. *Biochemical pharmacology* **23**(18): 2495-2531.

Del Bufalo D, Biroccio A, Leonetti C and Zupi G (1997) Bcl-2 overexpression enhances the metastatic potential of a human breast cancer line. *FASEB J* **11**(12): 947-953.

Denoyer D, Masaldan S, La Fontaine S and Cater MA (2015) Targeting copper in cancer therapy: 'Copper That Cancer'. *Metallomics : integrated biometal science* **7**(11): 1459-1476.

Didziapetris R, Japertas P, Avdeef A and Petrauskas A (2003) Classification analysis of P-glycoprotein substrate specificity. *J Drug Target* **11**(7): 391-406.

Dixon KM, Lui GY, Kovacevic Z, Zhang D, Yao M, Chen Z, Dong Q, Assinder SJ and Richardson DR (2013) Dp44mT targets the AKT, TGF-beta and ERK pathways via the metastasis suppressor NDRG1 in normal prostate epithelial cells and prostate cancer cells. *Br J Cancer* **108**(2): 409-419.

Dobritzsch D, Andersen B and Piskur J (2005) Crystallization and X-ray diffraction analysis of dihydropyrimidinase from Saccharomyces kluyveri. *Acta Crystallogr Sect F Struct Biol Cryst Commun* **61**(Pt 4): 359-362.

Dole M, Nunez G, Merchant AK, Maybaum J, Rode CK, Bloch CA and Castle VP (1994) Bcl-2 inhibits chemotherapy-induced apoptosis in neuroblastoma. *Cancer Res* **54**(12): 3253-3259.

Domagk G, Behnisch R, Mietzsch F and Schmidt H (1946) Uber eine neue, gegen Tuberkelbaeillin in vitro wirksame Verbindungsldasse. *Naturwissenschaften* **33**: 315.

Donovick R, Pansy F, Stryker G and Bernstein J (1950) The chemotherapy of experimental tuberculosis. I. The in vitro activity of thiosemicarbazides, thiosemicarbazones, and related compounds. *J Bacteriol* **59**(5): 667-674.

Doyle LA, Yang W, Abruzzo LV, Krogmann T, Gao Y, Rishi AK and Ross DD (1998) A multidrug resistance transporter from human MCF-7 breast cancer cells. *Proc Natl Acad Sci USA* **95**(26): 15665-15670.

Dunn KW and Maxfield FR (1992) Delivery of ligands from sorting endosomes to late endosomes occurs by maturation of sorting endosomes. *J Cell Biol* **117**(2): 301-310.

Dunn SE, Hardman RA, Kari FW and Barrett JC (1997) Insulin-like growth factor 1 (IGF-1) alters drug sensitivity of HBL100 human breast cancer cells by inhibition of apoptosis induced by diverse anticancer drugs. *Cancer Res* **57**(13): 2687-2693.

Duvvuri M, Konkar S, Funk RS, Krise JM and Krise JP (2005) A chemical strategy to manipulate the intracellular localization of drugs in resistant cancer cells. *Biochemistry* **44**(48): 15743-15749.

Dykes DJ, Bissery MC, Harrison SD, Jr. and Waud WR (1995) Response of human tumor xenografts in athymic nude mice to docetaxel (RP 56976, Taxotere). *Invest New Drugs* **13**(1): 1-11.

Egorin MJ, Clawson RE, Cohen JL, Ross LA and Bachur NR (1980) Cytofluorescence localization of anthracycline antibiotics. *Cancer Res* **40**(12): 4669-4676.

Ekhart C, Rodenhuis S, Smits PH, Beijnen JH and Huitema AD (2009) An overview of the relations between polymorphisms in drug metabolising enzymes and drug transporters and survival after cancer drug treatment. *Cancer Treat Rev* **35**(1): 18-31.

Elgie AW, Sargent JM, Williamson CJ, Lewandowicz GM and Taylor CG (1999) Comparison of P-glycoprotein expression and function with in vitro sensitivity to anthracyclines in AML. *Adv Exp Med Biol* **457**: 29-33.

Ellerby LM, Ellerby HM, Park SM, Holleran AL, Murphy AN, Fiskum G, Kane DJ, Testa MP, Kayalar C and Bredesen DE (1996) Shift of the cellular oxidation-reduction potential in neural cells expressing Bcl-2. *J Neurochem* **67**(3): 1259-1267.

Erdal H, Berndtsson M, Castro J, Brunk U, Shoshan MC and Linder S (2005) Induction of lysosomal membrane permeabilization by compounds that activate p53-independent apoptosis. *Proc Natl Acad Sci USA* **102**(1): 192-197.

Eskelinen EL (2006) Roles of LAMP-1 and LAMP-2 in lysosome biogenesis and autophagy. *Mol Aspects Med* **27**(5-6): 495-502.

Fais S, De Milito A, You H and Qin W (2007) Targeting vacuolar H+-ATPases as a new strategy against cancer. *Cancer Res* **67**(22): 10627-10630.

Farrugia LJ (1997) ORTEP-3 for Windows-a version of ORTEP-III with a Graphical User Interface (GUI). *J Appl Crystallography* **30**(5): 565-565.

Farrugia LJ (1999) WinGX suite for small-molecule single-crystal crystallography. *J Appl Cryst* **32**(4): 837-838.

Ferreira RJ, Ferreira MJ and dos Santos DJ (2013) Molecular docking characterizes substrate-binding sites and efflux modulation mechanisms within P-glycoprotein. *J Chem Inf Model* **53**(7): 1747-1760.

Finch RA, Liu M, Grill SP, Rose WC, Loomis R, Vasquez KM, Cheng Y and Sartorelli AC (2000) Triapine (3-aminopyridine-2-carboxaldehyde- thiosemicarbazone): A potent inhibitor of ribonucleotide reductase activity with broad spectrum antitumor activity. *Biochem Pharmacol* **59**(8): 983-991.

Fletcher JI, Haber M, Henderson MJ and Norris MD (2010) ABC transporters in cancer: more than just drug efflux pumps. *Nat Rev Cancer* **10**(2): 147-156.

Fojo AT, Ueda K, Slamon DJ, Poplack DG, Gottesman MM and Pastan I (1987) Expression of a multidrug-resistance gene in human tumors and tissues. *Proc Natl Acad Sci USA* **84**(1): 265-269.

Ford JM and Hait WN (1990) Pharmacology of drugs that alter multidrug resistance in cancer. *Pharmacol Rev* **42**(3): 155-199.

Fox E and Bates SE (2007) Tariquidar (XR9576): a P-glycoprotein drug efflux pump inhibitor. *Expert Rev Anticancer Ther* **7**(4): 447-459.

Fracasso PM, Brady MF, Moore DH, Walker JL, Rose PG, Letvak L, Grogan TM and McGuire WP (2001) Phase II study of paclitaxel and valspodar (PSC 833) in refractory ovarian carcinoma: a gynecologic oncology group study. *J Clin Oncol* **19**(12): 2975-2982.

French FA and Blanz EJ, Jr. (1966) The carcinostatic activity of thiosemicarbazones of formyl heteroaromatic compounds. 3. Primary correlation. *J Med Chem* **9**(4): 585-589.

Furuta K, Ikeda M, Nakayama Y, Nakamura K, Tanaka M, Hamasaki N, Himeno M, Hamilton SR and August JT (2001) Expression of lysosome-associated membrane proteins in human colorectal neoplasms and inflammatory diseases. *Am J Pathol* **159**(2): 449-455.

Gaal A, Orgovan G, Polgari Z, Reti A, Mihucz VG, Bosze S, Szoboszlai N and Streli C (2014) Complex forming competition and in-vitro toxicity studies on the applicability of di-2-pyridylketone-4,4,-dimethyl-3-thiosemicarbazone (Dp44mT) as a metal chelator. *J Inorg Biochem* **130**: 52-58.

Gaetke LM and Chow CK (2003) Copper toxicity, oxidative stress, and antioxidant nutrients. *Toxicology* **189**(1-2): 147-163.

Gaggelli E, Kozlowski H, Valensin D and Valensin G (2006) Copper homeostasis and neurodegenerative disorders (Alzheimer's, prion, and Parkinson's diseases and amyotrophic lateral sclerosis). *Chem Rev* **106**(6): 1995-2044.

Ganapathi R, Hoeltge G, Casey G, Grabowski D, Neelon R and Ford J (1996) Acquisition of doxorubicin resistance in human leukemia HL-60 cells is reproducibly associated with 7q21 chromosomal anomalies. *Cancer Genet Cytogenet* **86**(2): 116-119.

Gao J and Richardson DR (2001) The potential of iron chelators of the pyridoxal isonicotinoyl hydrazone class as effective antiproliferative agents, IV: The mechanisms involved in inhibiting cell-cycle progression. *Blood* **98**(3): 842-850.

Gazzaniga P, Gradilone A, Vercillo R, Gandini O, Silvestri I, Napolitano M, Albonici L, Vincenzoni A, Gallucci M, Frati L and Agliano AM (1996) Bcl-2/bax mRNA expression ratio as prognostic factor in low-grade urinary bladder cancer. *Int J Cancer* **69**(2): 100-104.

Gerlach JH, Bell DR, Karakousis C, Slocum HK, Kartner N, Rustum YM, Ling V and Baker RM (1987) P-glycoprotein in human sarcoma: evidence for multidrug resistance. *J Clin Oncol* **5**(9): 1452-1460.

Gerweck LE, Vijayappa S and Kozin S (2006) Tumor pH controls the in vivo efficacy of weak acid and base chemotherapeutics. *Mol Cancer Ther* **5**(5): 1275-1279.

Geuze HJ, Stoorvogel W, Strous GJ, Slot JW, Bleekemolen JE and Mellman I (1988) Sorting of mannose 6-phosphate receptors and lysosomal membrane proteins in endocytic vesicles. *J Cell Biol* **107**(6 Pt 2): 2491-2501.

Ghose AK and Crippen GM (1987) Atomic physicochemical parameters for three-dimensional-structure-directed quantitative structure-activity relationships. 2. Modeling dispersive and hydrophobic interactions. *J Chem Inf Comput Sci* **27**(1): 21-35.

Gibson L, Holmgreen SP, Huang DC, Bernard O, Copeland NG, Jenkins NA, Sutherland GR, Baker E, Adams JM and Cory S (1996) bcl-w, a novel member of the bcl-2 family, promotes cell survival. *Oncogene* **13**(4): 665-675.

Gilbert NE, O'Reilly JE, Chang CJ, Lin YC and Brueggemeier RW (1995) Antiproliferative activity of gossypol and gossypolone on human breast cancer cells. *Life Sci* **57**(1): 61-67.

Giles FJ, Fracasso PM, Kantarjian HM, Cortes JE, Brown RA, Verstovsek S, Alvarado Y, Thomas DA, Faderl S, Garcia-Manero G, Wright LP, Samson T, Cahill A, Lambert P, Plunkett W, Sznol M, DiPersio JF and Gandhi V (2003) Phase I and pharmacodynamic study of Triapine, a novel ribonucleotide reductase inhibitor, in patients with advanced leukemia. *Leuk Res* **27**(12): 1077-1083.

Gillet JP and Gottesman MM (2010) Mechanisms of multidrug resistance in cancer. *Methods Mol Biol* **596**: 47-76.

Gocheva V, Zeng W, Ke D, Klimstra D, Reinheckel T, Peters C, Hanahan D and Joyce JA (2006) Distinct roles for cysteine cathepsin genes in multistage tumorigenesis. *Genes Dev* **20**(5): 543-556.

Goldstein JL, Dana SE, Faust JR, Beaudet AL and Brown MS (1975) Role of lysosomal acid lipase in the metabolism of plasma low density lipoprotein. Observations in cultured fibroblasts from a patient with cholesteryl ester storage disease. *J Biol Chem* **250**(21): 8487-8495.

Goldstein LJ, Galski H, Fojo A, Willingham M, Lai SL, Gazdar A, Pirker R, Green A, Crist W, Brodeur GM and et al. (1989) Expression of a multidrug resistance gene in human cancers. *J Natl Cancer Inst* **81**(2): 116-124.

Gong Y, Duvvuri M and Krise JP (2003) Separate roles for the Golgi apparatus and lysosomes in the sequestration of drugs in the multidrug-resistant human leukemic cell line HL-60. *J Biol Chem* **278**(50): 50234-50239.

Gong Y, Duvvuri M, Duncan MB, Liu J and Krise JP (2006) Niemann-Pick C1 protein facilitates the efflux of the anticancer drug daunorubicin from cells according to a novel vesicle-mediated pathway. *J Pharmacol Exp Ther* **316**(1): 242-247.

Goodman VL, Brewer GJ and Merajver SD (2004) Copper deficiency as an anti-cancer strategy. *Endocr Relat Cancer* **11**(2): 255-263.

Gotink KJ, Broxterman HJ, Labots M, de Haas RR, Dekker H, Honeywell RJ, Rudek MA, Beerepoot LV, Musters RJ, Jansen G, Griffioen AW, Assaraf YG, Pili R, Peters GJ and Verheul HM (2011) Lysosomal sequestration of sunitinib: a novel mechanism of drug resistance. *Clin Cancer Res* **17**(23): 7337-7346.

Gottesman MM and Pastan I (1993) Biochemistry of multidrug resistance mediated by the multidrug transporter. *Annu Rev Biochem* **62**: 385-427.

Gottesman MM (2002) Mechanisms of cancer drug resistance. *Annu Rev Med* **53**: 615-627.

Gottesman MM, Fojo T and Bates SE (2002) Multidrug resistance in cancer: role of ATP-dependent transporters. *Nat Rev Cancer* **2**(1): 48-58.

Graham J, Ford T and Rickwood D (1994) The preparation of subcellular organelles from mouse liver in self-generated gradients of iodixanol. *Analytical biochemistry* **220**(2): 367-373.

Granger BL, Green SA, Gabel CA, Howe CL, Mellman I and Helenius A (1990) Characterization and cloning of lgp110, a lysosomal membrane glycoprotein from mouse and rat cells. *J Biol Chem* **265**(20): 12036-12043.

Green DA, Antholine WE, Wong SJ, Richardson DR and Chitambar CR (2001) Inhibition of malignant cell growth by 311, a novel iron chelator of the pyridoxal isonicotinoyl

hydrazone class: effect on the R2 subunit of ribonucleotide reductase. *Clin Cancer Res* **7**(11): 3574-3579.

Greenberg PL, Lee SJ, Advani R, Tallman MS, Sikic BI, Letendre L, Dugan K, Lum B, Chin DL, Dewald G, Paietta E, Bennett JM and Rowe JM (2004) Mitoxantrone, etoposide, and cytarabine with or without valspodar in patients with relapsed or refractory acute myeloid leukemia and high-risk myelodysplastic syndrome: a phase III trial (E2995). *J Clin Oncol* **22**(6): 1078-1086.

Greer DA and Ivey S (2007) Distinct N-glycan glycosylation of P-glycoprotein isolated from the human uterine sarcoma cell line MES-SA/Dx5. *Biochim Biophys Acta* **1770**(9): 1275-1282.

Gros P, Croop J and Housman D (1986) Mammalian multidrug resistance gene: complete cDNA sequence indicates strong homology to bacterial transport proteins. *Cell* **47**(3): 371-380.

Groth-Pedersen L, Ostenfeld MS, Hoyer-Hansen M, Nylandsted J and Jaattela M (2007) Vincristine induces dramatic lysosomal changes and sensitizes cancer cells to lysosome-destabilizing siramesine. *Cancer Res* **67**(5): 2217-2225.

Grover R and Wilson GD (1996) Bcl-2 expression in malignant melanoma and its prognostic significance. *Eur J Surg Oncol* **22**(4): 347-349.

Gupte A and Mumper RJ (2009) Elevated copper and oxidative stress in cancer cells as a target for cancer treatment. *Cancer Treat Rev* **35**(1): 32-46.

Gutierrez E, Richardson DR and Jansson PJ (2014) The anticancer agent di-2-pyridylketone 4,4-dimethyl-3-thiosemicarbazone (Dp44mT) overcomes prosurvival autophagy by two mechanisms: persistent induction of autophagosome synthesis and impairment of lysosomal integrity. *J Biol Chem* **289**(48): 33568-33589.

Gutierrez EM, Seebacher NA, Arzuman L, Kovacevic Z, Lane DJ, Richardson V, Merlot AM, Lok H, Kalinowski DS, Sahni S, Jansson PJ and Richardson DR (2016) Lysosomal membrane stability plays a major role in the cytotoxic activity of the anti-proliferative agent, di-2-pyridylketone 4,4-dimethyl-3-thiosemicarbazone (Dp44mT). *Biochim Biophys Acta* **1863**(7 Pt A): 1665-1681.

Gutteridge JM, Richmond R and Halliwell B (1979) Inhibition of the iron-catalysed formation of hydroxyl radicals from superoxide and of lipid peroxidation by desferrioxamine. *Biochem J* **184**(2): 469-472.

Gutteridge JM (1984) Copper-phenanthroline-induced site-specific oxygen-radical damage to DNA. Detection of loosely bound trace copper in biological fluids. *Biochem J* **218**(3): 983-985.

Gutteridge JM (1995) Lipid peroxidation and antioxidants as biomarkers of tissue damage. *Clin Chem* **41**(12 Pt 2): 1819-1828.

Haber F and Weiss J (1932) Über die Katalyse des Hydroperoxydes *Naturwissenschaften* **20**(51): 948-950.

Hall MD, Salam NK, Hellawell JL, Fales HM, Kensler CB, Ludwig JA, Szakacs G, Hibbs DE and Gottesman MM (2009) Synthesis, activity, and pharmacophore development for isatin-beta-thiosemicarbazones with selective activity toward multidrug-resistant cells. *J Med Chem* **52**(10): 3191-3204.

Hall MD, Brimacombe KR, Varonka MS, Pluchino KM, Monda JK, Li J, Walsh MJ, Boxer MB, Warren TH, Fales HM and Gottesman MM (2011) Synthesis and structure-activity evaluation of isatin-beta-thiosemicarbazones with improved selective activity toward multidrug-resistant cells expressing P-glycoprotein. *J Med Chem* **54**(16): 5878-5889.

Halliwell B (1978) Superoxide-dependent formation of hydroxyl radicals in the presence of iron chelates: is it a mechanism for hydroxyl radical production in biochemical systems? *FEBS letters* **92**(2): 321-326.

Hamre D, Bernstein J and Donovick R (1950) Activity of p-Aminobenzaldehyde, 3-Thiosemicarbazone on Vaccinia Virus in the Chick Embryo and in the Mouse. *Proc Soc Exp Bio Med* **73**(2): 275-278.

Herlevsen M, Oxford G, Owens CR, Conaway M and Theodorescu D (2007) Depletion of major vault protein increases doxorubicin sensitivity and nuclear accumulation and disrupts its sequestration in lysosomes. *Mol Cancer Ther* **6**(6): 1804-1813.

Hermine O, Haioun C, Lepage E, d'Agay MF, Briere J, Lavignac C, Fillet G, Salles G, Marolleau JP, Diebold J, Reyas F and Gaulard P (1996) Prognostic significance of bcl-2 protein expression in aggressive non-Hodgkin's lymphoma. Groupe d'Etude des Lymphomes de l'Adulte (GELA). *Blood* **87**(1): 265-272.

Herweijer H, Sonneveld P, Baas F and Nooter K (1990) Expression of mdr1 and mdr3 multidrug-resistance genes in human acute and chronic leukemias and association with stimulation of drug accumulation by cyclosporine. *J Natl Cancer Inst* **82**(13): 1133-1140.

Higgins CF and Gottesman MM (1992) Is the multidrug transporter a flippase? *Trends Biochem Sci* **17**(1): 18-21.

Higgins CF (2007) Multiple molecular mechanisms for multidrug resistance transporters. *Nature* **446**(7137): 749-757.

Hochman A, Sternin H, Gorodin S, Korsmeyer S, Ziv I, Melamed E and Offen D (1998) Enhanced oxidative stress and altered antioxidants in brains of Bcl-2-deficient mice. *J Neurochem* **71**(2): 741-748.

Holohan C, Van Schaeybroeck S, Longley DB and Johnston PG (2013) Cancer drug resistance: an evolving paradigm. *Nat Rev Cancer* **13**(10): 714-726.

Hsu SY, Kaipia A, McGee E, Lomeli M and Hsueh AJ (1997) Bok is a pro-apoptotic Bcl-2 protein with restricted expression in reproductive tissues and heterodimerizes with selective anti-apoptotic Bcl-2 family members. *Proc Natl Acad Sci USA* **94**(23): 12401-12406.

Hu ZY, Sun J, Zhu XF, Yang D and Zeng YX (2009) ApoG2 induces cell cycle arrest of nasopharyngeal carcinoma cells by suppressing the c-Myc signaling pathway. *J Transl Med* **7**: 74.

Huang DC and Strasser A (2000) BH3-Only proteins-essential initiators of apoptotic cell death. *Cell* **103**(6): 839-842.

Hundeshagen P, Hamacher-Brady A, Eils R and Brady NR (2011) Concurrent detection of autolysosome formation and lysosomal degradation by flow cytometry in a high-content screen for inducers of autophagy. *BMC Biol* **9**: 38.

Huotari J and Helenius A (2011) Endosome maturation. *EMBO J* **30**(17): 3481-3500.

Hurwitz SJ, Terashima M, Mizunuma N and Slapak CA (1997) Vesicular anthracycline accumulation in doxorubicin-selected U-937 cells: participation of lysosomes. *Blood* **89**(10): 3745-3754.

Hyafil F, Vergely C, Du Vignaud P and Grand-Perret T (1993) In vitro and in vivo reversal of multidrug resistance by GF120918, an acridonecarboxamide derivative. *Cancer Res* **53**(19): 4595-4602.

Imlay JA, Chin SM and Linn S (1988) Toxic DNA damage by hydrogen peroxide through the Fenton reaction in vivo and in vitro. *Science* **240**(4852): 640-642.

Inohara N, Ding L, Chen S and Nunez G (1997) harakiri, a novel regulator of cell death, encodes a protein that activates apoptosis and interacts selectively with survival-promoting proteins Bcl-2 and Bcl-X(L). *EMBO J* **16**(7): 1686-1694.

Irving H and Williams R (1953) The stability of transition-metal complexes. *J Chem Soc*: 3192-3210.

Ishiguro K, Lin ZP, Penketh PG, Shyam K, Zhu R, Baumann RP, Zhu YL, Sartorelli AC, Rutherford TJ and Ratner ES (2014) Distinct mechanisms of cell-kill by triapine and its terminally dimethylated derivative Dp44mT due to a loss or gain of activity of their copper(II) complexes. *Biochem Pharmacol* **91**(3): 312-322.

Izquierdo MA, van der Zee AG, Vermorken JB, van der Valk P, Belien JA, Giaccone G, Scheffer GL, Flens MJ, Pinedo HM, Kenemans P and et al. (1995) Drug resistance-associated marker Lrp for prediction of response to chemotherapy and prognoses in advanced ovarian carcinoma. *J Natl Cancer Inst* **87**(16): 1230-1237.

Jachez B, Nordmann R and Loor F (1993) Restoration of taxol sensitivity of multidrug-resistant cells by the cyclosporine SDZ PSC 833 and the cyclopeptolide SDZ 280-446. *J Natl Cancer Inst* **85**(6): 478-483.

Jager S, Bucci C, Tanida I, Ueno T, Kominami E, Saftig P and Eskelinen EL (2004) Role for Rab7 in maturation of late autophagic vacuoles. *J Cell Sci* **117**(Pt 20): 4837-4848.

Jansson PJ, Hawkins CL, Lovejoy DB and Richardson DR (2010a) The iron complex of Dp44mT is redox-active and induces hydroxyl radical formation: an EPR study. *J Inorg Biochem* **104**(11): 1224-1228.

Jansson PJ, Sharpe PC, Bernhardt PV and Richardson DR (2010b) Novel thiosemicarbazones of the ApT and DpT series and their copper complexes: identification of pronounced redox activity and characterization of their antitumor activity. *J Med Chem* **53**(15): 5759-5769.

Jansson PJ, Kalinowski DS, Lane DJ, Kovacevic Z, Seebacher NA, Fouani L, Sahni S, Merlot AM and Richardson DR (2015a) The renaissance of polypharmacology in the development of anti-cancer therapeutics: Inhibition of the "Triad of Death" in cancer by Di-2-pyridylketone thiosemicarbazones. *Pharmacol Res* **100**: 255-260.

Jansson PJ, Yamagishi T, Arvind A, Seebacher N, Gutierrez E, Stacy A, Maleki S, Sharp D, Sahni S and Richardson DR (2015b) Di-2-pyridylketone 4,4-dimethyl-3-thiosemicarbazone (Dp44mT) overcomes multidrug resistance by a novel mechanism involving the hijacking of lysosomal P-glycoprotein (Pgp). *J Biol Chem* **290**(15): 9588-9603.

Jayakumar K, Sithambaresan M and Prathapachandra Kurup MR (2011) (Z)-N,N-Dimethyl-2-[phen-yl(pyridin-2-yl)methyl-idene]hydrazinecarbothio-amide. *Acta Crystallogr Sect E Struct Rep Online* **67**(Pt 12): o3195.

Jayakumar K, Sithambaresan M, Aravindakshan AA and Kurup MP (2014) Synthesis and spectral characterization of copper (II) complexes derived from 2-benzoylpyridine-N 4, N 4-dimethyl-3-thiosemicarbazone: Crystal structure of a binuclear complex. *Polyhedron* **75**: 50-56.

Jiang SX, Sato Y, Kuwao S and Kameya T (1995) Expression of bcl-2 oncogene protein is prevalent in small cell lung carcinomas. *J Pathol* **177**(2): 135-138.

Jin MS, Oldham ML, Zhang Q and Chen J (2012) Crystal structure of the multidrug transporter P-glycoprotein from Caenorhabditis elegans. *Nature* **490**(7421): 566-569.

Joensuu H, Pylkkanen L and Toikkanen S (1994) Bcl-2 protein expression and long-term survival in breast cancer. *Am J Pathol* **145**(5): 1191-1198.

Johansson H, Svartstrom O, Phadnis P, Engman L and Ott MK (2010) Exploring a synthetic organoselenium compound for antioxidant pharmacotherapy--toxicity and effects on ROS-production. *Bioorganic & medicinal chemistry* **18**(5): 1783-1788.

Jones TR, Zamboni R, Belley M, Champion E, Charette L, Ford-Hutchinson AW, Frenette R, Gauthier JY, Leger S, Masson P and et al. (1989) Pharmacology of L-660,711 (MK-571): a novel potent and selective leukotriene D4 receptor antagonist. *Can J Physiol Pharmacol* **67**(1): 17-28.

Joseph M, Suni V, Kurup MRP, Nethaji M, Kishore A and Bhat SG (2004) Structural, spectral and antimicrobial studies of copper (II) complexes of 2-benzoylpyridine N (4)-cyclohexyl thiosemicarbazone. *Polyhedron* **23**(18): 3069-3080.

Juliano RL and Ling V (1976) A surface glycoprotein modulating drug permeability in Chinese hamster ovary cell mutants. *Biochim Biophys Acta* **455**(1): 152-162.

Kagedal K, Johansson U and Ollinger K (2001) The lysosomal protease cathepsin D mediates apoptosis induced by oxidative stress. *FASEB J* **15**(9): 1592-1594.

Kakehi Y, Kanamaru H, Yoshida O, Ohkubo H, Nakanishi S, Gottesman MM and Pastan I (1988) Measurement of multidrug-resistance messenger RNA in urogenital cancers; elevated expression in renal cell carcinoma is associated with intrinsic drug resistance. *J Urol* **139**(4): 862-865.

Kalinowski DS and Richardson DR (2005) The evolution of iron chelators for the treatment of iron overload disease and cancer. *Pharmacol Rev* **57**(4): 547-583.

Kalinowski DS, Yu Y, Sharpe PC, Islam M, Liao YT, Lovejoy DB, Kumar N, Bernhardt PV and Richardson DR (2007) Design, synthesis, and characterization of novel iron chelators: structure-activity relationships of the 2-benzoylpyridine thiosemicarbazone series and their 3-nitrobenzoyl analogues as potent antitumor agents. *J Med Chem* **50**(15): 3716-3729.

Kalinowski DS, Stefani C, Toyokuni S, Ganz T, Anderson GJ, Subramaniam NV, Trinder D, Olynyk JK, Chua A, Jansson PJ, Sahni S, Lane DJ, Merlot AM, Kovacevic Z, Huang ML, Lee CS and Richardson DR (2016) Redox cycling metals: Pedaling their roles in metabolism and their use in the development of novel therapeutics. *Biochimica et biophysica acta* **1863**(4): 727-748.

Kallunki T, Olsen OD and Jaattela M (2013) Cancer-associated lysosomal changes: friends or foes? *Oncogene* **32**(16): 1995-2004.

Kanamaru H, Kakehi Y, Yoshida O, Nakanishi S, Pastan I and Gottesman MM (1989) MDR1 RNA levels in human renal cell carcinomas: correlation with grade and prediction of reversal of doxorubicin resistance by quinidine in tumor explants. *J Natl Cancer Inst* **81**(11): 844-849.

Kartner N, Evernden-Porelle D, Bradley G and Ling V (1985) Detection of P-glycoprotein in multidrug-resistant cell lines by monoclonal antibodies. *Nature* **316**(6031): 820-823.

Kasuga NC, Sekino K, Ishikawa M, Honda A, Yokoyama M, Nakano S, Shimada N, Koumo C and Nomiya K (2003) Synthesis, structural characterization and antimicrobial activities of 12 zinc(II) complexes with four thiosemicarbazone and two semicarbazone ligands. *J Inorg Biochem* **96**(2ï 3): 298-310.

Katoh SY, Ueno M and Takakura N (2008) Involvement of MDR1 function in proliferation of tumour cells. *J Biochem* **143**(4): 517-524.

Keliher EJ, Reiner T, Earley S, Klubnick J, Tassa C, Lee AJ, Ramaswamy S, Bardeesy N, Hanahan D, Depinho RA, Castro CM and Weissleder R (2013) Targeting cathepsin E in

pancreatic cancer by a small molecule allows in vivo detection. *Neoplasia* **15**(7): 684-693.

Keller RP, Altermatt HJ, Nooter K, Poschmann G, Laissue JA, Bollinger P and Hiestand PC (1992) SDZ PSC 833, a non-immunosuppressive cyclosporine: its potency in overcoming P-glycoprotein-mediated multidrug resistance of murine leukemia. *Int J Cancer* **50**(4): 593-597.

Kemper EM, Verheij M, Boogerd W, Beijnen JH and van Tellingen O (2004) Improved penetration of docetaxel into the brain by co-administration of inhibitors of P-glycoprotein. *Eur J Cancer* **40**(8): 1269-1274.

Kenific CM, Thorburn A and Debnath J (2010) Autophagy and metastasis: another double-edged sword. *Curr Opin Cell Biol* **22**(2): 241-245.

Kessel D (1989) Exploring multidrug resistance using rhodamine 123. *Cancer Commun* **1**(3): 145-149.

Kessel D, Beck WT, Kukuruga D and Schulz V (1991) Characterization of multidrug resistance by fluorescent dyes. *Cancer Res* **51**(17): 4665-4670.

Kiefer MC, Brauer MJ, Powers VC, Wu JJ, Umansky SR, Tomei LD and Barr PJ (1995) Modulation of apoptosis by the widely distributed Bcl-2 homologue Bak. *Nature* **374**(6524): 736-739.

Kihara A, Kabeya Y, Ohsumi Y and Yoshimori T (2001) Beclin-phosphatidylinositol 3-kinase complex functions at the trans-Golgi network. *EMBO Rep* **2**(4): 330-335.

Kim HW, Chan Q, Afton SE, Caruso JA, Lai B, Weintraub NL and Qin Z (2012) Human macrophage ATP7A is localized in the trans-Golgi apparatus, controls intracellular copper levels, and mediates macrophage responses to dermal wounds. *Inflammation* **35**(1): 167-175.

Kim RB (2002) Drugs as P-glycoprotein substrates, inhibitors, and inducers. *Drug Metab Rev* **34**(1-2): 47-54.

Kimura Y, Matsuo M, Takahashi K, Saeki T, Kioka N, Amachi T and Ueda K (2004) ATP hydrolysis-dependent multidrug efflux transporter: MDR1/P-glycoprotein. *Curr Drug Metab* **5**(1): 1-10.

Kirshner JR, He S, Balasubramanyam V, Kepros J, Yang CY, Zhang M, Du Z, Barsoum J and Bertin J (2008) Elesclomol induces cancer cell apoptosis through oxidative stress. *Mol Cancer Ther* **7**(8): 2319-2327.

Kitada S, Leone M, Sareth S, Zhai D, Reed JC and Pellecchia M (2003) Discovery, characterization, and structure-activity relationships studies of proapoptotic polyphenols targeting B-cell lymphocyte/leukemia-2 proteins. *J Med Chem* **46**(20): 4259-4264.

Klayman DL, Bartosevich JF, Griffin TS, Mason CJ and Scovill JP (1979) 2-Acetylpyridine thiosemicarbazones. 1. A new class of potential antimalarial agents. *J Med Chem* **22**(7): 855-862.

Klionsky DJ, Abdelmohsen K, Abe A, Abedin MJ, Abeliovich H, Acevedo Arozena A, Adachi H, Adams CM, Adams PD, Adeli K, Adhihetty PJ, Adler SG, Agam G, Agarwal R, Aghi MK, Agnello M, Agostinis P, Aguilar PV, Aguirre-Ghiso J, Airoldi EM, Ait-Si-Ali S, Akematsu T, Akporiaye ET, Al-Rubeai M, Albaiceta GM, Albanese C, Albani D, Albert ML, Aldudo J, Algul H, Alirezaei M, Alloza I, Almasan A, Almonte-Beceril M, Alnemri ES, Alonso C, Altan-Bonnet N, Altieri DC, Alvarez S, Alvarez-Erviti L, Alves S, Amadoro G, Amano A, Amantini C, Ambrosio S, Amelio I, Amer AO, Amessou M, Amon A, An Z, Anania FA, Andersen SU, Andley UP, Andreadi CK, Andrieu-Abadie N,

Anel A, Ann DK, Anoopkumar-Dukie S, Antonioli M, Aoki H, Apostolova N, Aquila S, Aquilano K, Araki K, Arama E, Aranda A, Araya J, Arcaro A, Arias E, Arimoto H, Ariosa AR, Armstrong JL, Arnould T, Arsov I, Asanuma K, Askanas V, Asselin E, Atarashi R, Atherton SS, Atkin JD, Attardi LD, Auberger P, Auburger G, Aurelian L, Autelli R, Avagliano L, Avantaggiati ML, Avrahami L, Awale S, Azad N, Bachetti T, Backer JM, Bae DH, Bae JS, Bae ON, Bae SH, Baehrecke EH, Baek SH, Baghdiguian S, Bagniewska-Zadworna A, Bai H, Bai J, Bai XY, Bailly Y, Balaji KN, Balduini W, Ballabio A, Balzan R, Banerjee R, Banhegyi G, Bao H, Barbeau B, Barrachina MD, Barreiro E, Bartel B, Bartolome A, Bassham DC, Bassi MT, Bast RC, Jr., Basu A, Batista MT, Batoko H, Battino M, Bauckman K, Baumgarner BL, Bayer KU, Beale R, Beaulieu JF, Beck GR, Jr., Becker C, Beckham JD, Bedard PA, Bednarski PJ, Begley TJ, Behl C, Behrends C, Behrens GM, Behrns KE, Bejarano E, Belaid A, Belleudi F, Benard G, Berchem G, Bergamaschi D, Bergami M, Berkhout B, Berliocchi L, Bernard A, Bernard M, Bernassola F, Bertolotti A, Bess AS, Besteiro S, Bettuzzi S, Bhalla S, Bhattacharyya S, Bhutia SK, Biagosch C, Bianchi MW, Biard-Piechaczyk M, Billes V, Bincoletto C, Bingol B, Bird SW, Bitoun M, Bjedov I, Blackstone C, Blanc L, Blanco GA, Blomhoff HK, Boada-Romero E, Bockler S, Boes M, Boesze-Battaglia K, Boise LH, Bolino A, Boman A, Bonaldo P, Bordi M, Bosch J, Botana LM, Botti J, Bou G, Bouche M, Bouchecareilh M, Boucher MJ, Boulton ME, Bouret SG, Boya P, Boyer-Guittaut M, Bozhkov PV, Brady N, Braga VM, Brancolini C, Braus GH, Bravo-San Pedro JM, Brennan LA, Bresnick EH, Brest P, Bridges D, Bringer MA, Brini M, Brito GC, Brodin B, Brookes PS, Brown EJ, Brown K, Broxmeyer HE, Bruhat A, Brum PC, Brumell JH, Brunetti-Pierri N, Bryson-Richardson RJ, Buch S, Buchan AM, Budak H, Bulavin DV, Bultman SJ, Bultynck G, Bumbasirevic V, Burelle Y, Burke RE, Burmeister M, Butikofer P, Caberlotto L, Cadwell K, Cahova M, Cai D, Cai J, Cai Q, Calatayud S, Camougrand N, Campanella M, Campbell GR, Campbell M, Campello S, Candau R, Caniggia I, Cantoni L, Cao L, Caplan AB, Caraglia M, Cardinali C, Cardoso SM, Carew JS, Carleton LA, Carlin CR, Carloni S, Carlsson SR, Carmona-Gutierrez D, Carneiro LA, Carnevali O, Carra S, Carrier A, Carroll B, Casas C, Casas J, Cassinelli G, Castets P, Castro-Obregon S, Cavallini G, Ceccherini I, Cecconi F, Cederbaum AI, Cena V, Cenci S, Cerella C, Cervia D, Cetrullo S, Chaachouay H, Chae HJ, Chagin AS, Chai CY, Chakrabarti G, Chamilos G, Chan EY, Chan MT, Chandra D, Chandra P, Chang CP, Chang RC, Chang TY, Chatham JC, Chatterjee S, Chauhan S, Che Y, Cheetham ME, Cheluvappa R, Chen CJ, Chen G, Chen GC, Chen G, Chen H, Chen JW, Chen JK, Chen M, Chen M, Chen P, Chen Q, Chen Q, Chen SD, Chen S, Chen SS, Chen W, Chen WJ, Chen WQ, Chen W, Chen X, Chen YH, Chen YG, Chen Y, Chen Y, Chen Y, Chen YJ, Chen YQ, Chen Y, Chen Z, Chen Z, Cheng A, Cheng CH, Cheng H, Cheong H, Cherry S, Chesney J, Cheung CH, Chevet E, Chi HC, Chi SG, Chiacchiera F, Chiang HL, Chiarelli R, Chiariello M, Chieppa M, Chin LS, Chiong M, Chiu GN, Cho DH, Cho SG, Cho WC, Cho YY, Cho YS, Choi AM, Choi EJ, Choi EK, Choi J, Choi ME, Choi SI, Chou TF, Chouaib S, Choubey D, Choubey V, Chow KC, Chowdhury K, Chu CT, Chuang TH, Chun T, Chung H, Chung T, Chung YL, Chwae YJ, Cianfanelli V, Ciarcia R, Ciechomska IA, Ciriolo MR, Cirone M, Claerhout S, Clague MJ, Claria J, Clarke PG, Clarke R, Clementi E, Cleyrat C, Cnop M, Coccia EM, Cocco T, Codogno P, Coers J, Cohen EE, Colecchia D, Coletto L, Coll NS, Colucci-Guyon E, Comincini S, Condello M, Cook KL, Coombs GH, Cooper CD, Cooper JM, Coppens I, Corasaniti MT,

Corazzari M, Corbalan R, Corcelle-Termeau E, Cordero MD, Corral-Ramos C, Corti O, Cossarizza A, Costelli P, Costes S, Cotman SL, Coto-Montes A, Cottet S, Couve E, Covey LR, Cowart LA, Cox JS, Coxon FP, Coyne CB, Cragg MS, Craven RJ, Crepaldi T, Crespo JL, Criollo A, Crippa V, Cruz MT, Cuervo AM, Cuezva JM, Cui T, Cutillas PR, Czaja MJ, Czyzyk-Krzeska MF, Dagda RK, Dahmen U, Dai C, Dai W, Dai Y, Dalby KN, Dalla Valle L, Dalmasso G, D'Amelio M, Damme M, Darfeuille-Michaud A, Dargemont C, Darley-Usmar VM, Dasarathy S, Dasgupta B, Dash S, Dass CR, Davey HM, Davids LM, Davila D, Davis RJ, Dawson TM, Dawson VL, Daza P, de Belleroche J, de Figueiredo P, de Figueiredo RC, de la Fuente J, De Martino L, De Matteis A, De Meyer GR, De Milito A, De Santi M, de Souza W, De Tata V, De Zio D, Debnath J, Dechant R, Decuypere JP, Deegan S, Dehay B, Del Bello B, Del Re DP, Delage-Mourroux R, Delbridge LM, Deldicque L, Delorme-Axford E, Deng Y, Dengjel J, Denizot M, Dent P, Der CJ, Deretic V, Derrien B, Deutsch E, Devarenne TP, Devenish RJ, Di Bartolomeo S, Di Daniele N, Di Domenico F, Di Nardo A, Di Paola S, Di Pietro A, Di Renzo L, DiAntonio A, Diaz-Araya G, Diaz-Laviada I, Diaz-Meco MT, Diaz-Nido J, Dickey CA, Dickson RC, Diederich M, Digard P, Dikic I, Dinesh-Kumar SP, Ding C, Ding WX, Ding Z, Dini L, Distler JH, Diwan A, Djavaheri-Mergny M, Dmytruk K, Dobson RC, Doetsch V, Dokladny K, Dokudovskaya S, Donadelli M, Dong XC, Dong X, Dong Z, Donohue TM, Jr., Doran KS, D'Orazi G, Dorn GW, 2nd, Dosenko V, Dridi S, Drucker L, Du J, Du LL, Du L, du Toit A, Dua P, Duan L, Duann P, Dubey VK, Duchen MR, Duchosal MA, Duez H, Dugail I, Dumit VI, Duncan MC, Dunlop EA, Dunn WA, Jr., Dupont N, Dupuis L, Duran RV, Durcan TM, Duvezin-Caubet S, Duvvuri U, Eapen V, Ebrahimi-Fakhari D, Echard A, Eckhart L, Edelstein CL, Edinger AL, Eichinger L, Eisenberg T, Eisenberg-Lerner A, Eissa NT, El-Deiry WS, El-Khoury V, Elazar Z, Eldar-Finkelman H, Elliott CJ, Emanuele E, Emmenegger U, Engedal N, Engelbrecht AM, Engelender S, Enserink JM, Erdmann R, Erenpreisa J, Eri R, Eriksen JL, Erman A, Escalante R, Eskelinen EL, Espert L, Esteban-Martinez L, Evans TJ, Fabri M, Fabrias G, Fabrizi C, Facchiano A, Faergeman NJ, Faggioni A, Fairlie WD, Fan C, Fan D, Fan J, Fang S, Fanto M, Fanzani A, Farkas T, Faure M, Favier FB, Fearnhead H, Federici M, Fei E, Felizardo TC, Feng H, Feng Y, Feng Y, Ferguson TA, Fernandez AF, Fernandez-Barrena MG, Fernandez-Checa JC, Fernandez-Lopez A, Fernandez-Zapico ME, Feron O, Ferraro E, Ferreira-Halder CV, Fesus L, Feuer R, Fiesel FC, Filippi-Chiela EC, Filomeni G, Fimia GM, Fingert JH, Finkbeiner S, Finkel T, Fiorito F, Fisher PB, Flajolet M, Flamigni F, Florey O, Florio S, Floto RA, Folini M, Follo C, Fon EA, Fornai F, Fortunato F, Fraldi A, Franco R, Francois A, Francois A, Frankel LB, Fraser ID, Frey N, Freyssenet DG, Frezza C, Friedman SL, Frigo DE, Fu D, Fuentes JM, Fueyo J, Fujitani Y, Fujiwara Y, Fujiya M, Fukuda M, Fulda S, Fusco C, Gabryel B, Gaestel M, Gailly P, Gajewska M, Galadari S, Galili G, Galindo I, Galindo MF, Galliciotti G, Galluzzi L, Galluzzi L, Galy V, Gammoh N, Gandy S, Ganesan AK, Ganesan S, Ganley IG, Gannage M, Gao FB, Gao F, Gao JX, Garcia Nannig L, Garcia Vescovi E, Garcia-Macia M, Garcia-Ruiz C, Garg AD, Garg PK, Gargini R, Gassen NC, Gatica D, Gatti E, Gavard J, Gavathiotis E, Ge L, Ge P, Ge S, Gean PW, Gelmetti V, Genazzani AA, Geng J, Genschik P, Gerner L, Gestwicki JE, Gewirtz DA, Ghavami S, Ghigo E, Ghosh D, Giammarioli AM, Giampieri F, Giampietri C, Giatromanolaki A, Gibbings DJ, Gibellini L, Gibson SB, Ginet V, Giordano A, Giorgini F, Giovannetti E, Girardin SE, Gispert S, Giuliano S, Gladson CL, Glavic A, Gleave M, Godefroy N, Gogal RM, Jr., Gokulan K,

Goldman GH, Goletti D, Goligorsky MS, Gomes AV, Gomes LC, Gomez H, Gomez-Manzano C, Gomez-Sanchez R, Goncalves DA, Goncu E, Gong Q, Gongora C, Gonzalez CB, Gonzalez-Alegre P, Gonzalez-Cabo P, Gonzalez-Polo RA, Goping IS, Gorbea C, Gorbunov NV, Goring DR, Gorman AM, Gorski SM, Goruppi S, Goto-Yamada S, Gotor C, Gottlieb RA, Gozes I, Gozuacik D, Graba Y, Graef M, Granato GE, Grant GD, Grant S, Gravina GL, Green DR, Greenhough A, Greenwood MT, Grimaldi B, Gros F, Grose C, Groulx JF, Gruber F, Grumati P, Grune T, Guan JL, Guan KL, Guerra B, Guillen C, Gulshan K, Gunst J, Guo C, Guo L, Guo M, Guo W, Guo XG, Gust AA, Gustafsson AB, Gutierrez E, Gutierrez MG, Gwak HS, Haas A, Haber JE, Hadano S, Hagedorn M, Hahn DR, Halayko AJ, Hamacher-Brady A, Hamada K, Hamai A, Hamann A, Hamasaki M, Hamer I, Hamid Q, Hammond EM, Han F, Han W, Handa JT, Hanover JA, Hansen M, Harada M, Harhaji-Trajkovic L, Harper JW, Harrath AH, Harris AL, Harris J, Hasler U, Hasselblatt P, Hasui K, Hawley RG, Hawley TS, He C, He CY, He F, He G, He RR, He XH, He YW, He YY, Heath JK, Hebert MJ, Heinzen RA, Helgason GV, Hensel M, Henske EP, Her C, Herman PK, Hernandez A, Hernandez C, Hernandez-Tiedra S, Hetz C, Hiesinger PR, Higaki K, Hilfiker S, Hill BG, Hill JA, Hill WD, Hino K, Hofius D, Hofman P, Hoglinger GU, Hohfeld J, Holz MK, Hong Y, Hood DA, Hoozemans JJ, Hoppe T, Hsu C, Hsu CY, Hsu LC, Hu D, Hu G, Hu HM, Hu H, Hu MC, Hu YC, Hu ZW, Hua F, Hua Y, Huang C, Huang HL, Huang KH, Huang KY, Huang S, Huang S, Huang WP, Huang YR, Huang Y, Huang Y, Huber TB, Huebbe P, Huh WK, Hulmi JJ, Hur GM, Hurley JH, Husak Z, Hussain SN, Hussain S, Hwang JJ, Hwang S, Hwang TI, Ichihara A, Imai Y, Imbriano C, Inomata M, Into T, Iovane V, Iovanna JL, Iozzo RV, Ip NY, Irazoqui JE, Iribarren P, Isaka Y, Isakovic AJ, Ischiropoulos H, Isenberg JS, Ishaq M, Ishida H, Ishii I, Ishmael JE, Isidoro C, Isobe K, Isono E, Issazadeh-Navikas S, Itahana K, Itakura E, Ivanov AI, Iyer AK, Izquierdo JM, Izumi Y, Izzo V, Jaattela M, Jaber N, Jackson DJ, Jackson WT, Jacob TG, Jacques TS, Jagannath C, Jain A, Jana NR, Jang BK, Jani A, Janji B, Jannig PR, Jansson PJ, Jean S, Jendrach M, Jeon JH, Jessen N, Jeung EB, Jia K, Jia L, Jiang H, Jiang H, Jiang L, Jiang T, Jiang X, Jiang X, Jiang X, Jiang Y, Jiang Y, Jimenez A, Jin C, Jin H, Jin L, Jin M, Jin S, Jinwal UK, Jo EK, Johansen T, Johnson DE, Johnson GV, Johnson JD, Jonasch E, Jones C, Joosten LA, Jordan J, Joseph AM, Joseph B, Joubert AM, Ju D, Ju J, Juan HF, Juenemann K, Juhasz G, Jung HS, Jung JU, Jung YK, Jungbluth H, Justice MJ, Jutten B, Kaakoush NO, Kaarniranta K, Kaasik A, Kabuta T, Kaeffer B, Kagedal K, Kahana A, Kajimura S, Kakhlon O, Kalia M, Kalvakolanu DV, Kamada Y, Kambas K, Kaminskyy VO, Kampinga HH, Kandouz M, Kang C, Kang R, Kang TC, Kanki T, Kanneganti TD, Kanno H, Kanthasamy AG, Kantorow M, Kaparakis-Liaskos M, Kapuy O, Karantza V, Karim MR, Karmakar P, Kaser A, Kaushik S, Kawula T, Kaynar AM, Ke PY, Ke ZJ, Kehrl JH, Keller KE, Kemper JK, Kenworthy AK, Kepp O, Kern A, Kesari S, Kessel D, Ketteler R, Kettelhut Ido C, Khambu B, Khan MM, Khandelwal VK, Khare S, Kiang JG, Kiger AA, Kihara A, Kim AL, Kim CH, Kim DR, Kim DH, Kim EK, Kim HY, Kim HR, Kim JS, Kim JH, Kim JC, Kim JH, Kim KW, Kim MD, Kim MM, Kim PK, Kim SW, Kim SY, Kim YS, Kim Y, Kimchi A, Kimmelman AC, Kimura T, King JS, Kirkegaard K, Kirkin V, Kirshenbaum LA, Kishi S, Kitajima Y, Kitamoto K, Kitaoka Y, Kitazato K, Kley RA, Klimecki WT, Klinkenberg M, Klucken J, Knaevelsrud H, Knecht E, Knuppertz L, Ko JL, Kobayashi S, Koch JC, Koechlin-Ramonatxo C, Koenig U, Koh YH, Kohler K, Kohlwein SD, Koike M, Komatsu M, Kominami E, Kong D, Kong HJ,

Konstantakou EG, Kopp BT, Korcsmaros T, Korhonen L, Korolchuk VI, Koshkina NV, Kou Y, Koukourakis MI, Koumenis C, Kovacs AL, Kovacs T, Kovacs WJ, Koya D, Kraft C, Krainc D, Kramer H, Kravic-Stevovic T, Krek W, Kretz-Remy C, Krick R, Krishnamurthy M, Kriston-Vizi J, Kroemer G, Kruer MC, Kruger R, Ktistakis NT, Kuchitsu K, Kuhn C, Kumar AP, Kumar A, Kumar A, Kumar D, Kumar D, Kumar R, Kumar S, Kundu M, Kung HJ, Kuno A, Kuo SH, Kuret J, Kurz T, Kwok T, Kwon TK, Kwon YT, Kyrmizi I, La Spada AR, Lafont F, Lahm T, Lakkaraju A, Lam T, Lamark T, Lancel S, Landowski TH, Lane DJ, Lane JD, Lanzi C, Lapaquette P, Lapierre LR, Laporte J, Laukkarinen J, Laurie GW, Lavandero S, Lavie L, LaVoie MJ, Law BY, Law HK, Law KB, Layfield R, Lazo PA, Le Cam L, Le Roch KG, Le Stunff H, Leardkamolkarn V, Lecuit M, Lee BH, Lee CH, Lee EF, Lee GM, Lee HJ, Lee H, Lee JK, Lee J, Lee JH, Lee JH, Lee M, Lee MS, Lee PJ, Lee SW, Lee SJ, Lee SJ, Lee SY, Lee SH, Lee SS, Lee SJ, Lee S, Lee YR, Lee YJ, Lee YH, Leeuwenburgh C, Lefort S, Legouis R, Lei J, Lei QY, Leib DA, Leibowitz G, Lekli I, Lemaire SD, Lemasters JJ, Lemberg MK, Lemoine A, Leng S, Lenz G, Lenzi P, Lerman LO, Lettieri Barbato D, Leu JI, Leung HY, Levine B, Lewis PA, Lezoualc'h F, Li C, Li F, Li FJ, Li J, Li K, Li L, Li M, Li M, Li Q, Li R, Li S, Li W, Li W, Li X, Li Y, Lian J, Liang C, Liang Q, Liao Y, Liberal J, Liberski PP, Lie P, Lieberman AP, Lim HJ, Lim KL, Lim K, Lima RT, Lin CS, Lin CF, Lin F, Lin F, Lin FC, Lin K, Lin KH, Lin PH, Lin T, Lin WW, Lin YS, Lin Y, Linden R, Lindholm D, Lindqvist LM, Lingor P, Linkermann A, Liotta LA, Lipinski MM, Lira VA, Lisanti MP, Liton PB, Liu B, Liu C, Liu CF, Liu F, Liu HJ, Liu J, Liu JJ, Liu JL, Liu K, Liu L, Liu L, Liu Q, Liu RY, Liu S, Liu S, Liu W, Liu XD, Liu X, Liu XH, Liu X, Liu X, Liu X, Liu Y, Liu Y, Liu Z, Liu Z, Liuzzi JP, Lizard G, Ljujic M, Lodhi IJ, Logue SE, Lokeshwar BL, Long YC, Lonial S, Loos B, Lopez-Otin C, Lopez-Vicario C, Lorente M, Lorenzi PL, Lorincz P, Los M, Lotze MT, Lovat PE, Lu B, Lu B, Lu J, Lu Q, Lu SM, Lu S, Lu Y, Luciano F, Luckhart S, Lucocq JM, Ludovico P, Lugea A, Lukacs NW, Lum JJ, Lund AH, Luo H, Luo J, Luo S, Luparello C, Lyons T, Ma J, Ma Y, Ma Y, Ma Z, Machado J, Machado-Santelli GM, Macian F, MacIntosh GC, MacKeigan JP, Macleod KF, MacMicking JD, MacMillan-Crow LA, Madeo F, Madesh M, Madrigal-Matute J, Maeda A, Maeda T, Maegawa G, Maellaro E, Maes H, Magarinos M, Maiese K, Maiti TK, Maiuri L, Maiuri MC, Maki CG, Malli R, Malorni W, Maloyan A, Mami-Chouaib F, Man N, Mancias JD, Mandelkow EM, Mandell MA, Manfredi AA, Manie SN, Manzoni C, Mao K, Mao Z, Mao ZW, Marambaud P, Marconi AM, Marelja Z, Marfe G, Margeta M, Margittai E, Mari M, Mariani FV, Marin C, Marinelli S, Marino G, Markovic I, Marquez R, Martelli AM, Martens S, Martin KR, Martin SJ, Martin S, Martin-Acebes MA, Martin-Sanz P, Martinand-Mari C, Martinet W, Martinez J, Martinez-Lopez N, Martinez-Outschoorn U, Martinez-Velazquez M, Martinez-Vicente M, Martins WK, Mashima H, Mastrianni JA, Matarese G, Matarrese P, Mateo R, Matoba S, Matsumoto N, Matsushita T, Matsuura A, Matsuzawa T, Mattson MP, Matus S, Maugeri N, Mauvezin C, Mayer A, Maysinger D, Mazzolini GD, McBrayer MK, McCall K, McCormick C, McInerney GM, McIver SC, McKenna S, McMahon JJ, McNeish IA, Mechta-Grigoriou F, Medema JP, Medina DL, Megyeri K, Mehrpour M, Mehta JL, Mei Y, Meier UC, Meijer AJ, Melendez A, Melino G, Melino S, de Melo EJ, Mena MA, Meneghini MD, Menendez JA, Menezes R, Meng L, Meng LH, Meng S, Menghini R, Menko AS, Menna-Barreto RF, Menon MB, Meraz-Rios MA, Merla G, Merlini L, Merlot AM, Meryk A, Meschini S, Meyer JN, Mi MT, Miao CY, Micale L, Michaeli S,

Michiels C, Migliaccio AR, Mihailidou AS, Mijaljica D, Mikoshiba K, Milan E, Miller-Fleming L, Mills GB, Mills IG, Minakaki G, Minassian BA, Ming XF, Minibayeva F, Minina EA, Mintern JD, Minucci S, Miranda-Vizuete A, Mitchell CH, Miyamoto S, Miyazawa K, Mizushima N, Mnich K, Mograbi B, Mohseni S, Moita LF, Molinari M, Molinari M, Moller AB, Mollereau B, Mollinedo F, Mongillo M, Monick MM, Montagnaro S, Montell C, Moore DJ, Moore MN, Mora-Rodriguez R, Moreira PI, Morel E, Morelli MB, Moreno S, Morgan MJ, Moris A, Moriyasu Y, Morrison JL, Morrison LA, Morselli E, Moscat J, Moseley PL, Mostowy S, Motori E, Mottet D, Mottram JC, Moussa CE, Mpakou VE, Mukhtar H, Mulcahy Levy JM, Muller S, Munoz-Moreno R, Munoz-Pinedo C, Munz C, Murphy ME, Murray JT, Murthy A, Mysorekar IU, Nabi IR, Nabissi M, Nader GA, Nagahara Y, Nagai Y, Nagata K, Nagelkerke A, Nagy P, Naidu SR, Nair S, Nakano H, Nakatogawa H, Nanjundan M, Napolitano G, Naqvi NI, Nardacci R, Narendra DP, Narita M, Nascimbeni AC, Natarajan R, Navegantes LC, Nawrocki ST, Nazarko TY, Nazarko VY, Neill T, Neri LM, Netea MG, Netea-Maier RT, Neves BM, Ney PA, Nezis IP, Nguyen HT, Nguyen HP, Nicot AS, Nilsen H, Nilsson P, Nishimura M, Nishino I, Niso-Santano M, Niu H, Nixon RA, Njar VC, Noda T, Noegel AA, Nolte EM, Norberg E, Norga KK, Noureini SK, Notomi S, Notterpek L, Nowikovsky K, Nukina N, Nurnberger T, O'Donnell VB, O'Donovan T, O'Dwyer PJ, Oehme I, Oeste CL, Ogawa M, Ogretmen B, Ogura Y, Oh YJ, Ohmuraya M, Ohshima T, Ojha R, Okamoto K, Okazaki T, Oliver FJ, Ollinger K, Olsson S, Orban DP, Ordonez P, Orhon I, Orosz L, O'Rourke EJ, Orozco H, Ortega AL, Ortona E, Osellame LD, Oshima J, Oshima S, Osiewacz HD, Otomo T, Otsu K, Ou JH, Outeiro TF, Ouyang DY, Ouyang H, Overholtzer M, Ozbun MA, Ozdinler PH, Ozpolat B, Pacelli C, Paganetti P, Page G, Pages G, Pagnini U, Pajak B, Pak SC, Pakos-Zebrucka K, Pakpour N, Palkova Z, Palladino F, Pallauf K, Pallet N, Palmieri M, Paludan SR, Palumbo C, Palumbo S, Pampliega O, Pan H, Pan W, Panaretakis T, Pandey A, Pantazopoulou A, Papackova Z, Papademetrio DL, Papassideri I, Papini A, Parajuli N, Pardo J, Parekh VV, Parenti G, Park JI, Park J, Park OK, Parker R, Parlato R, Parys JB, Parzych KR, Pasquet JM, Pasquier B, Pasumarthi KB, Patschan D, Patterson C, Pattingre S, Pattison S, Pause A, Pavenstadt H, Pavone F, Pedrozo Z, Pena FJ, Penalva MA, Pende M, Peng J, Penna F, Penninger JM, Pensalfini A, Pepe S, Pereira GJ, Pereira PC, Perez-de la Cruz V, Perez-Perez ME, Perez-Rodriguez D, Perez-Sala D, Perier C, Perl A, Perlmutter DH, Perrotta I, Pervaiz S, Pesonen M, Pessin JE, Peters GJ, Petersen M, Petrache I, Petrof BJ, Petrovski G, Phang JM, Piacentini M, Pierdominici M, Pierre P, Pierrefite-Carle V, Pietrocola F, Pimentel-Muinos FX, Pinar M, Pineda B, Pinkas-Kramarski R, Pinti M, Pinton P, Piperdi B, Piret JM, Platanias LC, Platta HW, Plowey ED, Poggeler S, Poirot M, Polcic P, Poletti A, Poon AH, Popelka H, Popova B, Poprawa I, Poulose SM, Poulton J, Powers SK, Powers T, Pozuelo-Rubio M, Prak K, Prange R, Prescott M, Priault M, Prince S, Proia RL, Proikas-Cezanne T, Prokisch H, Promponas VJ, Przyklenk K, Puertollano R, Pugazhenthi S, Puglielli L, Pujol A, Puyal J, Pyeon D, Qi X, Qian WB, Qin ZH, Qiu Y, Qu Z, Quadrilatero J, Quinn F, Raben N, Rabinowich H, Radogna F, Ragusa MJ, Rahmani M, Raina K, Ramanadham S, Ramesh R, Rami A, Randall-Demllo S, Randow F, Rao H, Rao VA, Rasmussen BB, Rasse TM, Ratovitski EA, Rautou PE, Ray SK, Razani B, Reed BH, Reggiori F, Rehm M, Reichert AS, Rein T, Reiner DJ, Reits E, Ren J, Ren X, Renna M, Reusch JE, Revuelta JL, Reyes L, Rezaie AR, Richards RI, Richardson DR, Richetta C, Riehle MA, Rihn BH, Rikihisa Y, Riley BE, Rimbach G,

Rippo MR, Ritis K, Rizzi F, Rizzo E, Roach PJ, Robbins J, Roberge M, Roca G, Roccheri MC, Rocha S, Rodrigues CM, Rodriguez CI, de Cordoba SR, Rodriguez-Muela N, Roelofs J, Rogov VV, Rohn TT, Rohrer B, Romanelli D, Romani L, Romano PS, Roncero MI, Rosa JL, Rosello A, Rosen KV, Rosenstiel P, Rost-Roszkowska M, Roth KA, Roue G, Rouis M, Rouschop KM, Ruan DT, Ruano D, Rubinsztein DC, Rucker EB, 3rd, Rudich A, Rudolf E, Rudolf R, Ruegg MA, Ruiz-Roldan C, Ruparelia AA, Rusmini P, Russ DW, Russo GL, Russo G, Russo R, Rusten TE, Ryabovol V, Ryan KM, Ryter SW, Sabatini DM, Sacher M, Sachse C, Sack MN, Sadoshima J, Saftig P, Sagi-Eisenberg R, Sahni S, Saikumar P, Saito T, Saitoh T, Sakakura K, Sakoh-Nakatogawa M, Sakuraba Y, Salazar-Roa M, Salomoni P, Saluja AK, Salvaterra PM, Salvioli R, Samali A, Sanchez AM, Sanchez-Alcazar JA, Sanchez-Prieto R, Sandri M, Sanjuan MA, Santaguida S, Santambrogio L, Santoni G, Dos Santos CN, Saran S, Sardiello M, Sargent G, Sarkar P, Sarkar S, Sarrias MR, Sarwal MM, Sasakawa C, Sasaki M, Sass M, Sato K, Sato M, Satriano J, Savaraj N, Saveljeva S, Schaefer L, Schaible UE, Scharl M, Schatzl HM, Schekman R, Scheper W, Schiavi A, Schipper HM, Schmeisser H, Schmidt J, Schmitz I, Schneider BE, Schneider EM, Schneider JL, Schon EA, Schonenberger MJ, Schonthal AH, Schorderet DF, Schroder B, Schuck S, Schulze RJ, Schwarten M, Schwarz TL, Sciarretta S, Scotto K, Scovassi AI, Screaton RA, Screen M, Seca H, Sedej S, Segatori L, Segev N, Seglen PO, Segui-Simarro JM, Segura-Aguilar J, Seki E, Sell C, Selliez I, Semenkovich CF, Semenza GL, Sen U, Serra AL, Serrano-Puebla A, Sesaki H, Setoguchi T, Settembre C, Shacka JJ, Shajahan-Haq AN, Shapiro IM, Sharma S, She H, Shen CK, Shen CC, Shen HM, Shen S, Shen W, Sheng R, Sheng X, Sheng ZH, Shepherd TG, Shi J, Shi Q, Shi Q, Shi Y, Shibutani S, Shibuya K, Shidoji Y, Shieh JJ, Shih CM, Shimada Y, Shimizu S, Shin DW, Shinohara ML, Shintani M, Shintani T, Shioi T, Shirabe K, Shiri-Sverdlov R, Shirihai O, Shore GC, Shu CW, Shukla D, Sibirny AA, Sica V, Sigurdson CJ, Sigurdsson EM, Sijwali PS, Sikorska B, Silveira WA, Silvente-Poirot S, Silverman GA, Simak J, Simmet T, Simon AK, Simon HU, Simone C, Simons M, Simonsen A, Singh R, Singh SV, Singh SK, Sinha D, Sinha S, Sinicrope FA, Sirko A, Sirohi K, Sishi BJ, Sittler A, Siu PM, Sivridis E, Skwarska A, Slack R, Slaninova I, Slavov N, Smaili SS, Smalley KS, Smith DR, Soenen SJ, Soleimanpour SA, Solhaug A, Somasundaram K, Son JH, Sonawane A, Song C, Song F, Song HK, Song JX, Song W, Soo KY, Sood AK, Soong TW, Soontornniyomkij V, Sorice M, Sotgia F, Soto-Pantoja DR, Sotthibundhu A, Sousa MJ, Spaink HP, Span PN, Spang A, Sparks JD, Speck PG, Spector SA, Spies CD, Springer W, Clair DS, Stacchiotti A, Staels B, Stang MT, Starczynowski DT, Starokadomskyy P, Steegborn C, Steele JW, Stefanis L, Steffan J, Stellrecht CM, Stenmark H, Stepkowski TM, Stern ST, Stevens C, Stockwell BR, Stoka V, Storchova Z, Stork B, Stratoulias V, Stravopodis DJ, Strnad P, Strohecker AM, Strom AL, Stromhaug P, Stulik J, Su YX, Su Z, Subauste CS, Subramaniam S, Sue CM, Suh SW, Sui X, Sukseree S, Sulzer D, Sun FL, Sun J, Sun J, Sun SY, Sun Y, Sun Y, Sun Y, Sundaramoorthy V, Sung J, Suzuki H, Suzuki K, Suzuki N, Suzuki T, Suzuki YJ, Swanson MS, Swanton C, Sward K, Swarup G, Sweeney ST, Sylvester PW, Szatmari Z, Szegezdi E, Szlosarek PW, Taegtmeyer H, Tafani M, Taillebourg E, Tait SW, Takacs-Vellai K, Takahashi Y, Takats S, Takemura G, Takigawa N, Talbot NJ, Tamagno E, Tamburini J, Tan CP, Tan L, Tan ML, Tan M, Tan YJ, Tanaka K, Tanaka M, Tang D, Tang D, Tang G, Tanida I, Tanji K, Tannous BA, Tapia JA, Tasset-Cuevas I, Tatar M, Tavassoly I, Tavernarakis N, Taylor A, Taylor GS, Taylor GA, Taylor JP, Taylor MJ,

Tchetina EV, Tee AR, Teixeira-Clerc F, Telang S, Tencomnao T, Teng BB, Teng RJ, Terro F, Tettamanti G, Theiss AL, Theron AE, Thomas KJ, Thome MP, Thomes PG, Thorburn A, Thorner J, Thum T, Thumm M, Thurston TL, Tian L, Till A, Ting JP, Titorenko VI, Toker L, Toldo S, Tooze SA, Topisirovic I, Torgersen ML, Torosantucci L, Torriglia A, Torrisi MR, Tournier C, Towns R, Trajkovic V, Travassos LH, Triola G, Tripathi DN, Trisciuoglio D, Troncoso R, Trougakos IP, Truttmann AC, Tsai KJ, Tschan MP, Tseng YH, Tsukuba T, Tsung A, Tsvetkov AS, Tu S, Tuan HY, Tucci M, Tumbarello DA, Turk B, Turk V, Turner RF, Tveita AA, Tyagi SC, Ubukata M, Uchiyama Y, Udelnow A, Ueno T, Umekawa M, Umemiya-Shirafuji R, Underwood BR, Ungermann C, Ureshino RP, Ushioda R, Uversky VN, Uzcategui NL, Vaccari T, Vaccaro MI, Vachova L, Vakifahmetoglu-Norberg H, Valdor R, Valente EM, Vallette F, Valverde AM, Van den Berghe G, Van Den Bosch L, van den Brink GR, van der Goot FG, van der Klei IJ, van der Laan LJ, van Doorn WG, van Egmond M, van Golen KL, Van Kaer L, van Lookeren Campagne M, Vandenabeele P, Vandenberghe W, Vanhorebeek I, Varela-Nieto I, Vasconcelos MH, Vasko R, Vavvas DG, Vega-Naredo I, Velasco G, Velentzas AD, Velentzas PD, Vellai T, Vellenga E, Vendelbo MH, Venkatachalam K, Ventura N, Ventura S, Veras PS, Verdier M, Vertessy BG, Viale A, Vidal M, Vieira HL, Vierstra RD, Vigneswaran N, Vij N, Vila M, Villar M, Villar VH, Villarroya J, Vindis C, Viola G, Viscomi MT, Vitale G, Vogl DT, Voitsekhovskaja OV, von Haefen C, von Schwarzenberg K, Voth DE, Vouret-Craviari V, Vuori K, Vyas JM, Waeber C, Walker CL, Walker MJ, Walter J, Wan L, Wan X, Wang B, Wang C, Wang CY, Wang C, Wang C, Wang C, Wang D, Wang F, Wang F, Wang G, Wang HJ, Wang H, Wang HG, Wang H, Wang HD, Wang J, Wang J, Wang M, Wang MQ, Wang PY, Wang P, Wang RC, Wang S, Wang TF, Wang X, Wang XJ, Wang XW, Wang X, Wang X, Wang Y, Wang Y, Wang Y, Wang YJ, Wang Y, Wang Y, Wang YT, Wang Y, Wang ZN, Wappner P, Ward C, Ward DM, Warnes G, Watada H, Watanabe Y, Watase K, Weaver TE, Weekes CD, Wei J, Weide T, Weihl CC, Weindl G, Weis SN, Wen L, Wen X, Wen Y, Westermann B, Weyand CM, White AR, White E, Whitton JL, Whitworth AJ, Wiels J, Wild F, Wildenberg ME, Wileman T, Wilkinson DS, Wilkinson S, Willbold D, Williams C, Williams K, Williamson PR, Winklhofer KF, Witkin SS, Wohlgemuth SE, Wollert T, Wolvetang EJ, Wong E, Wong GW, Wong RW, Wong VK, Woodcock EA, Wright KL, Wu C, Wu D, Wu GS, Wu J, Wu J, Wu M, Wu M, Wu S, Wu WK, Wu Y, Wu Z, Xavier CP, Xavier RJ, Xia GX, Xia T, Xia W, Xia Y, Xiao H, Xiao J, Xiao S, Xiao W, Xie CM, Xie Z, Xie Z, Xilouri M, Xiong Y, Xu C, Xu C, Xu F, Xu H, Xu H, Xu J, Xu J, Xu J, Xu L, Xu X, Xu Y, Xu Y, Xu ZX, Xu Z, Xue Y, Yamada T, Yamamoto A, Yamanaka K, Yamashina S, Yamashiro S, Yan B, Yan B, Yan X, Yan Z, Yanagi Y, Yang DS, Yang JM, Yang L, Yang M, Yang PM, Yang P, Yang Q, Yang W, Yang WY, Yang X, Yang Y, Yang Y, Yang Z, Yang Z, Yao MC, Yao PJ, Yao X, Yao Z, Yao Z, Yasui LS, Ye M, Yedvobnick B, Yeganeh B, Yeh ES, Yeyati PL, Yi F, Yi L, Yin XM, Yip CK, Yoo YM, Yoo YH, Yoon SY, Yoshida K, Yoshimori T, Young KH, Yu H, Yu JJ, Yu JT, Yu J, Yu L, Yu WH, Yu XF, Yu Z, Yuan J, Yuan ZM, Yue BY, Yue J, Yue Z, Zacks DN, Zacksenhaus E, Zaffaroni N, Zaglia T, Zakeri Z, Zecchini V, Zeng J, Zeng M, Zeng Q, Zervos AS, Zhang DD, Zhang F, Zhang G, Zhang GC, Zhang H, Zhang H, Zhang H, Zhang H, Zhang J, Zhang J, Zhang J, Zhang J, Zhang JP, Zhang L, Zhang L, Zhang L, Zhang L, Zhang MY, Zhang X, Zhang XD, Zhang Y, Zhang Y, Zhang Y, Zhang Y, Zhang Y, Zhao M, Zhao WL, Zhao X, Zhao YG, Zhao Y, Zhao Y, Zhao YX,

Zhao Z, Zhao ZJ, Zheng D, Zheng XL, Zheng X, Zhivotovsky B, Zhong Q, Zhou GZ, Zhou G, Zhou H, Zhou SF, Zhou XJ, Zhu H, Zhu H, Zhu WG, Zhu W, Zhu XF, Zhu Y, Zhuang SM, Zhuang X, Ziparo E, Zois CE, Zoladek T, Zong WX, Zorzano A and Zughaier SM (2016) Guidelines for the use and interpretation of assays for monitoring autophagy (3rd edition). *Autophagy* **12**(1): 1-222.

Kluck RM, Bossy-Wetzel E, Green DR and Newmeyer DD (1997) The release of cytochrome c from mitochondria: a primary site for Bcl-2 regulation of apoptosis. *Science* **275**(5303): 1132-1136.

Knox JJ, Hotte SJ, Kollmannsberger C, Winquist E, Fisher B and Eisenhauer EA (2007) Phase II study of Triapine in patients with metastatic renal cell carcinoma: a trial of the National Cancer Institute of Canada Clinical Trials Group (NCIC IND.161). *Invest New Drugs* **25**(5): 471-477.

Kohen R, Szyf M and Chevion M (1986) Quantitation of single- and double-strand DNA breaks in vitro and in vivo. *Anal Biochem* **154**(2): 485-491.

Kondo Y, Kanzawa T, Sawaya R and Kondo S (2005) The role of autophagy in cancer development and response to therapy. *Nat Rev Cancer* **5**(9): 726-734.

Kondratskyi A, Yassine M, Slomianny C, Kondratska K, Gordienko D, Dewailly E, Lehen'kyi V, Skryma R and Prevarskaya N (2014) Identification of ML-9 as a lysosomotropic agent targeting autophagy and cell death. *Cell Death Dis* **5**: e1193.

Konopleva M, Watt J, Contractor R, Tsao T, Harris D, Estrov Z, Bornmann W, Kantarjian H, Viallet J, Samudio I and Andreeff M (2008) Mechanisms of antileukemic activity of the novel Bcl-2 homology domain-3 mimetic GX15-070 (obatoclax). *Cancer Res* **68**(9): 3413-3420.

Kos J and Lah TT (1998) Cysteine proteinases and their endogenous inhibitors: target proteins for prognosis, diagnosis and therapy in cancer (review). *Oncol Rep* **5**(6): 1349-1361.

Kovacevic Z and Richardson DR (2006) The metastasis suppressor, Ndrg-1: a new ally in the fight against cancer. *Carcinogenesis* **27**(12): 2355-2366.

Kovacevic Z, Kalinowski DS, Lovejoy DB, Quach P, Wong J and Richardson DR (2010) Iron Chelators: Development of Novel Compounds with High and Selective Anti-Tumour Activity. *Current drug delivery* **7**(3): 194-207.

Kovacevic Z, Chikhani S, Lovejoy DB and Richardson DR (2011) Novel thiosemicarbazone iron chelators induce up-regulation and phosphorylation of the metastasis suppressor N-myc down-stream regulated gene 1: a new strategy for the treatment of pancreatic cancer. *Mol Pharmacol* **80**(4): 598-609.

Kovacevic Z, Chikhani S, Lui GY, Sivagurunathan S and Richardson DR (2013) The iron-regulated metastasis suppressor NDRG1 targets NEDD4L, PTEN, and SMAD4 and inhibits the PI3K and Ras signaling pathways. *Antioxid Redox Signal* **18**(8): 874-887.

Kovala-Demertzi D, Yadav PN, Wiecek J, Skoulika S, Varadinova T and Demertzis MA (2006) Zinc(II) complexes derived from pyridine-2-carbaldehyde thiosemicarbazone and (1E)-1-pyridin-2-ylethan-1-one thiosemicarbazone. Synthesis, crystal structures and antiproliferative activity of zinc(II) complexes. *J Inorg Biochem* **100**(9): 1558-1567.

Kowol CR, Berger R, Eichinger R, Roller A, Jakupec MA, Schmidt PP, Arion VB and Keppler BK (2007a) Gallium(III) and iron(III) complexes of alpha-N-heterocyclic thiosemicarbazones: synthesis, characterization, cytotoxicity, and interaction with ribonucleotide reductase. *J Med Chem* **50**(6): 1254-1265.

Kowol CR, Eichinger R, Jakupec MA, Galanski M, Arion VB and Keppler BK (2007b) Effect of metal ion complexation and chalcogen donor identity on the antiproliferative activity of 2-acetylpyridine N,N-dimethyl(chalcogen)semicarbazones. *J Inorg Biochem* **101**(11-12): 1946-1957.

Kowol CR, Trondl R, Arion VB, Jakupec MA, Lichtscheidl I and Keppler BK (2010) Fluorescence properties and cellular distribution of the investigational anticancer drug triapine (3-aminopyridine-2-carboxaldehyde thiosemicarbazone) and its zinc(II) complex. *Dalton Trans* **39**(3): 704-706.

Kozopas KM, Yang T, Buchan HL, Zhou P and Craig RW (1993) MCL1, a gene expressed in programmed myeloid cell differentiation, has sequence similarity to BCL2. *Proc Natl Acad Sci USA* **90**(8): 3516-3520.

Kramer DL, Black JD, Mett H, Bergeron RJ and Porter CW (1998) Lysosomal sequestration of polyamine analogues in Chinese hamster ovary cells resistant to the S-adenosylmethionine decarboxylase inhibitor, CGP-48664. *Cancer Res* **58**(17): 3883-3890.

Krauter B, Nagel W, Hartmann HJ and Weser U (1989) Copper-thionein in melanoma. *Biochim Biophys Acta* **1013**(3): 212-217.

Kroemer G (1997) The proto-oncogene Bcl-2 and its role in regulating apoptosis. *Nat Med* **3**(6): 614-620.

Kunnath RJ, Prathapachandra Kurup MR and Ng SW (2012) Di-mu-azido-kappa(4)N(1):N(1')-bis-({1-[(E)-phen-yl(pyridin-2-yl-kappaN)methyl-id ene]thio-semi-carbazidato-kappa(2)N(1),S}copper(II)). *Acta Crystallogr Sect E Struct Rep Online* **68**(Pt 9): m1195.

Kuppens IE, Bosch TM, van Maanen MJ, Rosing H, Fitzpatrick A, Beijnen JH and Schellens JH (2005) Oral bioavailability of docetaxel in combination with OC144-093 (ONT-093). *Cancer Chemother Pharmacol* **55**(1): 72-78.

Kuppens IE, Witteveen EO, Jewell RC, Radema SA, Paul EM, Mangum SG, Beijnen JH, Voest EE and Schellens JH (2007) A phase I, randomized, open-label, parallel-cohort, dose-finding study of elacridar (GF120918) and oral topotecan in cancer patients. *Clin Cancer Res* **13**(11): 3276-3285.

Kurz T, Gustafsson B and Brunk UT (2006) Intralysosomal iron chelation protects against oxidative stress-induced cellular damage. *FEBS J* **273**(13): 3106-3117.

Kurz T, Eaton JW and Brunk UT (2010) Redox activity within the lysosomal compartment: implications for aging and apoptosis. *Antioxid Redox Signal* **13**(4): 511-523.

Kuwana T, Bouchier-Hayes L, Chipuk JE, Bonzon C, Sullivan BA, Green DR and Newmeyer DD (2005) BH3 domains of BH3-only proteins differentially regulate Bax-mediated mitochondrial membrane permeabilization both directly and indirectly. *Mol Cell* **17**(4): 525-535.

Lai SL, Goldstein LJ, Gottesman MM, Pastan I, Tsai CM, Johnson BE, Mulshine JL, Ihde DC, Kayser K and Gazdar AF (1989) MDR1 gene expression in lung cancer. *J Natl Cancer Inst* **81**(15): 1144-1150.

Lane DJ, Saletta F, Suryo Rahmanto Y, Kovacevic Z and Richardson DR (2013) N-myc downstream regulated 1 (NDRG1) is regulated by eukaryotic initiation factor 3a (eIF3a) during cellular stress caused by iron depletion. *PLoS One* **8**(2): e57273.

Le Blanc M, Russo J, Kudelka AP and Smith JA (2002) An in vitro study of inhibitory activity of gossypol, a cottonseed extract, in human carcinoma cell lines. *Pharmacol Res* **46**(6): 551-555.

Le NT and Richardson DR (2004) Iron chelators with high antiproliferative activity up-regulate the expression of a growth inhibitory and metastasis suppressor gene: a link between iron metabolism and proliferation. *Blood* **104**(9): 2967-2975.

Lee EF, Czabotar PE, van Delft MF, Michalak EM, Boyle MJ, Willis SN, Puthalakath H, Bouillet P, Colman PM, Huang DC and Fairlie WD (2008) A novel BH3 ligand that selectively targets Mcl-1 reveals that apoptosis can proceed without Mcl-1 degradation. *J Cell Biol* **180**(2): 341-355.

Leonard GD, Fojo T and Bates SE (2003) The role of ABC transporters in clinical practice. *Oncologist* **8**(5): 411-424.

Lessene G, Czabotar PE and Colman PM (2008) BCL-2 family antagonists for cancer therapy. *Nat Rev Drug Discov* **7**(12): 989-1000.

Letai A, Bassik MC, Walensky LD, Sorcinelli MD, Weiler S and Korsmeyer SJ (2002) Distinct BH3 domains either sensitize or activate mitochondrial apoptosis, serving as prototype cancer therapeutics. *Cancer Cell* **2**(3): 183-192.

Li J, Jaimes KF and Aller SG (2014) Refined structures of mouse P-glycoprotein. *Protein Sci* **23**(1): 34-46.

Li Ming X, Zhou J, Chen Chun L and Wang Jing P (2008) Synthesis, crystal structure and antitumor study of a zinc complex of the 2-benzoylpyridine thiosemicarbazone ligand. *Z Naturforsch B* **63**(3): 280.

Li MX, Chen CL, Zhang D, Niu JY and Ji BS (2010) Mn(II), Co(II) and Zn(II) complexes with heterocyclic substituted thiosemicarbazones: Synthesis, characterization, X-ray crystal structures and antitumor comparison. *Eur J Med Chem* **45**(7): 3169-3177.

Li P, Nijhawan D, Budihardjo I, Srinivasula SM, Ahmad M, Alnemri ES and Wang X (1997) Cytochrome c and dATP-dependent formation of Apaf-1/caspase-9 complex initiates an apoptotic protease cascade. *Cell* **91**(4): 479-489.

Liang XH, Kleeman LK, Jiang HH, Gordon G, Goldman JE, Berry G, Herman B and Levine B (1998) Protection against fatal Sindbis virus encephalitis by beclin, a novel Bcl-2-interacting protein. *J Virol* **72**(11): 8586-8596.

Liberta AE and West DX (1992) Antifungal and antitumor activity of heterocyclic thiosemicarbazones and their metal complexes: current status. *Biometals* **5**(2): 121-126.

Lim S, Price KA, Chong SF, Paterson BM, Caragounis A, Barnham KJ, Crouch PJ, Peach JM, Dilworth JR, White AR and Donnelly PS (2010) Copper and zinc bis(thiosemicarbazonato) complexes with a fluorescent tag: synthesis, radiolabelling with copper-64, cell uptake and fluorescence studies. *J Biol Inorg Chem* **15**(2): 225-235.

Lippard SJ (1999) Free copper ions in the cell? *Science* **284**(5415): 748-749.

Lithgow T, van Driel R, Bertram JF and Strasser A (1994) The protein product of the oncogene bcl-2 is a component of the nuclear envelope, the endoplasmic reticulum, and the outer mitochondrial membrane. *Cell Growth Differ* **5**(4): 411-417.

Liu MC, Lin TS and Sartorelli AC (1992) Synthesis and antitumor activity of amino derivatives of pyridine-2-carboxaldehyde thiosemicarbazone. *J Med Chem* **35**(20): 3672-3677.

Liu W, Xing F, Iiizumi-Gairani M, Okuda H, Watabe M, Pai SK, Pandey PR, Hirota S, Kobayashi A, Mo YY, Fukuda K, Li Y and Watabe K (2012) N-myc downstream regulated gene 1 modulates Wnt-beta-catenin signalling and pleiotropically suppresses metastasis. *EMBO Mol Med* **4**(2): 93-108.

Liu W, Yue F, Zheng M, Merlot A, Bae DH, Huang M, Lane D, Jansson P, Lui GY, Richardson V, Sahni S, Kalinowski D, Kovacevic Z and Richardson DR (2015) The proto-oncogene

c-Src and its downstream signaling pathways are inhibited by the metastasis suppressor, NDRG1. *Oncotarget* **6**(11): 8851-8874.

Liu X, Dai S, Zhu Y, Marrack P and Kappler JW (2003) The structure of a Bcl-xL/Bim fragment complex: implications for Bim function. *Immunity* **19**(3): 341-352.

Lobana TS, Khanna S and Butcher RJ (2012) 2-Benzoylpyridine thiosemicarbazone as a novel reagent for the single pot synthesis of dinuclear Cu(I)-Cu(II) complexes: formation of stable copper(II)-iodide bonds. *Dalton Trans* **41**(16): 4845-4851.

Lovejoy DB and Richardson DR (2002) Novel "hybrid" iron chelators derived from aroylhydrazones and thiosemicarbazones demonstrate selective antiproliferative activity against tumor cells. *Blood* **100**(2): 666-676.

Lovejoy DB, Jansson PJ, Brunk UT, Wong J, Ponka P and Richardson DR (2011) Antitumor activity of metal-chelating compound Dp44mT is mediated by formation of a redox-active copper complex that accumulates in lysosomes. *Cancer Res* **71**(17): 5871-5880.

Lovejoy DB, Sharp DM, Seebacher N, Obeidy P, Prichard T, Stefani C, Basha MT, Sharpe PC, Jansson PJ, Kalinowski DS, Bernhardt PV and Richardson DR (2012) Novel second-generation di-2-pyridylketone thiosemicarbazones show synergism with standard chemotherapeutics and demonstrate potent activity against lung cancer xenografts after oral and intravenous administration in vivo. *J Med Chem* **55**(16): 7230-7244.

Lübke T, Lobel P and Sleat DE (2009) Proteomics of the lysosome. *Biochim Biophys Acta* **1793**(4): 625-635.

Lui GY, Kovacevic Z, S VM, Kalinowski DS, Merlot AM, Sahni S and Richardson DR (2015) Novel thiosemicarbazones regulate the signal transducer and activator of transcription 3 (STAT3) pathway: inhibition of constitutive and interleukin 6-induced activation by iron depletion. *Mol Pharmacol* **87**(3): 543-560.

Lum BL, Kaubisch S, Yahanda AM, Adler KM, Jew L, Ehsan MN, Brophy NA, Halsey J, Gosland MP and Sikic BI (1992) Alteration of etoposide pharmacokinetics and pharmacodynamics by cyclosporine in a phase I trial to modulate multidrug resistance. *J Clin Oncol* **10**(10): 1635-1642.

Mahoney BP, Raghunand N, Baggett B and Gillies RJ (2003) Tumor acidity, ion trapping and chemotherapeutics. I. Acid pH affects the distribution of chemotherapeutic agents in vitro. *Biochem Pharmacol* **66**(7): 1207-1218.

Maliepaard M, van Gastelen MA, Tohgo A, Hausheer FH, van Waardenburg RC, de Jong LA, Pluim D, Beijnen JH and Schellens JH (2001) Circumvention of breast cancer resistance protein (BCRP)-mediated resistance to camptothecins in vitro using non-substrate drugs or the BCRP inhibitor GF120918. *Clin Cancer Res* **7**(4): 935-941.

Manero F, Gautier F, Gallenne T, Cauquil N, Gree D, Cartron PF, Geneste O, Gree R, Vallette FM and Juin P (2006) The small organic compound HA14-1 prevents Bcl-2 interaction with Bax to sensitize malignant glioma cells to induction of cell death. *Cancer Res* **66**(5): 2757-2764.

Martin C, Berridge G, Mistry P, Higgins C, Charlton P and Callaghan R (1999) The molecular interaction of the high affinity reversal agent XR9576 with P-glycoprotein. *Br J Pharmacol* **128**(2): 403-411.

Maruyama Y, Ono M, Kawahara A, Yokoyama T, Basaki Y, Kage M, Aoyagi S, Kinoshita H and Kuwano M (2006) Tumor growth suppression in pancreatic cancer by a putative metastasis suppressor gene Cap43/NDRG1/Drg-1 through modulation of angiogenesis. *Cancer Res* **66**(12): 6233-6242.

Mason KD, Carpinelli MR, Fletcher JI, Collinge JE, Hilton AA, Ellis S, Kelly PN, Ekert PG, Metcalf D, Roberts AW, Huang DC and Kile BT (2007) Programmed anuclear cell death delimits platelet life span. *Cell* **128**(6): 1173-1186.

McDonnell TJ, Troncoso P, Brisbay SM, Logothetis C, Chung LW, Hsieh JT, Tu SM and Campbell ML (1992) Expression of the protooncogene bcl-2 in the prostate and its association with emergence of androgen-independent prostate cancer. *Cancer Res* **52**(24): 6940-6944.

McNeil PL (2002) Repairing a torn cell surface: make way, lysosomes to the rescue. *J Cell Sci* **115**(Pt 5): 873-879.

Mellman I, Fuchs R and Helenius A (1986) Acidification of the endocytic and exocytic pathways. *Annu Rev Biochem* **55**: 663-700.

Merino D, Giam M, Hughes PD, Siggs OM, Heger K, O'Reilly LA, Adams JM, Strasser A, Lee EF, Fairlie WD and Bouillet P (2009) The role of BH3-only protein Bim extends beyond inhibiting Bcl-2-like prosurvival proteins. *J Cell Biol* **186**(3): 355-362.

Merino D, Khaw SL, Glaser SP, Anderson DJ, Belmont LD, Wong C, Yue P, Robati M, Phipson B, Fairlie WD, Lee EF, Campbell KJ, Vandenberg CJ, Cory S, Roberts AW, Ludlam MJ, Huang DC and Bouillet P (2012) Bcl-2, Bcl-x(L), and Bcl-w are not equivalent targets of ABT-737 and navitoclax (ABT-263) in lymphoid and leukemic cells. *Blood* **119**(24): 5807-5816.

Merlot AM, Pantarat N, Lovejoy DB, Kalinowski DS and Richardson DR (2010) Membrane transport and intracellular sequestration of novel thiosemicarbazone chelators for the treatment of cancer. *Molecular pharmacology* **78**(4): 675-684.

Merlot AM, Kalinowski DS and Richardson DR (2013) Novel chelators for cancer treatment: where are we now? *Antioxid Redox Signal* **18**(8): 973-1006.

Miklos W, Pelivan K, Kowol CR, Pirker C, Dornetshuber-Fleiss R, Spitzwieser M, Englinger B, van Schoonhoven S, Cichna-Markl M, Koellensperger G, Keppler BK, Berger W and Heffeter P (2015) Triapine-mediated ABCB1 induction via PKC induces widespread therapy unresponsiveness but is not underlying acquired triapine resistance. *Cancer Lett* **361**(1): 112-120.

Miletti-Gonzalez KE, Chen S, Muthukumaran N, Saglimbeni GN, Wu X, Yang J, Apolito K, Shih WJ, Hait WN and Rodriguez-Rodriguez L (2005) The CD44 receptor interacts with P-glycoprotein to promote cell migration and invasion in cancer. *Cancer Res* **65**(15): 6660-6667.

Miller TP, Grogan TM, Dalton WS, Spier CM, Scheper RJ and Salmon SE (1991) P-glycoprotein expression in malignant lymphoma and reversal of clinical drug resistance with chemotherapy plus high-dose verapamil. *J Clin Oncol* **9**(1): 17-24.

Minchinton AI and Tannock IF (2006) Drug penetration in solid tumours. *Nat Rev Cancer* **6**(8): 583-592.

Mistry P, Stewart AJ, Dangerfield W, Okiji S, Liddle C, Bootle D, Plumb JA, Templeton D and Charlton P (2001) In vitro and in vivo reversal of P-glycoprotein-mediated multidrug resistance by a novel potent modulator, XR9576. *Cancer Res* **61**(2): 749-758.

Miyashita T and Reed JC (1993) Bcl-2 oncoprotein blocks chemotherapy-induced apoptosis in a human leukemia cell line. *Blood* **81**(1): 151-157.

Mizushima N, Yoshimori T and Levine B (2010) Methods in mammalian autophagy research. *Cell* **140**(3): 313-326.

Mohammad RM, Goustin AS, Aboukameel A, Chen B, Banerjee S, Wang G, Nikolovska-Coleska Z, Wang S and Al-Katib A (2007) Preclinical studies of TW-37, a new nonpeptidic small-molecule inhibitor of Bcl-2, in diffuse large cell lymphoma xenograft model reveal drug action on both Bcl-2 and Mcl-1. *Clin Cancer Res* **13**(7): 2226-2235.

Molinari A, Calcabrini A, Meschini S, Stringaro A, Crateri P, Toccacieli L, Marra M, Colone M, Cianfriglia M and Arancia G (2002) Subcellular detection and localization of the drug transporter P-glycoprotein in cultured tumor cells. *Current protein & peptide science* **3**(6): 653-670.

Montazami N, Kheir Andish M, Majidi J, Yousefi M, Yousefi B, Mohamadnejad L, Shanebandi D, Estiar MA, Khaze V, Mansoori B, Baghbani E and Baradaran B (2015) siRNA-mediated silencing of MDR1 reverses the resistance to oxaliplatin in SW480/OxR colon cancer cells. *Cell Mol Biol* **61**(2): 98-103.

Mu FT, Callaghan JM, Steele-Mortimer O, Stenmark H, Parton RG, Campbell PL, McCluskey J, Yeo JP, Tock EP and Toh BH (1995) EEA1, an early endosome-associated protein. EEA1 is a conserved alpha-helical peripheral membrane protein flanked by cysteine "fingers" and contains a calmodulin-binding IQ motif. *J Biol Chem* **270**(22): 13503-13511.

Mukhopadhyay S, Panda PK, Sinha N, Das DN and Bhutia SK (2014) Autophagy and apoptosis: where do they meet? *Apoptosis* **19**(4): 555-566.

Munteanu E, Verdier M, Grandjean-Forestier F, Stenger C, Jayat-Vignoles C, Huet S, Robert J and Ratinaud MH (2006) Mitochondrial localization and activity of P-glycoprotein in doxorubicin-resistant K562 cells. *Biochemical pharmacology* **71**(8): 1162-1174.

Myhre O, Andersen JM, Aarnes H and Fonnum F (2003) Evaluation of the probes 2',7'-dichlorofluorescin diacetate, luminol, and lucigenin as indicators of reactive species formation. *Biochem Pharmacol* **65**(10): 1575-1582.

Nagai M, Vo NH, Shin Ogawa L, Chimmanamada D, Inoue T, Chu J, Beaudette-Zlatanova BC, Lu R, Blackman RK, Barsoum J, Koya K and Wada Y (2012) The oncology drug elesclomol selectively transports copper to the mitochondria to induce oxidative stress in cancer cells. *Free Radic Biol Med* **52**(10): 2142-2150.

Nakano K and Vousden KH (2001) PUMA, a novel proapoptotic gene, is induced by p53. *Mol Cell* **7**(3): 683-694.

Nemati F, de Montrion C, Lang G, Kraus-Berthier L, Carita G, Sastre-Garau X, Berniard A, Vallerand D, Geneste O, de Plater L, Pierre A, Lockhart B, Desjardins L, Piperno-Neumann S, Depil S and Decaudin D (2014) Targeting Bcl-2/Bcl-XL induces antitumor activity in uveal melanoma patient-derived xenografts. *PLoS One* **9**(1): e80836.

Nguyen M, Millar DG, Yong VW, Korsmeyer SJ and Shore GC (1993) Targeting of Bcl-2 to the mitochondrial outer membrane by a COOH-terminal signal anchor sequence. *J Biol Chem* **268**(34): 25265-25268.

Nicolini C, Belmont A, Parodi S, Lessin S and Abraham S (1979) Mass action and acridine orange staining: static and flow cytofluorometry. *J Histochem Cytochem* **27**(1): 102-113.

Nilsson E, Ghassemifar R and Brunk UT (1997) Lysosomal heterogeneity between and within cells with respect to resistance against oxidative stress. *Histochem J* **29**(11-12): 857-865.

Nooter K, Westerman AM, Flens MJ, Zaman GJ, Scheper RJ, van Wingerden KE, Burger H, Oostrum R, Boersma T, Sonneveld P and et al. (1995) Expression of the multidrug resistance-associated protein (MRP) gene in human cancers. *Clin Cancer Res* **1**(11): 1301-1310.

Noulsri E, Richardson DR, Lerdwana S, Fucharoen S, Yamagishi T, Kalinowski DS and Pattanapanyasat K (2009) Antitumor activity and mechanism of action of the iron chelator, Dp44mT, against leukemic cells. *Am J Hematol* **84**(3): 170-176.

Nowak-Sliwinska P, Weiss A, van Beijnum JR, Wong TJ, Kilarski WW, Szewczyk G, Verheul HM, Sarna T, van den Bergh H and Griffioen AW (2015) Photoactivation of lysosomally sequestered sunitinib after angiostatic treatment causes vascular occlusion and enhances tumor growth inhibition. *Cell Death Dis* **6**: e1641.

O'Brien S, Moore JO, Boyd TE, Larratt LM, Skotnicki AB, Koziner B, Chanan-Khan AA, Seymour JF, Gribben J, Itri LM and Rai KR (2009) 5-year survival in patients with relapsed or refractory chronic lymphocytic leukemia in a randomized, phase III trial of fludarabine plus cyclophosphamide with or without oblimersen. *J Clin Oncol* **27**(31): 5208-5212.

O'Connor L, Strasser A, O'Reilly LA, Hausmann G, Adams JM, Cory S and Huang DC (1998) Bim: a novel member of the Bcl-2 family that promotes apoptosis. *EMBO J* **17**(2): 384-395.

O'Day SJ, Eggermont AM, Chiarion-Sileni V, Kefford R, Grob JJ, Mortier L, Robert C, Schachter J, Testori A, Mackiewicz J, Friedlander P, Garbe C, Ugurel S, Collichio F, Guo W, Lufkin J, Bahcall S, Vukovic V and Hauschild A (2013) Final results of phase III SYMMETRY study: randomized, double-blind trial of elesclomol plus paclitaxel versus paclitaxel alone as treatment for chemotherapy-naive patients with advanced melanoma. *J Clin Oncol* **31**(9): 1211-1218.

Oda E, Ohki R, Murasawa H, Nemoto J, Shibue T, Yamashita T, Tokino T, Taniguchi T and Tanaka N (2000) Noxa, a BH3-only member of the Bcl-2 family and candidate mediator of p53-induced apoptosis. *Science* **288**(5468): 1053-1058.

Oda Y, Saito T, Tateishi N, Ohishi Y, Tamiya S, Yamamoto H, Yokoyama R, Uchiumi T, Iwamoto Y, Kuwano M and Tsuneyoshi M (2005) ATP-binding cassette superfamily transporter gene expression in human soft tissue sarcomas. *Int J Cancer* **114**(6): 854-862.

Odenike OM, Larson RA, Gajria D, Dolan ME, Delaney SM, Karrison TG, Ratain MJ and Stock W (2008) Phase I study of the ribonucleotide reductase inhibitor 3-aminopyridine-2-carboxaldehyde-thiosemicarbazone (3-AP) in combination with high dose cytarabine in patients with advanced myeloid leukemia. *Invest New Drugs* **26**(3): 233-239.

Ogihara T, Kamiya M, Ozawa M, Fujita T, Yamamoto A, Yamashita S, Ohnishi S and Isomura Y (2006) What kinds of substrates show P-glycoprotein-dependent intestinal absorption? Comparison of verapamil with vinblastine. *Drug Metab Pharmacokinet* **21**(3): 238-244.

Oh KJ, Barbuto S, Pitter K, Morash J, Walensky LD and Korsmeyer SJ (2006) A membrane-targeted BID BCL-2 homology 3 peptide is sufficient for high potency activation of BAX in vitro. *J Biol Chem* **281**(48): 36999-37008.

Ohkuma S, Moriyama Y and Takano T (1982) Identification and characterization of a proton pump on lysosomes by fluorescein-isothiocyanate-dextran fluorescence. *Proc Natl Acad Sci USA* **79**(9): 2758-2762.

Ohtsuki S, Kamoi M, Watanabe Y, Suzuki H, Hori S and Terasaki T (2007) Correlation of induction of ATP binding cassette transporter A5 (ABCA5) and ABCB1 mRNAs with differentiation state of human colon tumor. *Biol Pharm Bull* **30**(6): 1144-1146.

Oka M, Fukuda M, Sakamoto A, Takatani H, Soda H and Kohno S (1997) The clinical role of MDR1 gene expression in human lung cancer. *Anticancer Res* **17**(1B): 721-724.

Olie RA and Zangemeister-Wittke U (2001) Targeting tumor cell resistance to apoptosis induction with antisense oligonucleotides: progress and therapeutic potential. *Drug Resist Updat* **4**(1): 9-15.

Ollinger K and Brunk UT (1995) Cellular injury induced by oxidative stress is mediated through lysosomal damage. *Free Radic Biol Med* **19**(5): 565-574.

Oltersdorf T, Elmore SW, Shoemaker AR, Armstrong RC, Augeri DJ, Belli BA, Bruncko M, Deckwerth TL, Dinges J, Hajduk PJ, Joseph MK, Kitada S, Korsmeyer SJ, Kunzer AR, Letai A, Li C, Mitten MJ, Nettesheim DG, Ng S, Nimmer PM, O'Connor JM, Oleksijew A, Petros AM, Reed JC, Shen W, Tahir SK, Thompson CB, Tomaselli KJ, Wang B, Wendt MD, Zhang H, Fesik SW and Rosenberg SH (2005) An inhibitor of Bcl-2 family proteins induces regression of solid tumours. *Nature* **435**(7042): 677-681.

Oltvai ZN, Milliman CL and Korsmeyer SJ (1993) Bcl-2 heterodimerizes in vivo with a conserved homolog, Bax, that accelerates programmed cell death. *Cell* **74**(4): 609-619.

Ouar Z, Bens M, Vignes C, Paulais M, Pringel C, Fleury J, Cluzeaud F, Lacave R and Vandewalle A (2003) Inhibitors of vacuolar H+-ATPase impair the preferential accumulation of daunomycin in lysosomes and reverse the resistance to anthracyclines in drug-resistant renal epithelial cells. *Biochem J* **370**(Pt 1): 185-193.

Outten CE and O'Halloran TV (2001) Femtomolar sensitivity of metalloregulatory proteins controlling zinc homeostasis. *Science* **292**(5526): 2488-2492.

Palanimuthu D, Shinde SV, Somasundaram K and Samuelson AG (2013) In vitro and in vivo anticancer activity of copper bis(thiosemicarbazone) complexes. *J Med Chem* **56**(3): 722-734.

Pankiv S, Clausen TH, Lamark T, Brech A, Bruun JA, Outzen H, Overvatn A, Bjorkoy G and Johansen T (2007) p62/SQSTM1 binds directly to Atg8/LC3 to facilitate degradation of ubiquitinated protein aggregates by autophagy. *J Biol Chem* **282**(33): 24131-24145.

Pascu SI, Waghorn PA, Conry TD, Betts HM, Dilworth JR, Churchill GC, Pokrovska T, Christlieb M, Aigbirhio FI and Warren JE (2007) Designing Zn(II) and Cu(II) derivatives as probes for in vitro fluorescence imaging. *Dalton Trans*(43): 4988-4997.

Pascu SI, Waghorn PA, Conry TD, Lin B, Betts HM, Dilworth JR, Sim RB, Churchill GC, Aigbirhio FI and Warren JE (2008) Cellular confocal fluorescence studies and cytotoxic activity of new Zn(II) bis(thiosemicarbazonato) complexes. *Dalton Trans*(16): 2107-2110.

Pascu SI, Waghorn PA, Kennedy BW, Arrowsmith RL, Bayly SR, Dilworth JR, Christlieb M, Tyrrell RM, Zhong J, Kowalczyk RM, Collison D, Aley PK, Churchill GC and Aigbirhio FI (2010) Fluorescent copper(II) bis(thiosemicarbazonates): synthesis, structures, electron paramagnetic resonance, radiolabeling, in vitro cytotoxicity and confocal fluorescence microscopy studies. *Chem Asian J* **5**(3): 506-519.

Pattingre S, Tassa A, Qu X, Garuti R, Liang XH, Mizushima N, Packer M, Schneider MD and Levine B (2005) Bcl-2 antiapoptotic proteins inhibit Beclin 1-dependent autophagy. *Cell* **122**(6): 927-939.

Pearce HL, Safa AR, Bach NJ, Winter MA, Cirtain MC and Beck WT (1989) Essential features of the P-glycoprotein pharmacophore as defined by a series of reserpine analogs that modulate multidrug resistance. *Proc Natl Acad Sci USA* **86**(13): 5128-5132.

Petering HG, Buskirk HH and Crim JA (1967) The effect of dietary mineral supplements of the rat on the antitumor activity of 3-ethoxy-2-oxobutyraldehyde bis(thiosemicarbazone). *Cancer Res* **27**(6): 1115-1121.

Petros AM, Medek A, Nettesheim DG, Kim DH, Yoon HS, Swift K, Matayoshi ED, Oltersdorf T and Fesik SW (2001) Solution structure of the antiapoptotic protein bcl-2. *Proc Natl Acad Sci USA* **98**(6): 3012-3017.

Petrucci RH, Harwood WS and Herring FG (2002) *General Chemistry*. 8th ed. Prentics-Hall.

Piao S and Amaravadi RK (2015) Targeting the lysosome in cancer. *Ann N Y Acad Sci*.

Piche A, Grim J, Rancourt C, Gomez-Navarro J, Reed JC and Curiel DT (1998) Modulation of Bcl-2 protein levels by an intracellular anti-Bcl-2 single-chain antibody increases drug-induced cytotoxicity in the breast cancer cell line MCF-7. *Cancer Res* **58**(10): 2134-2140.

Pierzynska-Mach A, Janowski PA and Dobrucki JW (2014) Evaluation of acridine orange, LysoTracker Red, and quinacrine as fluorescent probes for long-term tracking of acidic vesicles. *Cytometry A* **85**(8): 729-737.

Pirker R, Goldstein LJ, Ludwig H, Linkesch W, Lechner C, Gottesman MM and Pastan I (1989) Expression of a multidrug resistance gene in blast crisis of chronic myelogenous leukemia. *Cancer Commun* **1**(2): 141-144.

Pirker R, Wallner J, Geissler K, Linkesch W, Haas OA, Bettelheim P, Hopfner M, Scherrer R, Valent P, Havelec L and et al. (1991) MDR1 gene expression and treatment outcome in acute myeloid leukemia. *J Natl Cancer Inst* **83**(10): 708-712.

Placzek WJ, Wei J, Kitada S, Zhai D, Reed JC and Pellecchia M (2010) A survey of the anti-apoptotic Bcl-2 subfamily expression in cancer types provides a platform to predict the efficacy of Bcl-2 antagonists in cancer therapy. *Cell Death Dis* **1**: e40.

Pohlmann R, Krentler C, Schmidt B, Schroder W, Lorkowski G, Culley J, Mersmann G, Geier C, Waheed A, Gottschalk S and et al. (1988) Human lysosomal acid phosphatase: cloning, expression and chromosomal assignment. *EMBO J* **7**(8): 2343-2350.

Ponka P, Borova J, Neuwirt J and Fuchs O (1979) Mobilization of iron from reticulocytes. Identification of pyridoxal isonicotinoyl hydrazone as a new iron chelating agent. *FEBS letters* **97**(2): 317-321.

Premzl A, Zavasnik-Bergant V, Turk V and Kos J (2003) Intracellular and extracellular cathepsin B facilitate invasion of MCF-10A neoT cells through reconstituted extracellular matrix in vitro. *Exp Cell Res* **283**(2): 206-214.

Pusztai L, Wagner P, Ibrahim N, Rivera E, Theriault R, Booser D, Symmans FW, Wong F, Blumenschein G, Fleming DR, Rouzier R, Boniface G and Hortobagyi GN (2005) Phase II study of tariquidar, a selective P-glycoprotein inhibitor, in patients with chemotherapy-resistant, advanced breast carcinoma. *Cancer* **104**(4): 682-691.

Puthalakath H, Villunger A, O'Reilly LA, Beaumont JG, Coultas L, Cheney RE, Huang DC and Strasser A (2001) Bmf: a proapoptotic BH3-only protein regulated by interaction with the myosin V actin motor complex, activated by anoikis. *Science* **293**(5536): 1829-1832.

Quach P, Gutierrez E, Basha MT, Kalinowski DS, Sharpe PC, Lovejoy DB, Bernhardt PV, Jansson PJ and Richardson DR (2012) Methemoglobin formation by triapine, di-2-pyridylketone-4,4-dimethyl-3-thiosemicarbazone (Dp44mT), and other anticancer thiosemicarbazones: identification of novel thiosemicarbazones and therapeutics that prevent this effect. *Mol Pharmacol* **82**(1): 105-114.

Rae JM, Creighton CJ, Meck JM, Haddad BR and Johnson MD (2007) MDA-MB-435 cells are derived from M14 melanoma cells--a loss for breast cancer, but a boon for melanoma research. *Breast Cancer Res Treat* **104**(1): 13-19.

Rae TD, Schmidt PJ, Pufahl RA, Culotta VC and O'Halloran TV (1999) Undetectable intracellular free copper: the requirement of a copper chaperone for superoxide dismutase. *Science* **284**(5415): 805-808.

Raisova M, Hossini AM, Eberle J, Riebeling C, Wieder T, Sturm I, Daniel PT, Orfanos CE and Geilen CC (2001) The Bax/Bcl-2 ratio determines the susceptibility of human melanoma cells to CD95/Fas-mediated apoptosis. *J Invest Dermatol* **117**(2): 333-340.

Rajagopal A and Simon SM (2003a) Subcellular Localization and Activity of Multidrug Resistance. *Mol Biol Cell* **14**(8): 3389-3399.

Rajagopal A and Simon SM (2003b) Subcellular localization and activity of multidrug resistance proteins. *Mol Biol Cell* **14**(8): 3389-3399.

Rao VA, Klein SR, Agama KK, Toyoda E, Adachi N, Pommier Y and Shacter EB (2009) The iron chelator Dp44mT causes DNA damage and selective inhibition of topoisomerase IIalpha in breast cancer cells. *Cancer Res* **69**(3): 948-957.

Rappa G, Lorico A, Liu MC, Kruh GD, Cory AH, Cory JG and Sartorelli AC (1997) Overexpression of the multidrug resistance genes MDR1, MDR3, and MRP in L1210 leukemia cells resistant to inhibitors of ribonucleotide reductase. *Biochem Pharmacol* **54**(6): 649-655.

Recklies AD, Poole AR and Mort JS (1982) A cysteine proteinase secreted from human breast tumours is immunologically related to cathepsin B. *Biochem J* **207**(3): 633-636.

Reichard P and Ehrenberg A (1983) Ribonucleotide reductase--a radical enzyme. *Science* **221**: 514-519.

Repnik U, Hafner Cesen M and Turk B (2014) Lysosomal membrane permeabilization in cell death: concepts and challenges. *Mitochondrion* **19 Pt A**: 49-57.

Richardson DR, Tran EH and Ponka P (1995) The potential of iron chelators of the pyridoxal isonicotinoyl hydrazone class as effective antiproliferative agents. *Blood* **86**(11): 4295-4306.

Richardson DR (1997) Mobilization of iron from neoplastic cells by some iron chelators is an energy-dependent process. *Biochimica et biophysica acta* **1320**(1): 45-57.

Richardson DR and Milnes K (1997) The potential of iron chelators of the pyridoxal isonicotinoyl hydrazone class as effective antiproliferative agents II: the mechanism of action of ligands derived from salicylaldehyde benzoyl hydrazone and 2-hydroxy-1-naphthylaldehyde benzoyl hydrazone. *Blood* **89**(8): 3025-3038.

Richardson DR, Sharpe PC, Lovejoy DB, Senaratne D, Kalinowski DS, Islam M and Bernhardt PV (2006) Dipyridyl thiosemicarbazone chelators with potent and selective antitumor activity form iron complexes with redox activity. *J Med Chem* **49**(22): 6510-6521.

Richardson DR, Kalinowski DS, Richardson V, Sharpe PC, Lovejoy DB, Islam M and Bernhardt PV (2009) 2-Acetylpyridine thiosemicarbazones are potent iron chelators and antiproliferative agents: redox activity, iron complexation and characterization of their antitumor activity. *J Med Chem* **52**(5): 1459-1470.

Riedl SJ and Salvesen GS (2007) The apoptosome: signalling platform of cell death. *Nat Rev Mol Cell Biol* **8**(5): 405-413.

Rink J, Ghigo E, Kalaidzidis Y and Zerial M (2005) Rab conversion as a mechanism of progression from early to late endosomes. *Cell* **122**(5): 735-749.

Ro J, Sahin A, Ro JY, Fritsche H, Hortobagyi G and Blick M (1990) Immunohistochemical analysis of P-glycoprotein expression correlated with chemotherapy resistance in locally advanced breast cancer. *Hum Pathol* **21**(8): 787-791.

Roberg K, Johansson U and Ollinger K (1999) Lysosomal release of cathepsin D precedes relocation of cytochrome c and loss of mitochondrial transmembrane potential during apoptosis induced by oxidative stress. *Free Radic Biol Med* **27**(11-12): 1228-1237.

Roberts AW, Davids MS, Pagel JM, Kahl BS, Puvvada SD, Gerecitano JF, Kipps TJ, Anderson MA, Brown JR, Gressick L, Wong S, Dunbar M, Zhu M, Desai MB, Cerri E, Heitner Enschede S, Humerickhouse RA, Wierda WG and Seymour JF (2016) Targeting BCL2 with Venetoclax in Relapsed Chronic Lymphocytic Leukemia. *N Engl J Med* **374**(4): 311-322.

Rodriguez A, Webster P, Ortego J and Andrews NW (1997) Lysosomes behave as Ca2+-regulated exocytic vesicles in fibroblasts and epithelial cells. *J Cell Biol* **137**(1): 93-104.

Rosenberg MF, Callaghan R, Modok S, Higgins CF and Ford RC (2005) Three-dimensional structure of P-glycoprotein: the transmembrane regions adopt an asymmetric configuration in the nucleotide-bound state. *J Biol Chem* **280**(4): 2857-2862.

Rossi A, Deveraux Q, Turk B and Sali A (2004) Comprehensive search for cysteine cathepsins in the human genome. *Biol Chem* **385**(5): 363-372.

Rothenberg ML, Mickley LA, Cole DE, Balis FM, Tsuruo T, Poplack DG and Fojo AT (1989) Expression of the mdr-1/P-170 gene in patients with acute lymphoblastic leukemia. *Blood* **74**(4): 1388-1395.

Rubin EH, de Alwis DP, Pouliquen I, Green L, Marder P, Lin Y, Musanti R, Grospe SL, Smith SL, Toppmeyer DL, Much J, Kane M, Chaudhary A, Jordan C, Burgess M and Slapak CA (2002) A phase I trial of a potent P-glycoprotein inhibitor, Zosuquidar.3HCl trihydrochloride (LY335979), administered orally in combination with doxorubicin in patients with advanced malignancies. *Clin Cancer Res* **8**(12): 3710-3717.

Rutherford AV and Willingham MC (1993) Ultrastructural localization of daunomycin in multidrug-resistant cultured cells with modulation of the multidrug transporter. *J Histochem Cytochem* **41**(10): 1573-1577.

Saftig P and Klumperman J (2009) Lysosome biogenesis and lysosomal membrane proteins: trafficking meets function. *Nat Rev Mol Cell Biol* **10**(9): 623-635.

Saftig P, Schröder B and Blanz J (2010) Lysosomal membrane proteins: life between acid and neutral conditions. *Biochem Soc Trans* **38**(6): 1420-1423.

Sandler A, Gordon M, De Alwis DP, Pouliquen I, Green L, Marder P, Chaudhary A, Fife K, Battiato L, Sweeney C, Jordan C, Burgess M and Slapak CA (2004) A Phase I trial of a potent P-glycoprotein inhibitor, zosuquidar trihydrochloride (LY335979), administered intravenously in combination with doxorubicin in patients with advanced malignancy. *Clin Cancer Res* **10**(10): 3265-3272.

Sartorelli AC, Moore EC, Zedeck MS and Agrawal KC (1970) Inhibition of ribonucleoside diphosphate reductase by 1-formylisoquinoline thiosemicarbazone and related compounds. *Biochem* **9**(23): 4492-4498.

Sartorelli AC, Agrawal KC and Moore EC (1971) Mechanism of inhibition of ribonucleoside diphosphate reductase by a-(N)-heterocyclic aldehyde thiosemicarbazones. *Biochem Pharmacol* **20**(11): 3119-3123.

Saryan LA, Ankel E, Krishnamurti C, Petering DH and Elford H (1979) Comparative cytotoxic and biochemical effects of ligands and metal complexes of alpha-N-heterocyclic carboxaldehyde thiosemicarbazones. *J Med Chem* **22**(10): 1218-1221.

Sato H, Gottesman MM, Goldstein LJ, Pastan I, Block AM, Sandberg AA and Preisler HD (1990a) Expression of the multidrug resistance gene in myeloid leukemias. *Leuk Res* **14**(1): 11-21.

Sato H, Preisler H, Day R, Raza A, Larson R, Browman G, Goldberg J, Vogler R, Grunwald H, Gottlieb A and et al. (1990b) MDR1 transcript levels as an indication of resistant disease in acute myelogenous leukaemia. *Br J Haematol* **75**(3): 340-345.

Sattler M, Liang H, Nettesheim D, Meadows RP, Harlan JE, Eberstadt M, Yoon HS, Shuker SB, Chang BS, Minn AJ, Thompson CB and Fesik SW (1997) Structure of Bcl-xL-Bak peptide complex: recognition between regulators of apoptosis. *Science* **275**(5302): 983-986.

Savitsky K, Sfez S, Tagle DA, Ziv Y, Sartiel A, Collins FS, Shiloh Y and Rotman G (1995) The complete sequence of the coding region of the ATM gene reveals similarity to cell cycle regulators in different species. *Hum Mol Genet* **4**(11): 2025-2032.

Schindler M, Grabski S, Hoff E and Simon SM (1996) Defective pH regulation of acidic compartments in human breast cancer cells (MCF-7) is normalized in adriamycin-resistant cells (MCF-7adr). *Biochemistry* **35**(9): 2811-2817.

Schmid D, Ecker G, Kopp S, Hitzler M and Chiba P (1999) Structure-activity relationship studies of propafenone analogs based on P-glycoprotein ATPase activity measurements. *Biochem Pharmacol* **58**(9): 1447-1456.

Schmitt CA, Rosenthal CT and Lowe SW (2000) Genetic analysis of chemoresistance in primary murine lymphomas. *Nat Med* **6**(9): 1029-1035.

Schneider DL (1981) ATP-dependent acidification of intact and disrupted lysosomes. Evidence for an ATP-driven proton pump. *J Biol Chem* **256**(8): 3858-3864.

Schneider J, Bak M, Efferth T, Kaufmann M, Mattern J and Volm M (1989) P-glycoprotein expression in treated and untreated human breast cancer. *Br J Cancer* **60**(6): 815-818.

Seebacher N, Lane DJ, Jansson PJ and Richardson D (2016a) Glucose modulation induces lysosome formation and increases lysosomotropic drug sequestration via the P-Glycoprotein drug transporter. *J Biol Chem* **291**(8): 3796-3820.

Seebacher N, Lane DJ, Richardson DR and Jansson PJ (2016b) Turning the gun on cancer: Utilizing lysosomal P-glycoprotein as a new strategy to overcome multi-drug resistance. *Free Radic Biol Med* **96**: 432-445.

Seebacher NA, Richardson DR and Jansson PJ (2015) Glucose modulation induces reactive oxygen species and increases P-glycoprotein-mediated multidrug resistance to chemotherapeutics. *Br J Pharmacol* **172**(10): 2557-2572.

Seebacher NA, Lane DJ, Jansson PJ and Richardson DR (2016c) Glucose modulation induces lysosome formation and increases lysosomotropic drug sequestration via the P-glycoprotein drug transporter. *J Biol Chem* **291**(8): 3796-3820.

Seelig A and Landwojtowicz E (2000) Structure-activity relationship of P-glycoprotein substrates and modifiers. *Eur J Pharm Sci* **12**(1): 31-40.

Seguin SJ, Morelli FF, Vinet J, Amore D, De Biasi S, Poletti A, Rubinsztein DC and Carra S (2014) Inhibition of autophagy, lysosome and VCP function impairs stress granule assembly. *Cell Death Differ* **21**(12): 1838-1851.

Senior AE, al-Shawi MK and Urbatsch IL (1995) The catalytic cycle of P-glycoprotein. *FEBS letters* **377**(3): 285-289.

Sestak V, Stariat J, Cermanova J, Potuckova E, Chladek J, Roh J, Bures J, Jansova H, Prusa P, Sterba M, Micuda S, Simunek T, Kalinowski DS, Richardson DR and Kovarikova P

(2015) Novel and potent anti-tumor and anti-metastatic di-2-pyridylketone thiosemicarbazones demonstrate marked differences in pharmacology between the first and second generation lead agents. *Oncotarget* **6**(40): 42411-42428.

Shao J, Ma Z-Y, Li A, Liu Y-H, Xie C-Z, Qiang Z-Y and Xu J-Y (2014) Thiosemicarbazone Cu(II) and Zn(II) complexes as potential anticancer agents: Syntheses, crystal structure, DNA cleavage, cytotoxicity and apoptosis induction activity. *J Inorg Biochem* **136**: 13-23.

Shapiro AB and Ling V (1997) Positively cooperative sites for drug transport by P-glycoprotein with distinct drug specificities. *Eur J Biochem* **250**(1): 130-137.

Sharom FJ (1997) The P-glycoprotein efflux pump: how does it transport drugs? *J Membr Biol* **160**(3): 161-175.

Sharom FJ, Lugo MR and Eckford PD (2005) New insights into the drug binding, transport and lipid flippase activities of the p-glycoprotein multidrug transporter. *J Bioenerg Biomembr* **37**(6): 481-487.

Sharom FJ (2011) The P-glycoprotein multidrug transporter. *Essays Biochem* **50**(1): 161-178.

Sharom FJ (2014) Complex Interplay between the P-Glycoprotein Multidrug Efflux Pump and the Membrane: Its Role in Modulating Protein Function. *Front Oncol* **4**: 41.

Sheldrick GM (2008) A short history of SHELX. *Acta Crystallogr A* **64**(Pt 1): 112-122.

Shibata MA, Liu ML, Knudson MC, Shibata E, Yoshidome K, Bandey T, Korsmeyer SJ and Green JE (1999) Haploid loss of bax leads to accelerated mammary tumor development in C3(1)/SV40-TAg transgenic mice: reduction in protective apoptotic response at the preneoplastic stage. *EMBO J* **18**(10): 2692-2701.

Shipman C, Jr., Smith SH, Drach JC and Klayman DL (1986) Thiosemicarbazones of 2-acetylpyridine, 2-acetylquinoline, 1-acetylisoquinoline, and related compounds as inhibitors of herpes simplex virus in vitro and in a cutaneous herpes guinea pig model. *Antiviral Res* **6**(4): 197-222.

Sinicrope FA, Hart J, Michelassi F and Lee JJ (1995) Prognostic value of bcl-2 oncoprotein expression in stage II colon carcinoma. *Clin Cancer Res* **1**(10): 1103-1110.

Skommer J, Wlodkowic D, Matto M, Eray M and Pelkonen J (2006) HA14-1, a small molecule Bcl-2 antagonist, induces apoptosis and modulates action of selected anticancer drugs in follicular lymphoma B cells. *Leuk Res* **30**(3): 322-331.

Sloane BF, Dunn JR and Honn KV (1981) Lysosomal cathepsin B: correlation with metastatic potential. *Science* **212**(4499): 1151-1153.

Slor H and Lev T (1971) Acid deoxyribonuclease activity in purified calf thymus nuclei. *Biochem J* **123**(5): 993-995.

Small DM, Burden RE, Jaworski J, Hegarty SM, Spence S, Burrows JF, McFarlane C, Kissenpfennig A, McCarthy HO, Johnston JA, Walker B and Scott CJ (2013) Cathepsin S from both tumor and tumor-associated cells promote cancer growth and neovascularization. *Int J Cancer* **133**(9): 2102-2112.

Soengas MS and Lowe SW (2003) Apoptosis and melanoma chemoresistance. *Oncogene* **22**(20): 3138-3151.

Solary E, Velay I, Chauffert B, Bidan JM, Caillot D, Dumas M and Guy H (1991) Sufficient levels of quinine in the serum circumvent the multidrug resistance of the human leukemic cell line K562/ADM. *Cancer* **68**(8): 1714-1719.

Sonneveld P, Marie JP, Huisman C, Vekhoff A, Schoester M, Faussat AM, van Kapel J, Groenewegen A, Charnick S, Zittoun R and Lowenberg B (1996) Reversal of multidrug

resistance by SDZ PSC 833, combined with VAD (vincristine, doxorubicin, dexamethasone) in refractory multiple myeloma. A phase I study. *Leukemia* **10**(11): 1741-1750.

Souers AJ, Leverson JD, Boghaert ER, Ackler SL, Catron ND, Chen J, Dayton BD, Ding H, Enschede SH, Fairbrother WJ, Huang DC, Hymowitz SG, Jin S, Khaw SL, Kovar PJ, Lam LT, Lee J, Maecker HL, Marsh KC, Mason KD, Mitten MJ, Nimmer PM, Oleksijew A, Park CH, Park CM, Phillips DC, Roberts AW, Sampath D, Seymour JF, Smith ML, Sullivan GM, Tahir SK, Tse C, Wendt MD, Xiao Y, Xue JC, Zhang H, Humerickhouse RA, Rosenberg SH and Elmore SW (2013) ABT-199, a potent and selective BCL-2 inhibitor, achieves antitumor activity while sparing platelets. *Nat Med* **19**(2): 202-208.

Souza P, Matesanz AI and Fernandez V (1996) Copper(II) and cobalt(II) complexes of methyl 2-pyridyl ketone thiosemicarbazone (HL); single-crystal structure of [Cu(HL)L]NCS. *Dalton Trans*(14): 3011-3013.

Sreekanth A and Kurup MRP (2003) Structural and spectral studies on four coordinate copper (II) complexes of 2-benzoylpyridine N (4), N (4)-(butane-1, 4-diyl) thiosemicarbazone. *Polyhedron* **22**(25): 3321-3332.

Stacy AE, Jansson PJ and Richardson DR (2013) Molecular pharmacology of ABCG2 and its role in chemoresistance. *Mol Pharmacol* **84**(5): 655-669.

Stadtman ER (1990) Metal ion-catalyzed oxidation of proteins: biochemical mechanism and biological consequences. *Free Radic Biol Med* **9**(4): 315-325.

Stanojkovic TP, Kovala-Demertzi D, Primikyri A, Garcia-Santos I, Castineiras A, Juranic Z and Demertzis MA (2010) Zinc(II) complexes of 2-acetyl pyridine 1-(4-fluorophenyl)-piperazinyl thiosemicarbazone: Synthesis, spectroscopic study and crystal structures ï Potential anticancer drugs. *J Inorg Biochem* **104**(4): 467-476.

Stariat J, Kovarikova P, Klimes J, Kalinowski DS and Richardson DR (2010) Development of an LC-MS/MS method for analysis of interconvertible Z/E isomers of the novel anticancer agent, Bp4eT. *Anal Bioanal Chem* **397**(1): 161-171.

Stefani C, Punnia-Moorthy G, Lovejoy DB, Jansson PJ, Kalinowski DS, Sharpe PC, Bernhardt PV and Richardson DR (2011) Halogenated 2'-benzoylpyridine thiosemicarbazone (XBpT) chelators with potent and selective anti-neoplastic activity: relationship to intracellular redox activity. *J Med Chem* **54**(19): 6936-6948.

Stefani C, Jansson PJ, Gutierrez E, Bernhardt PV, Richardson DR and Kalinowski DS (2013) Alkyl substituted 2'-benzoylpyridine thiosemicarbazone chelators with potent and selective anti-neoplastic activity: novel ligands that limit methemoglobin formation. *J Med Chem* **56**(1): 357-370.

Stefani C, Al-Eisawi Z, Jansson PJ, Kalinowski DS and Richardson DR (2015) Identification of differential anti-neoplastic activity of copper bis(thiosemicarbazones) that is mediated by intracellular reactive oxygen species generation and lysosomal membrane permeabilization. *J Inorg Biochem* **152**: 20-37.

Stein RC, Joseph AE, Matlin SA, Cunningham DC, Ford HT and Coombes RC (1992) A preliminary clinical study of gossypol in advanced human cancer. *Cancer Chemother Pharmacol* **30**(6): 480-482.

Stilgenbauer S, Eichhorst B, Schetelig J, Coutre S, Seymour JF, Munir T, Puvvada SD, Wendtner CM, Roberts AW, Jurczak W, Mulligan SP, Bottcher S, Mobasher M, Zhu M, Desai M, Chyla B, Verdugo M, Enschede SH, Cerri E, Humerickhouse R, Gordon G, Hallek M and Wierda WG (2016) Venetoclax in relapsed or refractory chronic

lymphocytic leukaemia with 17p deletion: a multicentre, open-label, phase 2 study. *Lancet Oncol*.

Stohs SJ and Bagchi D (1995) Oxidative mechanisms in the toxicity of metal ions. *Free Radic Biol Med* **18**(2): 321-336.

Stoorvogel W, Strous GJ, Geuze HJ, Oorschot V and Schwartz AL (1991) Late endosomes derive from early endosomes by maturation. *Cell* **65**(3): 417-427.

Strasser A, Harris AW and Cory S (1993) E mu-bcl-2 transgene facilitates spontaneous transformation of early pre-B and immunoglobulin-secreting cells but not T cells. *Oncogene* **8**(1): 1-9.

Sugawara I, Kataoka I, Morishita Y, Hamada H, Tsuruo T, Itoyama S and Mori S (1988) Tissue distribution of P-glycoprotein encoded by a multidrug-resistant gene as revealed by a monoclonal antibody, MRK 16. *Cancer Res* **48**(7): 1926-1929.

Sun J, Li ZM, Hu ZY, Zeng ZL, Yang DJ and Jiang WQ (2009) Apogossypolone inhibits cell growth by inducing cell cycle arrest in U937 cells. *Oncol Rep* **22**(1): 193-198.

Sun J, Zhang D, Zheng Y, Zhao Q, Zheng M, Kovacevic Z and Richardson DR (2013) Targeting the metastasis suppressor, NDRG1, using novel iron chelators: regulation of stress fiber-mediated tumor cell migration via modulation of the ROCK1/pMLC2 signaling pathway. *Mol Pharmacol* **83**(2): 454-469.

Szakacs G, Annereau JP, Lababidi S, Shankavaram U, Arciello A, Bussey KJ, Reinhold W, Guo Y, Kruh GD, Reimers M, Weinstein JN and Gottesman MM (2004) Predicting drug sensitivity and resistance: profiling ABC transporter genes in cancer cells. *Cancer Cell* **6**(2): 129-137.

Szakacs G, Paterson JK, Ludwig JA, Booth-Genthe C and Gottesman MM (2006) Targeting multidrug resistance in cancer. *Nat Rev Drug Discov* **5**(3): 219-234.

Terman A and Kurz T (2013) Lysosomal iron, iron chelation, and cell death. *Antioxid Redox Signal* **18**(8): 888-898.

Thiebaut F, Tsuruo T, Hamada H, Gottesman MM, Pastan I and Willingham MC (1987) Cellular localization of the multidrug-resistance gene product P-glycoprotein in normal human tissues. *Proc Natl Acad Sci USA* **84**(21): 7735-7738.

Thiebaut F, Tsuruo T, Hamada H, Gottesman MM, Pastan I and Willingham MC (1989) Immunohistochemical localization in normal tissues of different epitopes in the multidrug transport protein P170: evidence for localization in brain capillaries and crossreactivity of one antibody with a muscle protein. *J Histochem Cytochem* **37**(2): 159-164.

Thomas A, El Rouby S, Reed JC, Krajewski S, Silber R, Potmesil M and Newcomb EW (1996) Drug-induced apoptosis in B-cell chronic lymphocytic leukemia: relationship between p53 gene mutation and bcl-2/bax proteins in drug resistance. *Oncogene* **12**(5): 1055-1062.

Thomas S, Quinn BA, Das SK, Dash R, Emdad L, Dasgupta S, Wang XY, Dent P, Reed JC, Pellecchia M, Sarkar D and Fisher PB (2013) Targeting the Bcl-2 family for cancer therapy. *Expert Opin Ther Targets* **17**(1): 61-75.

Tidefelt U, Liliemark J, Gruber A, Liliemark E, Sundman-Engberg B, Juliusson G, Stenke L, Elmhorn-Rosenborg A, Mollgard L, Lehman S, Xu D, Covelli A, Gustavsson B and Paul C (2000) P-Glycoprotein inhibitor valspodar (PSC 833) increases the intracellular concentrations of daunorubicin in vivo in patients with P-glycoprotein-positive acute myeloid leukemia. *J Clin Oncol* **18**(9): 1837-1844.

Tomida A and Tsuruo T (1999) Drug resistance mediated by cellular stress response to the microenvironment of solid tumors. *Anticancer Drug Des* **14**(2): 169-177.

Tothova E, Fricova M, Stecova N, Kafkova A and Elbertova A (2002) High expression of Bcl-2 protein in acute myeloid leukemia cells is associated with poor response to chemotherapy. *Neoplasma* **49**(3): 141-144.

Traynor AM, Lee JW, Bayer GK, Tate JM, Thomas SP, Mazurczak M, Graham DL, Kolesar JM and Schiller JH (2010) A phase II trial of triapine (NSC# 663249) and gemcitabine as second line treatment of advanced non-small cell lung cancer: Eastern Cooperative Oncology Group Study 1503. *Invest New Drugs* **28**(1): 91-97.

Triller N, Korosec P, Kern I, Kosnik M and Debeljak A (2006) Multidrug resistance in small cell lung cancer: expression of P-glycoprotein, multidrug resistance protein 1 and lung resistance protein in chemo-naive patients and in relapsed disease. *Lung Cancer* **54**(2): 235-240.

Tse C, Shoemaker AR, Adickes J, Anderson MG, Chen J, Jin S, Johnson EF, Marsh KC, Mitten MJ, Nimmer P, Roberts L, Tahir SK, Xiao Y, Yang X, Zhang H, Fesik S, Rosenberg SH and Elmore SW (2008) ABT-263: a potent and orally bioavailable Bcl-2 family inhibitor. *Cancer Res* **68**(9): 3421-3428.

Tsuchihara K, Fujii S and Esumi H (2009) Autophagy and cancer: dynamism of the metabolism of tumor cells and tissues. *Cancer Lett* **278**(2): 130-138.

Tsujimoto Y, Cossman J, Jaffe E and Croce CM (1985) Involvement of the bcl-2 gene in human follicular lymphoma. *Science* **228**(4706): 1440-1443.

Turk B, Stoka V, Rozman-Pungercar J, Cirman T, Droga-Mazovec G, Oresic K and Turk V (2002) Apoptotic pathways: involvement of lysosomal proteases. *Biol Chem* **383**(7-8): 1035-1044.

Turk B and Turk V (2009) Lysosomes as "suicide bags" in cell death: myth or reality? *J Biol Chem* **284**(33): 21783-21787.

Türkkan B, Ülküseven B and Eroĵlu E (2015) Zinc (II) Complexes of Acetophenone and 5-Chloro-2-hydroxy-benzophenone Thiosemicarbazones. Synthesis, Characterization, and Nonlinear Optical Properties from Quantum Chemical Calculations. *Phosphorus, Sulfur, and Silicon and the Related Elemen* **190**(1): 53-65.

Urbatsch IL, al-Shawi MK and Senior AE (1994) Characterization of the ATPase activity of purified Chinese hamster P-glycoprotein. *Biochemistry* **33**(23): 7069-7076.

Urbatsch IL, Sankaran B, Weber J and Senior AE (1995) P-glycoprotein is stably inhibited by vanadate-induced trapping of nucleotide at a single catalytic site. *J Biol Chem* **270**(33): 19383-19390.

Valko M, Leibfritz D, Moncol J, Cronin MTD, Mazur M and Telser J (2007) Free radicals and antioxidants in normal physiological functions and human disease. *Int J Biochem Cell Biol* **39**(1): 44-84.

Vallee BL (1988) Zinc: biochemistry, physiology, toxicology and clinical pathology. *Biofactors* **1**(1): 31-36.

van Delft MF, Wei AH, Mason KD, Vandenberg CJ, Chen L, Czabotar PE, Willis SN, Scott CL, Day CL, Cory S, Adams JM, Roberts AW and Huang DC (2006) The BH3 mimetic ABT-737 targets selective Bcl-2 proteins and efficiently induces apoptosis via Bak/Bax if Mcl-1 is neutralized. *Cancer Cell* **10**(5): 389-399.

van der Holt B, Lowenberg B, Burnett AK, Knauf WU, Shepherd J, Piccaluga PP, Ossenkoppele GJ, Verhoef GE, Ferrant A, Crump M, Selleslag D, Theobald M, Fey MF, Vellenga E,

Dugan M and Sonneveld P (2005) The value of the MDR1 reversal agent PSC-833 in addition to daunorubicin and cytarabine in the treatment of elderly patients with previously untreated acute myeloid leukemia (AML), in relation to MDR1 status at diagnosis. *Blood* **106**(8): 2646-2654.

van der Valk P, van Kalken CK, Ketelaars H, Broxterman HJ, Scheffer G, Kuiper CM, Tsuruo T, Lankelma J, Meijer CJ, Pinedo HM and et al. (1990) Distribution of multi-drug resistance-associated P-glycoprotein in normal and neoplastic human tissues. Analysis with 3 monoclonal antibodies recognizing different epitopes of the P-glycoprotein molecule. *Ann Oncol* **1**(1): 56-64.

Van Giessen GJ, Crim JA, Petering DH and Petering HG (1973) Effect of heavy metals on the in vitro cytotoxicity of 3-ethoxy-2-oxobutyraldehyde bis (thiosemicarbazone) and related compounds. *J Natl Cancer Inst* **51**(1): 139-146.

Van Poznak C, Seidman AD, Reidenberg MM, Moasser MM, Sklarin N, Van Zee K, Borgen P, Gollub M, Bacotti D, Yao TJ, Bloch R, Ligueros M, Sonenberg M, Norton L and Hudis C (2001) Oral gossypol in the treatment of patients with refractory metastatic breast cancer: a phase I/II clinical trial. *Breast Cancer Res Treat* **66**(3): 239-248.

Vaux DL, Cory S and Adams JM (1988) Bcl-2 gene promotes haemopoietic cell survival and cooperates with c-myc to immortalize pre-B cells. *Nature* **335**(6189): 440-442.

Verhaegen M, Bauer JA, Martin de la Vega C, Wang G, Wolter KG, Brenner JC, Nikolovska-Coleska Z, Bengtson A, Nair R, Elder JT, Van Brocklin M, Carey TE, Bradford CR, Wang S and Soengas MS (2006) A novel BH3 mimetic reveals a mitogen-activated protein kinase-dependent mechanism of melanoma cell death controlled by p53 and reactive oxygen species. *Cancer Res* **66**(23): 11348-11359.

Viswanadhan VN, Chose AK, Revankar GR and Robins RK (1987) Atomic physiochemical parameters for 3-dimensional-structure directed quantitative structure-activity-relationships 4. Additional parameters for hydrophobic and dispersive interactions and their application for an automated superposition of certain naturally occurring nucleoside antibiotics. *JChem Inf Comput Sci* **29**: 163 - 172.

Voehringer DW and Meyn RE (2000) Redox aspects of Bcl-2 function. *Antioxid Redox Signal* **2**(3): 537-550.

Walensky LD, Pitter K, Morash J, Oh KJ, Barbuto S, Fisher J, Smith E, Verdine GL and Korsmeyer SJ (2006) A stapled BID BH3 helix directly binds and activates BAX. *Mol Cell* **24**(2): 199-210.

Wang G, Nikolovska-Coleska Z, Yang CY, Wang R, Tang G, Guo J, Shangary S, Qiu S, Gao W, Yang D, Meagher J, Stuckey J, Krajewski K, Jiang S, Roller PP, Abaan HO, Tomita Y and Wang S (2006) Structure-based design of potent small-molecule inhibitors of anti-apoptotic Bcl-2 proteins. *J Med Chem* **49**(21): 6139-6142.

Wang JQ, Du ZW, Gao XF, Wu M, Zhang YC, Pan Y, Wang Q and Zhang GZ (2013) The effect of Bcl-2 gene silencing on the sensitivity of cell line A549 to chemotherapeutic drugs. *Zhonghua Jie He He Hu Xi Za Zhi* **36**(3): 191-197.

Wang K, Yin XM, Chao DT, Milliman CL and Korsmeyer SJ (1996) BID: a novel BH3 domain-only death agonist. *Genes Dev* **10**(22): 2859-2869.

Watanabe A, Yasuhira S, Inoue T, Kasai S, Shibazaki M, Takahashi K, Akasaka T, Masuda T and Maesawa C (2013) BCL2 and BCLxL are key determinants of resistance to antitubulin chemotherapeutics in melanoma cells. *Exp Dermatol* **22**(8): 518-523.

Wei J, Stebbins JL, Kitada S, Dash R, Zhai D, Placzek WJ, Wu B, Rega MF, Zhang Z, Barile E, Yang L, Dahl R, Fisher PB, Reed JC and Pellecchia M (2011) An optically pure apogossypolone derivative as potent pan-active inhibitor of anti-apoptotic bcl-2 family proteins. *Front Oncol* **1**: 28.

Wei MC, Zong WX, Cheng EH, Lindsten T, Panoutsakopoulou V, Ross AJ, Roth KA, MacGregor GR, Thompson CB and Korsmeyer SJ (2001) Proapoptotic BAX and BAK: a requisite gateway to mitochondrial dysfunction and death. *Science* **292**(5517): 727-730.

Wei Y, Pattingre S, Sinha S, Bassik M and Levine B (2008) JNK1-mediated phosphorylation of Bcl-2 regulates starvation-induced autophagy. *Mol Cell* **30**(6): 678-688.

Weinlich G, Eisendle K, Hassler E, Baltaci M, Fritsch PO and Zelger B (2006) Metallothionein - overexpression as a highly significant prognostic factor in melanoma: a prospective study on 1270 patients. *Br J Cancer* **94**(6): 835-841.

Weinstein RS, Jakate SM, Dominguez JM, Lebovitz MD, Koukoulis GK, Kuszak JR, Klusens LF, Grogan TM, Saclarides TJ, Roninson IB and et al. (1991) Relationship of the expression of the multidrug resistance gene product (P-glycoprotein) in human colon carcinoma to local tumor aggressiveness and lymph node metastasis. *Cancer Res* **51**(10): 2720-2726.

Weiss LM, Warnke RA, Sklar J and Cleary ML (1987) Molecular analysis of the t(14;18) chromosomal translocation in malignant lymphomas. *N Engl J Med* **317**(19): 1185-1189.

Welch KD, Davis TZ, Van Eden ME and Aust SD (2002) Deleterious iron-mediated oxidation of biomolecules. *Free Radic Biol Med* **32**(7): 577-583.

Weller M, Malipiero U, Aguzzi A, Reed JC and Fontana A (1995) Protooncogene bcl-2 gene transfer abrogates Fas/APO-1 antibody-mediated apoptosis of human malignant glioma cells and confers resistance to chemotherapeutic drugs and therapeutic irradiation. *J Clin Invest* **95**(6): 2633-2643.

West DX, Ives JS, Krejci J, Salberg MM, Zumbahlen TL, Bain GA, Liberta AE, Valdes-Martinez J, Hernandez-Ortiz S and Toscano RA (1995) Copper(II) complexes of 2-benzoylpyridine 4N-substituted thiosemicarbazones. *Polyhedron* **14**(15ï 16): 2189-2200.

Whitnall M, Howard J, Ponka P and Richardson DR (2006) A class of iron chelators with a wide spectrum of potent antitumor activity that overcomes resistance to chemotherapeutics. *Proc Natl Acad Sci USA* **103**(40): 14901-14906.

Willis SN, Chen L, Dewson G, Wei A, Naik E, Fletcher JI, Adams JM and Huang DC (2005) Proapoptotic Bak is sequestered by Mcl-1 and Bcl-xL, but not Bcl-2, until displaced by BH3-only proteins. *Genes Dev* **19**(11): 1294-1305.

Willis SN, Fletcher JI, Kaufmann T, van Delft MF, Chen L, Czabotar PE, Ierino H, Lee EF, Fairlie WD, Bouillet P, Strasser A, Kluck RM, Adams JM and Huang DC (2007) Apoptosis initiated when BH3 ligands engage multiple Bcl-2 homologs, not Bax or Bak. *Science* **315**(5813): 856-859.

Withana NP, Blum G, Sameni M, Slaney C, Anbalagan A, Olive MB, Bidwell BN, Edgington L, Wang L, Moin K, Sloane BF, Anderson RL, Bogyo MS and Parker BS (2012) Cathepsin B inhibition limits bone metastasis in breast cancer. *Cancer Res* **72**(5): 1199-1209.

Wroblewski D, Mijatov B, Mohana-Kumaran N, Lai F, Gallagher SJ, Haass NK, Zhang XD and Hersey P (2013) The BH3-mimetic ABT-737 sensitizes human melanoma cells to apoptosis induced by selective BRAF inhibitors but does not reverse acquired resistance. *Carcinogenesis* **34**(2): 237-247.

Wu D (1989) An overview of the clinical pharmacology and therapeutic potential of gossypol as a male contraceptive agent and in gynaecological disease. *Drugs* **38**(3): 333-341.
Wu DW, Huang CC, Chang SW, Chen TH and Lee H (2015) Bcl-2 stabilization by paxillin confers 5-fluorouracil resistance in colorectal cancer. *Cell Death Differ* **22**(5): 779-789.
Wu YW, Chik CL and Knazek RA (1989) An in vitro and in vivo study of antitumor effects of gossypol on human SW-13 adrenocortical carcinoma. *Cancer Res* **49**(14): 3754-3758.
Yadav AA, Patel D, Wu X and Hasinoff BB (2013) Molecular mechanisms of the biological activity of the anticancer drug elesclomol and its complexes with Cu(II), Ni(II) and Pt(II). *J Inorg Biochem* **126**: 1-6.
Yamagishi T, Sahni S, Sharp DM, Arvind A, Jansson PJ and Richardson DR (2013) P-glycoprotein mediates drug resistance via a novel mechanism involving lysosomal sequestration. *J Biol Chem* **288**(44): 31761-31771.
Yang E, Zha J, Jockel J, Boise LH, Thompson CB and Korsmeyer SJ (1995) Bad, a heterodimeric partner for Bcl-XL and Bcl-2, displaces Bax and promotes cell death. *Cell* **80**(2): 285-291.
Yang J, Liu X, Bhalla K, Kim CN, Ibrado AM, Cai J, Peng TI, Jones DP and Wang X (1997) Prevention of apoptosis by Bcl-2: release of cytochrome c from mitochondria blocked. *Science* **275**(5303): 1129-1132.
Yang M, Lu Y-L, Li M-X, Xu X-W and Chen L (2013a) Synthesis, crystal structures and biological evaluation of 2-benzoylpyridine N (4)-cyclohexylthiosemicarbazone and its binuclear copper (II) complex. *Inorg Chem Commun* **35**: 117-121.
Yang M, Zhang Y-H, Li M-X, Lu Y-L and Zhang N (2013b) Synthesis, crystal structures, and cytotoxicity of 2-benzoylpyridine N(4)-cyclohexylthiosemicarbazone and its zinc(II) and diorganotin(IV) complexes. *J Coord Chem* **66**(19): 3327-3334.
Youle RJ and Strasser A (2008) The BCL-2 protein family: opposing activities that mediate cell death. *Nat Rev Mol Cell Biol* **9**(1): 47-59.
Young IS and Woodside JV (2001) Antioxidants in health and disease. *J Clin Pathol* **54**(3): 176-186.
Yu F, Chen Z, Wang B, Jin Z, Hou Y, Ma S and Liu X (2016) The role of lysosome in cell death regulation. *Tumour Biol* **37**(2): 1427-1436.
Yu H, Zhou Y, Lind SE and Ding WQ (2009a) Clioquinol targets zinc to lysosomes in human cancer cells. *Biochem J* **417**(1): 133-139.
Yu Y, Kalinowski DS, Kovacevic Z, Siafakas AR, Jansson PJ, Stefani C, Lovejoy DB, Sharpe PC, Bernhardt PV and Richardson DR (2009b) Thiosemicarbazones from the old to new: iron chelators that are more than just ribonucleotide reductase inhibitors. *J Med Chem* **52**(17): 5271-5294.
Yu Y and Richardson DR (2011) Cellular iron depletion stimulates the JNK and p38 MAPK signaling transduction pathways, dissociation of ASK1-thioredoxin, and activation of ASK1. *J Biol Chem* **286**(17): 15413-15427.
Yu Y, Suryo Rahmanto Y, Hawkins CL and Richardson DR (2011) The potent and novel thiosemicarbazone chelators di-2-pyridylketone-4,4-dimethyl-3-thiosemicarbazone and 2-benzoylpyridine-4,4-dimethyl-3-thiosemicarbazone affect crucial thiol systems required for ribonucleotide reductase activity. *Mol Pharmacol* **79**(6): 921-931.
Yu Y, Suryo Rahmanto Y and Richardson DR (2012) Bp44mT: an orally active iron chelator of the thiosemicarbazone class with potent anti-tumour efficacy. *Br J Pharmacol* **165**(1): 148-166.

Yu Z, Persson HL, Eaton JW and Brunk UT (2003) Intralysosomal iron: a major determinant of oxidant-induced cell death. *Free Radic Biol Med* **34**(10): 1243-1252.

Yuan J, Lovejoy DB and Richardson DR (2004) Novel di-2-pyridyl-derived iron chelators with marked and selective antitumor activity: in vitro and in vivo assessment. *Blood* **104**(5): 1450-1458.

Zalcberg J, Hu XF, Slater A, Parisot J, El-Osta S, Kantharidis P, Chou ST and Parkin JD (2000) MRP1 not MDR1 gene expression is the predominant mechanism of acquired multidrug resistance in two prostate carcinoma cell lines. *Prostate Cancer Prostatic Dis* **3**(2): 66-75.

Zelger B, Hittmair A, Schir M, Ofner C, Ofner D, Fritsch PO, Bocker W, Jasani B and Schmid KW (1993) Immunohistochemically demonstrated metallothionein expression in malignant melanoma. *Histopathology* **23**(3): 257-263.

Zhang H, Nimmer PM, Tahir SK, Chen J, Fryer RM, Hahn KR, Iciek LA, Morgan SJ, Nasarre MC, Nelson R, Preusser LC, Reinhart GA, Smith ML, Rosenberg SH, Elmore SW and Tse C (2007) Bcl-2 family proteins are essential for platelet survival. *Cell Death Differ* **14**(5): 943-951.

Zhitomirsky B and Assaraf YG (2015a) Lysosomal sequestration of hydrophobic weak base chemotherapeutics triggers lysosomal biogenesis and lysosome-dependent cancer multidrug resistance. *Oncotarget* **6**(2): 1143-1156.

Zhitomirsky B and Assaraf YG (2015b) The role of cytoplasmic-to-lysosomal pH gradient in hydrophobic weak base drug sequestration in lysosomes. *Cancer Cell Microenvironment* **2**(3).

Zhitomirsky B and Assaraf YG (2016) Lysosomes as mediators of drug resistance in cancer. *Drug Resist Updat* **24**: 23-33.

Zimmermann AK, Loucks FA, Schroeder EK, Bouchard RJ, Tyler KL and Linseman DA (2007) Glutathione binding to the Bcl-2 homology-3 domain groove: a molecular basis for Bcl-2 antioxidant function at mitochondria. *J Biol Chem* **282**(40): 29296-29304.

Zou H, Henzel WJ, Liu X, Lutschg A and Wang X (1997) Apaf-1, a human protein homologous to C. elegans CED-4, participates in cytochrome c-dependent activation of caspase-3. *Cell* **90**(3): 405-413.